



BIBLIOTHÈQUE

CÉGEP DE L'ABITIBI-TÉMISCAMINGUE
UNIVERSITÉ DU QUÉBEC EN ABITIBI-TÉMISCAMINGUE

Mise en garde

La bibliothèque du Cégep de l'Abitibi-Témiscamingue et de l'Université du Québec en Abitibi-Témiscamingue (UQAT) a obtenu l'autorisation de l'auteur de ce document afin de diffuser, dans un but non lucratif, une copie de son œuvre dans [Depositum](#), site d'archives numériques, gratuit et accessible à tous. L'auteur conserve néanmoins ses droits de propriété intellectuelle, dont son droit d'auteur, sur cette œuvre.

Warning

The library of the Cégep de l'Abitibi-Témiscamingue and the Université du Québec en Abitibi-Témiscamingue (UQAT) obtained the permission of the author to use a copy of this document for nonprofit purposes in order to put it in the open archives [Depositum](#), which is free and accessible to all. The author retains ownership of the copyright on this document.

UNIVERSITÉ DU QUÉBEC EN ABITIBI-TÉMISCAMINGUE

PERFORMANCES DE L'ÉLECTROCOAGULATION OU DES FERRATES
POUR LE TRAITEMENT DES CONTAMINANTS ÉMERGENTS PRÉSENTS
DANS LES EAUX MINIÈRES CONTAMINÉES

THÈSE

PRÉSENTÉE

COMME EXIGENCE PARTIELLE

DOCTORAT EN SCIENCES DE L'ENVIRONNEMENT

PAR

REEM SAFIRA

AVRIL 2024

UNIVERSITÉ DU QUÉBEC EN ABITIBI-TÉMISCAMINGUE

PERFORMANCE OF ELECTROCOAGULATION OR FERRATES FOR THE
TREATMENT OF CONTAMINANTS OF EMERGING CONCERNS FROM
NEUTRAL MINE WATER

PHD THESIS

PRESENTED

AS A PARTIAL REQUIREMENT

PHD IN ENVIRONMENTAL SCIENCES

BY

REEM SAFIRA

APRIL 2024

ACKNOWLEDGEMENT

First, I would like to sincerely thank my thesis supervisor, Lucie Coudert, whose support in the good and bad days, encouragement, and permanent availability, are what allowed me to finish this distinguished milestone in my academic journey. I would like also to thank my co-supervisor Carmen Mihaela Neculita for her continuous support, for giving me the great opportunity to learn from her wide experience and for teaching what is meant by being a researcher. A special thanks to my second co-supervisor Eric Rosa, who in the first place gave me this chance to pursue my studies, and for his contribution in my thesis to finish the work in the best way. I would like to thank all of you for your positive influence on my life, and for being by my side in the past five years. For me, you were like a family.

I would like to thank the great team and colleagues at URSTM. First, I like to thank Mélinda Gervais, who was the first person I met at URSTM and introduced me to the chemistry laboratories and who helped me a lot afterwards. I also want to thank from the bottom of my heart, Akué-Sylvette Awoh, the Director of URSTM and administrative director of RIME, for her continuous support and availability. A special mention to Étienne Bélanger, and sincere thanks for his collaboration in my project. The thanks are also due to the chemistry laboratory technicians, Julie Beaulieu and Roch Germain, from whom I learnt many analytical skills during my work at URSTM. Finally, I would like to thank Elvin Javier Basto for his support and continuous collaboration. Sincerely, I would like to thank my friends Marouen Jouini and T.V. Rakotonimaro (Koly), whose support in the hard days was the motivation to go forward and finish this journey successfully.

Last but not least, I would like to thank my partner, my beloved husband (JAD), who stand by my side and gave me all the support, strength, confidence that I am able to do it. My huge thanks are also for my family, my mother, my brothers and my sisters, who supported me along this interesting, hard journey.

DEDICATION

To my father;

To my beloved husband (JAD);

To my brother Maen;

To my dearest friend Wissam;

To my family and friends.

FOREWORD

The thesis consists of a general introduction (Chapter 1), a recent and relevant literature review (Chapter 2), a description of the methodology used (Chapter 3), three chapters in the form of scientific articles (Chapters 4 to 6), a discussion of the main results (Chapter 7) and a general conclusion (Chapter 8). As part of this research project, several papers were published, submitted or under revision for publication in peer-reviewed journals. In addition, several presentations were performed at national and international conferences as well as at the annual RIME symposium. These achievements were the result of the collaboration with my supervisor Lucie Coudert, and my co-supervisors Carmen M. Neculita and Eric Rosa, and they are listed below:

Publications in peer-reviewed journals:

Chapter 4. Safira, R., Coudert, L., Neculita, C.M., Rosa, E. (2024). Efficiency of electrocoagulation for simultaneous treatment of As and Mn in neutral mine water. *Minerals Engineering*, 207, 108546. <https://doi.org/10.1016/j.mineng.2023.108546>.

Credit authorship contribution statement: Reem Safira: Conceptualization, Methodology, Visualization, Formal analysis, Investigation, Writing - original draft. Lucie Coudert: Conceptualization, Methodology, Visualization, Formal analysis, Supervision, Project administration, Funding acquisition, Writing - review & editing. Carmen M. Neculita: Conceptualization, Methodology, Visualization, Formal analysis, Supervision, Funding acquisition, Writing - review & editing. Eric Rosa: Conceptualization, Methodology, Visualization, Formal analysis, Supervision, Writing - review & editing.

Chapter 5. Safira, R., Coudert, L., Neculita, C.M., Bélanger, E., Rosa, E. (2023). Performance of ferrates for simultaneous removal of As and Mn from circumneutral contaminated mine water. *Journal of Environmental Chemical Engineering* 11, 110421. <https://doi.org/10.1016/j.jece.2023.110421>.

Credit authorship contribution statement: Reem Safira: Conceptualization, Methodology, Visualization, Formal analysis, Investigation, Writing - original draft. Lucie Coudert: Conceptualization, Methodology, Formal analysis, Visualization, Supervision, Project administration, Funding acquisition, Writing - review & editing. Carmen M. Neculita: Conceptualization, Methodology, Visualization, Formal analysis, Supervision, Writing - review & editing, Funding acquisition. Étienne Bélanger: Methodology, Formal analysis, Writing – review & editing. Eric Rosa: Conceptualization, Methodology, Visualization, Formal analysis, Supervision, Writing - review & editing.

Chapter 6. Safira, R., Coudert, L., Benzaazoua, M., Elghali, A., Rosa, E., Neculita, C.M. (2024) Comparative assessment of As- and Mn-rich sludge stability from neutral mine water treatment by Fe(VI) and electrocoagulation. *Journal of Cleaner production* (in preparation).

Credit authorship contribution statement: Reem Safira: Conceptualization, Methodology, Visualization, Formal analysis, Investigation, Writing - original draft. Abdellatif Elghali: Formal analysis, Writing – review & editing. Mostafa Benzaazoua: Conceptualization, Formal analysis, Investigation, Writing – review & editing. Lucie Coudert: Conceptualization, Methodology, Visualization, Formal analysis, Supervision, Project administration, Funding acquisition, Writing - review & editing. Eric Rosa: Conceptualization, Methodology, Visualization, Formal analysis, Supervision, Writing - review & editing. Carmen M. Neculita: Conceptualization,

Methodology, Visualization, Formal analysis, Supervision, Project administration, Funding acquisition, Writing - review & editing.

Conferences and presentations:

Safira, R., Coudert, L., Neculita, C.M., Bélanger, E., Rosa, E. (2022). Performance of ferrates for As and Mn simultaneous removal from synthetic neutral effluents. URSTM Annual Colloque, RIME, UQAT-Polytechnique, Rouyn-Noranda, QC, Canada, 20 October.

Safira, R., Coudert, L., Neculita, C.M., Bélanger, E., Rosa, E. (2022). Efficiency assessment of ferrates to remove As and/or Mn from synthetic neutral mine water. 43rd Annual Meeting SETAC North America, Pittsburgh, PA, USA (and Online), 13-17 November.

Safira, R., Coudert, L., Neculita, C.M., Rosa, E. (2023). Évaluation de la toxicité sur *Daphnia magna* sur les effluents miniers après traitement de l'As et du Mn par les ferrates vs. l'électrocoagulation. Colloque conjoint ECOBIM EcotoQ, Quebec, QC, Canada, 31 May-2 June.

Safira, R., Coudert, L., Neculita, C.M., Rosa, E. (2023). Efficiency assessment of electrocoagulation for the removal of As and Mn from synthetic and surrogate neutral mine water. PEOPLE 2023 – Collaborative Solutions to Environmental Problems under Climate Change, Montreal, QC, Canada, 7-11 August.

Posters:

Safira, R., Coudert, L., Neculita, C.M., Rosa, E. (2021). Performance of electrocoagulation and ferrates for the treatment of contaminants of emerging concerns. Symposium 2021, (Virtual), Mines and the Environment, 14-16 June.

TABLE OF CONTENTS

FOREWORD.....	ix
TABLE OF CONTENTS.....	xiii
LIST OF FIGURES	xvii
LIST OF TABLES.....	xix
LIST OF ABBREVIATIONS	xxi
ABSTRACT	xxv
RÉSUMÉ.....	xxix
CHAPTER 1 GENERAL INTRODUCTION.....	1
1.1 Context of the study.....	1
1.2 Selection of the CECs studied in the present work	3
1.3 Knowledge gaps and originality	6
1.4 Hypotheses and Objectives	7
1.4.1 Hypotheses.....	7
1.4.2 Objectives	8
1.4.3 Thesis Structure.....	9
CHAPTER 2 LITTERATURE REVIEW	11
2.1 Arsenic and manganese in the environment and mine effluents	11
2.2 Technologies available for As and Mn treatment	17
2.3 Electrocoagulation.....	21
2.3.1 Principle and design	21
2.3.2 Mechanisms involved in contaminants removal during ECG	22
2.3.3 Operating parameters influencing the performance of ECG	27
2.3.4 Combining ECG with other processes	36
2.4 Ferrates	40
2.4.1 Principle.....	40
2.4.2 Synthesis and reactivity of Fe(VI)	41

2.4.3	Mechanisms involved in inorganic contaminants removal by Fe (VI) ..	44
2.4.4	Operating parameters influencing the performance of Fe(VI)	45
2.5	Toxicity of mine effluents: evaluation and regulations.....	53
2.6	Stability of treatment sludge.....	60
2.6.1	Stability of As-bearing residue	61
2.6.2	Stability of Mn-bearing residue	66
2.6.3	Stability of As- and Mn-bearing residues.....	67
CHAPTER 3 METHODOLOGICAL APPROACH		69
3.1	Preparation of synthetic and surrogate mine water	72
3.2	Electrocoagulation (ECG).....	73
3.3	Ferrate	74
3.4	Sludge characterization and mobility of As and Mn from the sludge	76
3.5	Preliminary techno-economic evaluation of ECG and Fe(VI) treatment and comparison of their performances	78
3.5.1	Techno-economic evaluation of ECG treatment.....	78
3.5.2	Techno-economic evaluation of Fe(VI) treatment	81
CHAPTER 4 EFFICIENCY OF ELECTROCOAGULATION FOR SIMULTANEOUS TREATMENT OF AS AND MN IN NEUTRAL MINE WATER.....		83
4.1	Abstract	84
4.2	Résumé.....	86
4.3	Introduction	88
4.4	Materials and methods	92
4.4.1	Preparation and characterization of mine water	92
4.4.2	ECG treatment.....	93
4.4.3	Analytical methods	97
4.4.4	Toxicity testing.....	98
4.5	Results and discussion	99
4.5.1	Performance of ECG on As and Mn removal from synthetic effluents S_{As} and S_{Mn}	99
4.5.2	Performance of ECG on simultaneous removal of As and Mn from S_{As+Mn}	107

4.5.3	Performance of ECG for As and Mn removal from surrogate mine water	110
4.5.4	Toxicity.....	111
4.6	Conclusion.....	114
CHAPTER 5 PERFORMANCES OF FERRATES FOR SIMULTANEOUS REMOVAL OF AS AND MN FROM CIRCUMNEUTRAL MINE WATER.....		
5.1	Abstract	120
5.2	Résumé.....	121
5.3	Introduction	123
5.4	Materials and Methods.....	127
5.4.1	Preparation and characterization of mine effluents and Fe(VI).....	127
5.4.2	Fe(VI) treatment.....	129
5.4.3	Analytical methods.....	133
5.4.4	Toxicity testing.....	134
5.5	Results and discussion	135
5.5.1	Characterization of synthetic and surrogate mine effluents	135
5.5.2	Performance of Fe(VI) on As and Mn removal from synthetic effluents	137
5.5.3	Performance of Fe(VI) on As and Mn removal from synthetic effluent S_{As+Mn}	145
5.5.4	Performance of Fe(VI) _s and Fe(III) on As and Mn removal from surrogate mine effluent.....	149
5.6	Conclusion.....	154
CHAPTER 6 COMPARATIVE ASSESSMENT OF AS- AND MN-RICH SLUDGE STABILITY FROM NEUTRAL MINE WATER TREATMENT BY FE(VI) VS ELECTROCOAGULATION		
6.1	Abstract	160
6.2	Résumé.....	162
6.3	Introduction	164
6.4	Materials and methods	168
6.4.1	Preparation of surrogate mine water and sludge production	168
6.4.2	Geochemical modeling and thermodynamic equilibrium calculations	170
6.4.3	Physicochemical and mineralogical composition of the sludge	171
6.4.4	Leaching tests.....	172
6.5	Results and discussion	174

6.5.1	Treatment performance, geochemical modelling, and thermodynamic equilibrium calculations.....	174
6.5.2	Chemical composition of post-treatment sludges	180
6.5.3	Mineralogical characterization of ECG- and Fe(VI)-sludge	183
6.5.4	Environmental characterization of the sludge.....	192
6.6	Conclusion.....	197
CHAPTER 7.....		205
GENERAL DISCUSSION.....		205
7.1	Effect of operating conditions on the simultaneous removal of As and Mn using ECG and Fe(VI)	206
7.1.1	Current density	207
7.1.2	Fe(VI) dose	209
7.1.3	Retention time	212
7.1.4	Effect of competing ions on treatment performance	215
7.2	Potential mobility of As and Mn from the sludge produced from ECG and Fe(VI)	218
7.3	Comparison between ECG and Fe(VI) performances	221
CHAPTER 8.....		225
GENERAL CONCLUSION.....		225
APPENDIX.....		229
RÉFÉRENCES		239

LIST OF FIGURES

Figure	Page
1.1 Definition of CECs based on scientific knowledge and actual regulations of different substances in mine water. REE: Rare earth elements; TDS: Total dissolved solids (Ryskie et al., 2021).....	2
2.1 Eh-pH mosaic diagram of aqueous As (a) and Mn (b) species in water at 25°C and 1 bar. The activity of As and Mn are 7.356×10^{-6} and 3.636×10^{-8} (Figure constructed using Geochemist's Workbench community software).....	12
2.2 A schematic representation of the mechanisms involved in the removal of As and Mn during treatment by ECG using Fe-electrode	25
2.3 A schematic representation of the mechanisms involved in the removal of As and Mn during treatment by ECG using Al-electrode	26
2.4 Impact of pH on the speciation of Fe(VI) (Wang et al., 2021).....	44
2.5 Mechanism involved in As(III) and Mn(II) removal by Fe(VI).....	47
3.1 Methodological approach used in this thesis project	70
3.2 Jar test setup (a) and 20 L-bucket experimental setup (b) used for Fe(VI) sludge production.....	76
4.1 Experimental approach used to identify the most performant operating conditions for the simultaneous removal of As and Mn from synthetic and surrogate mine water	95
4.2 Effect of CD on the removal efficiencies of As (a) and Mn (b) as well as energy and electrode consumption for As (c.) and Mn (d.) (operating conditions: two Fe-electrodes; EC: 1.50 mS/cm; pH: 6.0–6.5; retention time: 60 min; inter-electrode distance: 10 mm; [As] _i : 3.48 ± 0.12 mg/L or [Mn] _i : 4.32 ± 0.14 mg/L)	102
4.3 Evolution of As (a) and Mn (b) removal as well as energy consumption (for As (c) and Mn (d)) with retention time for different EC values (operating conditions: two Fe-electrodes; CD: 0.5 mA/cm ² for As and 2.0 mA/cm ² for Mn; pH: 6.0–6.5; inter- electrode distance: 10 mm; [As] _i : 3.38 ± 0.08 mg/L or [Mn] _i : 4.54 ± 0.16 mg/L).....	106

4.4	Evolution of As (a) and Mn (b) removal as well as energy consumption (c) from S_{As+Mn} at 0.5 and 2.0 mA/cm ² (operating conditions: two Fe-electrodes; pH: 6.0-6.5; electrolysis time: 60 min; inter-electrode distance: 10 mm; [As] _i : 3.23 mg/L and [Mn] _i : 4.10 mg/L).....	109
4.5	Mortality evolution of <i>D. magna</i> for (un)treated E_{low} (a) and E_{high} (b).....	113
5.1	Process steps followed for (a) Fe(VI) _{s/w} and (b) Fe(VI) _s +Fe(III) treatability tests on synthetic and surrogate mine effluents	131
5.2	Effect of Fe(VI) type at different doses and pH _a on As (a) and Mn (b) removal efficiency and residual salinity (c,d) from S_{As} and S_{Mn} (reaction time: 20 min; settling time: 30 min)	140
5.3	Evolution of As and Mn removal efficiency with time (Fe(VI) _s dose : 22 mg/L for As; 5 mg/L for Mn; pH _a = 5.5).....	143
5.4	Influence of Fe(VI) _s (a) and Fe(VI) _s +Fe(III) (b) on the simultaneous removal of As and Mn from the effluent S_{As+Mn} (pH _a : 5.5; reaction time: 5 min; settling time: 15 min)	147
5.5	Mortality evolution of <i>D. magna</i> for untreated and treated E_{low} (a) and E_{high} (b).	153
6.1	Experimental approach used for chemical and mineralogical characterization as well as stability assessment of As- and Mn-rich sludge from Fe(VI) and ECG treatment	173
6.2	Evolution of pH, pe and dissolved concentrations considered in the 5-steps Fe(VI) model.....	177
6.3	Evolution of pH, pe and dissolved concentrations considered in the 4-steps ECG model	179
6.4	Comparison of element concentrations measured in the Fe(VI) and ECG sludge	182
6.5	X-mapping of selected areas from (A) precipitate formed during ECG and (B) precipitate formed during Fe(VI) treatment of E_{high}	184
6.6	Multivariate analysis of EDS data in ECG sample	187
6.7	Multivariate analysis of EDS data in the precipitated minerals in Fe(VI) sample	188

LIST OF TABLES

Table	Page
1.1 Regulation evolution for As and Mn in Canada and around the world in drinking and mine-impacted water	5
2.1 Typical concentrations, sources and/or causes of As and Mn in groundwater, surface water and mine water worldwide.....	15
2.2 Available technologies for simultaneous removal of As and Mn from contaminated water	19
3.1 Variables considered for the estimation of preliminary operating costs for ECG and Fe(VI) treatment of circumneutral mine water contaminated by As and Mn.....	79
3.2 Variables considered for the estimation of preliminary operating costs for ECG and Fe(VI) treatment of circumneutral mine water contaminated by As and Mn	80
5.1 Physicochemical characteristics of synthetic, unspiked and spiked surrogate mine effluents before treatment compared to the real mine effluent	136
5.2 Effect of Fe(VI) _s dose on As (average [As] _{initial} : 3.5 ± 0.3 mg/L) or Mn (average [Mn] _i : 4.5 ± 0.2 mg/L) removal from S _{As} and S _{Mn} at pH _a = 5.5 (reaction time: 20 min; settling time: 30 min).....	141
5.3 Performance of Fe(VI) _s treatment on As and Mn removal from S _{As} and S _{Mn} (Fe(VI) dose: 22 mg/L for As and 5 mg/L for Mn; [As] _{initial} : 3.4 mg/L or [Mn] _{initial} : 4.7 mg/L; pH _a : 5.5; reaction time: 5 min and settling time: 15 min)	144
5.4 Effect of Fe(VI) _s +Fe(III) addition on As and Mn removal (pH _a : 5.5; reaction time: 5 min; settling time: 15 min) from E _{low} and E _{high}	151
6.1 Mineral phases selected during the geochemical modeling and corresponding reactions.....	176
6.2 Humidity and chemical composition of sludge produced from Fe(VI) and ECG treatment	180

6.3	Summary of the chemical composition (wt. %) of the identified groups as analyzed using SEM-EDS.	189
7.1	Effect of the co-occurrence of As and Mn on the CD required to achieve similar removals for S_{As} , S_{Mn} and S_{As+Mn}	208
7.2	Effect of the co-occurrence of As and Mn on the dose of Fe(VI) required to achieve similar removals for S_{As} , S_{Mn} and S_{As+Mn}	211
7.3	Effect of the presence of competing ions on the performances of ECG and Fe(VI) treatment for the simultaneous removal of As and Mn	216
7.4	Comparison between Fe(VI) and ECG performances for simultaneous removal of As and Mn from lowly-contaminated mine water	223
7.5	Preliminary OCs evaluation for the treatment of E_{high} by ECG and Fe(VI).....	224

LIST OF ABBREVIATIONS

ACAIE	Air cathode assisted iron electrocoagulation
AMD	Acid mine drainage
AOP	Advanced oxidation process
ASTM	American Society for Testing and Materials
BATEA	Best available technology economically achievable
CCME	Canadian Council of Ministers of Environment
CD	Current density
CEAEQ	Centre d'Expertise en Analyse Environnementale du Québec
CE	Conductivité électrique
CECs	Contaminants of emerging concerns
COD	Chemical oxygen demand
CRC	Canada Research Chairs Program
D	Inter-electrode distance
DC	Densité de courant
DI	Deionized Water
D019	Directive 019
DO	Dissolved oxygen
EC	Electrical conductivity
EC50	Median effective concentration
ECG	Electrocoagulation
ECG/OMF	Electrocoagulation coupled with oxidative media filtration
ECP	Electrochemical peroxidation process
Fe(VI)	Ferrates
FLT	Field leaching test
FLU	Fluoxetine
FLX	Fluvoxamine

IC	Ionic chromatography
ICP-MS	Inductively coupled plasma-mass spectroscopy
ICP-OES	Inductively coupled plasma – optical emission spectroscopy
INSPQ	Institut National de Santé Publique du Québec
IR	Ohmic drop
LC50	Median lethal concentration
MAC	Maximum allowable concentrations
MAMMC	Maximum authorized monthly mean concentration
MCL	Maximum concentration level
MDMER	Metal and Diamond Mining Effluent Regulations
MELCC	Ministère de l'Environnement et de la Lutte Contre les Changements Climatiques
MELCCFP	Ministère de l'Environnement, de la Lutte Contre les Changements Climatiques, de la Faune et des Parc
MEND	Mine Environment Neutral Drainage
N-SEP	Non-sequential selective extraction procedure
OC	Operating cost
OPEX	Operating expenses
ORP	Oxidation reduction potential
PECP	Photo-assisted electrochemical peroxidation process
pH	Potential hydrogen
pH _a	Adjusted pH
pH _{pzc}	pH of point of zero charge
PXRD	Powder X-ray diffraction
REE	Rare earth elements
RIME	Research institute on mines and environment
SEM-EDS	Scanning electron microscope-energy dispersive spectrometer
SMCL	Secondary maximum concentration level
SO	Specific objective

SPLP	Synthetic precipitation leaching procedure
SWQC	Surface water quality criteria
TUa	Acute toxic unit
TCLP	Toxic characteristic leaching procedure
TDS	Total dissolved solids
US CFR	United States Code of Federal Regulations
USGS	United States Geological Survey
USEPA	United States Environmental Protection Agency
UV-VIS	Ultraviolet-visible spectrophotometer
UQAT	University of Quebec in Abitibi-Temiscamingue
WHO	World Health Organization
XRD	X-Ray diffraction

ABSTRACT

Contaminated neutral mine water from low-grade gold deposits often contain contaminants such as As and Mn. Even at low concentrations, these contaminants can entail adverse effects on human health and the environment. Several treatment methods such as chemical co-precipitation, oxidative precipitation and neutralization have been investigated for the removal of As and Mn from contaminated mine water. Nevertheless, these approaches suffer from major limitations related to the amount of reactants needed, different pH and Fe/contaminants ratios required, among other factors. Such limitations are especially challenging when the treatment targets the simultaneous removal of As and Mn. These challenges highlight the need to explore novel As-Mn treatment methods, while electrocoagulation (ECG) and treatment by ferrates (Fe(VI)) represent promising options. Although ECG and Fe(VI) have been proven to efficiently remove As and Mn from synthetic and real effluents, key gaps related to : (1) the applicability of ECG and Fe(VI) for simultaneous removal of As and Mn; (2) the identification of the most performant treatment conditions; (3) the effect of operating parameters on the energy, electrode consumption and thus operating costs of ECG; (4) the toxicity after treatment of As-Mn contaminated mine water using ECG and Fe(VI) is not documented; and (5) the evaluation of generated sludge stability is poorly documented. Fitting in this context, this study aimed at: (1) evaluating ECG or Fe(VI) performances (i.e. removal efficiency, residual salinity, toxicity, sludge stability and operating cost) for the simultaneous removal of As and Mn, (2) investigating the effect of operating conditions on treatment performance; (3) assessing toxicity to *D. magna* before and after the treatment and (4) characterizing the produced sludge to evaluate their stability.

To achieve the objectives, the methodological approach first consisted of evaluating the performances of ECG or Fe(VI) treatment for removal of As and Mn from synthetic effluents (S_{As} , S_{Mn} , S_{As+Mn}), and surrogate mine water (E_{low} and E_{high}). For ECG treatment, two sets of experiments were performed to evaluate the effect of selected operating parameters: i) current density (CD; 0.25-10 mA/cm²) at 1.5 mS/cm, ii) electrical conductivity (EC; 0.25-2.5 mS/cm) at 0.5 mA/cm² for As and 2 mA/cm² for Mn, on removal of As and Mn from S_{As} and S_{Mn} . Afterward, another set of experiments was carried out for S_{As+Mn} treatment at different CD (0.5 and 2.0 mA/cm²) and, EC (0.25 and 2.5 mS/cm). The effect of retention time was also evaluated for S_{As+Mn} . Later, the most performant conditions (CD: 2 mA/cm², EC: 2.5 mS/cm, time: 1 h, D: 10 mm) were used for the treatment of E_{low} and E_{high} . Finally, the toxicity evaluation to *D. magna* of E_{low} and E_{high} before and after treatment was assessed. To evaluate the performance of Fe(VI) on the removal of As and Mn from S_{As} and S_{Mn} , the effect of Fe(VI) type (wet vs. solid), Fe(VI) dose (14-56 mg/L for As, 2-7 mg/L for Mn), pH_a (5.5 and 6 for As, 5.5 and 6.5 for Mn) and reaction time (0-20 min) was assessed. Then,

another set of experiments was realized for the treatment of S_{As+Mn} under the following conditions: $Fe(VI)_s$ dose (5-28 mg/L) alone, and $Fe(VI)_s$ dose (10, 12.5, 15 mg/L) with the addition of $Fe(III)$ at different doses (6, 8, 10 mg/L). Then, the most performant conditions ($[Fe(VI)]$: 12.5 mg/L, $[Fe(III)]$: 8 mg/L, pH_a : 5.5 and 5 min reaction time) were applied for the treatment of E_{low} and E_{high} . The final step was to evaluate the toxicity of E_{low} and E_{high} before and after $Fe(VI)+Fe(III)$ treatment to *D.magna*. The second step of this work was to assess the stability of As- and Mn-rich sludge produced from the ECG or $Fe(VI)$ treatment of E_{high} . To do so, geochemical modelling by PHREEQC was conducted. The physico-chemical, mineralogical and environmental composition of the sludge was determined. The third part of this project was to do a preliminary techno-economic analysis for ECG and $Fe(VI)$ treatment, mainly depending on energy consumption, electrode cost (for ECG only) and reagents cost. Finally, a comparison between the two treatment performances was done to select the most performant treatment between ECG and $Fe(VI)$ to simultaneously remove As and Mn from neutral mine water.

The results of ECG treatment tests suggest this method as a promising option for the removal of As and Mn. An enhancement of As removal from S_{As} (94%-99%) was noted as CD increased from 0.25 to 1.50 mA/cm², with no change at CD >2 mA/cm². The Mn removal from S_{Mn} was positively correlated (19-98%) with the increase in CD from 0.25 to 10 mA/cm². A significant increase in energy (from 0.007 to 4.36 kWh/m³) and electrode consumption (from 0.017 to 0.700 kg/m³) was observed with the improvement in As and Mn removal as CD increased. The most performant CD values identified were 0.5 mA/cm² for As, and 2 mA/cm² for Mn. The ionic strength (0.25-2.50 mS/cm) did not influence removal efficiency but influenced energy consumption. Maintaining the most performant CD value for As (0.5 mA/cm²) and for Mn (2 mA/cm²) resulted in a three times decrease in required energy (0.101 to 0.032 kWh/m³) for S_{As} , and six-fold decrease for S_{Mn} (0.914 to 0.179 kWh/m³) as the EC changed from 0.25 to 2.50 mS/cm. The ECG simultaneously and efficiently removed As (94–96%) and Mn (59–64%) from S_{As+Mn} , with the same efficiency as for As and Mn at the same CD (0.5 mA/cm² for As from S_{As} , 2 mA/cm² for Mn from S_{Mn}). These findings indicate the absence of antagonistic or synergistic effect between As and Mn during removal. Nevertheless, the efficient removal of As and Mn from S_{As+Mn} required the application of a higher CD (2 mA/cm²) and the volume of the produced wet sludge increased by a factor of 3.3 (16 mL at 0.5 mA/cm² vs. 53 mL at 2.0 mA/cm²). The results further revealed that As was removed faster (20 min) than Mn (60 min) at 2 mA/cm². The removal of As was greater for E_{high} than S_{As+Mn} (99% for E_{high} vs. 96% for S_{As+Mn}). This is attributed to the presence of Ca^{2+} entailing the production of larger Fe-hydroxide flocs in E_{high} , resulting in better adsorption of As on the flocs. An increased oxidation of As(III) in the presence of Cl^- is also likely to occur. Conversely, the removal of Mn was slightly less efficient for E_{high} (57% for E_{high} vs. 61% for S_{As+Mn}) due to potential electrode passivation by SO_4^{2-} . The toxicity evaluation

for E_{low} and E_{high} also suggested that the ECG did not add toxicity or produce toxic by-products.

The Fe(VI) showed promising results for the removal of As and Mn from S_{As} , S_{Mn} , $S_{\text{As+Mn}}$, E_{low} and E_{high} in a one-step treatment, within one minute. Despite the similar removal efficiencies obtained for S_{As} and S_{Mn} using wet (Fe(VI)_w) and solid (Fe(VI)_s) Fe(VI), the latter was selected for the remaining tests, due to the lower residual salinity when using Fe(VI)_s. At a dose of 22 mg Fe(VI)_s/L, at pH_a of 5.5, a nearly complete As removal was achieved (98% removal and [As]_{final}: 0.05 mg/L). A dose of 5 mg Fe(VI)_s/L, at pH_a of 5.5, was required to efficiently remove Mn (99% removal and [Mn]_{final}: 0.15 mg/L) from S_{Mn} . The Fe(VI)_s was also able to efficiently remove As (99%), and Mn (98%) from $S_{\text{As+Mn}}$. Nevertheless, a high dose of Fe(VI)_s (28 mg/L) was required for the simultaneous removal of As and Mn, which may reflect a competition between the two contaminants. Further experiments using a Fe(III) salt as a supporting coagulant showed improved results. The addition of 8 mg Fe(III)/L allowed for decreasing Fe(VI)_s to 12.5 mg/L, while efficiently removing As (99%) and Mn (97%) and decreasing the residual salinity and operating costs. An improvement for Mn removal from E_{high} was observed (99% vs. 97% from $S_{\text{As+Mn}}$), whereas similar removal was observed for As (99%). Finally, the Fe(VI) + Fe(III) treatment of E_{high} , initially acutely toxic, highlighted the possibility of eliminating the toxicity to *D.magna* using the Fe(VI) treatment.

Geochemical calculations performed using PHREEQC suggest that Fe oxides/hydroxides such as ferrihydrite and lepidocrocite are likely to precipitate during ECG and Fe(VI) treatments. These two mineral phases were as well identified by the powder X-ray diffraction (PXRD). The composition of the sludge indicated high water content for both ECG (78%) and Fe(VI) (80%) sludges. The ECG sludge contained higher Fe concentrations (520,000 mg/kg) than the Fe(VI) sludge (340,000 mg/kg). This difference in Fe content is introduced by the higher amount of Fe (133 mg/L) produced from Fe-sacrificial electrode dissolution. The 3.2- and 6.9-times higher concentrations of As and Mn measured in the Fe(VI) sludge in comparison to the ECG sludge could be an evidence for the better removal efficiency by Fe(VI) for Mn and As. The maps (backscattered/X-ray superimposed images) obtained from the SEM-EDS suggest the formation of relatively homogeneous precipitate during the ECG treatment and heterogeneous precipitate with the Fe(VI) treatment. The elemental analyses by EDS suggest that O and Fe are the main chemical species in the ECG and Fe(VI) sludges, consistent with geochemical calculations and PXRD analyses. The As fractionation, using a sequential extraction procedure, in the Fe(VI) sludge suggest that 97% of As is bound to the poorly crystalline Fe-(oxy-)hydroxides, while a 71% fraction was evaluated for the ECG sludge. These results suggest that the adsorption of As onto the Fe-(oxy)hydroxides surfaces is one of the As immobilization processes during ECG and Fe(VI). The field leaching test (FLT) results have shown that the As and Mn were

efficiently immobilized in the sludge at near-neutral pH. Very low amounts (< 0.1% of total amount) of As, Mn and Fe were leached from both sludges.

Overall, the results of this study provide new insights into the potential application of ECG and Fe(VI) for treating As- and Mn-contaminated mine water. In addition, the chemical, mineralogical and environmental characterization of the post-treatment sludges has contributed to filling the gaps on the composition and stability of the sludges, as well as the retention mechanisms of the targeted elements. Further studies will have to focus on evaluating the long-term sludge stability under conditions commonly encountered on mine sites.

Keywords: Advanced oxidation processes, metal(loid)s removal, toxicity, sludge stability, contaminated neutral mine water.

RÉSUMÉ

Les eaux minières neutres contaminées provenant de gisements d'or à faible teneur contiennent souvent des contaminants tels que l'As et le Mn. Même à de faibles concentrations, ces contaminants peuvent avoir des effets néfastes sur la santé humaine et l'environnement. Plusieurs méthodes de traitement telles que la co-précipitation chimique, la précipitation par oxydation et la neutralisation ont été étudiées pour enlever l'As et le Mn des eaux minières. Néanmoins, ces approches souffrent de limitations majeures liées notamment à la quantité de réactifs nécessaires, au pH et aux différents ratios Fe/contaminants requis. Ces limitations sont particulièrement difficiles à surmonter lorsque le traitement vise l'enlèvement simultané de l'As et du Mn. Ces défis soulignent la nécessité d'explorer de nouvelles méthodes de traitement de l'As-Mn des eaux minières. En ce sens, l'électrocoagulation (ECG) et le traitement par les ferrates (Fe(VI)) représentent des options prometteuses. Bien qu'il ait été prouvé que l'ECG et le Fe(VI) enlèvent efficacement l'As et le Mn des effluents synthétiques et réels, des lacunes importantes liées à (1) l'applicabilité de l'ECG et du Fe(VI) pour l'enlèvement simultané de l'As et du Mn des eaux minières contaminées ; (2) l'identification des conditions de traitement les plus performantes ; (3) l'évaluation de la toxicité après traitement par ECG et Fe(VI) des eaux minières contaminées par l'As et le Mn et (4) l'évaluation de la stabilité des boues générées. Dans ce contexte, cette étude visait à : (1) évaluer les performances (i.e. efficacité d'enlèvement, salinité résiduelle, toxicité, stabilité des boues et coûts d'exploitation) de l'ECG ou du Fe(VI) pour l'enlèvement simultané de l'As et du Mn présents dans des eaux minières contaminées, (2) étudier l'effet des conditions opératoires sur les performances du traitement, (3) évaluer la toxicité pour *D. magna* avant et après le traitement et (4) caractériser les boues produites et évaluer la mobilité potentielle de l'As et du Mn.

Pour atteindre les objectifs de l'étude, l'approche méthodologique adaptée a consisté à évaluer les performances de l'ECG ou du Fe(VI) pour l'enlèvement de l'As et du Mn des effluents synthétiques (S_{As} , S_{Mn} , S_{As+Mn}), et des eaux de mine de substitution (E_{low} et E_{high}). Pour le traitement ECG, deux séries d'expériences ont été réalisées pour évaluer l'effet des paramètres opératoires sélectionnés : i) densité de courant (DC; 0,25-10 mA/cm²) à 1,5 mS/cm, ii) conductivité électrique (CE; 0,25-2,5 mS/cm) à 0,5 mA/cm² pour As et 2 mA/cm² pour Mn, sur l'enlèvement de l'As et du Mn présents dans S_{As} et S_{Mn} . Ensuite, une autre série d'expériences a été réalisée pour le traitement de S_{As+Mn} à différentes DC (0,5 et 2 mA/cm²), et CE (0,25 et 2,5 mS/cm). L'effet du temps de rétention a également été évalué pour S_{As+Mn} . Par la suite, les conditions les plus performantes (DC : 2 mA/cm², CE : 2,5 mS/cm, temps : 1 h, D : 10 mm) ont été utilisées pour le traitement de E_{low} et E_{high} . Enfin, l'évaluation de la toxicité sur *D. magna* de E_{low} et E_{high} avant et après traitement a été réalisée. Pour évaluer les performances du Fe(VI), l'effet du type de Fe(VI) (humide ou solide), la

dose de Fe(VI) (14-56 mg/L pour As, 2-7 mg/L pour Mn), le pH_a (5,5 et 6 pour As, 5,5 et 6,5 pour Mn) et le temps de réaction (0-20 min) ont été évalués sur l'efficacité d'enlèvement de As et de Mn présents dans S_{As} et S_{Mn} . Ensuite, une autre série d'expériences a été réalisée pour le traitement de S_{As+Mn} dans les conditions suivantes : dose de Fe(VI)_s (5-28 mg/L) seul, et dose de Fe(VI)_s (10; 12,5 et 15 mg/L) avec ajout de Fe(III) à différentes doses (6; 8 et 10 mg/L). Ensuite, les conditions les plus performantes ([Fe(VI)_s] : 12,5 mg/L, [Fe(III)] : 8 mg/L, pH_a : 5,5 et temps de réaction de 5 min), ont été appliquées pour le traitement de E_{low} et de E_{high} . La dernière étape consistait à évaluer la toxicité sur *D.magna* de E_{low} et de E_{high} avant et après le traitement avec Fe(VI) + Fe(III). La deuxième étape de ce travail a consisté à évaluer la stabilité des boues riches en As et en Mn produites à partir du traitement par ECG ou Fe(VI) de E_{high} . Pour ce faire, une modélisation géochimique par PHREEQC a été réalisée. La composition physico-chimique, minéralogique et géo-environnementale des boues a été caractérisée. La troisième partie de ce projet consistait à réaliser une analyse technico-économique préliminaire des traitements par ECG et Fe(VI), en considérant principalement la consommation d'énergie, le coût des électrodes (pour ECG uniquement) et le coût des réactifs. Enfin, une comparaison entre les performances des deux traitements a été réalisée afin de sélectionner le traitement le plus performant entre ECG et Fe(VI) pour l'enlèvement simultané de l'As et du Mn présents dans les eaux minières neutres.

Les résultats des essais de traitement par ECG suggèrent que cette méthode représente une option prometteuse pour l'enlèvement simultané de l'As et du Mn. Une amélioration de l'enlèvement de l'As présent dans S_{As} (94-99%) a été notée lorsque la DC a été augmentée de 0,25 à 1,50 mA/cm², sans changement additionnel à DC > 2 mA/cm². L'enlèvement du Mn présent dans S_{Mn} était positivement corrélé (19%-98%) avec l'augmentation de la DC de 0,25 à 10 mA/cm². Une augmentation significative de l'énergie (de 0,007 à 4,36 kWh/m³) et de la consommation de l'électrode sacrificielle en Fe (de 0,017 à 0,700 kg/m³) a été observée avec l'amélioration de l'enlèvement de l'As et du Mn au fur et à mesure de l'augmentation de la DC. Les valeurs de DC les plus performantes identifiées étaient de 0,5 mA/cm² pour l'As et de 2 mA/cm² pour le Mn. La force ionique (0,25-2,50 mS/cm) n'a pas influencé l'efficacité du traitement mais a impacté la consommation d'énergie. Le maintien de la valeur de DC la plus performante pour l'As (0,5 mA/cm²) et pour le Mn (2 mA/cm²) a permis de diviser par trois la quantité d'énergie requise (de 0,101 à 0,032 kWh/m³) pour le traitement de S_{As} , et par six pour le traitement de S_{Mn} (de 0,914 à 0,179 kWh/m³) lorsque la conductivité électrique augmente de 0,25 à 2,50 mS/cm. L'ECG a permis d'enlever simultanément et efficacement l'As (94-96%) et le Mn (59-64%) de S_{As+Mn} , avec la même efficacité que pour l'As et le Mn à la même DC (0,5 mA/cm² pour As présent dans S_{As} , 2 mA/cm² pour Mn présent dans S_{Mn}). Ces résultats indiquent l'absence d'effet antagoniste ou synergique entre As et Mn lors de leur enlèvement à partir des effluents synthétiques. Néanmoins, l'enlèvement efficace de l'As et du Mn à

partir de S_{As+Mn} a nécessité l'application d'une DC plus élevée (2 mA/cm²) et le volume des boues produites a augmenté d'un facteur 3,3 (16 mL à 0,5 mA/cm² contre 53 mL à 2,0 mA/cm²). Les résultats ont également révélé que l'As était enlevé plus rapidement (20 min) que le Mn (60 min) à 2 mA/cm². L'enlèvement de l'As était plus important pour E_{high} que pour S_{As+Mn} (99% pour E_{high} contre 96% pour S_{As+Mn}). Ceci est attribué à la présence d'ions Ca^{2+} entraînant la production de floccs d'hydroxydes de fer plus importants dans E_{high} , ce qui entraîne une meilleure adsorption de l'As sur les floccs. Une oxydation accrue de l'As(III) en présence de Cl^- est également probable. À l'inverse, l'enlèvement du Mn était légèrement moins efficace pour E_{high} (57% pour E_{high} contre 61% pour S_{As+Mn}) en raison de la potentielle passivation de l'électrode par les ions SO_4^{2-} . L'évaluation de la toxicité pour E_{low} et E_{high} a suggéré que l'ECG n'ajoutait pas de toxicité ou ne produisait pas de sous-produits toxiques.

Le traitement par Fe(VI) a donné des résultats prometteurs pour l'enlèvement de l'As et du Mn présents dans S_{As} , S_{Mn} et S_{As+Mn} , E_{low} et E_{high} en une seule étape de traitement, en l'espace d'une minute. Malgré les efficacités d'enlèvement similaires obtenues pour S_{As} et S_{Mn} en utilisant les ferrates liquides (Fe(VI)_w) et solides (Fe(VI)_s), ce dernier a été sélectionné pour les tests restants, en raison de la salinité résiduelle plus faible lors de l'utilisation du Fe(VI)_s. À une dose de 22 mg de Fe(VI)/L avec un pH_a de 5,5, un enlèvement presque complet de l'As a été obtenu (98% d'enlèvement et $[As]_{final}$: 0,05 mg/L). Une dose de 5 mg Fe(VI)/L à un pH_a de 5,5 a été nécessaire pour enlever efficacement le Mn (99% d'enlèvement $[Mn]_{final}$: 0,15 mg/L) de S_{Mn} . Le Fe(VI)_s a également été capable de traiter efficacement l'As (99 %) et le Mn (98 %) de S_{As+Mn} . Néanmoins, une dose élevée de Fe(VI) (28 mg/L) a été nécessaire pour le traitement simultané, ce qui peut refléter une compétition entre les deux contaminants. D'autres expériences utilisant un sel de Fe(III) comme coagulant complémentaire ont donné de meilleurs résultats. L'ajout de 8 mg de Fe(III)/L a permis de réduire le Fe(VI)_s à 12,5 mg/L, tout en enlevant efficacement l'As (99%) et le Mn (97%) et en diminuant la salinité résiduelle et les coûts d'exploitation. Une amélioration de l'enlèvement du Mn à partir de E_{high} a été observée (99% contre 97% à partir de S_{As+Mn}), tandis qu'un enlèvement similaire a été observé pour l'As (99%). Enfin, le traitement au Fe(VI) + Fe(III) de E_{high} , initialement très toxique, a mis en évidence la possibilité d'éliminer la toxicité pour *D.magna* en utilisant le traitement au Fe(VI).

Les calculs géochimiques effectués à l'aide de PHREEQC suggèrent que des oxydes/hydroxydes de Fe tels que la ferrihydrite et la lépidocrocite sont susceptibles de précipiter au cours des traitements à l'ECG et au Fe(VI). Ces deux phases minérales ont également été identifiées par diffraction des rayons X sur poudre (PXRD). La composition des boues a indiqué une teneur élevée en eau pour les boues provenant du traitement par ECG (78%) et Fe(VI) (80%). La boue ECG contenait des concentrations de Fe plus élevées (520 000 mg/kg) que la boue Fe(VI) (340 000 mg/kg). Cette différence de teneur en Fe est due à la plus grande quantité de Fe (133 mg/L) produite

par la dissolution sacrificielle de l'électrode lors du traitement par ECG. Les concentrations d'As et de Mn 3,2 et 6,9 fois plus élevées mesurées dans les boues Fe(VI) par rapport aux boues ECG pourraient être une preuve de la meilleure efficacité d'enlèvement lors du traitement par Fe(VI) pour le Mn et l'As. Les cartes (images superposées rétrodiffusées/rayons X) obtenues à partir du MEB-EDS suggèrent la formation d'un précipité relativement homogène pour le traitement ECG et d'un précipité hétérogène avec le traitement au Fe(VI). Les analyses élémentaires par EDS suggèrent que O et Fe sont les principales espèces chimiques présentes dans les boues ECG et Fe(VI), ce qui est cohérent avec les calculs géochimiques et les analyses PXRD. Le fractionnement de l'As, déterminé à l'aide d'une extraction séquentielle, dans les boues de Fe(VI) suggère que 97% de l'As est lié aux oxyhydroxydes de Fe faiblement cristallins, alors qu'une fraction de 71% a été évaluée pour les boues ECG. Cela suggère que l'adsorption de l'As sur les surfaces d'oxyhydroxydes de Fe est l'un des processus d'immobilisation de l'As pendant l'ECG et le Fe(VI). Les résultats du test de lixiviation (FLT) ont montré que l'As et le Mn étaient efficacement immobilisés dans les boues à un pH presque neutre. De très faibles quantités (< 0,1% de la quantité totale) d'As, de Mn et de Fe ont été lessivées des deux boues.

Dans l'ensemble, les résultats de cette étude donnent un nouvel aperçu de l'applicabilité potentielle de l'ECG et du Fe(VI) pour le traitement des eaux minières faiblement contaminées. En outre, la caractérisation chimique, minéralogique et environnementale des boues de post-traitement a contribué à combler les lacunes concernant la composition et la stabilité des boues, ainsi que les mécanismes de rétention des éléments ciblés. D'autres études devront se concentrer sur l'évaluation de la stabilité à long terme des boues dans les conditions couramment rencontrées sur les sites miniers.

Mots-clés: Procédés d'oxydation avancés, traitement des métaux et métalloïdes, toxicité, stabilité des boues, eaux minières neutres contaminées.

CHAPTER 1

GENERAL INTRODUCTION

1.1 Context of the study

The mining industry is an important contributor to the economic growth of many countries including Canada, providing raw materials that are essential for our modern society (QMA, 2019). However, mineral extraction and processing produce large quantities of solid waste (e.g., waste rock, tailings) and contaminated mine water (mine drainage and contaminated mine effluents), that can result in socio-environmental impacts (Nordstrom et al., 2015). As a result, responsible management of contaminated mine water is deemed a challenge faced by the mining industry and governments.

Depending on the mineralogy of the deposit and the type of mining activities (e.g., excavation, ore transport and processing) and water management strategies (e.g., mixing of effluents), the quality of mine water is quite variable in terms of pH, sulfate and metal(loid)s contents from one mine site to another as well as the challenges related to the performant removal of these contaminants. Over the last years, contaminants of emerging concern (CECs) have raised serious concerns because of their complex and evolving chemistry, their persistence, and their toxicity to humans and the surrounding ecosystems (Neculita et al., 2018). In contaminated mine water, CECs could be classified into four categories: (1) new contaminants (e.g., Mn, Se); (2) contaminants that are persistent and difficult to treat (e.g., salinity); (3) common contaminants (e.g., As, Cu), but for which discharge standards are very low in sensitive

environments, especially in cold climates; and (4) N-based contaminants (e.g., ammonia, nitrites, nitrates) for which aquatic toxicity-based discharge criteria are upcoming (Neculita et al., 2018, 2019, 2020; Ryskie et al., 2021). A graphical definition of CECs based on scientific knowledge and actual regulations of different substances found in mine water is represented in Figure 1.1.

Appropriate management of contaminated mine water is required to meet the regulations in terms of physicochemical and toxicological parameters. The treatment of CECs is challenging because of (1) their complex chemistry; (2) insufficient knowledge of the effect of other contaminants from various sources (mixed contamination) on the efficiency of treatment processes; (3) the toxicity of final effluent related to residual salinity of treated water (Neculita et al., 2018) and (4) few information available on the sludge stability and adequate management.

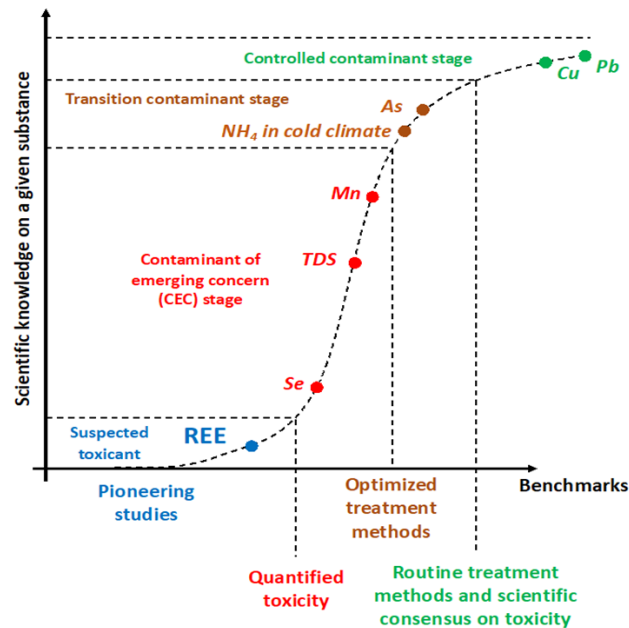


Figure 1.1 Definition of CECs based on scientific knowledge and actual regulations of different substances in mine water. REE: Rare earth elements; TDS: Total dissolved solids (Ryskie et al., 2021)

Several technologies exist for the treatment of contaminated mine water, including physicochemical, biological, and electrochemical processes (Bejan and Bunce; 2015; Ericsson and Hallmans, 1996; Johnson and Hallberg, 2005; Kuyucak et al., 2001; Neculita et al., 2007). Emerging technologies including electrocoagulation (ECG) and advanced oxidation processes (i.e., ferrates – Fe(VI)) have been developed to improve the removal of CECs from contaminated effluents, but research efforts are still needed to better understand the operating factors influencing treatment performances and extend their application to other contaminants.

1.2 Selection of the CECs studied in the present work

The present study focuses on the removal of As (transition CEC stage – Figure 1.1), and Mn (CEC stage – Figure 1.1) from lightly contaminated mine water. These contaminants are targeted due to (1) their increasing concentrations in mine-impacted and natural waters as a result of the growing exploitation of low-grade gold deposits; (2) the evolving regulation in mine/potable water; and (3) the dependency of their removal from contaminated effluents towards Eh-pH conditions and the presence of Fe, another well-known contaminant in mine water.

Recently, As and Mn are gaining more attention in several countries around the world due to their frequent co-occurrence in mine water as well as surface and groundwaters (Table 2.1). Arsenic and manganese mobilization from geogenic sources leads to natural contamination of surface (up to 0.147 mg As/L and up to 209 mg Mn/L) and groundwater (up to 1.34 mg As/L and up to 7.50 mg Mn/L) (Bondu et al., 2020; Buschmann et al., 2007). The growing mining activities associated to the exploitation of low-grade deposits, which often causes the dissolution of As- and Mn-bearing minerals and rocks (e.g., arsenates, arsenites or As sulfides; oxides and carbonates of

Mn) lead to an increase of As and Mn concentrations in the environment (Coudert et al., 2020; Neculita and Rosa, 2019). These natural (geogenic) and anthropogenic contamination raise significant health concerns, especially in areas where the population rely on private groundwater wells for drinking water supply, as is the case in many rural areas of southern Quebec (Bondu et al., 2020).

Based on their potential detrimental impacts on the environment and human health as well as the growing demand for safe supply of drinking water, the regulations and guidelines related to the maximum allowable concentrations (MAC) of both As and Mn in drinking water and in mine water are evolving (Table 1.1). Due to its non-biodegradability and bio-cumulative character, a progressive decrease in the MAC from 0.05 to 0.01 mg/L has been observed for As in drinking water since 1993 (McBeath et al., 2021; Pires et al., 2015; Smedley and Kinniburgh, 2002). For a long time, Mn was typically evaluated based on aesthetic issues as high concentrations may affect the colour and deteriorate the taste of water. Recently, Health Canada set a MAC of 0.12 mg/L in drinking water, based on its neurological effects particularly on sensitive population groups such as infants (Health Canada, 2016; Hu et al., 2019).

To protect aquatic life, a guideline has been proposed by the Ministry of Environment, Lands and Parks in British Columbia (Canada) for surface waters depending on its hardness. These regulated concentrations range from 0.6 to 1.9 mg Mn/L at a hardness increase from 0 to 325 mg CaCO₃/L (Reimer, 1999). Evolving quality criteria in respect to CECs including As and Mn are applied in some countries prior to the release of final mine effluents to limit the potential impacts of mining activities on the receiving environments. Based on the Metal and Diamond Mining Effluent Regulations (MDMER) in Canada, the Maximum Authorized Monthly Mean Concentration (MAMMC) is fixed at 0.3 mg As/L for mine sites in operation and at 0.1 mg As/L for mine sites starting their activities after June 1, 2021 (Ministry of Justice, 2021). In the province of Quebec, the MAMMC determined in the Directive 019 (D019) decreased from 1 mg/L in 1989 to 0.2 mg/L in 2012 (Directive 019, 2012). Manganese

concentration in final mine effluents is not yet regulated in both MDMER and D019, despite of its potential toxicity even at low concentrations (100 µg/L) (Ministry of Justice, 2015; Ying et al., 2017). However, a standard regulation of 2 mg/L was enforced for Mn in 1985 in the United States for mine water discharge (Code of Federal Regulations (CFR), 1985).

Table 1.1 Regulation evolution for As and Mn in Canada and around the world in drinking and mine-impacted water

Contaminant	Targeted water type	Regulation/guideline (mg/L)	Reference
As	Drinking water	MCL: 0.05	WHO (1993)
		MCL: 0.01	USEPA (2006); Health Canada (2006); WHO (2011)
	Mine effluent	MAMMC: 1	D019 (1989)
		MAMMC: 0.4	D019 (2005)
		MAMMC: 0.2	D019 (2012)
		MAMMC: 0.5	Ministry of Justice (1975)
		MAMMC: 0.3	Ministry of Justice (2019)
MAMMC: 0.1	Ministry of Justice (2021)		
Mn	Drinking water	SMCL: 0.05	USEPA (2018)
		MCL: 0.12	Health Canada (2016)
	Mine effluent	2	US CFR (1985)

D019: Directive 019; MCL: Maximum Contaminant Level; SMCL: Secondary Maximum Contaminant Level; WHO: World Health Organization; USEPA: United States Environmental Protection Agency; MAMMC: Maximum Authorized Monthly Mean Concentration

To comply with the evolvingly stringent regulations imposed on As and Mn concentrations in mine water, their treatment prior discharge to the environment is necessary. Treatment of As usually involves its chemical co-precipitation with Fe(III) at pH 4-7 (Coudert et al., 2020; MEND, 2014), while Mn(II) removal requires its oxidation to Mn(IV) prior to its precipitation as Mn-oxides at pH 9-10 (Chang et al., 006; Neculita and Rosa, 2019). Simultaneous and efficient removal of As and Mn

from mine water is still quite challenging due to the large amounts of chemicals required (addition of residual salinity and potential associated toxicity) as well as the differing pH-Eh conditions and Fe/contaminant ratio ($\text{Fe/As} > 4$ vs. $\text{Fe/Mn} < 4$) required.

1.3 Knowledge gaps and originality

Previous studies have demonstrated the efficiency of ECG and Fe(VI) for the removal of As or Mn from synthetic effluents (Gilhotra et al., 2018; Goodwill et al., 2016; Prucek et al., 2013; Shahreza et al., 2018; Wang et al., 2020), groundwater (Müller et al., 2021) and, to a lesser extent, mine water (Del Ángel et al., 2014; Nariyan et al., 2017; Reátegui-Romero et al., 2018) with variable concentrations (from few $\mu\text{g/L}$ to more than 100 mg/L). Despite promising As and Mn removal efficiencies, the performances of ECG and Fe(VI) to simultaneously remove As and Mn from lightly contaminated mine water are still poorly documented. Moreover, only few studies focused on the range of concentrations targeted in the present study for the treatment of lightly contaminated mine water ($< 10 \text{ mg/L}$). The associated residual toxicity of final effluents as well as the long-term stability of the produced sludge, which are crucial parameters to consider for the evaluation of the performances of treatment processes, remains poorly understood and evaluated. In addition, very few studies attempted to simultaneously remove As and Mn from mine water, despite their frequent co-occurrence. Hence, the main originality of this study was to compare the performances of ECG or Fe(VI) for the simultaneous removal of As and Mn from low contaminated synthetic effluents (solutions) and surrogate mine water at different selected operating parameters. The integration of As and Mn removal efficiencies, residual salinity, acute toxicity, sludge stability and operating costs to identify the most performant operating conditions to remove at the same time As and Mn by ECG or

Fe(VI) has never been used in previous studies. The assessment of acute toxicity of As- and Mn-contaminated mine water after treatment by ECG or Fe(VI) has not been previously reported in the literature and therefore represents an innovative contribution of this thesis. The assessment of the stability of the sludge is original as only few studies documented the potential leaching of both contaminants from the sludge with time.

1.4 Hypotheses and Objectives

1.4.1 Hypotheses

The hypotheses (H) that can be formulated based on the literature are the following,

- H1) The simultaneous removal of As and Mn from lightly contaminated mine water will result in the increase of CD for ECG and Fe(VI) dose for Fe(VI), as well as in the retention time to achieve satisfactory removal efficiencies compared to effluents containing only As or Mn;
- H2) The presence of competing ions commonly found in real mine water will negatively impact the performance of treatment processes, especially when using ECG;
- H3) The treatment of As and Mn from lightly contaminated mine water (<10 mg/L) is more performant (better contaminant removal efficiencies, shorter reaction times, and lower amounts of sludge produced and residual salinity of treated water) when using Fe(VI) than when using ECG process;

H4) The mobility of As and Mn from the sludge produced by Fe(VI) through incorporation of both contaminants in the structure of Fe-hydroxides nanoparticles is expected to be lower than for ECG.

1.4.2 Objectives

The general objective of the current study was to evaluate and compare the performances of ECG or Fe(VI) to simultaneously and efficiently remove As and Mn from low-contaminated mine water (<10 mg/L), while favoring minimal residual salinity and ensuring long-term stability of the produced sludge.

To realize the general objective, the specific objectives (SO) proposed are the following:

SO1) Evaluate the impact of different operating parameters (e.g., pH, CD, Fe(VI) dose, retention time) on treatment performance of ECG and Fe(VI) to maximize As and Mn removals, while reducing operating costs and residual salinity, this SO will answer to H1;

SO2) Compare the performance of the ECG and Fe(VI) in terms of: (1) efficiencies to remove As and Mn from synthetic vs. surrogate mine water (i.e., presence of competing ions); (2) toxicity of the treated effluent, this SO will answer to H2 and H3;

SO3) Evaluate the stability of the sludge produced from ECG and Fe(VI) treatment to select the favored treatment technology, this SO will answer to H4.

1.4.3 Thesis Structure

The present thesis is composed of eight chapters, three of them are presented in the form of scientific papers published or submitted to journals.

The first chapter presents a general introduction, which covers the context of the study, explains the main reasons for the selection of As and Mn as co-contaminants among the other CECs encountered in mine water. In addition, this chapter includes the originality of this research project, the formulated research hypotheses, as well as the general and the specific objectives.

The second chapter of the thesis is a critical, comprehensive literature review of recent, relevant articles and reviews, subdivided into 6 sections. The first section presents the chemistry of As and Mn, their typical concentrations in natural and mine water, and their toxicity effect on humans and the ecosystem. The second section reviews the conventional treatment technologies that have been applied for As and Mn removal from mine water, and their limitations, specifically for the simultaneous removal of As and Mn. The third and fourth sections present the principle and operating parameters affecting the performance of ECG and Fe(VI) treatments, which were identified as promising alternatives for conventional methods. The fifth section presents relevant information about the toxicity of As- or Mn-contaminated mine effluents. The last section presents the stability of the post-treatment sludge and the different factors that may affect this stability.

The third chapter describes in detail the methodological approach used to achieve the general and specific objectives, including: (i) the preparation and characterization of synthetic and surrogate mine effluent, (ii) the treatability testing using ECG and Fe(VI) to determine the most performant operating conditions, (iii) the assessment of the acute

toxicity to *D. magna* of E_{high} before and after ECG or Fe(VI) treatment, (iv) the evaluation of the stability of As- and Mn-rich sludge from ECG or Fe(VI) treatment and (v) the preliminary techno-economic analysis of ECG and Fe(VI) treatment.

Chapter 4, presented as an article published in Minerals Engineering, discussed the results related to the effect of operating conditions (i.e., CD, EC, retention time) on the performances of ECG treatment for the simultaneous removal of As and Mn from synthetic and surrogate mine effluents.

Chapter 5, presented as an article published in Journal of Environmental and Chemical Engineering, discussed the results related to the effect of operating conditions (i.e., type and dose of Fe(VI), addition of Fe(III) salt, pH_a , retention time) on the performances of Fe(VI) treatment for the simultaneous removal of As and Mn from synthetic and surrogate mine effluents.

Chapter 6, presented as a paper to be submitted to Journal of Cleaner Production, responds to the third SO about the stability of As- and Mn-rich sludge. In this chapter, the ECG- and Fe(VI)-sludge were characterized, and their short-term stability was evaluated through the assessment of potential metal(loid) leaching using static tests.

Chapter 7 presents a general discussion of the results, as well as a comparison between the performances of ECG and Fe(VI), and a preliminary techno-economic evaluation of ECG and Fe(VI) treatments. This chapter responds to the second SO and confirm/infirm all the research hypothesis.

Chapter 8 includes the main conclusions of this thesis based on the results obtained as well as suggested recommendations for future research work.

CHAPTER 2

LITTERATURE REVIEW

2.1 Arsenic and manganese in the environment and mine effluents

Arsenic is a metalloid and a deleterious substance for human, which can be found in both organic and inorganic forms. In natural waters, inorganic forms of As predominate, mainly as arsenite species (As(III)) under reducing environments, or as arsenate species (As(V)) under oxidizing environments (Smedley and Kinniburgh, 2002). Manganese is a transition metal that does not exist in a free form in the environment. Mn has 11 oxidation states but it naturally occurs in seven states (0, +2, +3, +4, +5, +6, and +7) (Pinsino et al., 2012). Among these oxidation states, only three are the most important in natural environments: (1) Mn(II) occurs in dissolved form; (2) Mn(III) is a transition state that exists in both dissolved and solid forms; and (3) Mn(IV) is present in insoluble oxide forms (MnO_x) (Davison, 1993). Different parameters including pH/Eh conditions can affect the speciation and mobility of the metal(loid)s in water. For example, under oxidizing conditions, As is prevalent in the form of H_2AsO_4^- species at low pH (<6.9), while at higher pH, the HAsO_4^{2-} becomes the predominant species (H_3AsO_4^0 and AsO_4^{3-} may be present in extremely acidic and alkaline conditions, respectively). Under reducing conditions and at pH lower than 9.2, the uncharged H_3AsO_3 will prevail (Figure 2.1a) (Prucek et al., 2013; Smedley and Kinniburgh, 2002). For Mn, under low Eh conditions and at pH less than 7, the solubility of Mn-bearing minerals increases, which leads to its reduction and make

Mn(II) the most predominant and stabilized form (Figure 2.1b). At pH greater than 8 and under aerobic conditions, Mn is mainly present as insoluble minerals.

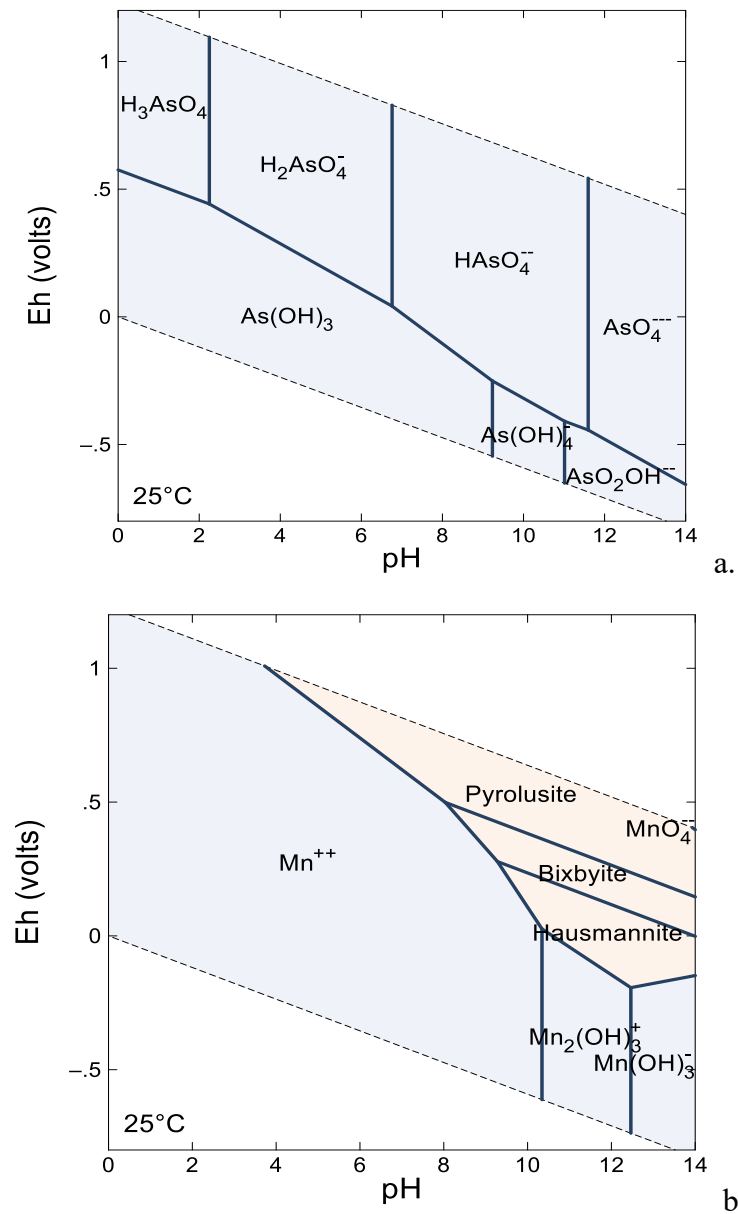


Figure 2.1 Eh-pH mosaic diagram of aqueous As (a) and Mn (b) species in water at 25°C and 1 bar. The activity of As and Mn are 7.356×10^{-6} and 3.636×10^{-8} (Figure constructed using Geochemist's Workbench community software)

Naturally occurring in different minerals, various geogenic and anthropogenic sources could be the cause of the presence of As and Mn in the different environments (i.e., surface water, groundwater, mine effluents) (Table 2.1). Concentrations of As ranging between 0.00001 and 0.147 mg/L (average value of 0.164 mg/L) have been reported in natural surface waters (Flem et al., 2018; Luo et al., 2020), while higher concentrations of Mn have been reported in natural surface water in the vicinity of mine sites with concentrations ranging between 0.0001 and 209 mg/L (average value of 17.7 mg/L) (Flem et al., 2018; Luo et al., 2020).

Variable concentrations of As and Mn have been measured in mine drainage from coal and metal mining, depending on the deposit mineralogy (Coudert et al., 2020; Oncel et al., 2013) (Table 2.1). For example, concentrations of As reaching up to 130 g/L have been measured in acid mine drainage at Svornost mine in Czech Republic (Majzlan et al., 2014). For Mn, concentrations reaching up to 282 mg/L (average: 49 mg/L) were found in mine drainage from different mine sites in the Harz Mountains and the nearby copper shale basins in Mining district St. Andreasberg, Germany (Bozau et al., 2017). Such high concentrations of As and Mn in natural or mine-impacted water can have negative impacts on the surrounding ecosystems, due to their toxic effects.

The toxicity of As and Mn has been widely discussed in the literature (Baig et al., 2016; Bouchard et al., 2006; Choong et al., 2007; Jain and Ali, 2000). Exposure to As has been reported as a cause for cancerous and non-cancerous impacts in both acute and, non-acute forms. For example, an As concentration of 3 µg/L in drinking water has been reported as potentially responsible of bladder and lung cancers (An et al., 2005). Furthermore, several diseases have been linked to As consumption, such as Ischemic heart disease (Hsueh et al., 1998), Blackfoot disease (Tseng et al., 1996), cardiovascular diseases (Wang et al., 2007), and Alzheimer's disease (Çöl et al., 1999). The toxicity of As varies with its forms, with its trivalent state (As(III)) being 60 times more toxic than its pentavalent state (As(V)) (Ratnaike, 2003).

At the same time, Mn is an important nutrient that supports the growth and development of plants, microorganisms, and animals to a certain level. However, above a certain deficiency limit, Mn can cause toxicity in aquatic and terrestrial ecosystems (Neculita and Rosa, 2019). Neurological disorder such as manganism, respiratory, reproductive, and developmental effects are examples of the impacts of inhalation of Mn airborne species. Another documented impact of exposure to Mn in drinking water is the intellectual impairment in school-age children (Bouchard et al., 2011).

Increasing mining of low-grade ore deposits are responsible for the progressive release of As and Mn into the environment (Gomes et al., 2007; Neculita and Rosa, 2019). The amounts of As and Mn released by mining activities depend on the presence of As- and Mn-bearing minerals exposed to weathering and on pH/Eh conditions, as well as microbial activity (Bondu et al., 2017; Neculita and Rosa, 2019). Considering As and Mn prevalence in the natural water due to geogenic or anthropogenic sources and evolving regulation to limit their toxicity to the environment, several technologies have been effectively used to remove these contaminants from contaminated water.

Table 2.1 Typical concentrations, sources and/or cause of As and Mn in groundwater, surface water and mine water worldwide

Location	# of samples	As (mg/L)	Mn (mg/L)	Sources / Causes	References
Groundwater					
California	18	0.011-0.016	0.072-0.106	Not specified	Chang et al. (2006)
Cambodia	131	0.001-1.34 (average: 0.16)	<0.1-3.1 (average: 0.6)	As: sediments / microbially induced reductive dissolution of As-coated iron oxides and MnO ₂ surfaces Mn: sediments / reductive dissolution of Mn oxides	Buschmann et al. (2007)
China	271	<0.0001-0.47	0.0044-4.47	As: sediments / reductive dissolution of Fe hydroxides Mn: sediments / reduction of Mn oxides	Ying et al. (2017)
Peru	57	<0.0005-0.72	0.003-3.69	As: sediments of Andean origin / microbially driven reductive dissolution of Fe-hydroxides Mn: sediments of Andean origin / reductive dissolution of Mn-oxides	de Meyer et al. (2017)
Southern Quebec, Canada	545 (Mn) 51 (As)	<0.001-0.28	<0.0004-7.5	As: sedimentary, hydrothermal rocks / reductive dissolution of As-rich Fe-Mn oxyhydroxides Mn: sedimentary, volcanic rocks / reductive dissolution of Fe-Mn oxyhydroxides	Bondu et al. (2020)
Southeastern Shaoguan, China	10	0.00015 - 0.0047 (average: 0.0011)	0.00063-0.16 (average: 0.0271)	As and Mn: acid mine drainage / mobilization from the mine site affects groundwater sources	Luo et al. (2020)
Surface water					
Southeastern Shaoguan, China	12	0.0009-0.15 (average: 0.0164)	0.007-209 (average: 17.7)	River flowing next to mine site receives acid mine effluents from the tailings pond and run-off from a treatment plant	Luo et al. (2020)
Europe	807	<0.00001-0.027	<0.0001-3.01	Water quality affected by natural and anthropogenic sources	Flem et al. (2018)

Table 2.1 (continued) Typical concentrations, sources and/or causes of As and Mn in groundwater, surface water and mine water worldwide

Location	# of samples	As (mg/L)	Mn (mg/L)	Sources / Causes	References
Mine effluents					
California, USA	180	850	119	Iron mountain mine, acid mine drainage	Nordstrom and Alpers (1999)
Almonaster la Real, SW of Spain	10 samplings (between 2006-2007)	0.3	19	Acid mine drainage	Caraballo et al. (2009)
Pahang, Malaysia	-	1.27	19.9	Abandoned iron mine Sungai Lembing / acid mine drainage	Hatar et al. (2013)
Turkey	-	0.000015	40.6	Coal mine drainage wastewater	Oncel et al. (2013)
Mining district St. Andreasberg, Germany	9	3-199	0.3-282 (average: 49)	Drainage from different ore mines in the Harz Mountains and the nearby copper shale basins	Bozau et al. (2017)
Bokaro coalfield, coal mine, India	15	0.0002-0.0007 (average: 0.0003)	0.0145-0.72 (average: 0.15)	Mine water pollution: natural mineralization; coal mining	Tiwari et al. (2017)

2.2 Technologies available for As and Mn treatment

Various chemical, electrochemical, and biological processes have been developed, and successfully applied to treat metal(oids), including As and Mn from surface, ground and mine water. Conventional methods for As and Mn removal from contaminated water, include coagulation/co-precipitation, filtration (e.g., reverse osmosis), adsorption and ion exchange (Chang et al., 2006; Coudert et al., 2020; Gordon et al., 1989; MEND, 2014; Tobiasson et al., 2016; USEPA, 2002). Coagulation/co-precipitation using ferric salts (e.g., ferric chloride; ferric sulfate) and pH adjustment at pH 4-7 to co-precipitate Fe and As followed by solid/liquid separation (e.g., decantation, microfiltration) is considered as the best available technology economically achievable (BATEA) for the removal of As from slightly ($<20 \mu\text{g/L}$) to highly contaminated mine water ($>500 \text{ mg/L}$) (Chang et al., 2006; Coudert et al., 2020; Inam et al., 2021; MEND, 2014). While initial As concentration seemed to not affect the effectiveness of this treatment process (USEPA, 2003), higher concentrations of As require higher Fe^{3+} doses, increasing the amount of sludge produced as well as residual associated salinity (Inam et al., 2021). The presence of Fe as a critical parameter impacting the efficient removal of As, with a favored Fe/As molar ratio $>4/1$ is well documented (Harris, 2000). Moreover, the removal of As(V) is more efficient than As(III), requiring a pre-oxidation step ($\text{As(III)} \rightarrow \text{As(V)}$) using strong oxidants such as chlorine, ozone and hydrogen peroxide (Eh: 0-0.6 V) prior to its sorption and/or co-precipitation as As(V) (Lee et al., 2003; Sharma et al., 2007). Nevertheless, the application of neutralizing agents (e.g., limestone, hydrated lime) to raise pH around 9-10, and of strong oxidants (e.g., sodium hypochlorite; ozone) to oxidize Mn(II) to Mn(IV) (Eh: 0.5-1 V) and precipitate Mn as Mn(OH)_2 or as MnO_2 is the most straightforward method used for Mn removal from contaminated water (Chang et al., 2006; Gordon et al., 1989). The presence of Fe must be considered during the

precipitation of Mn(IV) as Mn-oxides due to its potential inhibition effect. This phenomenon can be explained by the faster Fe(II) oxidation and precipitation compared to Mn(II). For example, dissolved oxygen and free chlorine quickly oxidize Fe(II) at pH 6.0-8.5, while Mn(II) oxidation is very slow (Tobiason et al., 2016). Due to the pH decrease following Fe precipitation, Mn remains in solution. The pH of the effluent to be treated must be increased to >8.5 to precipitate Mn-oxides. When the solution contains Fe(II), there will be a potential of reductive dissolution of Mn-oxides at Fe/Mn >4/1 (Neculita and Rosa, 2019). Sorption on natural (e.g., red mud, pyrolusite) or modified sorbents (e.g., Fe(III)-impregnated activated carbon, Mn-oxide coated filter) raise attention due to their efficiency (up to 99%) to remove As or Mn from mine water (e.g., As: 0.1-1 mg/L; Mn: 0.1-10 mg/L) (Mondal et al., 2007; Pietrelli et al., 2019).

The simultaneous removal of As and Mn from drinking water (Hu et al., 2019; Pietrelli et al., 2019), groundwater (Bora et al., 2018; McBeath et al., 2021) and mine water (Oncel et al., 2013) is the target of increasing concern. However, studies carried out on the simultaneous removal of As and Mn from mine water are relatively scarce (Safi and Gotoh, 2021). Some of the available methods for the simultaneous removal of As and Mn from different contaminated water are presented in Table 2.2. The treatment of As- and Mn-contaminated water usually requires the application of more than one-step process, such as oxidation using strong oxidizing agent (e.g., potassium permanganate, sodium hypochlorite) followed by coagulation with ferric chloride and adsorption on formed iron hydroxides (Bora et al., 2018; Chang et al., 2006), or adsorption on metal oxides (e.g., Mn-oxides) (Habib et al., 2020) or on natural sorbents (Pietrelli et al., 2019). Despite of the high removal efficiencies (50-99%) using these methods, the requirement of As pre-oxidation due to the higher toxicity and mobility of As(III) towards As(V), and the high pH values (pH >9) required for Mn removal, necessitated the development of treatment methods that provide both oxidation and coagulation in a one-step treatment .

Table 2.2 Available technologies for simultaneous removal of As and Mn from contaminated water

Technology	Targeted Contaminant (mg/L)	Operating parameters	Efficiency (%)	References
Groundwater				
Oxidation (NaOCl)/filtration/coagulation with ferric chloride	Fe: 0.06-0.085; Mn(II): 0.072-0.106; As: 0.011-0.016	Ferric chloride: 0-16 mg/L, pH: 7.89	Mn: 80; As: 69 (6 mg/L ferric chloride dose)	Chang et al. (2006)
Oxidation (KMnO ₄ /coagulation (FeCl ₃ ; Fe ²⁺)/adsorption at optimized pH	Fe(II): 2-23; Mn(II): 0.5-1.9; As(III): 0.025-0.091	pH adjusted: 7.3	Fe, Mn: 99 As: >99	Bora et al. (2018)
Ozonation/Mn greensand filtration/iron-based granular media adsorption	Mn(II): 0.134; As(III): 0.009	pH: 7.3	Mn: 100 As: 68.5	Hu et al. (2019)
Biological treatment	As: 0.023; Mn: 0.08; Fe: 2.9; NH ₄ ⁺ : 2.91 mg-N/L	Not specified	As: >56 Mn, Fe, NH ₄ ⁺ : 98-99	Lytle et al. (2020)
Electrocoagulation (ECG) Electrocoagulation coupled with oxidative media filtration (ECG/OMF)	Mn(II): 0.137; As: 0.009	pH: 7.34 Electrical conductivity (EC): 307 μS/cm	ECG + 5 min flocculation : Mn (II): 27 ECG: As: >80 ECG/OMF: Mn (II) <0.1 mg/L, As: 100	McBeath et al. (2021)
Synthetic water sample/Simulated groundwater				
Adsorption on Fe ³⁺ -impregnated activated carbon	Fe: 2.8; Mn (II): 0.6; As: 0.2	As(V): pH 5-7 As(III): pH 9-11 Mn(II): pH 2-11 Fe: pH 0-14	Fe: 100 Mn: 41 As: 95.5	Mondal et al. (2007)
Adsorption on synthesized Mn-oxide coated filter	Mn(II): 1-10; As(III): 0.3 and Mn(II): 2; As(III): 0.1-1	pH: 7	Mn: 100 As: 63 (with 1 mg/L Mn initially) As: 72 (with 10 mg/L Mn initially)	Habib et al. (2020)
Synthetic water sample/Simulated surface water				
Clarification (polyaluminum chloride, aluminum sulfate as coagulants)/ Chlorine oxidation	Mn(II): 0.12-1.12; As: 0.032-0.157	pH: 7.1 EC: 149.2-158.8 μS/cm; ORP: 427-439 mV	Mn: 77 As: 80-90	Pires et al. (2015)

Table 2.2 (continued) Available technologies for simultaneous removal of As and Mn from contaminated water

Synthetic water sample/Simulated drinking water				
Adsorption on metal oxides or natural sorbents (red mud and pyrolusite)	Mn(II): 2; As(III): 0.1	pH: 8.1	Red mud: Mn: 95.3, As: 99.3	Pietrelli et al. (2019)
Mine drainage				
ECG	As: 0.015 µg/L, Mn: 40.6 Cu, Zn, Mn, Cd, Cr, PO ₄ ³⁻	pH: 2.5	As, Mn: 99.9	Oncel et al. (2013)

ECG and Fe(VI) are examples of such emerging technologies for the removal of As and Mn that combines oxidation and coagulation mechanisms in a single treatment step. The principles and operating parameters that influence the removal of As and Mn from contaminated water using ECG or Fe(VI) are discussed in detail in Sections 2.3 and 2.4, respectively.

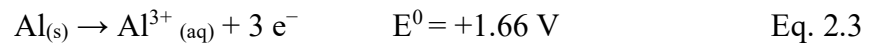
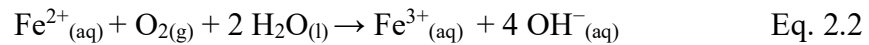
2.3 Electrocoagulation

2.3.1 Principle and design

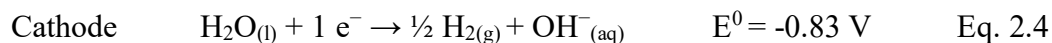
Electrocoagulation (ECG) is a green technology used to remove organic and inorganic contaminants from groundwater, potable water as well as contaminated industrial effluents (e.g., mining), as it combines both electrochemical and coagulation/flocculation treatments (Moussa et al., 2016). Usually, an ECG unit consists of an electrolytic cell equipped with anode(s) and cathode(s) immersed in the solution to be treated and connected externally to a DC power supply. The number of electrodes used depends on the operating conditions and the quality of the effluent to be treated (Emamjomeh and Sivakumar, 2009; Nariyan et al., 2018). Two main electrodes connection configurations, monopolar and bipolar, can be used when using several electrodes (at least four electrodes).

2.3.2 Mechanisms involved in contaminants removal during ECG

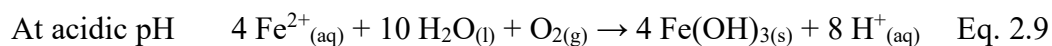
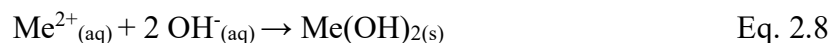
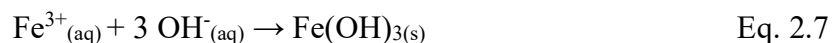
ECG treatment involves redox reactions, leading to the production of metallic cations at the anode, that act as coagulant to remove contaminants, and of OH⁻ ions at the cathode, that neutralize acidity and favor the precipitation of metals as hydroxides. Indeed, metallic cations (e.g., Fe²⁺, Fe³⁺, Al³⁺) are produced *in-situ* by anodic electro-dissolution of the anode material (e.g., Fe, Al), also known as sacrificial electrode (Hakizimana et al., 2017; Oncel et al., 2013). When using Fe as the anode, Fe(0) is oxidized into Fe(II) following the oxidation reaction presented in Equation 2.1 and leading to the anodic dissolution of the sacrificial Fe-electrode. The dissolved Fe(II) is then oxidized into Fe(III) by dissolved oxygen (Equation 2.2). When using Al(0) as the anode, it dissolves to Al(III) following the oxidation reaction described in Equation 2.3.



The cathode electrode undergoes a reduction reaction, generating hydroxyl ions (OH⁻) and hydrogen gas (H₂) bubbles as shown in Equations 2.4 and 2.5, respectively.



Once *in-situ* generated, OH^- will neutralize the acidity of the effluent to be treated and react with Fe^{2+} , Fe^{3+} or Al^{3+} to form intermediate monomeric (e.g., $\text{Fe}(\text{OH})^{2+}$, $\text{Fe}(\text{OH})_2^+$, $\text{Fe}(\text{H}_2\text{O})_4(\text{OH})^{2+}$, $\text{Al}(\text{OH})^{2+}$, $\text{Al}(\text{OH})_2^+$, $\text{Al}(\text{OH})_4^-$) and polymeric species (e.g., $\text{Fe}_2(\text{H}_2\text{O})_8(\text{OH})_2^{4+}$, $\text{Fe}_2(\text{H}_2\text{O})_6(\text{OH})_4^{2+}$, $\text{Al}_2(\text{OH})_2^{4+}$, $\text{Al}_6(\text{OH})_{15}^{3+}$, $\text{Al}_7(\text{OH})_{17}^{4+}$), that have the ability to coagulate with the counter ions in the solution (Garcia-Segura et al., 2017). Oxyhydroxides and polymeric hydroxides formed *in-situ* during ECG were reported as more efficient coagulants than those used in the conventional chemical coagulation (Reátegui- Romero et al., 2018). Finally, all these monomeric and polymeric species will be transformed to $\text{Fe}(\text{OH})_{2(s)}$ or $\text{Fe}(\text{OH})_{3(s)}$ (Equations 2.6-2.7 and 2.9) or to $\text{Al}(\text{OH})_{3(s)}$ (Equation 2.10) (Chen, 2004; Mollah et al., 2001).



Several mechanisms have been reported for the removal of inorganic contaminants including As or Mn from contaminated water by ECG when using Fe- and Al- electrodes as described in Figures 2.2 and 2.3, respectively (Ali et al., 2012; Kobya et al., 2011; Oncel et al., 2013; Shafaei et al., 2010).

The mechanisms involved in the removal of As(III) by ECG can be divided into two groups: i) the oxidation of As(III) to As(V) by the reactive oxidant species (e.g., hydroxyl radical (OH^\bullet), superoxide ($\text{O}_2^{\bullet-}$)); ii) the sorption and/or co-precipitation of As(V) with the produced Fe(III)- or Al(III)-oxyhydroxides (Figures 2.2 and 2.3). At near-neutral pH, As(V) species were reported to sorb onto the surface of $\text{Fe}(\text{OH})_2$ or $\text{Fe}(\text{OH})_3$ and replace the hydroxyl group to produce insoluble complexes such as FeHAsO_4 or $\text{FeAsO}_4 \cdot x\text{H}_2\text{O}$ (Kobyas et al., 2011; Li et al., 2012). In the final step, the flocs settle, and a subsequent sedimentation or filtration process is required to separate As-bearing precipitates from the treated water (Kobyas et al., 2011, Li et al., 2012).

For Mn, the mechanisms involved in its removal by ECG are not fully understood, probably because of a limited number of studies available. A previous study reported that *in situ* produced OH^- react with Mn(II) to form Mn-hydroxides ($\text{Mn}(\text{OH})_{2(s)}$) at $\text{pH} > 7$ as presented in Equation 2.11, leading to the precipitation of Mn (Shafaei et al., 2010). Eventually, the removal of generated Mn-hydroxides can be improved by sorption and/or co-precipitation with the Fe- or Al-hydroxides (Shafaei et al., 2010; Xu et al., 2017). Cathodic deposition of Mn(II) could enhance its removal from the solution, as well as its trapping (sweep coagulation) by the hydroxides formed (Oncel et al., 2013; Shafaei et al., 2010).

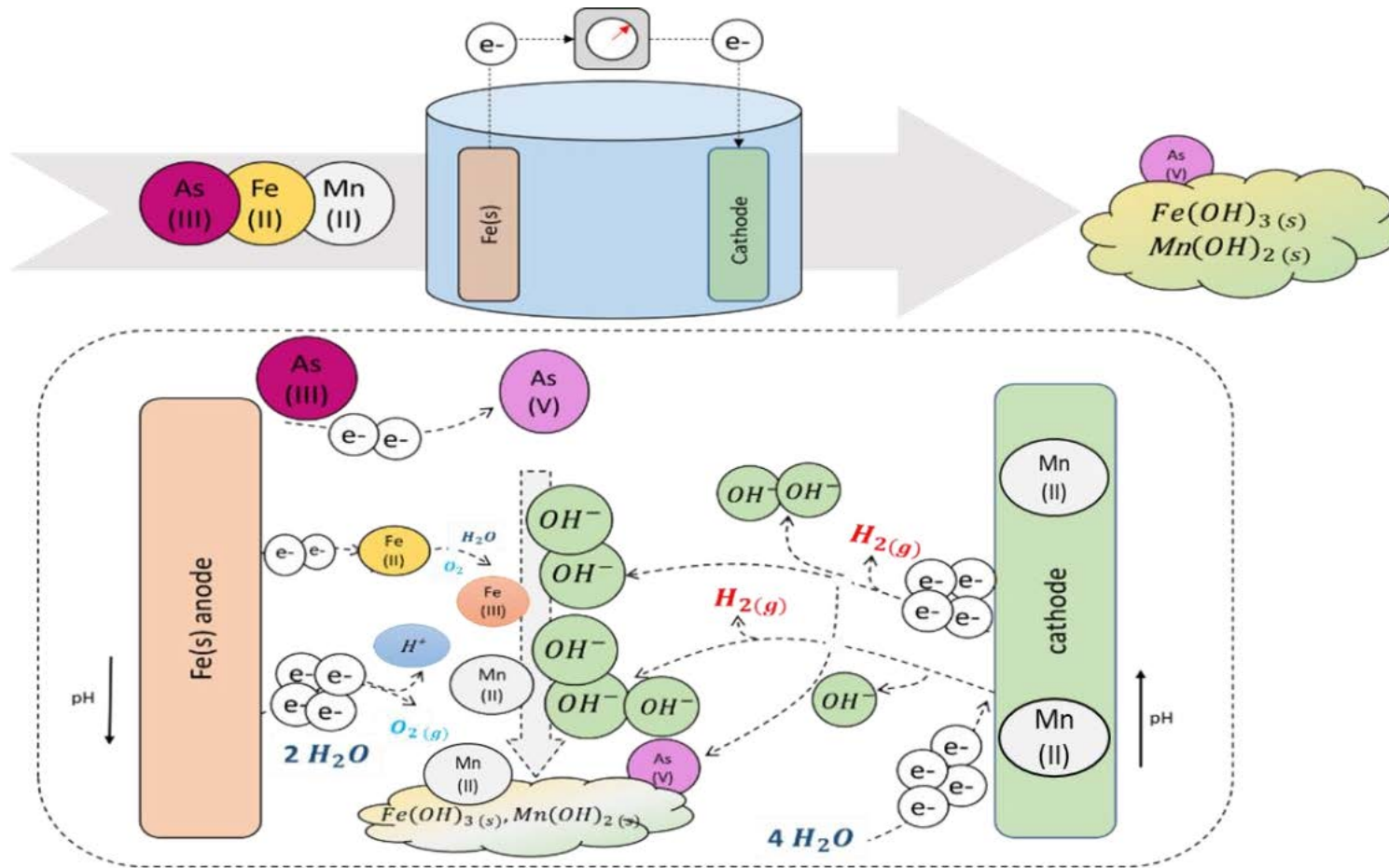


Figure 2.2 A schematic representation of the mechanisms involved in the removal of As and Mn during treatment by ECG using Fe-electrode

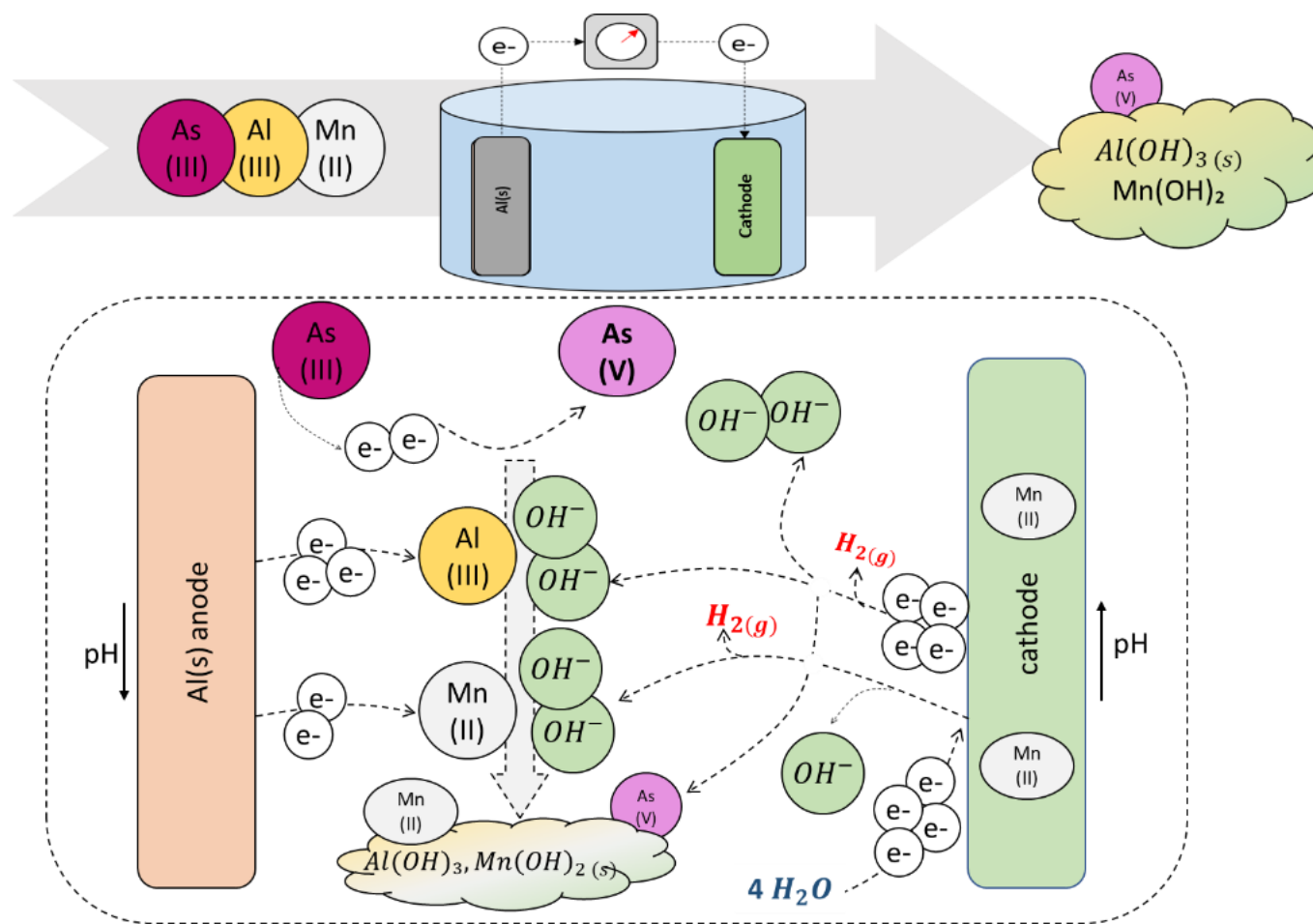


Figure 2.3 A schematic representation of the mechanisms involved in the removal of As and Mn during treatment by ECG using Al-electrode

Moreover, chlorides may further enhance Mn(II) oxidation to Mn(IV) and its subsequent precipitation as MnO₂ (Xu et al., 2017) (more details are provided at Section 2.3.3).



Considering the different mechanisms (e.g., oxidation, coagulation, (co-)precipitation, sorption) involved in the removal of As or Mn from contaminated water, several parameters (e.g., operational, effluent chemistry) can influence the performances of ECG.

2.3.3 Operating parameters influencing the performance of ECG

The performances of the most relevant studies on ECG to remove As and/or Mn from synthetic and real effluents are summarized in Table 2.3. Data show that both operating conditions (e.g., nature and number of electrodes, inter-electrode distance, current density (CD), retention time) and the quality of the effluent to be treated (e.g., initial pH, salinity, presence of anionic species or impurities) can impact the removal of As or Mn from contaminated water. For specific parameters (e.g., pH, nature of electrode), consensus are reached in the literature for the most performant conditions, but not for all. For example, better As removal efficiencies were observed under slightly acidic to neutral conditions, while Mn removal seemed to be more efficient under neutral to slightly alkaline conditions (Balasubramanian et al., 2009; Kobya et al., 2011;

Lakshmanan et al., 2009). From Table 2.3, it can be noticed that satisfactory removal efficiencies (>93%) were obtained for the removal of As and Mn from synthetic or real effluents, no matter the nature of electrodes used (Fe-Fe, Al-Al, Al-Fe, steel). However, most of the studies were performed using Fe- and Al-electrodes. This can be due to the following: i) availability, ii) low cost, iii) high valence of the cations produced from anodic dissolution, iv) low toxicity of Fe-and Al- hydroxides formed by precipitation (Fayad, 2017; Hakizimana et al., 2017; Moussa et al., 2016). In the current study, the discussion is limited to the most relevant operating parameters affecting the ECG performance for the removal of As and Mn from synthetic or surrogate effluents and for which the identification of optimal conditions is not obvious and seems to be dependent on the initial composition of the effluents to be treated or other operating conditions.

- Current density

Current density (CD - expressed in mA/cm²) is defined as the amount of electric current (I in mA) divided by the effective area of the sacrificial anode (S in cm²) (Fayad, 2017). CD is a crucial parameter in ECG, known for controlling the amounts of metallic ions and gas bubbles produced as well as the size and growth of the flocs (Moussa et al., 2016). Optimal CD values reported in the literature varies between 0.2 and 70 mA/cm² (Table 2.3), with respect to water quality and other operational parameters (e.g., configuration, voltage, electrode surface) (Banerji and Chaudhari, 2016; Nariyan et al., 2017). Several studies have reported that an increase in CD increases the dissolution of sacrificial electrodes, resulting in higher amounts of Fe-hydroxide and therefore in better metal(loid) removals (Fayad, 2017). Indeed, an important increase in Mn removal (from 35.8 to 87.9%) has been observed when increasing CD from 1.5 to 9.4 mA/cm² ([Mn(II)];: 100 mg/L, pH;: 7, retention time: 30 min, Al-Al electrodes) (Shafaei et al., 2010). A slight improvement of As removal from slightly contaminated synthetic effluent has been recorded (from 93.5 to 94.1%) with the slight

increase of CD from 0.25 to 0.50 mA/cm² ([As]_i: 0.15 mg/L, pH_i: 6.5, retention time: 12.5 min) (Kobyta et al., 2011). In addition, CD can impact the kinetic of metal(loid)s removal. A faster removal of As (<10 µg/L) has been noticed when increasing CD (150 min needed at 1.72 mA/cm² vs. 180 min needed at 0.86 mA/cm² and 240 min needed at 0.49 mA/cm²) (Müller et al., 2021). However, this increase in CD results in an important increase of energy consumption and therefore, operating costs.

Therefore, a compromise should be found between the removal efficiencies of the targeted contaminants and the economic feasibility of the treatment. Some studies showed that the selection of the best CD may be affected by other operating parameters such as pH or temperature (Moussa et al., 2016).

- Retention time

The retention time plays a key role in the performance of the ECG treatment (Nariyan et al., 2017; 2018). In the literature, the reported retention time for the removal of As and Mn from contaminated water varies from few minutes (5 min) to several hours (2-3 h). As expected, higher contaminant removal efficiencies are observed when increasing the retention time (Oncel et al., 2013). For example, the removal of Mn from a synthetic effluent ([Mn(II)]_i: 100 mg/L, CD: 6.25 mA/cm², pH_i: 7) increases from only 34.1% after 10 min to 94.4% after 60 min (Shafaei et al., 2010). A lower enhancement in As removal (from 93.0 to 97.2%) with increasing retention time from 30 to 60 min was recorded using Al-Al electrodes (Gomes et al., 2007).

Table 2.3 Examples of ECG performances for the removal of As and Mn from synthetic or real effluents

Effluent Type	Targeted contaminants	pH _i / pH _a *	pH _f	Electrodes				Retention time (min)	CD (mA/cm ²)	Efficiency (%)	References
	(mg/L)			Nature	Number	Configuration	D (mm)				
As removal											
Synthetic effluent	As: 1-1000	pH _a : 2.4-10	-	Fe-Fe	2	Vertical	30	60, 120	30.3	99.6	Gomes et al. (2007)
			-	Al-Fe	2	Vertical	30	60	30	78.9-99.6	
			-	Al-Al	2	Vertical	30	120	3	97.8	
Synthetic effluent	As: 50	pH _i : 7	-	Fe-stainless-steel	2	Monopolar	15	55	15	94	Balasubramanian et al. (2009)
Synthetic effluent	As: 0.15	pH _i : 6.5	7.8	Fe-Fe	2	Monopolar	13	7.5	0.5	94.1	Koby et al. (2011)
		pH _i : 7	7.6	Al-Al	2	Monopolar	13	4	0.75	96.5	
Synthetic effluent	As: 2-5	pH _i : 5	-	Al-Fe	2	Monopolar	10	12	3V	99	Ali et al. (2012)
Synthetic effluent	As: 0.5	pH _i : 7	-	Fe-Fe	2	Monopolar	10	180	0.2	90	Banerji and Chaudhari (2016)
Synthetic effluent	As(III): 55-100	pH _i : 5.2	-	Stainless steel	2	-	15	20	2	99.6	Gilhotra et al. (2018)
Synthetic effluent	As(V): 100	-	-	Fe-Fe	2	-	20	120	12	>98	Hansen et al. (2007)

*pH_i: pH initial, pH_a: adjusted at the beginning of the test, **CD is calculated

Table 2.3 (continued) Examples of ECG performances for the removal of As and Mn from synthetic or real effluents

Effluent Type	Targeted contaminants (mg/L)	pH _i / pH _a *	pH _f	Electrodes				Retention time (min)	CD (mA/cm ²)	Efficiency (%)	References
				Nature	Number	Configuration	D (mm)				
Synthetic effluent	As(III): 50	pH _a : 4	-	Fe-Fe	12	Vertical	50	45	0.54	99.5	Can et al. (2014)
Synthetic effluent	As(III): 25	pH _a : 6.5-7	-	Mild steel	12	-	2	40	5.2	99	Lakshmipathiraj et al. (2010)
Groundwater	As: 2.86	pH _i : 2.86	6.36 (without air injection) 8.3 (with air injection)	Fe-Fe	2	Monopolar	6	1.5	4.6	95.54 >99	Parga et al. (2005)
Abandoned mine drainage	As: 0.024 SO ₄ ²⁻ : 3567	pH _a : 7	-	Al-Al	3 anodes 4 cathodes	Monopolar	6	15	4	As: 93 SO ₄ ²⁻ : 53	Del Ángel et al. (2014)
Groundwater samples	As: 3.25-14.6	pH _i : 6.8-7.4	-	Steel plates	4	Monopolar parallel	10; 20	60; 180; 40	0.35; 0.86; 1.72	>99.9	Müller et al. (2021)

*pH_i: pH initial, pH_a: adjusted at the beginning of the test, **CD is calculated

Table 2.3 (continued) Examples of ECG performances for the removal of As and Mn from synthetic or real effluents

Effluent Type	Targeted contaminants (mg/L)	pH _i /pH _a *	pH _f	Electrodes				Retention time (min)	Current density (mA/cm ²)	Efficiency (%)	References
				Nature	Number	Configuration	Distance (mm)				
Mn removal											
Synthetic effluent	Mn: 100	pH _a : 7	6.97	Al-Al	2	Monopolar	10	30	6.25	80	Shafaei et al. (2010)
Synthetic effluent	Mn: 360	pH _a : 9		Al-Al	2	parallel	20	195	-	92	Shahreza et al. (2018)
Real mine effluent	Mn: 8.34; Fe: 25.1	pH _i : 6.62	-	Fe-Fe	7	Vertical	30	45	2.23	Mn: 99.7; Fe: 99.2	Reátegui-Romero et al. (2018)
Real mine effluent	Mn: 49; Fe: 770; SO ₄ ²⁻ : 13000	pH _i : 2.68	-	Fe, Al-stainless steel	2	Monopolar	5	60	70	Mn: 23.4; Fe: 74.9; SO ₄ ²⁻ : 7.9; (Fe-steel); Mn neglectable (low pH); Fe: 67.9; SO ₄ ²⁻ : 13.9 (Al-steel)	Nariyan et al. (2017)
Real industrial wastewater	Mn: 5; Cu: 5; Zn: 10	pH _i : 6	7.87	Fe-Fe	2	Vertical	20 or 40	90	42**	Mn: 94 (20 mm); 73 (40 mm)	Gatsios et al. (2015)
			6.65	Al-Fe	2	Vertical	20 or 40	90	42**	Mn: 69 (20 mm); 76 (40 mm)	

* pH_i: pH initial, pH_a: adjusted at the beginning of the test, **CD is calculated

- Inter-electrode distance

Another important parameter to consider in an ECG system is the distance between the anode and the cathode, as called inter-electrode distance (D). Inter-electrode distance is a controlling parameter in ECG because it can affect contaminant removal efficiencies and ECG cell size, the consumption of energy and, as a result, the operating costs (Sahu et al., 2014). Ohmic drop (IR), which is the potential drop due to the resistivity of the solution, is directly proportional to the D (Equation 2.12). The decrease of D was reported to lead to a decrease of the ohmic drop, of the electrical power required (Equation 2.13) and the associated OPEX.

$$IR = I \times D / S \times K \quad \text{Eq. 2.12}$$

$$P = U \times I = I \times R^2 \quad \text{Eq. 2.13}$$

where, IR is the solution resistance or the ohmic drop (Ω), I is the current intensity (A), D is the inter-electrode distance (m), S is the active electrode surface area (m^2), K is the solution conductivity (mS/m), P is the electric power (W) and U is the voltage (V).

Several studies showed that higher contaminant removal efficiencies are obtained for smaller D (Gatsios et al., 2015; Thella et al., 2008). Inter-electrode distance of 5-30 mm has been reported in the literature for the removal of As or Mn from synthetic and real effluents (Table 2.3). The impact of D on the removal of As from a synthetic effluent ([As]_i: 15 mg/L, pH_i: 4, CD: 7.5 mA/cm², reaction time: 30 min) using Fe-Fe electrodes was evaluated. A small decrease of As removal efficiency (from 100 to 94.6%) was reported when increasing D from 10 to 40 mm (Thella et al., 2008). The difference observed in removal efficiency could be attributed to the lower movement of ions and

electrons between electrodes when increasing D (Sahu et al., 2014). However, a recent study showed that D can be increased to 90 mm without affecting the removal efficiency of arsenic from sulfate-chloride spent brine (Li et al., 2023). The effect of D was also evaluated for the removal of metals, including Mn, from a real industrial wastewater ([Mn(II)]: 5 mg/L, pH: 6, CD: 42 mA/cm², reaction time: 90 min) using Fe-electrodes. Results showed that the removal of Mn decreases from 94 to 73%, when increasing the D from 20 to 40 mm (Gatsios et al., 2015).

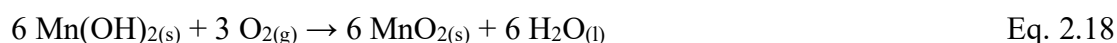
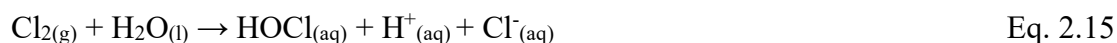
- Air bubbling

Some studies reported the importance of air bubbling during the ECG process, which does not only oxidize Fe(II) to Fe(III), but enhances the coagulation/flocculation process as well because of the turbulence caused by air bubbles in the ECG cell. Metal(loid)s removals may be enhanced upon air bubbling (Banerji and Chaudhari, 2016; Hansen et al., 2007). For example, a significant increasing in As removal, from 15 to 80%, has been noticed when adding air bubbling in the ECG unit (Hansen et al., 2007).

- Effect of salinity and anion species

The nature of electrolyte (i.e., Cl⁻, SO₄²⁻, CO₃²⁻ and HCO₃⁻) may affect contaminants removal efficiency during ECG treatment. The presence of anions can positively or negatively affect the removal of metals by ECG. For example, the presence of Cl⁻ (50 mM) alone or in combination with SO₄²⁻ (50 mM) seems to slightly improve the removal of Mn from synthetic effluent. Indeed, the final Mn concentration were around 156 mg/L (50 mM Cl⁻), 181 mg/L (50 mM Cl⁻+SO₄²⁻) and 200 mg/L (50 mM SO₄²⁻). The favorable effect of Cl⁻ on Mn removal may be attributed to higher oxidizing

conditions related to the production of hypochlorite and oxygen (Equations 2.14-2.18), resulting in Mn(II) oxidation to Mn(IV) and its precipitation as Mn-oxides (Xu et al., 2017).



The beneficial effect of Cl^{-} ions, and the negative effect of SO_4^{2-} on Mn removal by ECG have also been reported for As by several studies (Banerji and Chaudhari, 2016; Lakshmipathiraj et al., 2010; Maitlo et al., 2018). The removal of 98% of As was achieved in the presence of NaCl (0.01 M) whereas it decreased to 80% and 75% in the presence of Na_2SO_4 (0.01 M) and NaNO_3 (0.01 M), respectively (Lakshmipathiraj et al., 2010). The positive effect of Cl^{-} ions can be explained by the prevention of the formation of a passivation layer on the surface of the electrodes, resulting in higher amounts of Fe-hydroxides produced and increased As removal. At the same time, the inhibition effect of SO_4^{2-} and NO_3^{-} ions on the removal of As was mainly attributed to the formation of a passive layer that hinder the electrode dissolution (Lakshmipathiraj et al., 2010). The presence of HCO_3^{-} ions (20 mM) was also found to hinder the As(V) sorption or co-precipitation with Al(III)-hydroxides, because of the competition of HCO_3^{-} with HAsO_4^{2-} and HAsO_4^{3-} for the surface sites of Al(III)-hydroxides (Maitlo et al., 2018).

2.3.4 Combining ECG with other processes

ECG as sole treatment process may not be efficient enough to remove the targeted contaminants below the regulated discharge limit. Combining ECG with other advanced oxidation processes (AOP - e.g., Fenton, ozonation) can improve the removal of organic and inorganic contaminants, while producing lower amounts of sludge, as well as decreasing the retention time and the operating costs (Babu et al., 2019). Successfully applied to the removal of organic contaminants (biological oxygen demand, chemical oxygen demand) from industrial wastewater (Babu et al., 2019; Torres-Sánchez et al., 2014), little is known about the efficiency of combining ECG with other processes on the removal of inorganic contaminant including As and Mn. Table 2.4 presents selected examples on the application of ECG process combined with a second oxidation process for the removal of As and Mn. Most of the studies are focusing on the simultaneous production of Fe^{2+} and hydroxyl radicals ($\cdot\text{OH}$) through the addition of H_2O_2 in the ECG cell or its *in-situ* production (Bandaru et al., 2020; Montefalcon et al., 2020). A recent study showed that H_2O_2 can be *in-situ* generated using an air diffusion cathode, that replaces the conventional Fe-cathode in the ECG cell, through the cathodic reduction of O_2 diffused from the air inside the electrode. This air cathode assisted ECG process enhances the kinetics of As(III) oxidation and removal by orders of magnitude ($[\text{As}_f] < 0.001$ mg/L with the advanced ECG vs. 0.3 mg/L with ECG alone). The improvement in As(III) oxidation and subsequent removal can be explained by the enhanced oxidation of Fe(II) of almost 4 orders of magnitude by the *in situ* generated H_2O_2 compared to O_2 , in addition to the production of more reactive intermediates such as Fe(IV), which enhances the oxidation of As(III) as well (Bandaru et al., 2020). An electrochemical peroxidation process, with an external source of H_2O_2 (5 mg/L) to the ECG unit, has been developed, leading to a significant increase in As removal (from 11 to 44%) in a shorter retention time (from

27.6 to 6.7 min) (Montefalcon et al., 2020). The *in situ* production of hydroxyl radicals through H_2O_2 photolysis (Equation 2.19), Fenton's reaction (Equation 2.20) or photoreduction of $\text{Fe}(\text{OH})_2^+$ (Equation 2.21) has been investigated in the photo-assisted electrochemical peroxidation process (PECP) as well. The removal of As was improved (78%), while reducing the retention time to 4.9 minutes only. This increase in As(III) removal was attributed to the production of Fe(IV) species, which are strong intermediate oxidants, while the contribution of hydroxyl radicals seemed to be insignificant.



A pilot treatment system was developed for the treatment of contaminated groundwater (Vinkovci County, Eastern Croatia), containing 0.138 mg/L As, 1.2 mg/L NH_4^+ and 3.5 mg/L PO_4^{3-} . This system included a combined electrochemical treatment (ECG), using 24 Fe- and 24 Al-electrode plates with simultaneous ozonation, followed by a post-treatment with UV, O_3 and H_2O_2 . The combination of ECG with AOP completely removed all the targeted contaminants (Orescanin et al., 2014). The simultaneous removal of As and Mn from a raw groundwater ($[\text{As}_i] = 9.77 \mu\text{g/L}$, $[\text{Mn}_i] = 137 \mu\text{g/L}$) has been evaluated using ECG alone or combined with an oxidative media filtration (McBeath et al., 2021). Based on the results, ECG alone was effective, decreasing As concentration below 3 $\mu\text{g/L}$, while the flocculation step allowed the removal of Mn to values below 98.97 $\mu\text{g/L}$. The combination of ECG with filtration onto an oxidative

media composed of silica sand coated with MnO_2 (Greensand Plus[®]) increased the removal of As ($<0.1 \mu\text{g/L}$) and Mn ($<40 \mu\text{g/L}$). Generally, the advanced ECG processes were proven to be efficient to remove As and Mn from contaminated groundwater, achieving very low final concentrations.

In summary, ECG has been proved efficient ($>80\%$) for As or Mn removal, separately, from synthetic and real effluents, while minimizing residual salinity relative to conventional precipitation because Fe(III) ions are produced from the electrical dissolution of sacrificial electrodes. Moreover, the ECG process was found to be more effective than the chemical precipitation with respect to the removal efficiency, amount of sludge generated and operating cost (Oncel et al., 2013). Nevertheless, despite a relatively good scientific understanding of the effects of operating conditions on ECG treatment, the identification of the most performant ones for the simultaneous removal of As and Mn from contaminated mine water is still ongoing. In addition, the previous studies that were performed on the Mn removal indicated that its efficient removal may require higher operating conditions, for example higher CD or pH in comparison to As. Therefore, the efficient simultaneous removal of As and Mn would potentially force the selection of the higher operating conditions required for Mn. Moreover, the performance of ECG can be improved through its combination with AOP, which will result in undesirable increase in operating costs. Further to the challenges highlighted above, the evaluation of acute and chronic toxicity has become a requirement for mine effluent discharge in several legislations. However, there is few information available about toxicity assessment of effluents treated by ECG, especially for As and Mn contaminated water (Foudhaili et al., 2020a; Lach et al., 2022; Radić et al., 2014).

Table 2.4 Relevant studies on advanced ECG processes for the removal of As and/or Mn

Technology	Effluent type / Targeted contaminants (mg/L)	Test conditions	Final concentration (mg/L)		Reference
			ECG alone	ECG combined with AOP	
ECG; Air cathode Assisted Iron Electrocoagulation (ACAIE)	Synthetic effluent / As (III); 1.464	Fe-electrodes; 60 min	As: 0.3	As: 0.001	Bandaru et al. (2020)
ECG; simultaneous ozonation; post-treatment with ozone, UV	Groundwater/As(III); 0.138; PO ₄ ³⁻ : 3.5 ; NH ₄ ⁺ : 1.2; suspended solids: 3	pH: 8.14	As: 0; PO ₄ ³⁻ : 0; NH ₄ ⁺ : 1.2; suspended solids: 0	As: 0; PO ₄ ³⁻ : 0; NH ₄ ⁺ : 0; suspended solids: 0	Orescanin et al. (2014)
ECG; ECG-ECP; ECG-PECP*	Synthetic effluent simulating a groundwater / As(III); 0.5	pH _a : 7	As: 0.4427 (after 27.6 min)	EC-ECP: As: 0.2822 (after 6.7 min)	Montefalcon et al. (2020)
		Electrodes: 2 mild steel		EC-PECP: As: 0.116 (after 4.9 min)	
		Distance: 20 mm			
		Electrodes: set of 24 Fe-electrodes, set of 24 Al-electrodes			
		Distance: 5 mm			
ECG; ECG-oxidative media filtration (Greensand Plus)	Groundwater / As; 0.0098; Mn; 0.1372	Electrodes: steel-stainless steel; CD: 0.03 mA/cm ²	As: <0.003	As: <0.0001	McBeath et al. (2021)
			Mn: 0.099	Mn: <0.04	

*ECG-ECP: ECG-electrochemical peroxidation, ECG-PECP: EGC- photo-assisted electrochemical peroxidation

2.4 Ferrates

2.4.1 Principle

Ferrates, which are high oxidation state of iron species (from Fe(IV) to Fe(VIII), with Fe(VI) as the most stable and easier to produce species), are gaining more and more attention for the treatment of wastewater (Goodwill et al., 2016; Kong et al., 2023; Machala et al., 2020; Prucek et al., 2013; Rai et al., 2018; Sharma, 2002; Sharma et al., 2016; Wang et al., 2020a). Characterized by their oxidizing power ($E^\circ = +2.20$ V in acidic media, $E^\circ = +0.72$ V in alkaline media), and their ability to generate *in-situ* coagulant (e.g., Fe(III) species), ferrates (Fe(VI) – FeO_4^{2-}) are highly efficient species for the removal of metal(loid)s from contaminated water (Goodwill et al., 2016; Lee et al., 2003; Machala et al., 2020; Munyengabe et al., 2020). Fe(VI) are able to efficiently remove inorganic contaminants in a single-treatment process through: i) oxidation of reduced species (e.g., As(III) to As(V) or Mn(II) to Mn(IV)), ii) coagulation through *in-situ* production of Fe(III), and iii) sorption onto Fe(III)-hydroxides (Sharma, 2002; Sharma et al., 2005). The main advantages of using Fe(VI) compared to conventional precipitation processes using Fe(III) salts are related to the low amount of highly stable sludge produced. While the main drawbacks are related to the time-consuming and expensive methods required to synthesize Fe(VI), its instability in aqueous phases and the addition of residual salinity in the treated effluent due to the low purity of Fe(VI) (20-40%) (Machala et al., 2020; Sharma, 2002; Wang et al., 2020a).

2.4.2 Synthesis and reactivity of Fe(VI)

Current research focuses on the synthesis of sodium (Na_2FeO_4) or potassium (K_2FeO_4) ferrate salts (Gonzalez-Merchan et al., 2016; Machala et al., 2020; Rai et al., 2018). Potassium ferrate is among the most known derivatives of Fe(VI) due to its stability and ease of production (Sharma, 2002). Fe(VI) can be synthesized by three different processes, including: 1) wet chemical, 2) electrochemical, and 3) thermal methods. Wet chemical and electrochemical approaches produce a highly pure and wet Fe(VI) sample (98%). However, the amount of the product is relatively low (Machala et al., 2020). These synthesis methods are not suitable for a large-scale production. Moreover, the thermal synthesis, which is the most commonly used, results in higher amount of solid Fe(VI) (up to kilograms per one synthetic cycle). Nevertheless, its purity is relatively low (20-40%), because of self-decay of Fe(VI) at high temperatures (Machala et al., 2020).

An important characteristic of Fe(VI) relative to other advanced or conventional oxidants is its self-decay in the presence of oxygen or water, requiring its use upon its production or storage as solid in non-humid conditions (Sharma et al., 2016). When Fe(VI) reacts with water, Fe(III)-hydroxides, oxygen and OH^- ions are produced, resulting in very alkaline solutions (Rush and Bielski, 1989; Schreyer and Ockerman, 1951).

The self-decay or instability of Fe(VI) in solid and aqueous phases is an important feature to be considered when this treatment is applied for large-scale applications. Strongly related to its oxidation ability, its self-decay in aqueous phase is influenced by several conditions (e.g., initial Fe(VI) concentration, temperature, presence of other species, pH) (Barisci and Dimoglo, 2016; Schreyer and Ockerman, 1951). However,

the mechanisms of Fe(VI) self-decay under different experimental conditions are still controversial.

- Initial Fe(VI) concentration

The decomposition rate of Fe(VI) can be influenced by the initial concentration of Fe(VI) used. For example, a total degradation of Fe(VI) was observed after 1 h for a solution of 0.03 M of Fe(VI), while only 11% of the Fe(VI) were degraded under the same period for lower concentrations (<0.025 M). The critical concentration of Fe(VI) was identified as 0.025 M (Schreyer and Ockerman, 1951). This higher degradation rate observed at high initial Fe(VI) concentrations is explained by the presence of higher amounts of Fe(III) species, resulting from the reduction of highly oxidant Fe(VI) to Fe(III) in solution (Li et al., 2005; Schreyer and Ockerman, 1951). This degradation rate is more important when the pH is very acidic as Fe(III) remains in solution. The identification of the appropriate Fe(VI)/contaminant ratio to be used to avoid the addition of too high amounts of Fe(VI), which will result in a higher degradation rate of the oxidant and lower contaminant removal efficiencies is therefore critical.

- Temperature

The stability of Fe(VI) can be affected by the temperature of the solution. For example, Fe(VI) solution stored at 0.5°C was reported to remain stable (~2% of Fe(VI) reduction) after 2 hours, while a 10% decrease in Fe(VI) concentration was observed when stored at 25°C during the same period (Wagner et al., 1952).

- Presence of salts

The addition of salts to a solution containing Fe(VI) could either accelerate or delay its decomposition, depending on the nature of the salt added. For example, an increase in the decomposition of Fe(VI) was observed in the presence of NaCl (0.5 M), while the presence of KCl (0.5 M) or KNO₃ (0.5 M) led to a decrease of Fe(VI) decomposition. A complete decomposition of Fe(VI) occurred within only 15 minutes in the presence of NaCl, while it took 35 minutes without any salt addition, and lasted 60 minutes in the presence of KCl or KNO₃ to achieve the complete degradation of Fe(VI) (Schreyer and Ockerman, 1951).

- pH

The stability as well as the speciation of Fe(VI) and its reactivity towards inorganic contaminants are pH-dependent. Four different species of Fe(VI) can exist depending on the pH (Figure 2.4). The FeO₄²⁻ is predominant in alkaline medium, while HFeO₄⁻, which is a stronger oxidant due to its larger spin density, dominates in slightly acidic-neutral conditions (Barisci and Dimoglo, 2016; Kamachi et al., 2005). The lowest degradation rate of Fe(VI) occurs at pH 9.2-9.4, indicating that Fe(VI) is more stable under slightly alkaline conditions, while under acidic conditions (pH ~ 6), Fe(VI) is quite unstable with more than 60% of Fe(VI) degraded within several minutes (Graham et al., 2004; Tiwari et al., 2007). This can be explained by the high oxidation potential of Fe(VI) under acidic conditions, leading to a rapid degradation of Fe(VI) and the production of O₂ and Fe(III). At pH above 10, the stability of Fe(VI) tends to decrease with the increase of pH (20% of Fe(VI) degradation at pH 11 vs. 60% at pH 12 within 10 minutes), but the mechanisms involved in Fe(VI) degradation are still not fully understood (Graham et al., 2004).

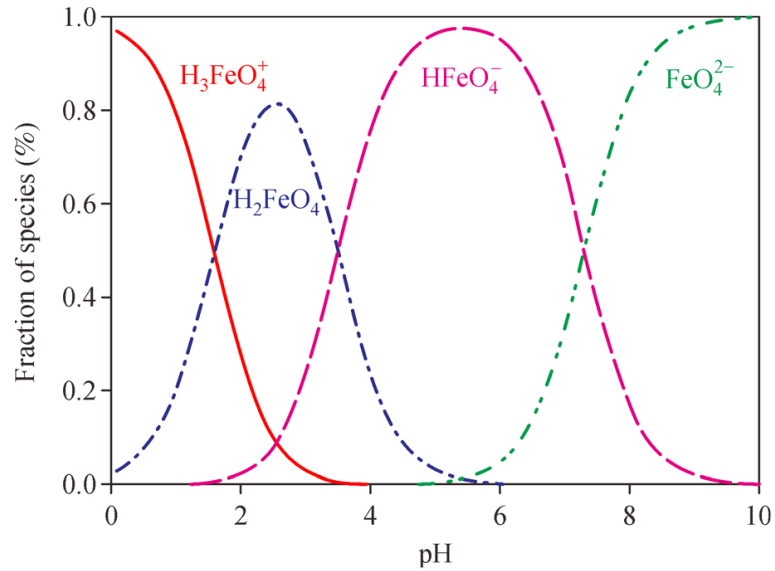


Figure 2.4 Impact of pH on the speciation of Fe(VI) (Wang et al., 2021)

2.4.3 Mechanisms involved in inorganic contaminants removal by Fe (VI)

Different potential pathways have been identified for the removal of inorganic contaminants by Fe(VI) (Goodwill et al., 2016; Pucek et al., 2013; Sharma, 2010; 2011; Wang et al., 2020). Fe(VI) provides multi-functional removal strategy, where it acts as an oxidant for the compounds present in their reduced forms and as a coagulant/sorbent upon the *in situ* formation of Fe(III)-hydroxides (Pucek et al., 2013; Sharma, 2011). The mechanisms involved in As and Mn removal from contaminated water by Fe(VI), which involved a 2-electrons transfer, are described in Figure 2.5 (Sharma, 2010; 2011). For As(III), the redox reaction occurring with Fe(VI) involves a combined transfer of oxygen atom and $2 e^-$, leading to its oxidation into As(V). Once oxidized, As(V) is removed from contaminated water through its co-precipitation with

or sorption on Fe(III)-hydroxides. According to Pucek et al. (2013), 20% of As(V) removal occurred through its incorporation into the structure of Fe(III)-hydroxides nanoparticles formed *in situ*, leading to the production of more stable sludge. The pH affected the sorption of As(V) on the generated Fe(III)-hydroxide nanoparticles (Pucek et al., 2013), as the pH of the solution drives the isoelectric point of the solid phase surfaces, which will be discussed in detail in Section 2.4.4. The mechanisms involved in the removal of Mn(II) are not yet fully elucidated. However, Goodwill et al. (2016) proposed a Mn(II) removal mechanism occurring via its oxidation to Mn(IV) followed by precipitation of Mn-oxide nanoparticles. This last study also recommended that the dosage of Fe(VI) should be carefully defined to avoid the oxidation of Mn(II) to Mn(VII), which are soluble.

2.4.4 Operating parameters influencing the performance of Fe(VI)

The performances of Fe(VI) to remove As and Mn from contaminated water are affected by several operating parameters, such as the initial solution pH, the Fe(VI) dose and the retention time (Goodwill et al., 2016; Lee et al., 2003; Pucek et al., 2013). Some of the relevant studies evaluating the performances of Fe(VI) to remove As and Mn from synthetic and real effluents, under different operating conditions are presented in Table 2.5.

Several studies have been conducted on the removal of As by Fe(VI), while the removal of Mn(II) using this process is poorly documented. Most of the studies focus on the treatment of synthetic effluents rather than real effluents, so the influence of other contaminants including salinity is not fully evaluated. Based on the information presented in Table 2.5, Fe(VI) are highly efficient (90–100%) for the removal of As and Mn from synthetic or real water. However, there is no consensus on the most

appropriate operating conditions, including the best pH for the oxidation of As(III) or for the removal of Mn(II) and the optimal Fe(VI)/contaminant molar ratio, especially for slightly-contaminated water containing both contaminants. The effect of the different operating parameters reported in the most relevant studies influencing the removal of As and Mn by Fe(VI) will be discussed in the following sections.

- Influence of pH on Fe(VI) performance

Metal(loid) speciation, including As and Mn, as well as Fe(VI) speciation/stability is strongly pH-dependent. Several studies have reported that the reaction rate of Fe(VI) with the inorganic contaminants increases with the decrease of pH (from 10 to 6.5), which can be explained by the higher oxidizing power of Fe(VI) at acidic-neutral pH relative to alkaline conditions (Dong et al., 2019; Pucek et al., 2013; Sharma et al., 2005; Sharma, 2011). An important increase of As removal (from 80 to >99%) has been observed with the decrease of pH from 10 to 6.0, identifying pH 6.6 as optimal (Pucek et al., 2013). A pH of 6.0-6.6 was identified as optimal for the removal of As(III) or As(V) by Fe(VI) in most of the studies (Table 2.5). This can be explained by the formation of Fe(III)-hydroxide nanoparticles, which has a pH_{pzc} of 6.8 (Yang et al., 2018).

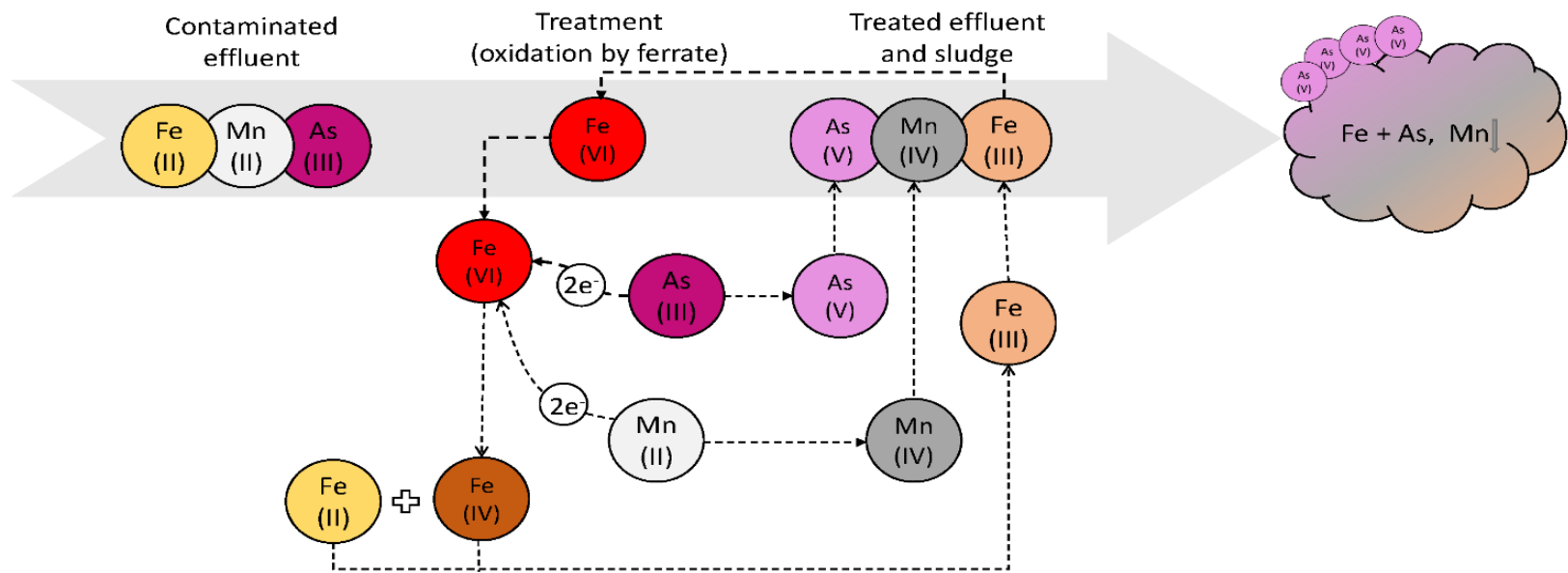


Figure 2.5 Mechanism involved in As(III) and Mn(II) removal by Fe(VI)

Table 2.5 Examples of Fe(VI) performances for the removal of As or Mn from synthetic or real effluents

Effluent Type	Targeted contaminant (mg/L)	Scale	pH _i /pH _a	Molar ratio (Fe(VI)/As)	Molar ratio (Fe(VI)/Mn (II))	K ₂ FeO ₄ (mg/L)	Retention time (min)	Efficiency (%)	References
As removal									
Synthetic effluent	As(III,V): 100	Batch	pH _i : 6.6–10	5.8/1*	-	200 (as Fe)	60	80-100	Prucek et al. (2013)
Synthetic effluent	As(III): 2; Sb: 2	Batch	pH _i : 4–7	5.7/1*	-	50	-	As: >98.5 (pH 6.5) Sb: 27 (pH _i :7), >96 (pH _i : 3.5)	Lan et al. (2016)
Synthetic effluent	As(III): 0.5; Sb: 0.5	Batch	pH _a : 3–12 pH optimal: 4-5	3.7/1*	-	8	20	As: 100 (pH: 4-7) Sb: 65 (pH: 4-5.5)	Wang et al. (2020)
Synthetic effluent	As(III): 2.99**	Batch	pH _a : 7.5	9/1	-	-	-	100	Sharma et al. (2007)
River water	As(III): 0.517	Batch	pH _i : 7.8; pH _a : 6.3–6.6	11/1*	-	2 (as Fe)	60	90	Lee et al. (2003)
Groundwater	As: 0.1	Semi-pilot	pH _a : 7	Not specified	-	15	20	>95	Hermankova et al. (2020)
Raw drinking water	As: 38.66	Pilot plant batch mode	pH _a : 6	7/1	-	-	30	97	Bujanovic et al. (2016)
Mn removal									
Synthetic effluent	Mn: 5.5**	Batch	pH _a : 3, 6, 11	-	15/1*	39.1 (as Fe)	-	73	Lim and Kim (2010)
Synthetic effluent	Mn: 0.26**	Batch	pH _a : 6.2	-	2/3	-	45	-	Goodwill et al. (2016)
Raw water	Mn: 10	Batch	pH _i : 5–8 (optimal: 7.5)	-	0.6/1*	3 (as Fe)	55	100	White and Franklin (1998)

*: Molar ratio is calculated from available data; **: As/Mn concentration is calculated from available data; pH_i: initial pH; pH_a: adjusted pH

Under alkaline conditions ($\text{pH} > 6.8$), both Fe(III)-hydroxides and As(V) species are negatively charged, which results in electrostatic repulsion between both species that may hinder As removal through co-precipitation or sorption. More recently, Wang et al. (2020) showed that a decrease of the pH from 6.5 to 4.0 led to a slight increase of As removal, which can be due to the higher oxidizing properties of Fe(VI) under acidic conditions as well as the lower solubility of produced $\text{Fe}(\text{OH})_3$, favoring the formation of stable flocs and sorption activity. These results also showed that the amount of Fe(VI) required for the removal of As can be reduced (Fe(VI)/As molar ratio of 3.7/1) compared to the other studies (Fe(VI)/As molar ratio between 5.8/1 and 9/1) as the pH was fixed at 4-5 (Table 2.5). This decrease in the amount of Fe(VI) is beneficial in terms of operating costs, residual salinity and sludge production.

For the removal of Mn, Goodwill et al. (2016) reported that Fe(VI) can oxidize Mn(II) to Mn(IV), which then precipitate as Mn-oxides, at almost neutral pH (6.2-7.5). The results showed that the rate of reaction decreased as the pH increased from 8.8 to 9.2. Another study reported that Mn removal efficiency increased from 40 to 80% as the pH increased from 3 to 6 and remained stable at 80% at pH 11 (Lim and Kim, 2010). The enhanced Mn removal observed at high pH (pH 6 and 11) was attributed to the presence of stable Fe(VI) species in neutral and alkaline conditions, which can react with divalent metals (Me^{2+} - including Cu^{2+} , Zn^{2+} and Mn^{2+}) in the solution and form precipitates such as $\text{Me}(\text{HFeO}_4)_2$ and $\text{Me}(\text{FeO}_4)$. Similar improved Mn removal efficiencies with pH increase (from 5 to 8) were observed by White and Franklin (1998) in the treatment of a raw water sample, with an optimal pH at 7.5.

- Fe(VI) dose or Fe(VI)/contaminant molar ratio

Several studies have reported the effect of Fe(VI) dose or Fe(VI)/contaminant molar ratio on the efficient removal of As or Mn species from synthetic and real water at

various initial concentrations (0.5 to 100 mg/L) (Goodwill et al., 2016; Lan et al., 2016; Lee et al., 2003; Lim and Kim, 2010; Prucek et al., 2013). The relation between As removal and Fe(VI) dose is positive, indicating that increasing applied Fe(VI) dose will lead to a better As removal (Lee et al., 2003; Prucek et al., 2013). For example, an increase of the molar Fe(VI)/As ratio from 11/1 to 34/1 led to an increase of As removal from 90 to >99% for a lowly contaminated river water ($[As]_i$: 0.517 mg/L). The optimal Fe(VI)/As ratio was fixed at 11/1, leading to 90% As removal (Lee et al., 2003). Prucek et al. (2013) also observed that the removal of As(III) and As(V) from synthetic effluents initially containing 100 mg/L of As increased with increasing applied Fe(VI) concentration (from 100 to 1000 mg/L as Fe). The As was almost completely removed at a Fe/As weight ratio of 2/1 (equivalent to Fe(VI)/As molar ratio of 5.8/1), with the same efficiency observed for As(III) and As(V). While, a Fe(VI)/As molar ratio of 5.7/1 was reported as optimal by Lan et al. (2016), for an initial concentration of 2 mg As/L. These results indicate that the most suitable Fe(VI)/As ratio seems to be affected by the initial As concentration present in the effluent to be treated, the type of effluent (synthetic effluent or real effluent) and the pH of the solution (Table 2.5).

Only few studies were found on the removal of Mn by Fe(VI). Unlike the positive relation between Fe(VI) added dose and As removal, overdosing of Fe(VI) can further oxidizes insoluble Mn(VI) to soluble Mn(VII) species (apparition of a persistent pink color), decreasing Mn removal efficiencies (Goodwill et al., 2016). The oxidation of Mn(II) to Mn(IV) and its subsequent removal from a synthetic effluent was found to be optimal at a molar stoichiometry Fe(VI)/Mn of 2/3 at an initial Mn concentration of 0.26 mg/L (Goodwill et al., 2016). However, a higher optimal molar Fe(VI)/Mn ratio (15/1) was reported by Lim and Kim (2010) for the treatment of a synthetic effluent (initial Mn concentration of 5.5 mg/L). White and Franklin (1998) found an optimal Fe(VI)/Mn molar ratio of 0.6/1 for the removal of Mn from a real effluent ($[Mn]_i$: 10 mg/L). Based on these results, the most suitable Fe(VI)/Mn molar ratio ranges from 0.6/1 to 15/1, with respect to the quality of the effluent to be treated.

- Retention time and kinetic studies

The reaction of Fe(VI) with the different inorganic contaminants is very fast, from few milliseconds to 1 h (Fan et al., 2007; Sharma et al., 2005; Sharma et al., 2008). As presented in Table 2.5, the reaction is usually conducted within 1 h in most studies. The oxidation of As or Mn usually occurs within the first minute, while the remaining time is necessary to allow the flocculation and precipitation of Fe(III)-hydroxide nanoparticles and the subsequent sorption, incorporation or co-precipitation of As(V) (Prucek et al., 2013) and precipitation of Mn-oxide (Goodwill et al., 2016). Increased settling time after the reaction could improve the removal of targeted contaminants, because of the enhanced sorption of As and Mn on Fe(III)-hydroxides and the sweeping of remaining species in the solution (Wang et al., 2020). For As removal, it was observed that As(V) is adsorbed in the first 3 to 4 minutes and partially incorporated (~20%) into the structure of γ -Fe₂O₃ or γ -FeOOH nanoparticles formed. This immobilization mechanism through incorporation could enhance the stability of the generated product (Heřmánková et al., 2020; Prucek et al., 2013).

The reaction rate of Fe(VI) with different inorganic contaminants was evaluated through kinetic studies and calculation of reaction rate and reaction constants ($k - M^{-1}s^{-1}$). The results reveal that most of the inorganic compounds can be removed at a time scale of few milliseconds to seconds at pH 7-8. Indeed, Fe(VI) can oxidize As(III) very fast ($k > 1 \times 10^3 M^{-1}s^{-1}$) with half-life time ($t_{1/2}$) lower than one second (Lee et al., 2003; Sharma, 2011), while Mn(II) oxidation by Fe(VI) occurs within one minute ($k > 1 \times 10^4 M^{-1}s^{-1}$) (Goodwill et al., 2016), under optimal pH conditions. For example, the reaction rate constants between Fe(VI) and As(III) are estimated at $2.0 \times 10^4 M^{-1}s^{-1}$ at pH 9; which are quite comparable to those measured for Mn(II) at pH 9.2 and 8.8 ($k = 1.0 \times 10^4$ and $5.6 \times 10^4 M^{-1}s^{-1}$, respectively) (Goodwill et al., 2016; Lee et al., 2003). The kinetic studies conducted by Lee et al. (2003) showed that the reaction of As(III) with Fe(VI) follows a first-order reaction with respect to both reactants.

A non-linear decrease of the second order rate constant at 25°C from $3.5 \times 10^5 \text{ M}^{-1}\text{s}^{-1}$ to $1.2 \times 10^3 \text{ M}^{-1}\text{s}^{-1}$ was observed with the increase of pH from 8.4 to 12.9. A similar evolution of the second order rate constants of the reaction between Fe(VI) and most inorganic compounds was also observed (Sharma et al., 2007; Sharma, 2010). The inverse relationship between the second order rate constant and the pH may be related to the speciation of Fe(VI) and its higher oxidizing properties under acidic conditions compared to alkaline ones. Indeed, the protonated form HFeO_4^- reacts more readily than the unprotonated species (FeO_4^{2-}) with As. Moreover, this decrease in the rate constant with the pH increase correlates with the fact that under alkaline conditions, Fe(VI) and As(V) species are negatively charged. Hence, the electrostatic repulsion between the two negatively charged species may influence the removal of As oxyanions. As observed for As removal, some studies reported that the oxidation of Mn(II) by Fe(VI) slightly decreases with the increase of pH. For example, Goodwill et al. (2016) conducted kinetic studies at different pH values and reported that the maximum reaction rate was obtained at pH of 6.2-7.5 ($k = 9 \times 10^4 \text{ M}^{-1}\text{s}^{-1}$), while the reaction rate constant slightly decreased from $5.6 \times 10^4 \text{ M}^{-1}\text{s}^{-1}$ to $1 \times 10^4 \text{ M}^{-1}\text{s}^{-1}$ at pH 8.8 and 9.2, respectively.

In summary, despite promising As and Mn removal efficiencies (>80%), the potential use of Fe(VI) to simultaneously remove As and Mn from mine water has not yet been reported in the literature. Moreover, optimal treatment conditions (e.g., Fe(VI) dose, pH, retention time) for low-contaminated mine water containing both As and Mn are yet to be developed. However, according to the previous studies on the removal of As and Mn by Fe(VI), showing that the As removal seems to consume higher dose of Fe(VI) compared to Mn, it could be expected that their simultaneous removal will require higher Fe(VI) dose in relative to the applied dose for their separate removal. In addition, most of the studies on the use of Fe(VI) to remove As and Mn from contaminated water evaluated its efficiency rather than its performances (removal efficiency, regulations, residual salinity, toxicity of treated effluent, and operating

costs). Only a few studies have evaluated the toxicity of the final effluent after treatment by Fe(VI), mostly targeting the removal of emerging organic contaminants such as pharmaceutical products (Han et al., 2015; Yang et al., 2016; Zhang et al., 2022).

2.5 Toxicity of mine effluents: evaluation and regulations

As previously mentioned, final mine water should respect both physicochemical and toxicological (acute and chronic) criteria to allow their responsible and safe discharge in the environment. Mine water toxicity is usually evaluated through acute and chronic toxicity tests, which may vary depending on the legislation (MDMER, 2018; USEPA, 2018). For example, in the Canadian context (Table 2.6), acute toxicity must be assessed on rainbow trout fish (*Oncorhynchus mykiss*) and water fleas (*Daphnia magna*) in both federal (Ministry of Justice, 2021) and Quebec's provincial (MELCC, 2012) legislation. The sublethal or chronic toxicity assessment on algae species *Pseudokirchneriella subcapitata* is also required in the federal legislation (Ministry of Justice, 2021). Several organisms have been used for the assessment of mine water toxicity (Table 2.6). *D. magna* is one of the most widely used organism by mining companies to evaluate acute toxicity due to its wide distribution, ease of cultivation in laboratory, sensitivity, high reproduction rate and short life cycle (Lee et al., 2015).

There are several potential sources of acute and chronic toxicity in mine water including the pH, the ionic strength (or salinity) as well as the concentration of some metal(loid)s and sulfates (Byrne et al., 2013; Foudhaili et al., 2020a; Lee et al., 2015; Pereira et al., 2014; Soucek et al., 2000; Williamson et al., 2013). This section will briefly discuss the main causes of toxicity expected from the treatment of As- and

Mn-contaminated mine water using ECG and Fe(VI). The Table 2.7 presents some studies, which evaluated the toxicity effect of As, Mn and Fe in terms of acute and chronic toxicity towards *D. magna*.

Table 2.6 Toxicity tests recommended in the federal and Quebec's provincial legislation (MELCC, 2012; Ministry of Justice, 2021)

Toxicity test	Common name of organism	Latin name of organism	Legislation
Acute toxicity	Rainbow trout fish	<i>Oncorhynchus mykiss</i>	D019; MDMER
	Water fleas	<i>Daphnia magna</i>	D019; MDMER
Sublethal toxicity	Fathead minnow	<i>Pimephales promelas</i>	MDMER
	Green algae	<i>Pseudolirchneriella subcapitata</i>	MDMER
	Small water lentils	<i>Lemna minor</i>	MDMER
	Small water fleas	<i>Ceriodaphnia dubia</i>	MDMER

- Arsenic

The toxicity of As to *D. magna* has been reported in the literature; with As(III) being exhibited to be more toxic than As(V) and organic forms of As (Suhendrayatna et al., 1999; Tisler and Zagorc- Koncan, 2002; Wang et al., 2016). The toxicity of As(III) is due to its high affinity for sulfhydryl groups of biomolecules. The bonds formed between As(III) and sulfhydryl groups lead to inhibition of critical enzymatic functions within the cells. On the other hand, the toxicity of As(V) is mainly associated to its potential for phosphate replacement (Zeng et al., 2017). Information on the toxicity effect of As to freshwater species were available for 21 species of fish, 14 species of invertebrates, and 14 species of plants (CCME, 2001). Rainbow trout (*Oncorhynchus mykiss*) and climbing perch (*Anabas testudineus*), which were identified as the most

sensitive fish, seem to be as sensitive as invertebrates such as copepods (*Cyclops vernalis*) and daphnids (*D. magna*) to As content in water. For example, the lethal concentration (LC₅₀) for *O. mykiss* and *A. testudineus* is 550 µg/L (21 days), while the effective concentration (EC₅₀) to detect an effect on the reproduction of *D. magna* is 520 µg/L (CCME, 2001).

- Manganese

Manganese is a toxic element mostly overlooked in the evaluation of effluent toxicity, even though it is a prevalent contaminant in discharges from mining activities (Ferrari et al., 2018). Manganese in water can be considerably bio-concentrated by biota at lower trophic levels, favoring its adsorption and bioaccumulation by aquatic invertebrates and fish (Howe et al., 2004). The toxicity of dissolved Mn is related to the water quality, in particular the hardness and pH. This relationship is explained by the competition between major ions (e.g., Ca²⁺, Mg²⁺, H⁺) and Mn for binding sites on/in organisms. Hence, the higher risk of Mn toxicity to fish and invertebrates is in the acidic, Ca-deficient waters as these conditions can significantly promote the uptake and toxicity of metals, including Mn (Harford et al., 2015). Freshwater streams, rivers and lakes are among the environments that are most sensitive to elevated concentrations of Mn (>1 mg/L) (Howe et al., 2004). The results of various toxicity tests performed on various organisms in aquatic biota, such as microalgae (e.g., diatoms), protozoa, invertebrates (e.g., worms; daphnia; crustaceans), fish and amphibians in the presence of Mn(II) are reported in a report from the World Health Organization (WHO) (Howe et al., 2004). Adverse impacts such as inhibition of growth, reduction in total cell volume, inhibition of reproduction rate, abnormal larval development, and significant embryonic mortality have been reported among others (Howe et al., 2004). For example, a 48h-LC₅₀/EC₅₀ values in the range of 0.8 mg/L (*Daphnia magna*) to 1389 mg/L (*Crangonyx pseudogracilis*) were reported, with the lowest LC₅₀ found at low water hardness (25 mg CaCO₃/L) (Howe et al., 2004).

Table 2.7 Examples of the effect of the toxicity generated on *D. magna*

Effluent conc. (mg/L)	Objective of study	Toxicity test; organism	Test conditions	Results	Observations	References
As						
Synthetic As(III) effluent: 0.1-2 mg/L; synthetic As(V) water: 1-20 mg/L	Test bioaccumulation; biotransformation, tolerance of arsenic compounds by <i>D. magna</i>	24 h LC ₅₀ <i>D. magna</i> (0.5-2.0 mm in length size)	24 h exposure, 20°C	24h LC ₅₀ : As(III): 1.7 mg/L As(V): 5 mg/L	The survival of <i>D. magna</i> not affected by increase of As(III) concentration up to 1.5 mg As/L	Suhendrayatna et al. (1999)
Synthetic effluent of As(III), different concentrations (not specified)	Evaluate acute, chronic toxicity of As(III) on different organisms	24 h, 48 h acute toxicity; 21-days chronic toxicity; <i>D. magna</i> (neonates)	24 h; 48 h; 21 days exposure; 21°C; 16 h light; 8 h dark	24 h-EC ₅₀ : 2.7 mg/L (2.6-2.9); 48 h-EC ₅₀ : 2.5 mg/L (2.4-2.7); 21d-LC ₅₀ : 1.9 mg/L	As(III) is not highly toxic to <i>D. magna</i> in short duration of exposure	Tisler and Zagorc-Koncan (2002)
Synthetic effluent of 23 metals, including As(III), Fe(II), Mn(II) (prepared separately)	Evaluate acute toxicities of 23 metal ions to <i>D. magna</i>	48 h acute toxicity EC ₅₀ ; <i>D. magna</i>	48 h exposure	48 h-EC ₅₀ : As(III): 6.23 mg/L; Fe(II): 7.20 mg/L; Mn(II): 8.28 mg/L	Among the 23 metals tested, mercury (Hg) was the most toxic, antimony (Sb) the least toxic (low solubility)	Khargarot and Ray (1989)

Table 2.7 (continued) Examples of the effect of the toxicity generated on *D. magna*

Effluent conc. (mg/L)	Objective of study	Toxicity test; organism	Test conditions	Results	Observations	References
Manganese						
Synthetic effluent of Cd (0.006-61.32 mg/L); Zn (0.01-113.7 mg/L); Pb (6.26-6256 mg/L); Mn (0.03-325 mg/L)	Evaluate the sensitivity of two bacterial tests in comparison to the standard acute <i>D. magna</i> test, against Cd, Zn, Mn and Pb	24 h; 48 h acute toxicity; LC ₅₀ ; <i>D. magna</i> (neonates)	24 h; 48 h exposure; 20°C; 16 h light; 8 h dark	24 h; 48 h-LC ₅₀ : Mn: 32.5 mg/L; Cd: 0.61 mg/L; Zn: 1.14 mg/L; Pb: 62.56 mg/L	Manganese appears to be slightly toxic to <i>D. magna</i> and non-toxic to the two tested bacteria. Conclusion: even in regions with high background concentrations, manganese would not act as a confusing factor	Teodorovic et al. (2009)
Synthetic effluent of Mn(II); [Mn(II)]: <i>D. magna</i> : 30-80 mg/L ; <i>C. silvestrii</i> : 3-9 mg/L	Evaluate effects of acute manganese toxicity to <i>D. magna</i> ; <i>C. silvestrii</i>	48 h acute toxicity; <i>D. magna</i> ; <i>C. silvestrii</i> (neonates <24 h)	48 h exposure; 16 h light, 8 h darkness; 20°C (<i>D. magna</i>); 25°C (<i>C. silvestrii</i>)	48 h-LC ₅₀ : 51.66 mg/L (<i>D. magna</i>); 5.93 mg/L (<i>C. silvestrii</i>)	Significant difference in LC ₅₀ between the two species; due to hardness effect; <i>D. magna</i> (hard water); protective effect; <i>C. silvestrii</i> (soft water)	Ferrari et al. (2018)

Table 2.7 (continued) Examples of the effect of the toxicity generated on *D. magna*

Effluent conc. (mg/L)	Objective of study	Toxicity test; organism	Test conditions	Results	Observations	References
Iron						
AMD-impacted water (pH: 3.29-3.77; Fe: 0.77-6.56 mg/L)	Examine acute toxicity of water impacted by AMD on <i>D. magna</i>	Acute 48 h LC ₅₀ ; <i>D. magna</i> (5-day-old)	48 h exposure acute toxicity tests	LC ₅₀ (%): 27-69	Water chemistry with low pH, high metal content including Fe is probably the cause of toxicity	Soucek et al. (2000)
Synthetic effluent of FeCl ₃ ·6H ₂ O	Examine the toxicity of different elements including Fe(III) to <i>D. magna</i>	<i>D. magna</i> neonates (<24 h)	48 h exposure; Light/dark cycle: 16/18 h; temp.: 21C°, pH: 6.5-8.5	EC ₅₀ : 6.7 mg/L	The study considered the Fe to have low toxicity to <i>D. magna</i>	Okamoto et al. (2014)

Table 2.7 (continued) Examples of the effect of the toxicity generated on *D. magna*

Effluent conc. (mg/L)	Objective of study	Toxicity test; organism	Test conditions	Results	Observations	References
Salinity						
<p>Solution of NaCl Acute: (4.4-7.09 g/L; <i>D. magna</i>) (2.5-4.03 g/L; <i>D. longispina</i>) Chronic: (3.42-5.5 g/L; <i>D. magna</i>) (1.55-2.5 g/L <i>D. longispina</i>)</p>	<p>Study the acute and chronic effects of salinity in <i>D. magna</i> and <i>D. longispina</i></p>	<p>Acute and chronic (EC₅₀); <i>D. magna</i> and <i>D. longispina</i> (neonates)</p>	<p>Acute: 48 h exposure; Chronic: 21 days exposure</p>	<p><i>D. magna</i>: EC₅₀ 5.9 g/L (acute); EC₅₀ 5.0 g/L (chronic) <i>D. longispina</i>: EC₅₀ 2.9 g/L (acute); EC₅₀ 2.2 g/L (chronic)</p>	<p><i>D. magna</i> is more tolerant than <i>D. longispina</i>; Chronic exposure, salinity caused a significant reduction in fecundity; developmental delay, decrease in growth rate of daphnids</p>	<p>Gonçalves et al. (2007)</p>
<p>Solutions with salinities (1-11 g/L)</p>	<p>Determine <i>D. magna</i> tolerance to salinity; suitability for tests with estuarine water; sediments</p>	<p>Acute (LC₅₀); <i>D. magna</i> (1 to 30-days-old)</p>	<p>2-21 days exposure; 21-25°C</p>	<p>LC₅₀: 5.10 to 7.81g/L</p>	<p><i>D. magna</i> survive; reproduce well in water with salinities <4 g/L; demonstrate potential usefulness in monitoring toxicity from both freshwater and estuarine</p>	<p>Schuytema et al. (1997)</p>

Guidelines have been defined for Mn in freshwater in some countries or jurisdictions to protect aquatic life. For example, in British Columbia (Canada), guideline ranging from 0.1 to 1 mg/L Mn in freshwaters were reported by the Canadian Council of Ministers of Environment (CCME) in 1995. However, these guidelines were later adjusted by the Ministry of Environment, Lands and Parks for the protection of aquatic life to a range of 0.6 mg/L at a hardness of zero to 1.9 mg/L at a water hardness of 325 mg/L CaCO₃ to consider the hardness effect on Mn toxicity (Reimer, 1999).

2.6 Stability of treatment sludge

The treatment of mine water slightly contaminated by As or Mn produces As- or Mn-bearing residues that can represent a secondary source of pollution, if not properly managed. A performant treatment process should be defined as a technology that provides: i) an efficient removal of the targeted contaminant in combination; ii) the compliance of the regulations in terms of both physicochemical and toxicological parameters and iii) the long-term stability of the produced sludge or post-treatment residue. The stability of As- or Mn-residues can be affected by several parameters including: (1) the composition of the sludge/residues (e.g., nature and crystallinity of the precipitates formed as well as the particles size of the sludge); (2) the quality of the effluent to be treated (e.g., presence of impurities or competing species such as calcium, sulfates); (3) the site-related disposal conditions (Coudert et al., 2020; Nazari et al., 2017). Redox conditions, pH and salinity are critical parameters that control the potential mobilization of As and Mn from post-treatment residues during their long-term management (Bourg and Loch, 1995; Coudert et al., 2020; Neculita and Rosa, 2019; Neil et al., 2014; Northrup et al., 2018). Several methods such as mineralogical characterization, static tests (e.g., water leaching; toxic characteristic

leaching procedure (TCLP); field leaching test (FLT)) and kinetic tests (e.g., weathering cells) have been used to evaluate the short and long-term stability of the sludge or post-treatment residues from mine water treatment (Ahmad et al., 2019; Coudert et al., 2020; Hageman, 2007; Le Bourre et al., 2020). The mineralogical composition of As-bearing sludge originated from conventional treatment (co-precipitation with Fe(III) salt addition and pH adjustment) and the potential transformation of these precipitates to other forms with time have been extensively studied (Clancy et al., 2013; Harris, 2000; Welham et al., 2000). On the contrary, the characterization of Mn-bearing residues from mine water treatment using conventional precipitation as Mn-oxides and their stability over time is less documented (Butler 2011; Ginder-Vogel and Remucal, 2016; Le Bourre et al., 2020). However, the mineralogical characterization of As- and Mn-bearing sludge produced from the treatment of real mine effluents can be quite challenging (Nazari et al., 2017; Pantuzzo and Ciminelli, 2010) depending on the initial composition of the effluent to be treated and the elapsed time between treatment and characterization. ECG and Fe(VI) have been proven to be efficient in the removal of As and Mn from contaminated mine water, but the stability of the produced sludge is poorly documented in the literature. Pucek et al. (2013) showed that 20% of the As(V) was incorporated into the structure of Fe(III)-hydroxides, which can be associated with an improved stability of the sludge even if no leaching tests were conducted to confirm/infirm this hypothesis.

2.6.1 Stability of As-bearing residue

Co-precipitation and sorption of As(V) are the main mechanisms involved during the treatment of contaminated effluents using conventional treatment approaches. The production of thermodynamically and kinetically resistant precipitates is required to ensure the long-term safe disposal of As-bearing residues. This section will focus only

on the stability of As-bearing precipitates using Fe(III) as coagulant, even if As(V) can efficiently be precipitated as Ca-arsenate, because of the low stability of the produced sludge, except in specific conditions (i.e., absence of moisture and minimal fall events) (Harris, 2000; Wang et al., 2020; Zhang et al., 2020) (Table 2.8).

Among the methods used for As(V) treatment from contaminated effluents, its precipitation as scorodite ($\text{FeAsO}_4 \cdot 2\text{H}_2\text{O}$) is recommended for the safe disposal of As-bearing residues because of: (1) its high As content (25-30 wt%), (2) its low Fe requirements (Fe/As molar ratio 1-1.5/1), (3) the low solubility of As under TCLP conditions ($< 5 \text{ mg/L}$) and (4) its high short-term stability in slightly acidic (As release of 0.35-1.61 mg/L for $\text{pH} > 2$) and neutral conditions comparative to alkaline pH (As release of 45-787 mg/L for $\text{pH} > 8$) and very acidic conditions (As release of 20-206 mg/L for $\text{pH} < 2$) (Coudert et al., 2020). Under slightly alkaline conditions ($\text{pH} > 8$), the short and long-term stability of scorodite is low, leading to the release of high amounts of As in the environment (Demopoulos, 2005; Harris, 2000; Nazari et al., 2017). This could be explained by the dissolution of Fe(III)-bearing residues under alkaline conditions. Despite its long-term stability under acidic to near-neutral conditions, scorodite may decompose to goethite ($\alpha\text{-FeOOH}$), releasing As into the environment (Cruz-Hernández et al., 2017; Nazari et al., 2017). Scorodite is known to be stable under oxic conditions up to $\text{pH} 6.5$ at 22°C , while it tends to dissolve under anoxic conditions or under the effect of reducing bacteria (Demopoulos, 2005; Lagno et al., 2010; Revesz et al., 2015). For example, high amounts of As ($\sim 200 \text{ mg/L}$) were released from freshly precipitated scorodite after 6 weeks of disposal under reducing conditions (Lagno et al., 2010).

Ferric arsenates, with the formula of $\text{FeAsO}_4 \cdot 4\text{-}7\text{H}_2\text{O}$, are another example of the most common As-bearing precipitates formed during the treatment of As contaminated water using conventional technologies. These precipitates are stable at $\text{pH} 3\text{-}4$ and have very low solubility ($< 5 \text{ mg/L}$ of As leached during the TCLP test) (Harris, 2000).

Crystalline and high-iron amorphous ferric arsenates are considered the most suitable forms for safe As disposal due to their low solubility under the normal aqueous disposal conditions (Harris, 2000). More recently, the effect of salinity (e.g., SO_4^{2-} , Cl^-) on the stability of As-bearing minerals has been investigated (Liu et al., 2014; Northrup et al., 2018; Xu et al., 2012; Zhang et al., 2020). Unlike, the well-known effect of pH and redox conditions on As release, the relationship between the salinity and the mobility of As from As-bearing minerals remains unclear (Northrup et al., 2018). For example, a minor impact of the presence of SO_4^{2-} (300 mg/L – 3 mM) was observed on the sorption of As(V) on hydrous ferric oxide at pH 5-10 (Meng et al., 2000). This could be explained by the weaker binding affinity of SO_4^{2-} for the ferric oxide compared with As(V) and As(III). The presence of SO_4^{2-} or Cl^- , at concentrations of 1 M, have also shown negligible effect on As desorption from As-bearing Fe-oxyhydroxides (Liu et al., 2014).

Recent studies investigated the use of different sources of Fe(III) including the addition of hematite or magnetite powders as well as its *in-situ* production through the addition of Fe(VI) to promote As(V) precipitation from synthetic effluents and improve the long-term stability of Fe(III)-As(V) precipitates formed (Cai et al., 2019; Iizuka et al., 2018; Prucek et al., 2013). The immobilization of As(V) from a synthetic effluent by scorodite formation was affected by the direct addition of hematite powder, producing coarser faceted scorodite particles (Iizuka et al., 2018). The authors observed the formation of a gel-like precursor from the Fe(II) ions originally present in the synthetic effluent, which convert to a well-crystallized scorodite with the addition of hematite. The stability of the sludge produced through the addition of hematite to a Fe(II)-As(V) containing synthetic effluent seemed to be better under oxic conditions (O_2 blowing for 1 h at pH 3.1) in comparison with a scorodite produced from Fe(III) ions of a hematite precursor (Iizuka et al., 2018).

The addition of magnetite as an *in-situ* Fe-donor was also found to enhance As(V) removal (>99.9%, [As]_i: 10.3 g/L) from a metallurgical waste acid, and to improve formed crystalline scorodite. Indeed, the magnetite pre-dissolution under controlled test conditions (6-h room temperature pre-dissolution, pH 2, 12-h atmospheric reaction at 90°C) produces Fe ions which act as a coagulant for As(V) co-precipitation and as active surface for scorodite nucleation and growth, leading to more crystalline and stable scorodite (Cai et al., 2019). The addition of Fe(VI) in a synthetic effluent containing As(III) or As(V) led to the *in situ* production of nanoparticles of crystalline γ -Fe₂O₃ and γ -FeOOH, improving As removal efficiencies (Prucek et al., 2013). No As(III) was detected in the precipitate formed during the treatment with Fe(VI). A high-resolution X-ray photoelectron spectroscopy coupled with a Fe-Mössbauer spectroscopy showed that a significant proportion (20%) of As removed was incorporated into the crystal structure of the Fe(III)-precipitates formed, while the remaining proportion of the As removed was strongly sorbed onto the surface of Fe(III)-nanoparticles. Based on the species formed during the treatment, the improvement of long-term stability of the sludge was deemed important but no static or kinetic tests were performed to evaluate As mobility.

Table 2.8 Summary of the stability of most common As-bearing precipitates found on As-bearing sludge (adapted from Coudert et al., 2020)

Mineral group	Mineral	Formula	Stability pH range	Solubility (mg/L) in TCLP test	Reference
Ca-arsenate	Wellite	CaHAsO ₄	Unstable under slightly acidic pH (pH <6) and in contact with CO ₂ , HCO ₃ ⁻ and CO ₃ ²⁻ . Require absence of moisture and minimal rain events, suitable for Fe-deficient As-containing wastewaters	>2000	Valenzuela (2000); Zhang et al. (2020)
	Guerinite	Ca ₅ (AsO ₄) ₂ (AsO ₃ OH) ₂ •9H ₂ O		>1000	
	Phamacolie	CaHAsO ₄ •2H ₂ O		>3000	
	Haidingerite	Ca(AsO ₃ OH)•H ₂ O		>3000	
Fe-arsenate	Scorodite	FeAsO ₄ •3.5H ₂ O	Stable at pH around 4-5; As solubilization observed at pH 1 (>10 mg/L) and pH 8 (>100 mg/L)	<5	Harris (2000)
	Jarosite	Fe ₃ (SO ₄) ₂ (OH) ₆	Stable at pH around 6; As solubilization observed at pH 2 after 500 h and at pH 8 after 1500 h	<0.5 from jarosite residue containing 0.5wt% of As	Harris (2000); Kerr et al. (2015)
	Schwertmannite	Fe ₈ O ₈ (OH) _x (SO ₄) _y H ₂ O	Stable at pH near 3; dissolves at acidic pH (pH below 2) and neutral pH (pH above 7)	<0.1	Harris (2000)
	Ferric arsenate	FeAsO ₄ •4-7 H ₂ O	Stable at pH 3-4, suitable for Fe-rich As-containing wastewaters	<5	Harris (2000); Zhang et al. (2020)

2.6.2 Stability of Mn-bearing residue

Precipitation of Mn at high pH (>9) using neutralizing agents (e.g, lime, sodium hydroxide), or the oxidation of Mn(II) to Mn(IV) using strong oxidants (e.g., ozone, sodium hypochlorite, potassium permanganate), followed by the precipitation of Mn(IV)-oxides are among the most applied technologies for Mn removal from mine water (Freitas et al., 2013; Macingova et al., 2016; Neculita and Rosa, 2019). Furthermore, the oxidative precipitation of Mn(II) is known to produce more stable Mn-bearing residue comparatively to the precipitation of Mn(II) at high pH (Watzlaf, 1987). However, the addition of strong oxidants can be costly (Watzlaf, 1987; Watzlaf and Casson, 1990). The sorption of Mn onto reactive surfaces of Fe(III)-hydroxides and MnO₂ at near-neutral pH is also effective for Mn removal (Macingova et al., 2016; Neculita and Rosa, 2019; Watzlaf and Casson, 1990). This section will discuss the different parameters that may affect the stability of the Mn-bearing residue produced from the mentioned treatments. The stability of Mn-bearing residues is strongly influenced by several factors including the pH, the ionic strength, the redox conditions, the sludge aging period, and the treatment method (Butler 2011; Ginder-Vogel and Remucal, 2016; Watzlaf, 1987; Watzlaf and Casson, 1990). Mn-bearing residues generated by precipitation at high pH or sorption onto Fe(III)-hydroxides are quite unstable upon pH decrease (Watzlaf, 1987). Indeed, previous studies highlighted that a slight decrease of the pH led to an important increase in the amount of Mn released from high-pH Mn(II)-precipitates (30% of Mn released at pH 7.5 vs. 78% at pH 6.0) (Watzlaf, 1987). For Mn-bearing sludge originating from the use of strong oxidants (e.g., NaOCl, KMnO₄) during the treatment, their stability seemed to be satisfactory even at pH as low as 3.5 (Watzlaf and Casson, 1990). Ionic strength is another important parameter controlling the stability of Mn-bearing residues.

For example, an increase of Mn release from mine drainage impacted sediments was observed with the increase of the ionic strength of the solution (5.5 mg/kg at 2 M vs. 4.0 mg/kg at 0.7 mM) (Butler, 2009). This increase in Mn release can be explained by an ionic exchange of the metals associated with Fe-hydroxides particles (Butler, 2009). Anaerobic conditions, commonly encountered in tailings impoundment facilities, can affect the stability of Mn-bearing residues, resulting in Mn release through the reductive dissolution of hydrous Mn-oxides (Butler, 2011; Ginder-Vogel and Remucal, 2016; Tobiasson et al., 2016). Generally, Mn-bearing residues seems to become more stable with time (Watzlaf, 1987; Watzlaf and Casson, 1990). A significant decrease of Mn release (-50%) was observed for a 3-month aged Mn-precipitates compared to a fresh one upon pH decrease to 3, for a high-pH Mn precipitate (Watzlaf, 1987). Another study reported that aged residues were found to be more stable when stored in contact with air (aerobic conditions) than under water (anaerobic conditions), even at pH as low as 3. Indeed, a 3% Mn release was observed from the air-aged sludge, while more than 69% of Mn was released from the water-aged sludge stored, while the reason behind the difference in terms of stability has not been clearly stated (Watzlaf and Casson, 1990).

2.6.3 Stability of As- and Mn-bearing residues

Simultaneous removal of As and Mn from contaminated mine water results in the production of sludge containing various precipitates, including Fe(III)-As(V)-hydroxides, Fe(III)-hydroxides and Mn-oxides. Previously, Mn-oxides have been proven efficient sorbent for metal(loid)s removal from contaminated effluents, including As (Ettler et al., 2015; Lafferty et al., 2011). Therefore, it can be expected that some of the As present in the effluent to be treated can sorb onto Mn-oxides formed during the treatment. This section will briefly discuss the stability

of Mn-oxides on which As is sorbed and the conditions that can lead to the release of As or Mn from the sludge produced. The stability of Mn-oxides resulting from As sorption is influenced by several conditions such as: pH, Eh and the presence of competing ions. The release of As from the surface of Mn-oxides decreased by 60% in the neutral pH conditions (pH 6.5-7), whereas its leaching increased in both acidic (pH 3) and alkaline conditions (pH 8) (Ettler et al., 2015). The reductive dissolution of Mn-oxides, occurring under reducing conditions, causes the release of Mn as well as of metal(loid)s adsorbed on their surfaces (Butler, 2011; Ginder-Vogel and Remucal, 2016; Tobiasson et al., 2016). The presence of competing ions such as PO_4^{3-} may compete for the sorption sites on the surfaces of Mn-oxides, leading to the mobilization of previously sorbed As. This can be explained by the fact that PO_4^{3-} ions are chemically similar to the As(V) ions, therefore they have the potential for competing with As for the sorption sites on the Mn-oxides. Lafferty et al. (2011) showed that Ca^{2+} ions also had the potential to re-mobilize As(V) from Mn-oxides, however to a lesser extent compared with PO_4^{3-} ions. This desorption phenomena of As(V) by Ca^{2+} ions was explained by the potential reaction of Ca^{2+} ions with $\delta\text{-MnO}_2$ vacancy sites and edge sites onto which As(V) was firstly adsorbed.

In summary, post-treatment sludge could have variable physical characteristics and chemical composition depending on the applied treatment and the operating parameters used. The evaluation of sludge stability could be challenging. Despite the information available on the stability of As-bearing, Mn-bearing and As-Mn-bearing residues, the stability of these residues produced after the treatment by ECG and Fe(VI) is poorly discussed or documented. Hence, the endeavors of the current study to evaluate the stability of the ECG and Fe(VI) post-treatment sludge could be an original addition to the evaluation of the treatment performances.

CHAPTER 3

METHODOLOGICAL APPROACH

The main objective of this research project was to evaluate the performance (in terms of contaminant removal efficiency, final concentrations of targeted contaminants and pH in regards to the regulation, residual salinity, acute toxicity, stability of the produced sludge and preliminary operating costs) of ECG and Fe(VI) for the simultaneous removal of As and Mn from slightly contaminated synthetic (S_{As} , S_{Mn} , and S_{As+Mn}) and surrogate mine water (E_{low} and E_{high}). To achieve the endeavours of this study, the research approach, illustrated in Figure 3.1, was based on:

- Literature review: focused on the chemistry of As and Mn, their presence in the environment and in mine water, the available technologies for their removal (when present alone or together) including ECG and Fe(VI), the toxicity of treated water as well as the stability of produced sludge (Chapter 2).
- Preparation of single (S_{As} – containing 3.5 mg As/L, S_{Mn} – containing 4.5 mg Mn/L) and binary (S_{As+Mn} – containing 3.5 mg As/L and 4.5 mg Mn/L) synthetic effluents (solutions) from chemical products as well as surrogate mine water (E_{low} and E_{high}) from the washing of mine tailings originating from the Eleonore mine site.
- Application of ECG for the treatment of S_{As} , S_{Mn} , S_{As+Mn} , E_{low} and E_{high} : the main operating parameters tested were CD, ionic strength, and retention time. The acute toxicity of E_{low} and E_{high} towards *D. magna* before and after treatment was assessed (Chapter 4).

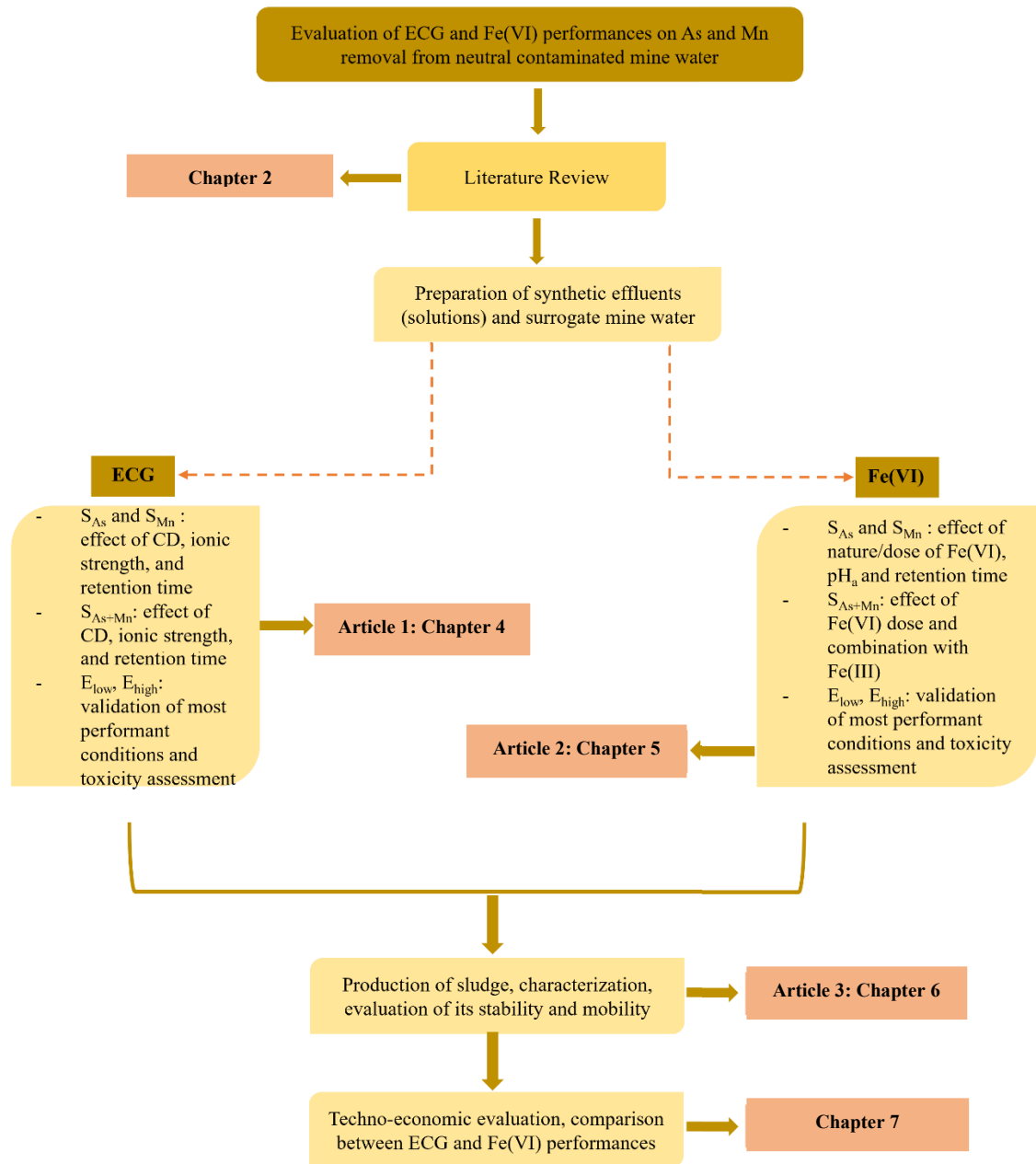


Figure 3.1 Methodological approach used in this thesis project

- Evaluation of the performance of Fe(VI) alone or in combination with Fe(III) salt for the removal of As and Mn from S_{As} , S_{Mn} , S_{As+Mn} , E_{low} and E_{high} : the effect of Fe(VI) nature/dose, the adjusted pH (pH_a) and the retention time on both As and Mn removal from synthetic effluents was evaluated. The most performant conditions were applied to the surrogate mine water (E_{low} and E_{high}) and the acute toxicity of untreated and treated effluent towards *D. magna* was evaluated (Chapter 5).
- Evaluation of the mobility of As and Mn from the sludge produced from ECG and Fe(VI) treatment of the surrogate mine water (E_{high}). A mineralogical and chemical characterization of the sludge produced from ECG and Fe(VI) treatment was performed using scanning electron microscope equipped with an energy dispersive spectrometer (SEM-EDS) and powder X-ray diffraction (PXRD) techniques, in addition to chemical composition and parallel extraction. The potential mobility of As and Mn from the produced sludge was also evaluated using a field leaching test (FLT) to evaluate its short-term stability (Chapter 6).
- Lastly, a preliminary techno-economic analysis of ECG and Fe(VI) treatment was performed. The performances of ECG and Fe(VI) in terms of contaminants removal efficiencies, respect of final effluent quality with regulations, residual salinity, toxicity of final effluent, sludge stability and treatment costs were then compared to define the most promising technology for the simultaneous removal of As and Mn from circum-neutral mine water (Chapter 7).

3.1 Preparation of synthetic and surrogate mine water

The first series of experiments, aimed to optimize the operating parameters for both ECG and Fe(VI) treatments, were executed using synthetic effluents of simple composition. Three synthetic effluents were prepared by dissolving the required amount of NaAsO₂ and MnSO₄·H₂O: (i) S_{As} containing only 3.5 mg As/L; (ii) S_{Mn} containing only 4.5 mg Mn/L and (iii) S_{As+Mn} containing 3.5 mg As/L and 4.5 mg Mn/L. Before each ECG test, the electrical conductivity (EC) of the effluent was adjusted by adding sodium chloride salt (NaCl). For ECG and Fe(VI), the most performant operating conditions identified using single and binary synthetic effluents were tested on surrogate mine water, which was prepared from the washing of desulfurized and filtered mine tailings using deionized water (S/L: 1/1). Two surrogate mine water were prepared: (1) the first one is the unspiked effluent (E_{low}) containing lower concentrations of As and Mn than the targeted concentrations with synthetic effluents, and (2) the second effluent is the spiked effluent (E_{high}). For E_{high}, required amounts of NaAsO₂ and MnSO₄·H₂O were added to obtain As and Mn concentrations similar to the synthetic effluents (S_{As}, S_{Mn} and S_{As+Mn}). For each series of experiments, synthetic effluents and surrogate mine water were characterized to determine their physicochemical parameters (pH, ORP, EC), before and after treatment. Metal(loid)s concentrations were determined using an inductively coupled plasma-optical emission spectroscopy (ICP-OES - Agilent 5800-Vertical Dual View, Canada). For E_{low} and E_{high} only, the concentrations of anionic species (i.e., SO₄²⁻ and Cl⁻) were determined using an ion chromatography (IC - Metrohm 940 Professional IC Vario, Switzerland).

3.2 Electrocoagulation (ECG)

ECG experiments were performed in a 2 L Pyrex reactor (Fig. S4.2) equipped with 2 Fe-electrodes (D): 10 mm) connected to a DC power supply. During the ECG treatment, air was injected to maintain a dissolved oxygen (DO) content around 8-9 mg/L, while the agitation was continuously fixed at 200 rpm. The tests were run for 60 min, followed by 30 min of settling (to favor solid to liquid separation by decantation). Later, a 5 mL sample was taken to analyze Fe(II) by UV-VIS spectroscopy at 507 nm using the 1,10-phenanthroline complexation method (Christian, 1994). For metal(loid)s analyses by ICP-OES, samples were filtered (porosity: 0.45 μm) and acidified (2% HNO_3), before and after the treatment.

The first series of tests ($n = 26$) was performed to investigate the effect of selected operating parameters (CD: 0.25-10 mA/cm^2 , ionic strength: 0.25, 1.5 and 2.5 mS/cm , retention time: 0-60 min) on the removal of As and Mn from S_{As} and S_{Mn} , respectively. A set of triplicate tests was conducted to evaluate the reproducibility of the treatment at 0.5 mA/cm^2 for S_{As} and 2 mA/cm^2 for S_{Mn} and at ionic strength of 0.25 and 2.5 mS/cm . In addition, one test was realized with an inter-electrode distance of 50 mm to assess the effect of D on the removal efficiency of As and Mn from S_{As} and S_{Mn} and on the reaction kinetics.

The second series of tests ($n = 4$) was done to evaluate the performance of ECG treatment for the simultaneous removal of As and Mn from $S_{\text{As+Mn}}$. The tests were conducted under the following conditions, which were identified from the previous experiments performed on S_{As} and S_{Mn} : (i) CD of 0.5 and 2 mA/cm^2 ; (ii) ionic strength of 0.25 and 2.5 mS/cm , (iii) D of 10 mm, (iv) retention time of 60 min, (v) pH_a of 6.0-6.50. Samples were collected, before and after treatment, for metal(loid) analyses by ICP-OES.

The third series of experiments ($n = 1$) was conducted on the surrogate mine water (E_{low} and E_{high}) to evaluate the performances of the most performant treatment parameters identified previously with $S_{\text{As+Mn}}$ (CD: 2 mA/cm², D: 10 mm and retention time: 60 min) on “real” effluents. Samples were collected before and after the treatment of E_{low} and E_{high} for: (i) metal(loid) analyses by ICP-OES, (ii) anions analyses by IC, and (iii) toxicity assessment to *D. magna*.

Lastly, a series of tests ($n = 10$) was conducted with E_{high} to produce enough amount of sludge for chemical and mineralogical characterization (5 g) and the evaluation of contaminant mobility through FLT (1 g - further details in Section 3.4).

3.3 Ferrate

Fe(VI) experiments were performed in 750 mL beakers installed on a jar tester to control the agitation during the reaction (fast agitation at 250 rpm) and the flocculation (slow agitation at 60 rpm) (Fig. 3.2a). For each series of experiments performed with Fe(VI) only (Fig. 5.1a), the required dose of Fe(VI) was added to the solution to be treated and mixed vigorously for 3 min before adjusting the pH at the desired value. Then, the mixing agitation was slow down to 60 rpm and the pulp was mixed for 20 min. Then, the agitation was stopped, and the solution was let to settle for 30 min before to collect the supernatant for analyses. For the experiments performed with Fe(VI) and Fe(III), the same procedure was followed, except that Fe(III) was added to the solution after the 3-min fast mixing and before the adjustment of the pH to the desired value (Fig. 5.1b)

The first series of experiments ($n = 17$) was conducted using *in-situ* prepared wet or solid Fe(VI), named Fe(VI)_w and Fe(VI)_s respectively, to evaluate the performance of Fe(VI) for the removal of As and Mn from S_{As} and S_{Mn}. In this series of experiments, the effect of Fe(VI) type (wet vs. solid) and dose (14-56 mg Fe(VI)/L for S_{As} and 2-7 mg Fe(VI)/L for S_{Mn}), as well as pH_a (5.5 and 6.0 for S_{As} vs. 5.5 and 6.5 for S_{Mn}), reaction time (0-20 min) and settling time (15 and 30 min) on the removal of As and Mn was assessed. Additional tests were performed using Fe(VI)_s to select the optimal dose for the efficient removal of As and Mn. Later, the tests were realized in triplicate using Fe(VI)_s at the most performant Fe(VI)_s dose (22 mg/L for As, 5 mg/L for Mn), pH_a 5.5, 5 min reaction time and 15 min settling time to evaluate the reproducibility of the Fe(VI) treatment.

The second series of experiments ($n = 10$) was executed to evaluate the performance of Fe(VI)_s at several doses (5-28 mg/L) for the removal of As and Mn from S_{As+Mn}. Due to the high dose of Fe(VI)_s (28 mg/L) required for the efficient and simultaneous removal of As and Mn, the addition of an external source of Fe(III) (Fe₂(SO₄)₃) as a supplementary coagulant was tested at several doses (6, 8 and 10 mg Fe(III)/L).

For the third series of experiments ($n = 1$), the most performant treatment conditions using Fe(VI)_s+Fe(III) (12.5 mg Fe(VI)_s/L + 8 mg Fe(III)/L, pH_a 5.5, 5 min reaction time and 15 min settling time) were applied for the treatment of surrogate mine water (E_{low} and E_{high}). Samples were collected, before and after treatment, to evaluate the effect of Fe(VI) treatment on the toxicity of water on *D.magna* before and after treatment.

Lastly, a series of 4 experiments was conducted, using a 20L-bucket equipped with a mechanical stirrer (Figure 3.2b), on E_{high} using the most performant conditions to produce enough sludge (3 g) for its physicochemical and mineralogical

characterization as well as for the evaluation of As and Mn release from produced sludge using FLT (further details in Section 3.4).

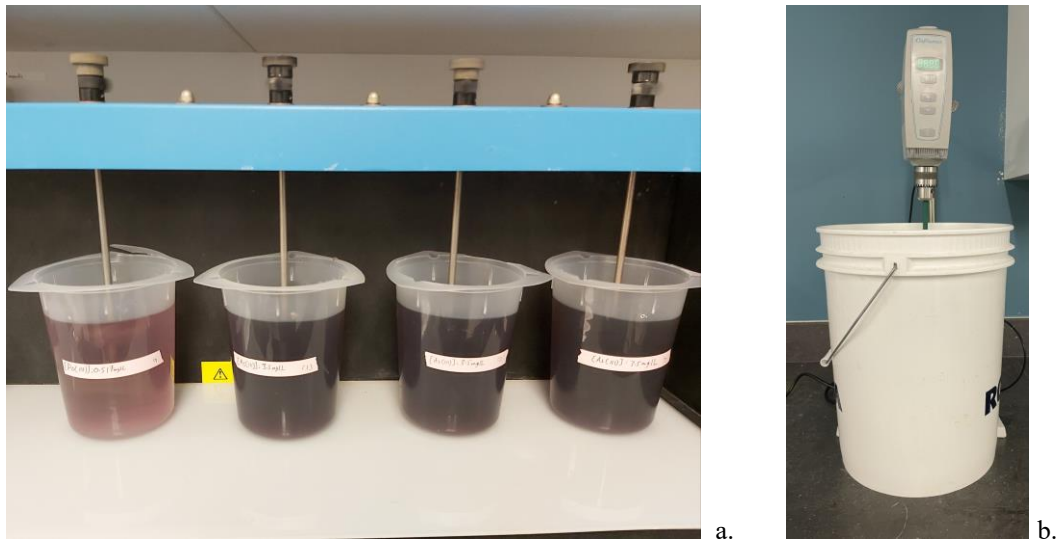


Figure 3.2 Jar test setup (a) and 20 L-bucket experimental setup (b) used for Fe(VI) sludge production

3.4 Sludge characterization and mobility of As and Mn from the sludge

Several experiments using ECG and Fe(VI) treatments were performed to treat E_{high} and to produce the required amounts of the sludge for further physicochemical and mineralogical characterization as well as the evaluation of the potential mobility of As and Mn from the sludge using a static test (FLT).

First, the chemical composition of the sludge produced from ECG and Fe(VI) treatment was determined using microwave-assisted acid digestion followed by ICP-MS analysis in an external laboratory. A mineralogical characterization of the sludge produced was carried out using various techniques (scanning electron microscopy-energy dispersive X-ray spectroscopy - SEM-EDS and powder X-ray diffraction - XRD) to better understand the mechanisms involved during the removal of As and Mn from surrogate mine water using ECG and Fe(VI) treatments and their potential release from the sludge with time. A geochemical simulation was done using the software PHREEQC to identify the secondary minerals that can be formed during Fe(VI) and ECG treatments and compare the results obtained using the mineralogical characterization.

Second, a parallel selective extraction procedure was used to determine the speciation of As and Mn in the sludge produced and, therefore, better understand the potential mechanisms involved in As and Mn removal during the treatments. By identifying if As and Mn were bound to poorly-crystalline/amorphous Fe-(hydr)oxides, adsorbed or co-precipitated on/with crystalline Fe-(hydr)oxides, this parallel extraction procedure also give information about the potential release of these contaminants with time (Rakotonimaro et al., 2021). The potential mobility of As and Mn from the produced sludge was also assessed using the FLT procedure (Hageman, 2007). This fast (5 min), efficient and simple test was developed by the U.S Geological Survey (USGS) to evaluate the potential leaching of contaminants, including metalloids, from solid mine waste.

3.5 Preliminary techno-economic evaluation of ECG and Fe(VI) treatment and comparison of their performances

A preliminary techno-economic analysis was performed for the ECG and Fe(VI) processes developed in the present study to estimate the operating costs. The values of all variables used for the determination of preliminary operating costs as well as the price for unit of consumables are presented in Tables 3.1 and 3.2, while the calculations are detailed in the following sub-sections. It should be noted that for simplification the costs related to the air injection as well as for the purchase of the equipment (e.g., tanks, settlers, pumps) and the space needed to implement the technologies were not considered.

3.5.1 Techno-economic evaluation of ECG treatment

For the ECG treatment, the operating costs (OC) were estimated in terms of energy consumption (C_{energy}), reagents requirements for pH adjustment before the treatment (C_{reagent}) and sacrificial Fe-electrodes consumption ($C_{\text{electrodes}}$) according to Equation 3.1.

$$\text{OC } (\$/\text{m}^3) = C_{\text{energy}} (\$/\text{m}^3) + C_{\text{reagent}} (\$/\text{m}^3) + C_{\text{electrodes}} (\$/\text{m}^3) \quad \text{Eq. 3.1}$$

Table 3.1 Variables considered for the estimation of preliminary operating costs for ECG and Fe(VI) treatment of circumneutral mine water contaminated by As and Mn

Parameter	Amount required	Unit
<u>ECG</u>		
<u>Energy</u>		
Current intensity	0.25	A
Voltage	2	V
Reaction time	1	h
Treated volume	0.0018	m ³
Energy required	0.28	kWh/m ³
<u>Neutralizing agent</u>		
Quantity of HCl used	0.034	mL
Volume treated	0.0018	m ³
<u>Electrodes</u>		
Type of electrode	Fe	
Amount of electrode	0.15	kg Fe/m ³
<u>Fe(VI)</u>		
Reaction time	8	min
Treated volume	10	L
<u>Reagents</u>		
Solid Fe(VI)	827	mg
Fe(III) salt	712	mg
Deionized water-Fe(VI) solution	210	mL
Deionized water-Fe(III) solution	80	mL
H ₂ SO ₄	0.108	mL
NaOH	3.2	mg
<u>Equipment</u>		
Flow rate	100	m ³ /day
Reservoir volume	0.67	m ³
Reservoir cost	75 026	\$/m ³
Total volume of effluent to be treated for 10 years	365,000	m ³

Table 3.2 Variables considered for the estimation of preliminary operating costs for ECG and Fe(VI) treatment of circumneutral mine water contaminated by As and Mn

Consumable	Formula	Unitary price	Unit	Reference
<u>Reagents</u>				
Hydrochloric acid	HCl	0.23	\$/kg	Zuorro et al. (2021)
Solid ferrates	K ₂ FeO ₄	30	\$/kg	Thimons et al. (2022); Quino-Favero et al. (2018)
Fe(III) salt	Fe ₂ (SO ₄) ₃	0.4	\$/kg	Turan et al. (2023)
Sodium hydroxide	NaOH	0.25	\$/kg	Turan et al. (2023)
Sulfuric acid	H ₂ SO ₄	0.76	\$/kg	Turan et al. (2023)
<u>Other</u>				
Water	-	0.5	\$/m ³	
Electricity	-	0.3	\$/kWh	Dubuc et al. (2022)

Considering that hydroelectricity is the main source of electricity in Canada, the costs related to the consumption of energy (C_{energy}) were calculated by accounting for the price per unit of hydroelectricity ($\text{PPU}_{\text{hydro}}$) following Equation 3.2.

$$C_{\text{energy}} (\$/\text{m}^3) = E_{\text{cell}} \times I \times t \times \text{PPU}_{\text{hydro}} / (V \times 1000) \quad \text{Eq. 3.2}$$

Where E_{cell} is the cell voltage (V), I is the current (A), t is the retention time (h), V is volume of effluent to be treated (m³) and $\text{PPU}_{\text{hydro}}$ is the price for unit of hydroelectricity (\$/kWh)

Reagent costs (HCl used for the adjustment of the pH of the effluent to be treated) were estimated following Equation 3.3.

$$C_{\text{reagent}} (\$/\text{m}^3) = m_{\text{reagent}} \times \text{PPU}_{\text{HCl}} / V \quad \text{Eq. 3.3}$$

Where m_{reagent} is the mass of reagent required (kg), PPU_{HCl} is the price per unit of HCl (\$/kg – Zuorro et al., 2021) and V is volume of effluent to be treated (m³)

Costs related to the consumption of sacrificial Fe-electrodes were estimated following Equation 3.4 (Ebba et al., 2021).

$$C_{\text{électrode}} (\$/\text{m}^3) = I \times t \times M \times \text{PPU}_{\text{électrode}} / (n \times F \times V \times 1000) \quad \text{Eq. 3.4}$$

Where I is the current (A), t is the retention time (s), M is the molecular mass of Fe (55.85 g/mol), $\text{PPU}_{\text{électrode}}$ is the price for unit of hydroelectricity (\$/kWh), n is the number of electrons transferred, F is the Faraday's constant (96 500 C/mol) and V is volume of effluent to be treated (m^3)

3.5.2 Techno-economic evaluation of Fe(VI) treatment

The operating costs for the treatment of circumneutral mine water contaminated by As and Mn using Fe(VI) + Fe(III) were estimated in respect to the consumption of reagents used (i.e., Fe(VI), Fe(III), H_2SO_4 and NaOH) as well as the consumption of water required for the preparation of the stock solutions of Fe(VI)_s and Fe(III). The capital costs related to the acquisition of the tanks for the treatment were estimated for a plant unit with a capacity of 100 m^3/d (0.06\$/ m^3) and 1 000 m^3/d (0.02 \$/ m^3), with an equipment lifetime of 10 years. The costs of reagents were estimated following the Equation 3.5.

$$C_{\text{reagent}} (\$/\text{m}^3) = m_{\text{reagent}} \times \text{PPU}_{\text{reagent}} / V \quad \text{Eq. 3.5}$$

Where m_{reagent} is the mass of reagent required (kg), $\text{PPU}_{\text{reagent}}$ is the price per unit of the reagent ($\$/\text{kg}$) and V is volume of effluent to be treated (m^3)

3.5.3 Comparison of ECG and Fe(VI) performances

Several criteria were defined to evaluate and compare the performances of ECG and Fe(VI) for the treatment of As- and Mn-contaminated circumneutral mine water including: (1) the removal efficiency of As and Mn; (2) the requirements in terms of physicochemical regulations (i.e., final pH and As content); (3) the residual salinity; (4) the toxicity of final effluent, (5) the amount of produced sludge; (6) the potential mobility of As and Mn from the sludge (using FLT results) and (7) the operating costs. As previously mentioned, the efficient removal is assessed in respect to the final contaminant concentration that complies with the selected guidelines or regulations. For As, the guideline applied in the current study is a final concentration $< 0.20 \text{ mg/L}$ (Directive 019, 2012), while for Mn which is not regulated in most countries, the criteria is $< 2 \text{ mg/L}$ (U.S. Code of Federal Regulations (US CFR, 1985). Because of its effect on toxicity to aquatic organisms, salinity is a variable to be considered in evaluating treatment performance, but to a lesser extent compared to other criteria, because this criterion is already included in the toxicity assessment. The amount of produced sludge is an important parameter to consider for a performant treatment, because of challenges associated to its handling and long-term storage, while its stability is another important criterion as produced sludge could become a secondary source of contamination if not properly managed.

CHAPTER 4

EFFICIENCY OF ELECTROCOAGULATION FOR SIMULTANEOUS TREATMENT OF AS AND MN IN NEUTRAL MINE WATER

EFFICACITÉ DE L'ÉLECTROCOAGULATION POUR L'ENLÈVEMENT SIMULTANÉ DE L'AS ET DU MN PRÉSENTS DANS LES EAUX MINIÈRES

Reem Safira¹, Lucie Coudert^{1, *}, Carmen M. Neculita¹, Eric Rosa^{1, 2}

¹Research Institute on Mines and Environment (RIME), University of Québec in
Abitibi-Témiscamingue (UQAT), Rouyn-Noranda, QC, Canada

²Groupe de Recherche sur l'Eau Souterraine (GRES - Groundwater Research Group),
RIME, UQAT, Amos, QC, Canada

This article has been published in Minerals Engineering
(<https://doi.org/10.1016/j.mineng.2023.108546>)

4.1 Abstract

Despite the efficiency and ease of implementation of electrocoagulation (ECG), its industrial application for the treatment of contaminated mine water is limited due to high energy and electrode consumption. The main objective of the present study was to identify the most performant ECG conditions using Fe-electrodes for the simultaneous removal of As(III) and Mn(II) from synthetic and surrogate neutral mine water, while limiting energy and electrode consumption. Treatability tests were performed on i) single synthetic effluents containing only 3.5 mg/L As (S_{As}) or 4.5 mg/L Mn (S_{Mn}), ii) binary synthetic effluents containing both As and Mn (S_{As+Mn}), and iii) surrogate mine water (E_{low} and E_{high}). The effect of current density (CD), ionic strength, and retention time were first evaluated for the treatment of S_{As} , S_{Mn} , and S_{As+Mn} . Then, the most performant conditions were used to treat E_{low} and E_{high} . The toxicity to *Daphnia magna* of E_{low} and E_{high} was evaluated before and after ECG treatment. The results showed that the increase of CD from 0.25 to 10 mA/cm² greatly improved the removal of Mn and to a lesser extent of As, as well as energy and electrode consumption. Despite a negligible effect on the removal efficiency of As and Mn, the ionic strength (from 0.25 to 2.5 mS/cm) and inter-electrode distance (from 10 to 50 mm) strongly affected the energy consumption. Results showed that ECG efficiently removed As (>97%) from S_{As} at low CD (0.5 mA/cm²), while Mn required a four-fold higher CD to achieve satisfactory removal (>60%) from S_{Mn} . For the treatment of S_{As+Mn} , As removal was more efficient and faster than Mn removal (99 vs. 60% and 20 vs. 60 min, respectively) at a CD of 2.0 mA/cm². However, the simultaneous removal of As and Mn at 2.0 mA/cm² produced a volume of sludge 3.3 times greater than at 0.5 mA/cm². Lastly, high As (99%) and variable Mn (40–57%) removal efficiencies were obtained after E_{low} and E_{high} treatment, with potential positive effect of the presence of Ca²⁺ and Cl⁻ on the removal of As, while SO₄²⁻ may

have negatively affected the removal of Mn. After ECG treatment, no addition of toxicity to *D. magna* was observed for E_{low} and E_{high} . The outcomes of this study may provide promising insights for the application of ECG for simultaneous removal of metal(loid)s from contaminated mine water.

Keywords: electrochemical treatment, advanced oxidation process, metal(loid)s removal, toxicity, contaminated mine water.

4.2 Résumé

Bien que l'électrocoagulation (ECG) soit efficace et facile à mettre en place, son utilisation à l'échelle industrielle pour le traitement des eaux minières contaminées est limitée en raison de la consommation d'énergie et des électrodes élevée. L'objectif principal de cette étude était d'identifier les conditions opératoires les plus efficaces du traitement ECG en présence d'électrodes en Fe pour enlever simultanément l'As(III) et le Mn(II) présents dans des eaux minières synthétiques et de substitution, tout en réduisant la consommation d'énergie et des électrodes sacrificielles. Des tests de traitabilité ont été effectués sur : (i) des effluents synthétiques simples contenant seulement 3,5 mg/L d'As (S_{As}) ou 4,5 mg/L de Mn (S_{Mn}), (ii) des effluents synthétiques binaires contenant à la fois de l'As et du Mn (S_{As+Mn}), et (iii) des eaux minières de substitution (E_{faible} et $E_{elevé}$). Premièrement, l'effet de la densité de courant (DC), de la force ionique et du temps de rétention a été évalué pour le traitement de S_{As} , S_{Mn} et S_{As+Mn} . Ensuite, les conditions les plus performantes ont été utilisées pour traiter E_{faible} et $E_{elevé}$. La toxicité de E_{faible} et $E_{elevé}$ pour *Daphnia magna* a été évaluée avant et après le traitement par ECG. Les résultats ont montré que l'augmentation de la DC de 0,25 à 10 mA/cm² améliorerait considérablement l'enlèvement du Mn et dans une moindre mesure de l'As, ainsi que la consommation d'énergie et des électrodes sacrificielles. En dépit d'un effet négligeable sur l'efficacité d'enlèvement de l'As et du Mn, la force ionique (de 0,25 à 2,5 mS/cm) et la distance inter-électrodes (de 10 à 50 mm) ont fortement affecté la consommation d'énergie. Les résultats ont indiqué que l'ECG enlevait efficacement l'As (> 97 %) de S_{As} à faible DC (0,5 mA/cm²), tandis que le Mn nécessitait une DC quatre-fois plus élevée pour obtenir un enlèvement satisfaisant (>60 %) pour le traitement de S_{Mn} . Pour le traitement de S_{As+Mn} , l'enlèvement de l'As était plus efficace et plus rapide que celui du Mn (99 contre 60% et 20 contre 60 min, respectivement) à une DC de 2,0 mA/cm². Néanmoins, l'enlèvement simultané de l'As

et du Mn à 2,0 mA/cm² a produit un volume de boues 3,3 fois supérieur à celui obtenu lors du traitement à 0,5 mA/cm². Enfin, des efficacités d'enlèvement élevées de l'As (99%) et variables du Mn (40 à 57%) ont été obtenues après le traitement de E_{faible} et E_{élevé}, avec un effet positif potentiel de la présence de Ca²⁺ et Cl⁻ sur l'enlèvement de l'As, tandis que le SO₄²⁻ peut avoir affecté négativement l'enlèvement du Mn. Après le traitement par ECG, aucun ajout de toxicité pour *D. magna* n'a été observé pour E_{faible} et E_{élevé}. Les résultats de la présente étude peuvent fournir des connaissances prometteuses pour l'application de l'ECG pour l'enlèvement simultané des métaux/métalloïdes présents dans les eaux de minières contaminées.

Mots clés: traitement électrochimique, procédé d'oxydation avancé, enlèvement des métaux/métalloïdes, toxicité, eau minière contaminée.

4.3 Introduction

Mining activities produce large volumes of mine water contaminated by metal(loid)s, requiring performant treatment to meet increasingly stringent regulations for their discharge to the environment (Ryskie et al., 2021; Shahedi et al., 2023). Arsenic and manganese, which can be toxic to humans and aquatic ecosystems at moderate to high concentrations, are common contaminants in gold mine effluents (Thakur et al., 2021). Due to its efficiency (50–99%) and ease of implementation, (co-)precipitation is the most commonly used treatment to remove As or Mn from mine water (Coudert et al., 2020; Neculita and Rosa, 2019). However, large amounts of chemicals are required, leading to increased residual salinity and associated toxicity (Gonçalves et al., 2007; Van Dam et al., 2014). Furthermore, different pH conditions (4–7 for As vs. 9–11 for Mn) and contradictory Fe concentrations (Fe/contaminant ratio $>4/1$ for As vs. $<4/1$ for Mn) are required for optimal treatment, leading to major hurdles for the removal of both As and Mn by (co-)precipitation (Bora et al., 2018; Chang et al., 2006; Habib et al., 2020; Safwat et al., 2023). Therefore, improved methods for the simultaneous treatment of As and Mn from mine water, while decreasing the consumption of chemicals and associated residual salinity, are still necessary.

Combining electrochemistry and coagulation, electrocoagulation (ECG) has proven effective for the removal of (in-)organic contaminants from contaminated groundwater and wastewater from different sources including domestic, hospital, pulp and paper as well as brewery, automobile and mining industries (Boinpally et al., 2023; Gilhotra et al., 2018; Kobya et al., 2020; Müller et al., 2021; Shahedi et al., 2023; Shahreza et al., 2018). A recent and relevant review on the use of ECG for the treatment of contaminated mine water showed that most of the studies focused on the removal of sulfates, iron and/or total suspended solids from mine water, while only few of them

documented the removal of As and Mn (Table S4.1) (Shahedi et al., 2023). ECG treatment is based on redox reactions leading to the in-situ production of cations (e.g., Fe^{3+} , Al^{3+}) at the anode as a result of electrical dissolution of the sacrificial electrode, that act as a coagulant, and OH^- ions at the cathode, that neutralize the acidity and favor the precipitation of metal hydroxides (McBeath et al., 2021; Kobya et al., 2022; Safwat et al., 2023). The mechanisms involved in As removal are well documented, and include (co-)precipitation and sorption on newly formed Fe- or Al-hydroxides (Fig. S4.1) (Kobya et al., 2022; Li et al., 2012). For Mn, the removal mechanisms are less understood but are known to mainly depend on the electrode material and the final pH (Oncel et al., 2013; Shafaei et al., 2010). The precipitation of $\text{Mn}(\text{OH})_2$ at $\text{pH} > 7$, sorption on Al-, Ti- or Fe-hydroxides produced in-situ, trapping (sweep coagulation) by these hydroxides, or deposition on the cathode surface are among the proposed mechanisms for Mn removal by ECG (Oncel et al., 2013; Shafaei et al., 2010; Xu et al., 2017). The presence of Cl^- in the effluent may enhance the oxidation of Mn(II) to Mn(IV), and eventually favors precipitation of MnO_2 (Xu et al., 2017). Fe- and Al-electrodes are mainly used for the removal of As, while Al-, Ti- electrodes and to a lesser extent Fe-electrodes are generally recommended for Mn (Hakizimana et al., 2017; Moussa et al., 2016; Reátegui- Romero et al., 2018; Safwat et al., 2023; Shahreza et al., 2018). Despite its efficiency in removing (in-)organic contaminants, including As and Mn, from contaminated wastewater, the main drawbacks of ECG limiting its industrial application are related to the operating costs (0.25-3.88 US\$/ m^3) and the need to reduce energy and electrode consumption (Kobya et al., 2014, 2020; Shahedi et al., 2023; Touahria et al., 2016).

Previous studies evaluated the effect of operating factors on the removal efficiencies of As and Mn from synthetic or real mine water (Table S4.1), while only few of them deals with their impact on the consumption of energy and sacrificial electrodes and therefore associated operating costs (Ebba et al., 2021; Shahedi et al., 2023; Thakur and Mondal, 2016). Current density (CD) and pH are among the main operating factors

influencing As and Mn removal using ECG. The CD is known to control the amount of soluble metal produced from anode electro-dissolution as well as the production rate of gas bubbles, and the size and growth of the flocs. Optimal CD identified in previous studies ranges from 0.3 to 70 mA/cm² (mainly between 5 and 15 mA/cm²) (Table S4.1), depending on the water quality (Banerji and Chaudhari, 2016; Nariyan et al., 2017; Moussa et al., 2016). ECG shows better As removal efficiencies under slightly acidic to neutral conditions since electro-dissolution of sacrificial Fe- and Al-electrodes is higher under acidic conditions, producing larger amounts of coagulant and Fe- or Al- hydroxides; in contrast, Mn removal is more efficient under neutral to slightly alkaline conditions (Balasubramanian et al., 2009; Kobya et al., 2011; Lakshmanan et al., 2009). Inter-electrode distance (D) usually ranges between 5 and 30 mm (Gatsios et al., 2015; Sahu et al., 2014), although this distance can be increased to 90 mm without affecting the removal efficiency of arsenic from sulfate-chloride spent brine (Li et al., 2023). The addition of an electrolyte (e.g., NaCl) to increase the electrical conductivity (EC) and to limit the electrode passivation and energy consumption is common practice during the ECG process, even if this increases the operating costs related to the consumption of this chemical and the volume of sludge produced (Gomes et al., 2007, Shafaei et al., 2010; Touahria et al., 2016; Ucar et al., 2013). The amount of added electrolyte is correlated with the targeted EC. For instance, 4 g/L NaCl was used to remove As from a synthetic effluent to limit the formation of a passivation layer on the Al-electrodes (Hansen et al., 2007) or to increase EC and decrease passivation of the steel anode (Gomes et al., 2007). Only few studies evaluated the performances of ECG for the treatment of neutral contaminated water at low ionic strength (< 1.5 mS/cm), without the addition of supporting electrolyte (Touahria et al., 2016). Previous studies documented that the co-occurrence of As and other ions (i.e., F⁻, hydrated silica, sulfates) influenced the removal of As from contaminated groundwater using ECG, due to competition for sorption sites on Fe-hydroxides, but there is no information related to the co-occurrence of As and Mn and their impact on the performances of ECG in terms of removal efficiencies as well

as energy and electrode consumption (Kabya et al., 2020, Thakur and Mondal, 2016; Valentin-Reyes et al., 2022). Nevertheless, despite a scientific understanding of the effects of CD, pH, and EC on ECG treatment, the identification of the most performant operating conditions for the simultaneous removal of As and Mn from contaminated mine water as well as on energy and electrode consumption is still ongoing.

Further to the challenges highlighted above, acute and chronic toxicity assessments have become a requirement for mine water discharge in several legislations. In the Canadian context, acute toxicity must be assessed on water fleas (*Daphnia magna*) and rainbow trout (*Oncorhynchus mykiss*) in both Quebec's provincial and federal legislation (MELCC, 2012; Ministry of Justice, 2021). However, toxicity assessment of water treated by ECG is poorly documented, while inconsistencies on the effects of ECG on toxicity persist (Foudhaili et al., 2020a; Lach et al., 2022; Radić et al., 2014). For example, a decrease in the lethality of *D. magna* has been observed after the ECG treatment of a synthetic textile effluent contaminated by azo dye (EC_{50%} of 5.87% for untreated and 40.2% for treated effluent) (Lach et al., 2022). Conversely, an increase in toxicity (immobility and mortality) towards *Daphnia magna* and *Daphnia pulex* was reported after the treatment of sulfate-rich mine drainage using ECG, although the cause is still to be elucidated (Foudhaili et al., 2020a).

In this context, the main objective of the present study was to evaluate the performance of ECG for the simultaneous removal of As(III) and Mn(II) from circumneutral low-contaminated synthetic and surrogate mine water, including a toxicity assessment of untreated and treated water. To the best of the authors' knowledge, although the removal of As and Mn using ECG have been studied with different quality of wastewater, there is no study investigating the effect of operating conditions on the simultaneous removal of As and Mn from circumneutral mine water, including the determination of energy and electrode consumption as well as the amount of sludge produced and the toxicity of the final effluent.

4.4 Materials and methods

4.4.1 Preparation and characterization of mine water

A combination of synthetic and surrogate mine water was used. Synthetic effluents containing only As (S_{As} ; 3.5 mg/L) or Mn (S_{Mn} ; 4.5 mg/L), or both contaminants (S_{As+Mn} ; 3.5 mg/L As + 4.5 mg/L Mn) were prepared from stock solutions (50 mg/L each) of $NaAsO_2$ (99% purity, Sigma-Aldrich) and $MnSO_4 \cdot H_2O$ (99%, Laboratory MAT). Because stock solutions were prepared before each series of experiments, small variations in terms of initial As and Mn concentrations can be observed. However, such variations are expected on industrial mine site. The composition of the synthetic effluents was based on a previous characterization of real mine water ($n = 292$, from 2016 to 2021) from an active mine site located in Northern Quebec (Safira et al., 2023). Before each ECG test, the pH and EC of the synthetic effluents were adjusted to 6.0–6.5 using NaOH or HCl (1 M) and to 0.25–2.5 mS/cm using NaCl, respectively. Surrogate mine water was prepared by rinsing desulfurized and filtered tailing samples, collected from the mine site on which the synthetic effluents were based, with water (solid/liquid ratio of 1/1) to produce an effluent representative of the mine drainage occurring on the site. Two surrogate mine water samples, E_{low} and E_{high} , were prepared for ECG testing. E_{low} (unspiked surrogate effluent) initially contained 1.43 mg/L As and 0.05 mg/L Mn. For E_{high} (spiked surrogate effluent), required amounts of $NaAsO_2$ and $MnSO_4 \cdot H_2O$ salts were added to yield 3.5 mg/L and 4.5 mg/L for As and Mn, respectively.

4.4.2 ECG treatment

4.4.2.1 ECG experimental set-up

ECG experiments were conducted in a 2 L Pyrex reactor (Fig. S4.2). Two iron electrodes (dimensions: 110 mm × 110 mm × 2 mm; total submerged area: 121 cm²; purity: ≥99.5%) were connected to a DC power supply (ARKSEN 605D, USA; voltage: 0–30 V; electrical current: 0–10 A). The interelectrode distance (D) was fixed at 10 mm. Before each experiment, the electrodes were abraded with sandpaper, dipped in 10% HCl for 10 min, and then cleaned with tap water and deionized water. The dried electrodes were weighed before and after each test to measure the mass loss, which is correlated to the amounts of soluble metals resulting from anode electro-dissolution. All experiments were conducted at ambient (~22°C) temperature. The working volume was fixed at 1.8 L. During treatment, the effluent was mixed continuously at a speed of 200 rpm using a digital stirrer (Fig. S4.2). Air was injected in the system during the ECG treatment to maintain a dissolved O₂ content around 8–9 mg/L and to avoid reducing conditions (Fig. S4.2). After 1 h of ECG treatment, treated effluents were left to settle for 30 min into a 250 mL-graduated cylinder. After 30 min of settling, the volume of wet sludge was measured. The supernatant was then collected, filtered for Fe(II) analyses, and acidified for inductively coupled plasma optical emission spectroscopy (ICP-OES) analyses for As, Mn, and total Fe. The produced sludge was air-dried for 24 h to determine the amount of dry sludge.

4.4.2.2 Effluent treatability tests

A series of three different tests were conducted to evaluate the performance of ECG on the removal of As and Mn from synthetic and surrogate mine water (Fig. 4.1). Two series of experiments were performed to evaluate the effect of operating parameters on As and Mn removal from S_{As} and S_{Mn} as well as energy and electrode consumptions with i) the CD (0.25 to 10 mA/cm²) at an EC of 1.5 mS/cm and ii) the EC (0.25 to 2.5 mS/cm) at a CD of 0.5 mA/cm² for As and 2.0 mA/cm² for Mn. A treatability test with the most performant conditions was conducted in triplicate to evaluate the reproducibility of the treatment process. Another series of experiments was conducted to evaluate the effect of CD at 0.5 mA/cm² for As and 2.0 mA/cm² for Mn, as well as the effect of EC at 0.25 and 2.5 mS/cm, on the removal of As and Mn from S_{As+Mn} , and on the energy consumption.

The effect of retention time was also evaluated for the simultaneous removal of As and Mn from S_{As+Mn} . Then, (un)spiked surrogate mine water (E_{low} and E_{high}) was treated under the most performant conditions identified from the previous tests with S_{As} , S_{Mn} , and S_{As+Mn} .

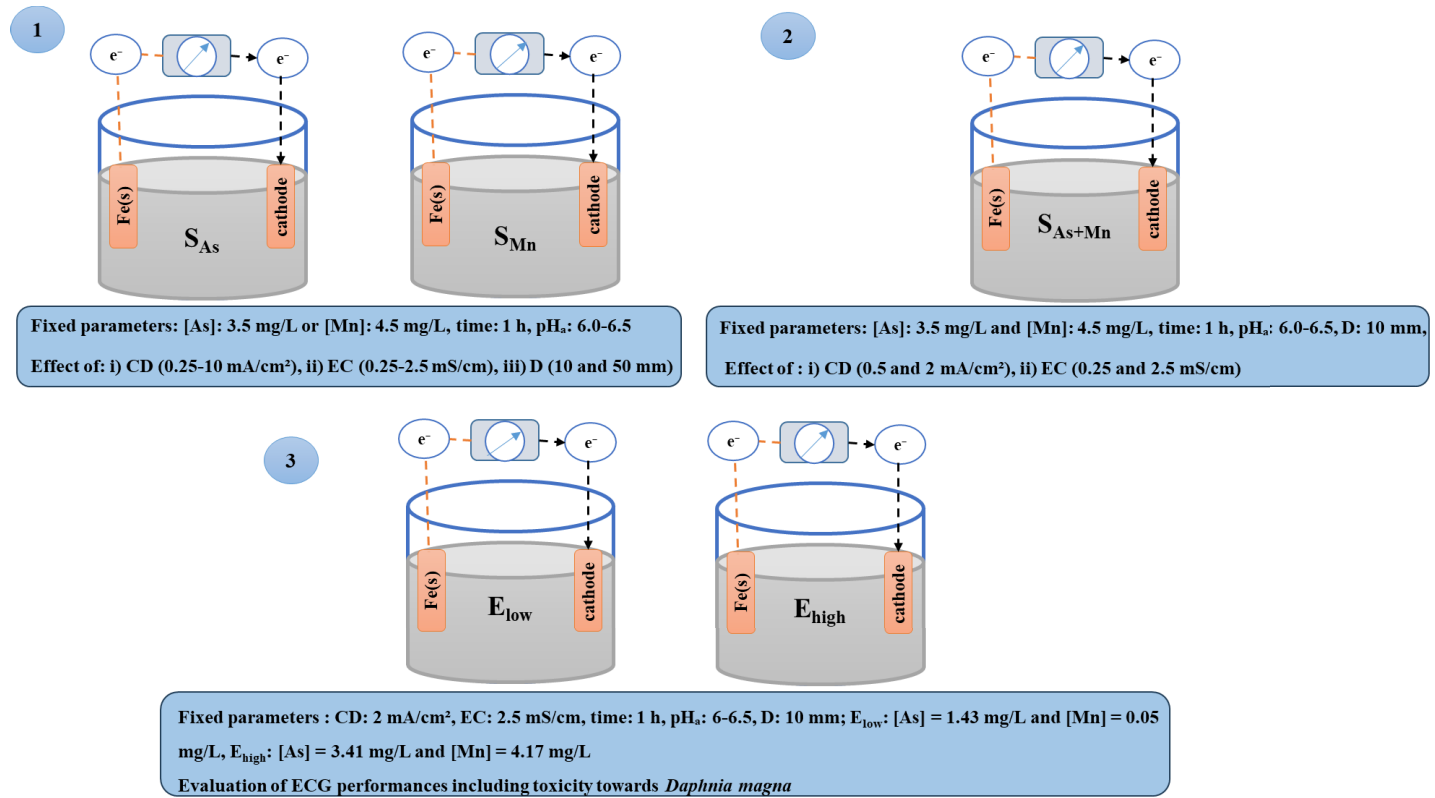


Figure 4.1 Experimental approach used to identify the most performant operating conditions for the simultaneous removal of As and Mn from synthetic and surrogate mine water

4.4.2.3 Determination of energy and electrode consumption

Energy and electrode consumption are important criteria to be considered when evaluating the performances of ECG treatment as they are directly related to operating conditions. The energy consumption was estimated using the following equation (Koby et al., 2022):

$$C_{\text{energy}} (\text{kWh/m}^3) = U \times I \times t / (V \times 1000)$$

Where U is the cell voltage (V), I is the current (A), t is the retention time (h), V is volume of effluent to be treated (m^3).

The consumption of sacrificial Fe-electrodes was estimated by subtracting the initial and final weight of the electrode before and after treatment ($C_{\text{electrode-experimental}}$) and by using the following equation ($C_{\text{electrode-calculated}}$) (Koby et al., 2022):

$$C_{\text{electrode-calculated}} (\text{kg/m}^3) = I \times t \times M / (n \times F \times V \times 1000)$$

Where I is the current (A), t is the retention time (s), M is the molecular mass of Fe (55.85 g/mol), n is the number of electrons transferred, F is the Faraday's constant (96,500 C/mol) and V is volume of effluent to be treated (m^3).

4.4.3 Analytical methods

Before and after each ECG treatment, the pH, redox potential (ORP), and EC were measured using calibrated electrodes. A VWR Symphony[®] multimeter (Canada) equipped with an Orion 915 BNWP double junction Ag/AgCl electrode and an Orbisint CPS 12D Pt electrode were used to measure the pH and ORP, respectively. A VWR Traceable[®] Expanded Range Conductivity Meter equipped with an epoxy probe was used to determine the EC. Before each ECG test, the dissolved oxygen concentration was measured using an HQ30d portable meter kit with a calibrated LDO101 dissolved oxygen probe. The concentrations of dissolved As, Mn, and Fe were measured using an ICP-OES (Agilent 5800-Vertical Dual View (VDV)) after sample filtration using syringe filter (pore size of 0.45 μm , diameter of 30 mm). The calibration of the ICP- OES was validated for each series of measurements using certified multi-element standard solutions (Agilent Technologies; TruQ). For E_{low} and E_{high} , anion concentrations were measured using ion chromatography (Metrohm 940 Professional IC Vario, Switzerland; CEAEQ, 2014). The different anions were eluted from the Supp 5 (150 \times 4.0 mm) separation column (Metrohm) using a carbonate buffer (1.0 mM NaHCO_3 , 3.2 mM Na_2CO_3) at 0.7 mL/min. The 1,10-phenanthroline complexation method was used to measure dissolved Fe(II) by UV-Visible spectroscopy (Christian, 1994).

4.4.4 Toxicity testing

Acute toxicity to *D. magna* was assessed on untreated and treated E_{low} and E_{high} following the standard analysis method (MA. 500-D.mag 1.1R3m) of the Center of Expertise in Environmental Analysis of Quebec (CEAEQ, 2021). (Un)treated effluents were kept at 4°C directly after sampling until testing in the laboratories of Bureau Veritas (Sainte-Foy, QC, Canada). The samples were brought to room temperature and homogenized. Physicochemical parameters (pH, dissolved oxygen, EC, temperature, and hardness) were measured before starting the experiment and immediately after the counting of immobile or dead organisms. Dilution waters were mixed with E_{low} and E_{high} in different proportions (0, 6.25, 12.5, 25, 50, 100% - v/v) to achieve a final volume of 10 mL for each vessel. The dilution waters consisted of hard water reconstituted to a 170 mg/L $CaCO_3$ hardness to ensure *D. magna* survival. Five neonates (newborn organisms < 24 h old) from a *D. magna* culture raised in the laboratories of Bureau Veritas were added to each vessel to achieve a density of 2.0 mL/daphnia. The neonates were incubated at $20 \pm 2^\circ C$ for 48 h (two series of a 16 h photoperiod followed by an 8 h darkness period) (CEAEQ, 2021). To confirm the quality of the results, neonates were exposed to a positive control containing potassium dichromate as a toxicant. Immobile and dead organisms were counted. Immobility is defined as the inability to swim for 15 s after a slight agitation of the solution, while mortality is defined by the absence of movement of the appendages and antennas, and by the absence of a heartbeat. Effluents resulting in $\leq 50\%$ mortality of the exposed *D. magna* population after 48 h were deemed as non-acutely toxic, while effluents causing $> 50\%$ mortality (LC_{50}) were considered acutely toxic (MELCC, 2012; Minister of Justice, 2021).

4.5 Results and discussion

4.5.1 Performance of ECG on As and Mn removal from synthetic effluents S_{As} and S_{Mn}

4.5.1.1 Effect of current density on ECG performance

The effect of CD was evaluated in the range of 0.25–10 mA/cm² for the treatment of slightly contaminated S_{As} and S_{Mn} , as CD is one of the most critical operating parameters for the removal As and Mn by ECG as well as for energy and electrode consumption (Kobyra et al., 2022; Moussa et al., 2016). The results of the tests, which were performed for 60 min, are presented in Table 4.1 and Fig. 4.2. The findings are consistent with previous studies, showing a positive correlation between CD and As and Mn removal efficiency (Table 4.1). An important increase in As removal (from 92 to up to 100%) was observed as CD increased from 0.25 to 1.5 mA/cm², while a plateau was reached at CD >2.0 mA/cm².

This slight improvement of As removal can be attributed to the greater amount of Fe(III)-hydroxides produced, which is consistent with the observed increase in Fe-electrode mass loss (from 0.018 to 0.70 kg of electrode consumed/m³ with CD increase from 0.25 to 10 mA/cm²) (Table 4.1). Indeed, according to the Faraday's law, higher CD results in larger amounts of solubilized Fe from sacrificial electrodes as well as OH⁻ ions at the cathode and therefore an increase in the amount of amorphous Fe(III)-hydroxides with high surface area produced, which will trap more As (Kobyta et al., 2016; Ucar et al., 2013). For Mn, removal efficiency seems to be positively correlated with the applied CD (results not shown; Mn removal (%) = 23.9 ln(CD) + 47; R² = 0.9707). These results could potentially be explained by the larger surface of Fe(III)-hydroxides produced as CD increased, leading to trapping or sorption of Mn ions onto Fe(III)-hydroxides (Nariyan et al., 2017; Oncel et al., 2013; Shafaei et al., 2010). Although increasing CD enhances As and Mn removal, an important increase in energy (from 0.007 to 4.36 kWh/m³) and electrode consumption (from 0.017 to 0.700 kg/m³) was observed, which is consistent with previous studies (Kobyta et al., 2014; Touahria et al., 2016). Values of experimental electrode consumption (C_{electrode-experimental}) were closed to the theoretical electrode consumption (C_{electrode-calculated}) for all the conditions tested, which is consistent with a current efficiency of 105-118%.

As energy and electrode consumption and associated operating costs are positively correlated to the CD applied to the ECG unit, the identification of the lowest CD value allowing a satisfactory removal of the target contaminant is critical ([As]_f < 0.2 mg/L (MELCC; 2012) and [Mn]_f < 2 mg/L (US CFR, 1996)). New experiments were performed with the CD ranging from 0.25 to 2.5 mA/cm² to identify the most performant CD for As and Mn removal from S_{As} and S_{Mn} (Fig. 4.2). Despite improving As and Mn removal, the increase in CD led to an increase in both energy (from 0.0067 to 0.45 kWh/m³) and electrode (from 0.0175 to 0.1751 kg/m³) consumption. An important decrease in the amount of As removed per amount of Fe consumed (from 0.3

to 0.005 mgAs/mgFe) was observed when increasing CD from 0.5 to 2.5 mA/cm², while a slight increase was observed between 0.25 and 0.5 mA/cm².

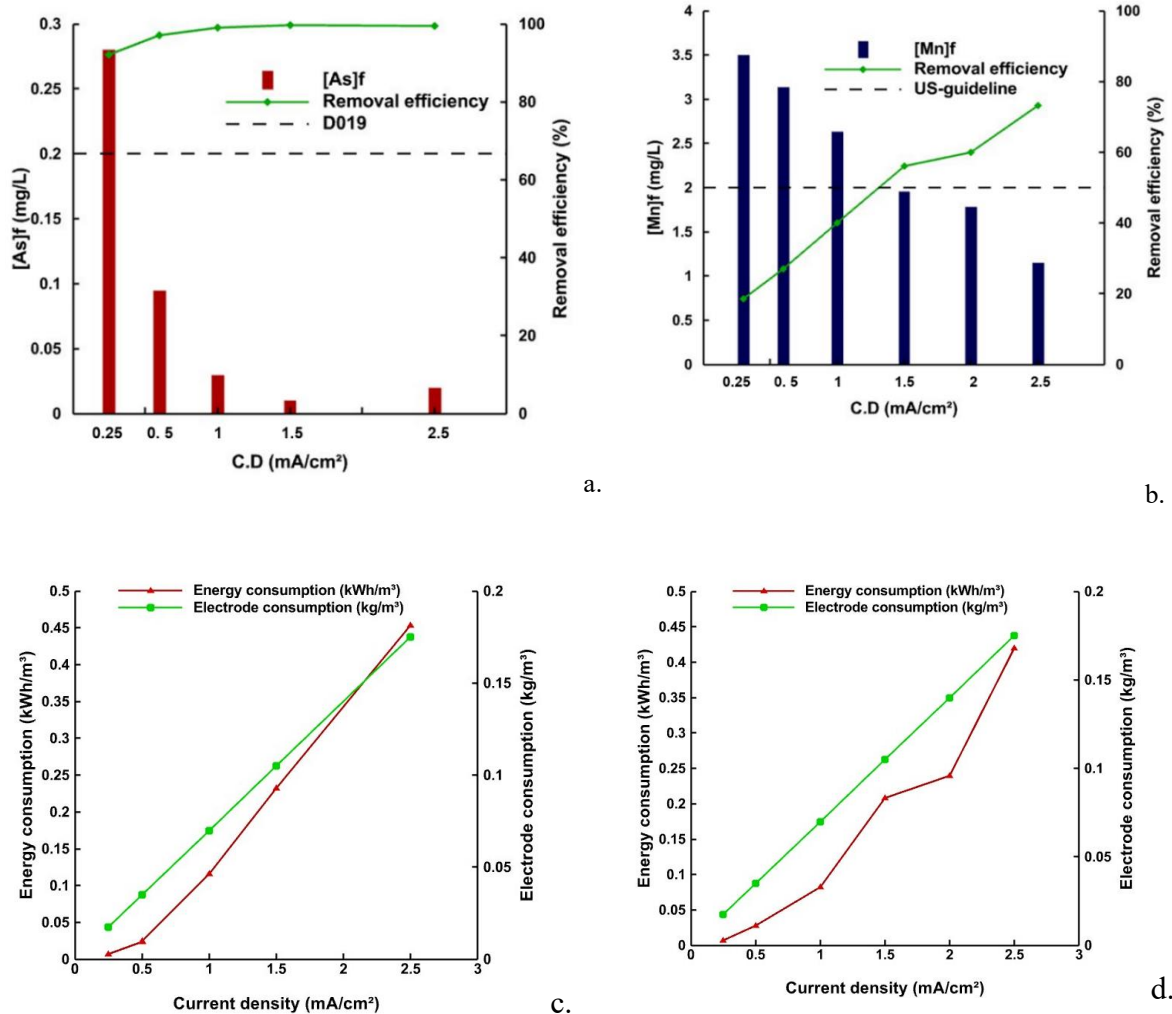


Figure 4.2 Effect of CD on the removal efficiencies of As (a) and Mn (b) as well as energy and electrode consumption for As (c) and Mn (d.) (operating conditions: two Fe-electrodes; EC: 1.50 mS/cm; pH: 6.0–6.5; retention time: 60 min; inter-electrode distance: 10 mm; [As]_i: 3.48 ± 0.12 mg/L or [Mn]_i: 4.32 ± 0.14 mg/L)

For Mn, the increase in CD from 0.25 to 2.5 mA/cm² led to a gradual decrease in the amount of Mn removed per amount of Fe consumed ranging from 0.14 to 0.02 mgMn/mgFe. The most performant CDs were 0.5 mA/cm² for As and 2.0 mA/cm² for Mn, with final concentrations below criteria. It can be noticed that an efficient Mn removal required a CD four times greater than that for As. Other tests were performed with an inter-electrode distance of 50 mm (instead of 10 mm) to determine if this distance can be increased to reduce operating costs without affecting contaminant removal. Similar As and Mn removal efficiencies were obtained for both inter-electrode distances. While increasing the inter-electrode distance from 10 to 50 mm led to a two-fold and three-fold increase of the voltage required and the energy consumption, respectively, to maintain the target CD. Therefore, the inter-electrode distance was fixed at 10 mm for the remaining experiments.

4.5.1.2 Effect of ionic strength on ECG performance

For the treatment of low ionic strength effluents, ECG usually requires the addition of supporting electrolytes (e.g., NaCl, Na₂SO₄) to improve current diffusion and to limit the ohmic drop as well as the associated increase in energy required to maintain a target CD (Balasubramanian et al., 2009; Shafaei et al., 2010; Ucar et al., 2013). Previous studies showed that a higher ionic strength has a negligible influence on the removal of As (EC from 0.4 to 2.5 mS/cm; Ucar et al., 2013) or Mn (EC from 2.5 to 7 mS/cm; Shafaei et al., 2010) at variable CDs (3.3–10 mA/cm²), while affecting the voltage required to obtain the targeted CD.

Experiments were conducted on As- and Mn-contaminated effluents with EC ranging from 0.25 to 2.5 mS/cm (Table 4.2) at CD values of 0.5 and 2.0 mA/cm² for As and Mn, respectively, to better understand the effect of ionic strength on As and Mn removal and energy consumption at low CD. Similar removal efficiencies were observed after 60 min of treatment for As (96–98%) and Mn (58–67%), at both low and high EC. However, the increase in EC from 0.25 to 2.5 mS/cm led to a three-fold decrease in the energy required to apply the targeted CD for the treatment of S_{As} (from 0.101 to 0.032 kWh/m³), and a six-fold decrease for S_{Mn} (from 0.914 to 0.179 kWh/m³).

Table 4.2 Effect of ionic strength on As and Mn removal as well as energy consumption (two Fe-electrodes; CD: 0.5 mA/cm² for As, 2.0 mA/cm² for Mn; pH 6.0-6.5; retention time: 60 min; inter-electrode distance: 10 mm).

	EC (mS /cm)	0.25	0.5	1	1.5	2.5
Treatment of S _{As}	[cont.] _f (mg/L)	0.08	0.1	0.15	0.1	0.14
	Removal (%)	98	97	96	97	96
	pH _f	6.42	6.5	6.5	6.4	6.4
	C _{energy} (kWh/m ³)	0.101	0.042	0.040	0.037	0.032
Treatment of S _{Mn}	[cont.] _f (mg/L)	1.55	1.97	1.77	1.78	1.8
	Removal (%)	67	58	61	60	58
	pH _f	6.13	6.15	6.2	6.2	6.15
	C _{energy} (kWh/m ³)	0.914	0.471	0.296	0.239	0.179

[cont.]_f: final concentration of contaminant; pH_f: final pH

Because varying the ionic strength resulted in negligible effects after 60 min of ECG treatment, additional experiments were performed to assess its potential impact on the kinetics of As and Mn removal and identify the most performant retention time (Fig. 4.3). No major differences were observed in terms of As and Mn removal with the retention time for the three EC tested, suggesting that ionic strength did not impact the kinetics of ECG treatment. However, 60 min of treatment were required to reach

the targeted final concentrations for both As and Mn (0.2 mg/L As and 2 mg/L Mn), consistent with previous studies (Shafaei et al., 2010). As the retention time was independent of the ionic strength of the solution to be treated, the increase in current requirements to maintain the target CD with the decrease of ionic strength from 2.5 to 0.25 mS/cm resulted in a reasonable increase of energy consumption for As (from 0.02 to 0.09 kWh/m³), while resulting in an important increase for Mn (from 0.27 to 1.23 kWh/m³).

ECG treatments were further conducted in triplicate under the most performant conditions to evaluate the reproducibility of the approach (Table 4.3). Coefficient of variation values of 6–8% for As and 7–11% for Mn were obtained, indicating a small extent of variation among the conducted triplicates. Thus, the ECG process can be considered reproducible for removing As and Mn from effluents with low or high ionic strength effluents. Based on these results, ECG can be efficiently used for the treatment of As and Mn at low CD without the addition of salts to increase ionic strength, resulting in lower residual salinity and potential associated toxicity.

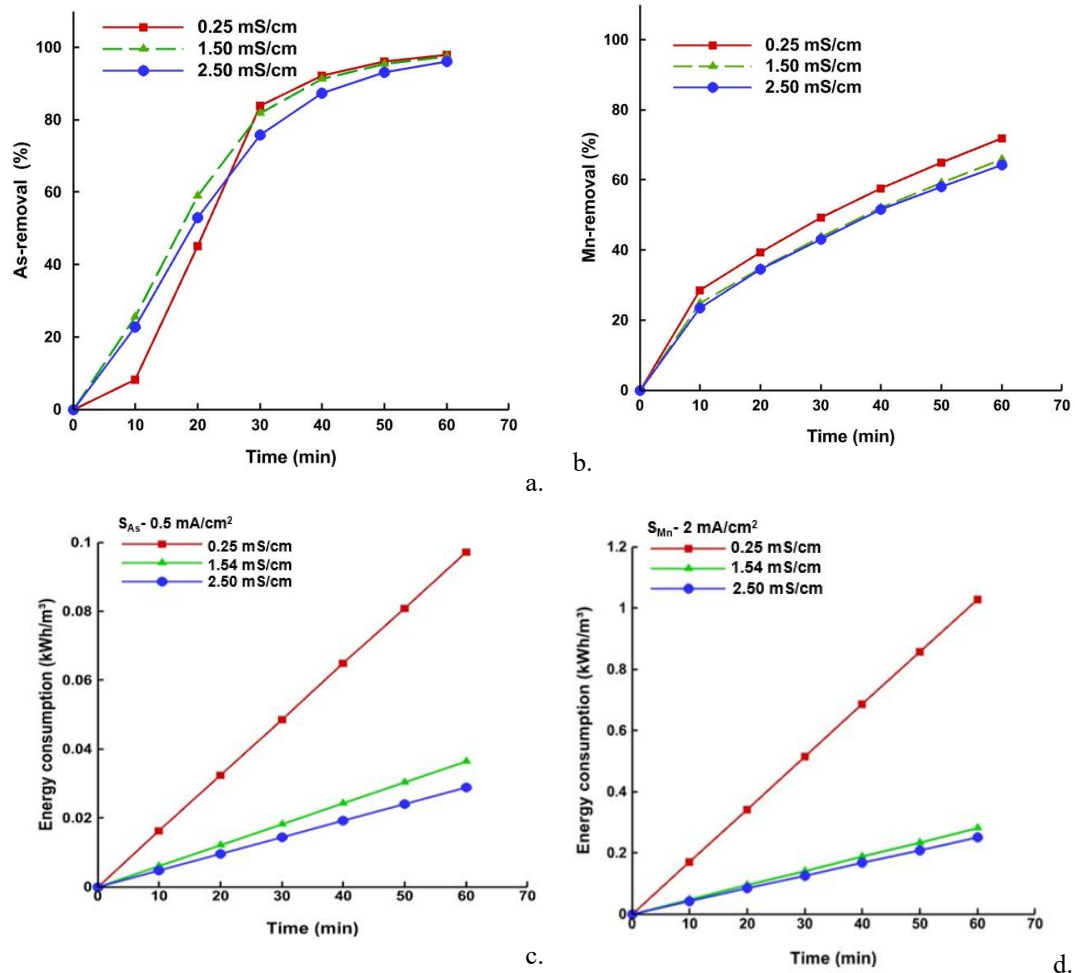


Figure 4.3 Evolution of As (a) and Mn (b) removal as well as energy consumption (for As (c) and Mn (d)) with retention time for different EC values (operating conditions: two Fe-electrodes; CD: 0.5 mA/cm² for As and 2.0 mA/cm² for Mn; pH: 6.0–6.5; inter-electrode distance: 10 mm; [As]_i: 3.38 ± 0.08 mg/L or [Mn]_i: 4.54 ± 0.16 mg/L)

Table 4.3 Reproducibility assessment of the ECG process for the removal of As and Mn from S_{As} and S_{Mn} at low and high EC (operating conditions: two Fe-electrodes; pH: 6.0–6.5; retention time: 60 min; inter-electrode distance: 10 mm; $[As]_i$: 3.31 ± 0.04 mg/L or $[Mn]_i$: 4.29 ± 0.08 mg/L).

Cont.*	EC _i (mS/cm)	Replicate	[cont.] _f (mg/L)	Removal (%)	pH _f	EC _f (mS/cm)
As	0.25	1	0.10	97.01	6.21	0.25
		2	0.10	97.01	6.30	0.26
		3	0.09	97.25	6.14	0.25
	2.50	1	0.14	95.72	6.10	2.51
		2	0.13	96.02	6.23	2.60
		3	0.12	96.33	6.10	2.52
Mn	0.25	1	1.45	66.59	6.18	0.25
		2	1.49	64.52	6.17	0.27
		3	1.20	71.43	6.20	0.26
	2.50	1	1.61	62.73	6.13	2.50
		2	1.49	65.51	6.19	2.51
		3	1.71	60.96	6.15	2.53

*cont.: contaminant; [cont.]_f: final concentration of the contaminant, pH_f: final pH, EC_{i/f}: initial or final EC

4.5.2 Performance of ECG on simultaneous removal of As and Mn from S_{As+Mn}

As different optimal CDs were previously identified for the removal of As and Mn from S_{As} and S_{Mn} , respectively, experiments for the treatment of S_{As+Mn} were conducted using two CDs (0.5 and 2.0 mA/cm²). The evolution of As and Mn removal from S_{As+Mn} with time using two different CDs and ECs is presented in Fig. 4.4. Similar removal efficiencies were obtained for S_{As+Mn} (94–96% for As and 59–64% for Mn) as for S_{As} (96–98% As) and S_{Mn} (58–67% Mn) under the optimal CD (0.5 mA/cm² for As and

2.0 mA/cm² for Mn), suggesting no antagonistic or synergistic effects for their simultaneous removal after 60 min of treatment. However, the removal of As was three times faster at higher CD (2.0 vs. 0.5 mA/cm²), requiring only 20 min compared to 60 min. The removal of Mn was very low (<30%) and slow (>60 min) at low CD (0.5 mA/cm²), as previously observed during the experiments performed on S_{Mn}. The results also showed that at high CD, As was removed before Mn, probably due to differing pH requirements: As can be removed at a lower final pH, whereas Mn requires higher pH values (Parga et al., 2005). Indeed, the increase in CD led to an increase of the amount of OH⁻ ions at the cathode, which results in the gradual increase of pH during the treatment (Shafaei et al., 2010; Xu et al., 2017). A slight decrease in energy consumption after 60 minutes of ECG treatment was observed for S_{As+Mn} compared to S_{As} (0.063 vs. 0.097 kWh/m³ at 0.25 mS/cm and 0.017 vs. 0.029 kWh/m³ at 2.5 mS/cm) and S_{Mn} (0.098 vs. 1.027 at 0.25 mS/cm and 0.210 vs. 0.250 kWh/m³ at 2.5 mS/cm).

The simultaneous and efficient removal of both contaminants was achieved at the highest CD, after 60 min of treatment. The efficient removal of As and Mn obtained at 2.0 mA/cm² is probably due to the production of sufficient amounts of OH⁻ ions and Fe(III)-hydroxides for the sorption or (co)-precipitation of As and Mn. This is consistent with the 3.3x increase in the volume of produced sludge (16 mL at 0.5 mA/cm² vs. 53 mL at 2.0 mA/cm²), providing greater numbers of sorption sites for As and Mn removal. Despite the increased sludge volume, the higher CD value was selected for the treatment of surrogate effluents to ensure that both contaminants would be removed below the targeted values.

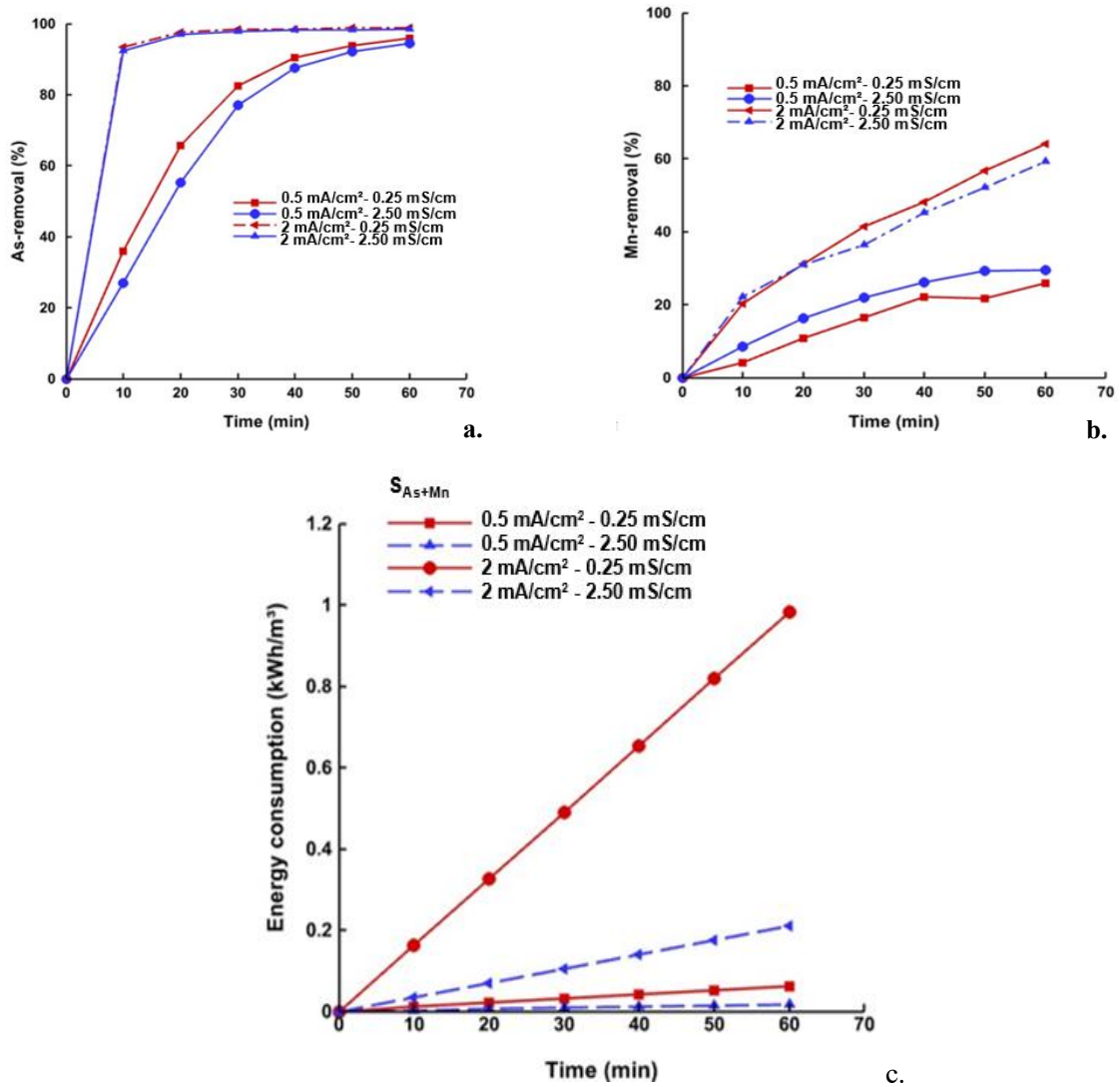


Figure 4.4 Evolution of As (a) and Mn (b) removal as well as energy consumption (c) from S_{As+Mn} at 0.5 and 2.0 mA/cm² (operating conditions: two Fe-electrodes; pH: 6.0-6.5; electrolysis time: 60 min; inter-electrode distance: 10 mm; [As]_i: 3.23 mg/L and [Mn]_i: 4.10 mg/L)

4.5.3 Performance of ECG for As and Mn removal from surrogate mine water

4.5.3.1 Removal of inorganic contaminants from E_{low} and E_{high} using ECG

E_{low} and E_{high} were treated using the Fe-ECG process under the optimal conditions identified from the previous experiments conducted on the $S_{\text{As+Mn}}$ effluent. Physicochemical parameters for E_{low} and E_{high} met the Quebec's provincial and Canadian's federal regulations, indicating that ECG was efficient for removing contaminants and increasing the pH (Table 4.4). High As removal efficiencies (99%) were obtained for E_{low} and E_{high} , while Mn removal efficiencies were variable (40% for E_{low} and 57% for E_{high}).

An improvement in As removal was observed for E_{high} as compared to $S_{\text{As+Mn}}$ (99% for E_{high} vs. 96% for $S_{\text{As+Mn}}$), which had similar initial As and Mn concentrations. This enhancement can be partially attributed to the production of larger Fe-hydroxide flocs due to the presence of Ca (215–230 mg/L) in E_{high} , leading to better adsorption of As on the surface of the flocs (Ruiping et al., 2007). The superior oxidation of As(III) in the presence of Cl^- , leading to the production of strong oxidants (i.e., ClO^-) during ECG treatment, could be another potential cause for the noted improvement (Banerji and Chaudhari, 2016). At the same time, the removal of Mn was less efficient (57% for E_{high} vs. 61% for $S_{\text{As+Mn}}$). The presence of SO_4^{2-} (916–1,006 mg/L), which can hinder the effective dissolution of the Fe-electrode through the formation of a passivating film over time, could probably explain this decreased efficiency; Mn removal seemed to be slower than As removal (El-Taweel et al., 2015; Lakshmipathiraj et al., 2010).

Table 4.4 Physicochemical characterization of E_{low} and E_{high} before and after treatment by ECG (operating conditions: two Fe-electrodes; CD: 2.0 mA/cm²; pH: 6.0-6.5; retention time: 60 min; inter-electrode distance: 10 mm).

Effluent	Regulation*	E_{low}		E_{high}		E_{high} **	
		Initial	Final	Initial	Final	Initial	Final
pH	6.5–9.5	6.51	7.27	6.54	7.15	7.89	6.14
ORP (mV)	-	-	136	-	136	270	448
EC (mS/cm)	-	2.61	2.61	2.50	2.50	3.03	3.08
As (mg/L)	0.2	1.43	0.02	3.41	0.02	4.05	0.01
Mn (mg/L)	2	0.05	0.03	4.17	1.81	4.27	0.04
Fe (mg/L)	3	0.12	0.78	0.09	0.89	0.23	0.22
Al (mg/L)	-	0.05	0.03	0.05	0.03	0.06	0.04
Ba (mg/L)	-	118	116	115	112	435	420
Ca (mg/L)	-	233	231	219	215	483	472
K (mg/L)	-	118	117	115	112	125	120
Na (mg/L)	-	275	275	265	261	535	522
SO ₄ ²⁻ (mg/L)	-	1,006	996	947	918	1,784	1,771
Cl ⁻ (mg/L)	-	171	152	143	138	72	68
Hardness (mgCaCO ₃ /L)		696	606	561	567	1,221	1,202

* MELCC (2012); ** Results from a previous study published (Safira et al., 2023)

4.5.4 Toxicity

Toxicity assessments conducted on E_{low} and E_{high} before and after the treatment by ECG showed that the mine water samples were non-toxic to *D. magna* (Fig. 4.5). For untreated E_{high} , the non-toxicity is inconsistent with a previous study performed on a similar effluent composition (4.05 mg/L As and 4.27 mg/L Mn) showing acute toxicity (48 h-LC50 of 85.4% (v/v)) (Safira et al., 2023). These results could be partially

attributed to slight variations in terms of E_{high} water quality before treatment. For example, some variation of the tolerance of *D. magna* to high concentrations of Na, depending on the water hardness, was previously reported (Okamoto et al., 2014). Indeed, acute toxic effects of Na towards *D. magna* were observed at different concentrations, depending on water hardness (1,600 mg/L vs. 423 mg/L for hardness values of 45 mgCaCO₃/L and 240 mgCaCO₃/L, respectively). In the present study, both hardness and Na concentrations of non-toxic E_{high} (561 mg/L CaCO₃ and 265 mg/L Na) were lower than the toxic E_{high} from the previous study (1,221 mg/L CaCO₃ and 535 mg/L Na; Safira et al., 2023). Another potential source of this inconsistent toxicity for untreated E_{high} might be the higher salinity and sulfate content of the water from the previous study (Safira et al., 2023) vs. the present one (Table 4.4). This is consistent with previously reported observations on the *D. magna* tolerance at lower salinities (Schuytema et al., 1997; Semsari and Megateli, 2007). A total absence of mortality was noted for untreated E_{low} (Fig. 4.5a) and treated E_{high} (Fig. 4.5b) for all dilutions, while 5% mortality was reported for untreated E_{high} at concentrations of 6.25% and 100%. Considering that 5% mortality only represents one dead organism of *D. magna*, these effects are considered to be biologically insignificant (CEAEQ, 2021; Foudhaili et al., 2020b). However, 30% mortality and 15% immobility were observed for treated E_{low} at a concentration of 100%, despite a slight decrease in the concentrations of all the chemical elements that were initially present. The reason for this increase in immobility and mortality after ECG treatment for E_{low} remains unclear but could be partially attributed to the residual concentration of sulfate (997 mg/L), as previously documented in the literature (Radić et al., 2014; Foudhaili et al., 2020b). However, the non-toxicity of treated E_{low} and E_{high} effluents emphasizes the potential advantages of ECG for environmental protection applications.

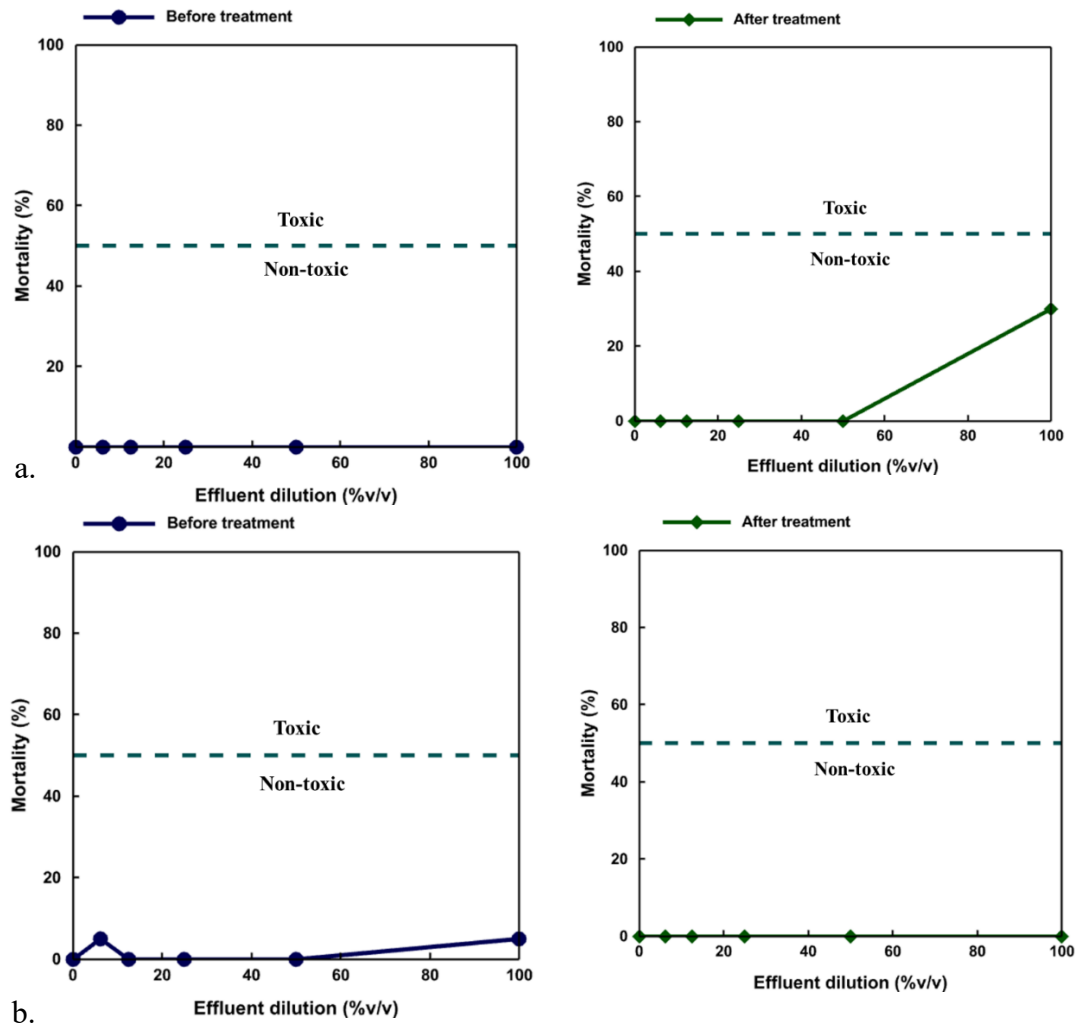


Figure 4.5 Mortality evolution of *D. magna* for (un)treated E_{low} (a) and E_{high} (b)

4.6 Conclusion

The effect of operating conditions (CD, ionic strength, and retention time) on the efficient and simultaneous removal of As and Mn from synthetic effluents containing As (S_{As}), Mn (S_{Mn}), or As+Mn (S_{As+Mn}) and two surrogate (E_{low} : unspiked and E_{high} : spiked) neutral mine water was evaluated using Fe-electrode ECG. CD was identified as the one of the most critical operating parameters affecting the removal of Mn (19-98%), while highly efficient removal of As (94-99%) was obtained, regardless of the CD applied. Satisfactory Mn removal (60%) was achieved at a CD four times higher than that used for As removal, confirming that Mn requires higher ORP and pH conditions relative to As. The inter-electrode distance did not influence the removal efficiency, although it led to a two- or three-fold increase in the required voltage, energy consumption, and associated operating costs. The increase in the ionic strength of the effluent to be treated (from 0.25 to 2.5 mS/cm) was found to decrease the required voltage by three- or six-fold, with a negligible impact on the removal efficiency of As (96-98%) or Mn (58-67%). The results showed that ECG can efficiently treat S_{As} and S_{Mn} , even at low CD and ionic strength, resulting in residual salinity and potentially low toxicity. Neither antagonistic nor synergistic effects were observed for the simultaneous removal of As and Mn from S_{As+Mn} using the most performant conditions identified for S_{As} and S_{Mn} . However, as observed for S_{As} and S_{Mn} , a higher CD was needed for the efficient removal of Mn from S_{As+Mn} , while As removal from S_{As+Mn} was highly efficient at both low and high CD. The removal of As was faster and more efficient from S_{As+Mn} than Mn (20 vs. 60 min and 97-98% vs. 59-64%, respectively) at a CD of 2.0 mA/cm². Finally, efficient removal of As and Mn was obtained for E_{low} and E_{high} , with no addition of toxicity toward *D. magna* after the ECG treatment. These results suggest that ECG could be a promising option for the simultaneous removal of As and Mn from real mine waters in a one-step treatment.

Further studies will be needed to investigate the mechanisms involved in simultaneous removal of As and Mn by ECG as well as the stability of the produced sludge to ensure the performance of this process for the long-term treatment of mine water.

Credit authorship contribution statement

Reem Safira: Conceptualization, Methodology, Visualization, Formal analysis, Investigation, Writing - original draft. Lucie Coudert: Conceptualization, Methodology, Visualization, Formal analysis, Supervision, Project administration, Funding acquisition, Writing - review & editing. Carmen M. Neculita: Conceptualization, Methodology, Visualization, Formal analysis, Supervision, Funding acquisition, Writing - review & editing. Eric Rosa: Conceptualization, Methodology, Visualization, Formal analysis, Supervision, Writing - review & editing.

Declaration of competing interest

The authors declare that there is no conflict of interest.

Acknowledgements

This study was funded by the Natural Sciences and Engineering Research Council of Canada (NSERC), Canada Research Chairs Program (CRC) and the industrial partners of the Research Institute on Mines and Environment (RIME) - University of Québec in Abitibi-Témiscamingue (UQAT) - Polytechnique Montréal, including Agnico Eagle Mines, Newmont Éléonore, Iamgold, Canadian Malartic Mine, Raglan Mine – a Glencore Company and Rio Tinto.

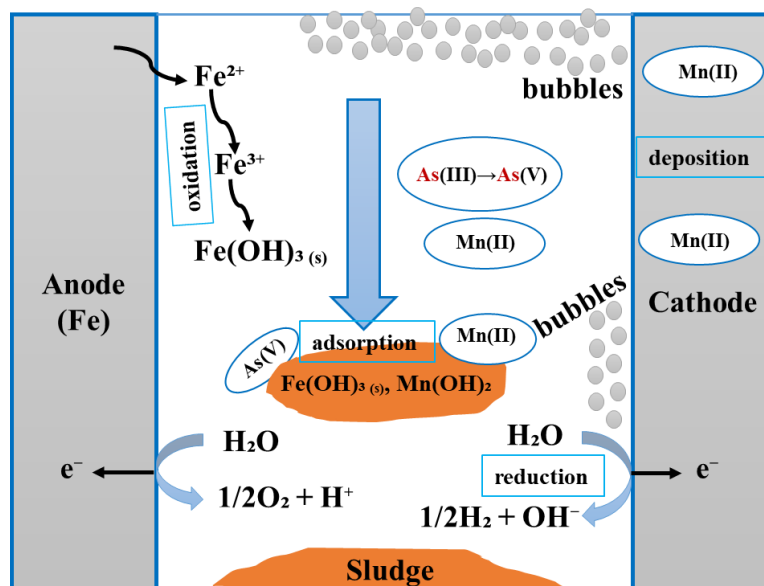


Figure S4.1 Mechanisms involved in As and Mn removal using Fe- electrocoagulation

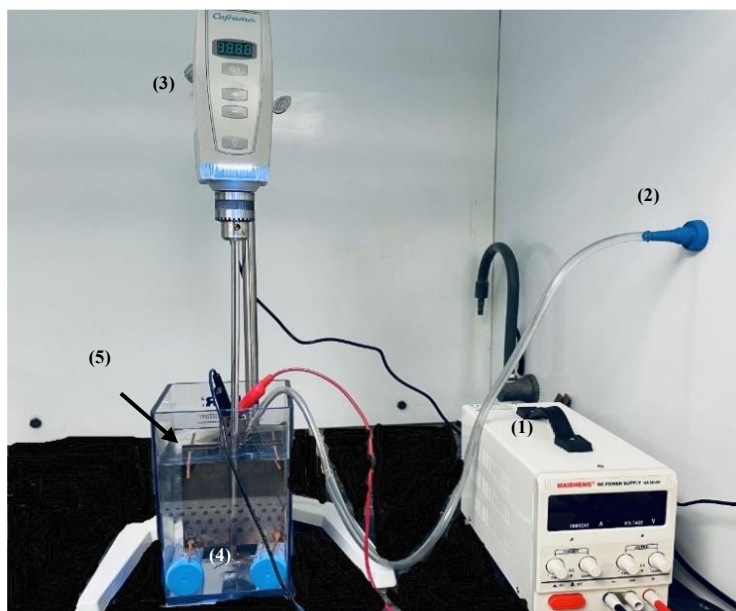


Figure S4.2 Electrocoagulation experimental set-up: (1) power supply, (2) air source, (3) digital stirrer, (4) Pyrex reactor, (5) Fe-electrode

Table S4.1 Examples of the ECG applications for the removal of As and Mn from synthetic or real effluents.

Concentration of contaminant (mg/L)	pH _i / pH _a *	Nature of electrodes	Inter-electrodes distance (mm)	Retention time (min)	Current density (mA/cm ²)	Removal efficiency (%)	References
Synthetic effluent							
As: 50	pH _i : 7	Fe-stainless-steel	15	55	15	94	Balsubramanian et al. (2009)
As: 0.15	pH _i : 6.5	Fe-Fe	13	7.5	0.5	94.1	Kobyas et al. (2011)
	pH _i : 7	Al-Al	13	4	0.75	96.5	
As: 2-5	pH _i : 5	Al-Fe	10	12	3V	99	Ali et al. (2012)
As: 0.5	pH _i : 7	Fe-Fe	10	180	0.2	90	Banerji and Chaudhari (2016)
As(III): 25	pH _a : 6.5–7	Mild steel	2	40	5.2	99	Lakshmi pathiraj et al. (2010)
As: 0.55	pH _i : 7	Al-Al	10	95	10	98.5	Thakur and Mondal (2016)
Mn: 50-200	pH _a : 4-9	Al-Al	5	35	15	40-65	Hanay and Hasar (2011)
Mn: 100	pH _a : 7	Al-Al	10	30	6.25	80	Shafaei et al. (2010)
Mn: 2	pH _i : 7	Ti-Ti	20	60	10	96.5	Safwat et al. (2023)

* pH_i/pH_a: initial/adjusted pH; D: inter-electrode distance; CD: current density

Table S4.1 (continued) Examples of the ECG applications for the removal of As and Mn from synthetic or real effluents.

Concentration of contaminant (mg/L)	pH _i / pH _a *	Nature of electrodes	Inter-electrodes distance (mm)	Retention time (min)	Current density (mA/cm ²)	Removal efficiency (%)	References
Groundwater							
As: 1	pH _a : 3 – 6 and 9	Al-Al	-	40	10	99.9	Demirel et al. (2022)
As: 2.86	pH _i : 2.86	Fe-Fe	6	1.5	4.6	95.54	Parga et al. (2005)
Real mine/industrial effluent							
As: 0.15 Mn: 40.6	pH _i : 2.43	Fe-Fe	10	40	200-500	As: >99 Mn: 25-99.9	Oncel et al. (2013)
As: 0.55	pH _i : 7.7	Al-Al	10	30	10	76.3	Touahria et al. (2016)
Mn: 8.34	pH _i : 6.62	Fe-Fe	30	45	2.23	99.7	Reátegui- Romero et al. (2018)
Mn: 5	pH _i : 6	Fe-Fe Al-Al	20; 40	90	42	94 69 (Al-Al)	Gatsios et al. (2015)

* pH_i/pH_a: initial/adjusted pH; D: inter-electrode distance; CD: current density

CHAPTER 5

PERFORMANCES OF FERRATES FOR SIMULTANEOUS REMOVAL OF AS AND MN FROM CIRCUMNEUTRAL MINE WATER

PERFORMANCES DES FERRATES POUR L'ENLÈVEMENT SIMULTANÉ DE L'AS ET DU MN PRÉSENTS DANS LES EAUX MINIÈRES CONTAMINÉES

Reem Safira¹, Lucie Coudert^{1, *}, Carmen M. Neculita¹, Étienne Bélanger¹, Eric
Rosa^{1, 2}

¹Research Institute on Mines and Environment (RIME), University of Québec in
Abitibi-Témiscamingue (UQAT), Rouyn-Noranda, QC, Canada

²Groupe de Recherche sur l'Eau Souterraine (GRES - Groundwater Research Group),
RIME, UQAT, Amos, QC, Canada

This article has been published in Journal of Environmental Chemical Engineering

(<https://doi.org/10.1016/j.jece.2023.110421>)

5.1 Abstract

Despite being efficient in removing (in)organic contaminants from effluents, ferrate (Fe(VI)) have scarcely been used for the removal of metal(loid)s from mine effluents. The present study evaluated the performance of wet vs. solid ferrate to remove As(III) and Mn(II) from synthetic and surrogate neutral mine effluents. The experiments were done using single (S_{As} or S_{Mn} containing 3.5 mg As/L or 4.5 mg Mn/L, respectively) and binary (S_{As+Mn} containing 3.5 mg As/L and 4.5 mg Mn/L) synthetic effluents as well as surrogate mine effluents (E_{low} and E_{high}). Firstly, Fe(VI) type, optimal dose, adjusted pH (pH_a), and retention time were assessed to evaluate their effect on the treatment of S_{As} and S_{Mn} . Then, the performance of Fe(VI)_s, alone or combined with Fe(III), was tested for the removal of As and Mn from S_{As+Mn} . Lastly, the most performant conditions were applied to E_{low} and E_{high} ; the toxicity to *D. magna* was evaluated before and after treatment. The results showed that at pH_a of 5.5, Fe(VI)_s efficiently removed As (>98%) and Mn (>97%) from both S_{As} , S_{Mn} , and S_{As+Mn} within the first minute. The Fe(VI)_s dose required had to be adjusted depending on the contaminant to be removed (S_{As} or S_{Mn} vs. S_{As+Mn}). The use of Fe(VI)_s+Fe(III) showed improved removal efficiencies for As (99%) and Mn (>99%), while requiring a lower Fe(VI) dose. Moreover, the Fe(VI) treatment of E_{high} , initially acutely toxic, entailed the elimination of *D. magna* toxicity. These findings provide new insights for the potential application of Fe(VI) in the removal of metal(loid)s from mine water.

Keywords: Advanced oxidation process (AOPs), metal(loid)s removal, toxicity, residual salinity, contaminated mine water

5.2 Résumé

Bien qu'efficaces pour le traitement d'effluents contaminés par des composés (in-)organiques, peu d'études se sont intéressées à l'utilisation des ferrates (Fe(VI)) pour l'enlèvement des métaux et métalloïdes présents dans les eaux minières. La présente étude a évalué la performance des ferrates, solides vs. liquides, pour enlever l'As(III) et le Mn(II) présents dans des eaux minières neutres synthétiques et de substitution (produites à partir de rejets miniers réels). Les expériences ont été réalisées sur des effluents synthétiques simples (S_{As} ou S_{Mn} contenant 3,5 mg As/L ou 4,5 mg Mn/L) ou binaires (S_{As+Mn} contenant 3,5 mg As/L et 4,5 mg Mn/L) ainsi que des eaux minières de substitution (E_{faible} et $E_{élevé}$). Tout d'abord, l'effet de la nature et de la dose de Fe(VI), du $pH_{ajusté}$ (pH_a) et du temps sur l'efficacité d'enlèvement de l'As et du Mn présents dans S_{As} et S_{Mn} a été évalué. La performance des Fe(VI), seuls ou combinés à des sels de Fe(III), sur l'enlèvement de l'As et du Mn présents dans S_{As+Mn} a été évaluée. Enfin, les conditions les plus performantes ont été appliquées au traitement de E_{faible} et $E_{élevé}$ et la toxicité envers *D. magna* a été évaluée sur l'effluent avant et après traitement. Les résultats montrent qu'à pH_a de 5,5, Fe(VI)_s enlève efficacement l'As (>98%) et le Mn (>97%) présents dans S_{As} , S_{Mn} et S_{As+Mn} en seulement une minute. La dose de Fe(VI) requise nécessite d'être ajustée en fonction du contaminant présent (S_{As} ou S_{Mn} vs. S_{As+Mn}). L'utilisation de Fe(VI)_s+Fe(III) a montré une amélioration des efficacités d'enlèvement de l'As (99%) et du Mn (>99%), tout en diminuant la dose de Fe(VI) ajoutée. De plus, le traitement par les Fe(VI) de $E_{élevé}$, effluent initialement toxique, a permis d'éliminer la toxicité envers *D. magna*. Ces résultats offrent de nouvelles perspectives pour l'application potentielle des Fe(VI) pour le traitement des eaux minières contaminées.

Mots-clés: procédé d'oxydation avancé, enlèvement des métaux/métalloïdes, toxicité, eau minière contaminée, salinité résiduelle.

5.3 Introduction

Over the last decade, As and Mn have been the target of increasing concerns due to their frequent co-occurrence in surface water, groundwater, and mine-impacted water (Bondu et al., 2020; Luo et al., 2020; Tiwari et al., 2017). Growing mining activities associated with the exploitation of low-grade deposits is partially responsible for the higher As and Mn concentrations in mine and natural water (Coudert et al., 2020; Neculita and Rosa, 2019). Increasing concentrations of As and Mn in water raise significant health concerns, especially in public areas and where private wells provide the main source of drinking water (Bondu et al., 2020; Buschmann et al., 2007; Oza et al., 2021). As proof of the current awareness of As and Mn toxicity, regulations controlling concentrations in mine effluents and drinking water are evolving (Health Canada, 2019; INSPQ, 2017; MELCC, 2012; Ministry of Justice, 2022; US CFR, 1996), leading to new treatment challenges to reach lower As and Mn concentrations. The conventional method for As treatment is chemical co-precipitation in the presence of Fe(III) as a coagulant, at pH 4–7 (Chang et al., 2006; Coudert et al., 2020; Inam et al., 2021; MEND, 2014), while Mn(II) is usually oxidized to Mn(IV) prior to its precipitation as Mn-oxides at pH 9–10 (Chang et al., 2006; Gordon et al., 1989; Neculita and Rosa, 2019). Despite satisfactory removal efficiencies (50-99%), conventional treatment methods show limitations and challenges, particularly for the simultaneous removal of both contaminants. The high amounts of required chemicals for the oxidation of As(III) and Mn(II), the differing pH conditions for (co-)precipitation, and the contradictory Fe/contaminant ratios required ($\text{Fe/As} > 4/1$ vs. $\text{Fe/Mn} < 4/1$) are some of the main factors limiting the simultaneous removal of As and Mn using conventional methods (Bora et al., 2018; Chang et al., 2006; Habib et al., 2020). Therefore, there is a real need to develop innovative methods to remove As and Mn from mine effluents with a one-step treatment.

Ferrates, highly oxidized iron species (from Fe(IV) to Fe(VIII), with Fe(VI) as the most stable and easier to produce), are a promising option for the simultaneous removal of As and Mn from mine water. Known for their strong oxidizing power ($E^\circ = +2.20$ V in acidic media, $E^\circ = +0.72$ V in alkaline media) and their ability to generate in situ environmentally-friendly coagulants (Fe(III)-hydroxides), Fe(VI) are highly efficient species for the removal of metal(loid)s from contaminated water (Goodwill et al., 2016; Lee et al., 2003; Machala et al., 2020; Munyengabe et al., 2021). Because solid ferrate (K_2FeO_4) had low purity (20-40 %), high amounts are needed to reach the Fe(VI)/contaminant target ratio, leading to increased residual salinity and potential associated toxicity. Ferrates are able to remove As or Mn from contaminated water through: (i) the oxidation of As(III) to As(V) and Mn(II) to Mn(IV), (ii) the (co-)precipitation of $FeAsO_4$ and MnO_2 and/or incorporation of As(V) into Fe(III)-hydroxide nanoparticles, and (iii) the sorption of As(V) onto Fe(III)-hydroxides formed in situ; while generating a low amount of highly stable sludge (Sharma, 2002; Sharma et al., 2005). Previous studies have demonstrated the effectiveness of Fe(VI) for the removal of As (> 99%) (Lan et al., 2016; Prucek et al., 2013; Wang et al., 2020) or Mn (90%) (Goodwill et al., 2016; Lim and Kim, 2010; Munyengabe et al., 2021) from synthetic and real effluents. The efficiencies of As and Mn removal were found to be dependent on: i) the type (wet vs. solid) and dose of Fe(VI); and ii) the adjusted pH (pH_a) of the solution, which drives the isoelectric point of formed Fe(III)-hydroxides (Goodwill et al., 2016; Lee et al., 2003; Lim and Kim, 2010; Sharma et al., 2005; Wang et al., 2020). Previous studies showed that the removal of As and Mn was more efficient under neutral to slightly acidic conditions, with optimal pH_a varying from 6 to 7.5 for both contaminants (Goodwill et al., 2016; Lan et al., 2016; Lee et al., 2003; Lee et al., 2015; Lim and Kim, 2010; Prucek et al., 2013). For example, an increase of As removal from 80 to up to 100% was observed when decreasing the pH from 10 to 6.6 (Prucek et al., 2013). A recent study showed that decreasing the pH from 6.5 to 4.0 led to a slight increase of As removal, while decreasing the amount of Fe(VI) dose (Wang et al., 2020). Lim and Kim (2010) observed that Mn removal

increased from 40 to almost 65% when increasing the pH from 3 to 6. Some studies also reported the combination of Fe(III)-based coagulants (Jain et al., 2009; Lee et al., 2003; Quino-Favero et al., 2021) or Al-based coagulants (Kong et al., 2023) with Fe(VI) in As removal for economic purposes. Despite promising As and Mn removal efficiencies, optimal treatment conditions (e.g., Fe(VI) dose, pH) for low-contaminated mine effluents containing both contaminants are yet to be developed.

Advanced oxidation processes (AOPs) have been widely used in water and wastewater treatment. However, previous studies mainly focused on the efficiency of AOPs rather than their performance (removal efficiency, regulations, residual salinity, toxicity of treated effluent, and operating costs) (Goodwill et al., 2016; Munyengabe et al., 2021; Pucek et al., 2013). In addition, by-products with higher toxicity than the original contaminant can be formed during AOPs, depending on initial water quality (Olmez-Hanci et al., 2014; Rueda-Márquez et al., 2020). Only a few studies have evaluated the toxicity of the final effluent after treatment by Fe(VI), mostly targeting the removal of emerging organic contaminants such as pharmaceutical products (Han et al., 2015; Yang et al., 2016; Zhang et al., 2022). To date, there is no consensus about the role of Fe(VI) in the elimination of toxicity of the effluents. A negligible contribution of Fe(VI) treatment to the toxicity has been observed with a toxic effluent initially containing organic contaminants (Han et al., 2015; Malik et al., 2017; Zhang et al., 2022). For example, the degradation of bisphenol from a synthetic effluent using Fe(VI) generated aromatic intermediates (e.g., benzoquinone, hydroquinone, styrene), leading to an increased toxicity to marine luminescent bacteria (*Vibrio fischeri*) in the first 5 min. A longer retention time (up to 60 min) allowed the diminution of the toxicity towards *V. fischeri*, which was explained by the degradation and/or mineralization of these toxic by-products (Han et al., 2015). In another study, comparative performance of coagulation, ozone, a three-step treatment (coagulation + ozone + coagulation), and Fe(VI) to remove chemical oxygen demand (COD) and color from highly contaminated wastewater, including a toxicity assessment through a seed germination test using

spinach seeds (*Spinacia oleracea*) was evaluated (Malik et al., 2017). Effluent treated by Fe(VI) + FeSO₄ showed the highest toxicity removal (75%), while treatment by coagulation alone, ozone alone, or coagulation + ozone + coagulation showed lower toxicity removal (32%, 45%, and 58%, respectively) (Malik et al., 2017). Consistently, the toxicity of two pharmaceuticals, fluoxetine (FLU) and fluvoxamine (FLX), to protozoa (*Spirostomum ambiguum*) was evaluated before and after treatment with Fe(VI). The 24h-EC50 was estimated at 0.99 mg/L for FLU and 1.59 mg/L for FLX before treatment. After treatment using 400 mg/L of Fe(VI), the toxicity of FLU decreased 3.5–4.2-fold, while for FLX toxicity removal was more efficient and decreased 7-fold (Drzewicz et al., 2018). Previous studies showed that the salinity, which can be added during the treatment with Fe(VI) due to its low purity (20-40%), is a potential source of toxicity to aquatic species, including *Daphnia Magna*, through several pathways: (i) increase of osmotic pressure from the combined effect of all constituents, (ii) the individual toxicity of ions and (iii) ion imbalance; causing extreme, sometimes irreversible, alterations in the structure of freshwater communities (Gonçalves et al., 2007; Van Dam et al., 2014). Therefore, residual salinity is an important factor to consider when evaluating the performances of a process treatment, considering its potential impact on the toxicity to *D. magna*. Nevertheless, to the authors' best knowledge, there is no previous study that evaluates the toxicity on *D. magna* of mine effluents initially containing As and Mn, before and after treatment by Fe(VI).

In this context, the main objective of the present study was to evaluate the performance of Fe(VI), alone or in combination with Fe(III), for the simultaneous removal of As(III) and Mn(II) from synthetic and surrogate neutral mine effluents. To this end, the effect of operating conditions (e.g., type and dose of Fe(VI), pH, retention time) on As and Mn removal from a single synthetic effluent (i.e., S_{As}, S_{Mn}) using Fe(VI) was evaluated. Then, the performance of Fe(VI) alone or in combination with Fe(III) to simultaneously remove As and Mn from a binary synthetic effluent (i.e., S_{As+Mn}) was assessed. Finally,

the optimal operating conditions were tested on surrogate mine effluents (E_{low} and E_{high}) and their toxicity to *D. magna*, before and after treatment with Fe(VI) and Fe(III), was evaluated.

5.4 Materials and Methods

5.4.1 Preparation and characterization of mine effluents and Fe(VI)

5.4.1.1 Preparation of synthetic effluents — S_{As} , S_{Mn} , and $S_{\text{As+Mn}}$

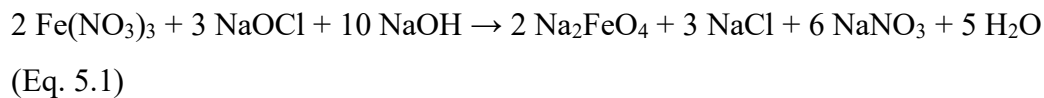
Stock solutions (50 mg/L) of As(III) and Mn(II) were freshly prepared before each series of tests by dissolving the required amount of sodium arsenite (87 mg NaAsO_2 , 99% purity, Sigma-Aldrich) or manganese sulfate (154 mg $\text{MnSO}_4 \cdot \text{H}_2\text{O}$, 99% purity, Laboratoire MAT) in 1 L of deionized water. Synthetic effluents S_{As} , S_{Mn} , and $S_{\text{As+Mn}}$ containing 3.5 mg As/L and/or 4.5 mg Mn/L were then prepared by diluting the stock solution with deionized water. The concentrations of As and Mn used in the present study were selected based on the mean composition of a real mine effluent ($n = 292$, monitoring data from 2016 to 2021) collected at an active gold mine site in Northern Quebec, QC, Canada (Table 5.1). The pH of the As solution was adjusted to neutral pH using 1 M H_2SO_4 before the tests. Effluents S_{As} , S_{Mn} , and $S_{\text{As+Mn}}$ were characterized for physicochemical parameters and metal(loid) concentrations, before and after the treatment, as described in Section 5.4.3.

5.4.1.2 Preparation of E_{low} and E_{high}

Due to the complexity of obtaining large volumes of real mine water, the performance of Fe(VI) was evaluated on surrogate mine effluents (E_{low} and E_{high}) prepared by washing desulfurized and filtered tailings from the active gold mine site in Northern Quebec (data collected and presented in Table 5.1) to simulate the generation of mine drainage occurring on the site. The washing was performed with deionized water at a solid-to-liquid ratio of 1:1. The surrogate mine effluent, referred to as unspiked surrogate effluent or E_{low} , was characterized for its physicochemical parameters before and after treatment. A second surrogate effluent, named spiked surrogate effluent or E_{high} , was prepared using the same approach; As and Mn were added to E_{high} using the NaAsO_2 and $\text{MnSO}_4 \cdot \text{H}_2\text{O}$ salts to achieve initial concentrations similar to the ones used in the treatability tests performed on S_{As} , S_{Mn} , and $S_{\text{As+Mn}}$ (Table 5.1). E_{low} and E_{high} were treated under the most performant operating conditions, which were identified based on treatability tests carried out with S_{As} , S_{Mn} , and $S_{\text{As+Mn}}$.

5.4.1.3 Preparation of wet and solid ferrate

Wet sodium ferrate, Fe(VI)_{w} , was synthesized using an adapted protocol based on previous studies (Ciampi and Daly, 2009; Gonzalez-Merchan et al., 2016; Thompson et al., 1951; Van Dam et al., 2014). Synthesis required: (i) a source of Fe^{3+} (e.g., $\text{Fe(NO}_3)_3$), (ii) a suitable oxidant (e.g., NaOCl), and (iii) strong alkaline conditions (e.g., NaOH) to assure Fe(VI)_{w} stability (Eq. 5.1).



Solid potassium ferrate, Fe(VI)_s, was obtained from NANOIRON Future Technology, Czechia (Nanoiron Envifer, 2023). The purity of Fe(VI)_s was checked prior to Fe(VI) solution preparation using UV-VIS (ultraviolet-visible) spectroscopy at 510 nm by dissolving a given amount of Fe(VI)_s (40 mg as K₂FeO₄) in 100 mL of deionized water, which was selected after performing several tests using different solvents such as a carbonate buffer and tap water (Thompson et al., 1951). The purity of the solid Fe(VI) used was 25%. For the treatability tests, a stock solution of Fe(VI)_s (600 mg/L as Fe(VI)) was freshly prepared at the beginning of each series of experiments to avoid variations related to the dissolution of small amounts of solid Fe(VI) in the effluent to be treated and to improve the reproducibility of the treatment. The concentration of the stock solution of Fe(VI)_s was confirmed before each treatment using UV-VIS spectroscopy at 510 nm. For the experiments performed with Fe(VI)_s and Fe(III), ferric sulfate (Fe₂(SO₄)₃·5H₂O, Anachemia) was used to prepare a 500 mg/L Fe(III) stock solution.

5.4.2 Fe(VI) treatment

The protocol included three sets of Fe(VI) treatability testing: (i) one set of 17 treatability tests to evaluate the effect of the type (solid vs wet) and dose of Fe(VI), pH_a, and retention time on the removal of As and Mn from effluents S_{As} and S_{Mn}; (ii) one set of 10 tests to investigate the effect of Fe(VI)_s dose and the addition of Fe(III)

on the performance of the simultaneous removal of As and Mn from effluent S_{As+Mn} ; and (iii) one experiment conducted on the unspiked and spiked surrogate mine effluents (E_{low} and E_{high}) to evaluate the performance (including toxicity assessment) of the most performant treatment conditions identified from previous experiments conducted on synthetic effluents.

5.4.2.1 Fe(VI) experimental set-up

Laboratory-scale experiments were performed in 750 mL beakers installed on a six-paddle jar tester (Phipps and Bird LU-09-0905, Richmond, Virginia, USA) to control the reaction and flocculation mixing time. The same sequence was used to conduct Fe(VI)-alone treatability testing on effluents S_{As} , S_{Mn} , and S_{As+Mn} (Fig. 5.1a). Each beaker was filled with 500 mL of the solution to be treated and the required amount of $Fe(VI)_w$ or $Fe(VI)_s$ was added to achieve the target Fe(VI)/contaminant molar ratio. The mixture was stirred at 250 rpm for 3 min. The pH was then adjusted to the required pH using a 1 M H_2SO_4 solution and the mixture was mixed at 60 rpm for 20 min. Then, the agitation was stopped, and the mixture was left to settle for 30 min. The mixing duration and speed of each step (addition of Fe(VI), pH adjustment and settling) were selected based on previous studies (Lee et al., 2003; Wang et al., 2020) and visual changes in solution color (from purple to slightly orange for S_{As} and brown reddish for S_{Mn} and S_{As+Mn}) and apparition of flocs.

For the $Fe(VI)_s+Fe(III)$ treatability tests performed on effluents S_{As+Mn} , E_{low} , and E_{high} (Fig. 5.1b), $Fe(VI)_s$ was added to the effluent and the mixture was stirred at 250 rpm for 3 min. Then, the required dose of Fe(III) was added, the pH was adjusted with NaOH to 5.5, the reaction was run for 5 min at 60 rpm, and left to settle for 15 min.

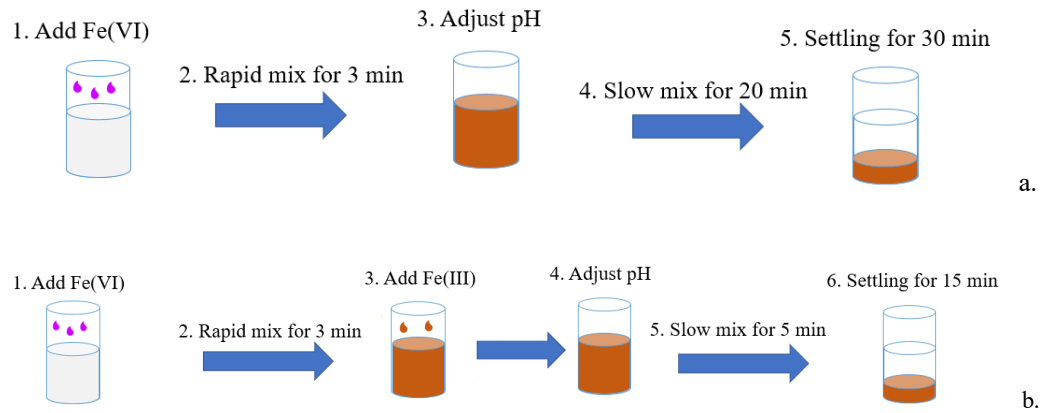


Figure 5.1 Process steps followed for (a) $\text{Fe(VI)}_{s/w}$ and (b) $\text{Fe(VI)}_s + \text{Fe(III)}$ treatability tests on synthetic and surrogate mine effluents

5.4.2.2 Single synthetic effluent treatability tests

Two series of experiments were performed to evaluate the effect of operating parameters on As and Mn removal from effluents S_{As} and S_{Mn} : (i) the type (solid vs. wet) and dose (14 to 56 mg/L for As and 2 to 7 mg/L for Mn) of Fe(VI) ; the doses were selected based on previous relevant studies on As or Mn removal by Fe(VI) ; at pH_a of 5.5 and 6.0 for As and 5.5 and 6.5 for Mn; and (ii) the reaction time (0 to 20 min) under the most performant conditions previously identified. Then, a treatability test was performed in triplicate with the most performant conditions to evaluate the reproducibility of the treatment process.

5.4.2.3 Binary synthetic effluent treatability tests

Two series of experiments were conducted on the effluent S_{As+Mn} to evaluate the effect of operating conditions on the simultaneous removal of As and Mn as follows: (i) $Fe(VI)_s$ dose (from 5 to 28 mg/L) alone, and (ii) $Fe(VI)_s$ dose (10, 12.5, 15 mg/L) with the addition of $Fe(III)$ at different doses (6, 8, 10 mg/L). These tests were conducted at the most performant pH_a and reaction time identified in Section 5.5.2.

5.4.2.4 Unspiked and spiked surrogate mine effluent treatability tests

E_{low} and E_{high} collected after the washing of desulfurized and filtered tailings were treated with $Fe(VI)_s+Fe(III)$ under the most performant conditions identified from the previous tests with synthetic effluents (pH_a : 5.5, reaction time: 5 min, settling time: 15 min). E_{low} was the unspiked surrogate sample containing 1.6 mg As/L and 0.05 mg Mn/L, and E_{high} was the spiked surrogate effluent containing 3.5 mg/L of As and 4.5 mg/L of Mn. The concentrations of $Fe(VI)_s$ and $Fe(III)$ were adjusted to 4.3 and 2.0 mg/L, respectively, for E_{low} and at 12.5 and 8 mg/L for E_{high} to maintain the same contaminant/ $Fe(VI)+Fe(III)$ ratio than for the effluent S_{As+Mn} . Finally, the toxicity on *D. magna* was assessed for E_{low} and E_{high} before and after treatment (Section 5.5.4).

5.4.3 Analytical methods

The main physicochemical parameters (pH, redox potential (ORP), electrical conductivity (EC)) were measured before and after treatment, with Fe(VI)_{s/w} alone or Fe(VI)_s+Fe(III). The pH and ORP were measured with calibrated electrodes (Orion 915 BNWP double junction Ag/AgCl for pH and Orbisint CPS 12D Pt for ORP) connected to a VWR Symphony[®] multimeter (VWR, Canada). A value of 220 mV for the standard ORP was used. EC was measured with a VWR Traceable[®] Expanded Range Conductivity Meter equipped with an epoxy probe calibrated using a 1,413 $\mu\text{S}/\text{cm}$ conductivity standard (VWR, Canada). Dissolved As, Mn, and Fe concentrations were measured before and after each treatability test using inductively coupled plasma optical emission spectroscopy (ICP-OES, Agilent 5800-Vertical Dual View (VDV), Canada) after sample filtration using syringe filter (pore size of 0.45 μm , diameter of 30 mm). The quality of the measurement was ensured using two certified multi-element standard solutions (Agilent Technologies; TruQ, Canada). Anion concentrations were assessed for E_{low} and E_{high} only by ion chromatography (Metrohm 940 Professional IC Vario, Switzerland) (CEAEQ, 2014) with a Supp 5 (150 \times 4.0 mm) separation column (Metrohm), a 945 professional detector, and an 858 professional sample processor. A carbonate buffer (1.0 mM NaHCO₃, 3.2 mM Na₂CO₃) was injected in the separation column at 0.7 mL/min to eluate the different anions. Two quality control solutions (6 and 15 ppm) prepared from a 1,000 ppm stock solution containing all anions (SCP Science, Canada) were used for quality control. Dissolved Fe(II) was measured, directly after the treatment and filtration of the sample using syringe filter (pore size of 0.45 μm , diameter of 30 mm), by UV-VIS spectroscopy at 507 nm using the 1,10-phenanthroline complexation method (Christian, 1994). The Fe(II) concentration was calculated and confirmed based on a calibration curve of a

known ferrous ammonium sulfate solution ($\text{Fe}(\text{NH}_4)_2(\text{SO}_4)_2 \cdot 6\text{H}_2\text{O}$, 98.5% purity, Laboratoire MAT, Canada).

5.4.4 Toxicity testing

Acute toxicity to *D. magna* was tested based on the standard analysis method (SPE 1/RM/14) of the Environmental Technology Centre of Environment Canada (Environment Canada, 2000) at Bureau Veritas (Sainte-Foy, QC, Canada). Being characterized by its broad distribution in wide range of habitats, ease of cultivation in laboratory, sensitivity, high reproduction rate and short life cycle, *D. magna* is an extensively used organism for the evaluation of acute toxicity in the Quebec's provincial and Canadian's federal regulations (Foudhaili et al., 2020a; Lee et al., 2015; MELCC, 2012; Ministry of Justice, 2022). Untreated and treated effluents were stored at 4°C. Prior to testing, samples were conditioned to room temperature and physicochemical parameters (pH, EC, dissolved oxygen (DO), temperature, and hardness) were measured. Toxicity tests consisted of mixing the effluents with dilution water in different proportions (0, 6.25, 12.5, 25, 50, 100% - v/v), to obtain a final volume of 150 mL for each test vessel. The dilution water was hard water reconstituted at the laboratory to a hardness of 170-180 mg/L CaCO_3 to ensure *D. magna* survival. Neonates (< 24 h old) from a *D. magna* culture raised in the laboratories of Bureau Veritas were used for the toxicity tests. To obtain a density of 15.0 mL/daphnia (equivalent to 67 *Daphnia*/L), 10 neonates were added to each vessel. As per the standard method, the neonates were exposed to a 16 h photoperiod and an 8 h darkness period over 48 h (Environment Canada, 2000). Immobile (inability to swim for 15 s after a slight agitation of the solution) and dead (absence of movement of the appendages and antennas and absence of heartbeat) organisms were counted after the

48 h-period of incubation at 20 ± 2 °C. Potassium dichromate was used as a toxicant for quality control. Physicochemical parameters (pH, temperature, DO, and EC) were measured directly after the counting for all dilutions, including the control (dilution water). Based on Directive 019 (D019) (MELCC, 2012) and Metal and Diamond Mining Effluent Regulations (MDMER) (Ministry of Justice, 2022), effluents resulting in the mortality of $> 50\%$ (LC50) of the exposed *D. magna* after 48 h of exposure were considered acutely toxic, while effluent mixtures causing the mortality of $\leq 50\%$ of the population were classified as non-acutely toxic.

5.5 Results and discussion

5.5.1 Characterization of synthetic and surrogate mine effluents

The main physicochemical characteristics of all the solutions and effluents used in the treatability tests are presented in Table 5.1. As mentioned previously, the concentrations of As and Mn in effluents S_{As} , S_{Mn} , and S_{As+Mn} were selected to simulate a real gold mine effluent. The real mine effluent had neutral to alkaline pH (from 7.5 to 11) and contained 0.16-39 mg/L As (average: 3.5 mg/L) and 0.03-4.5 mg/L Mn (average: 0.9 mg/L). The surrogate mine effluents, referred to as E_{low} and E_{high} , showed neutral to slightly alkaline conditions consistent with the real mine effluent, with pH of 7.71 and 7.89, respectively.

Table 5.1 Physicochemical characteristics of synthetic, unspiked and spiked surrogate mine effluents before treatment compared to the real mine effluent

Parameter (unit)		As (mg/L)	Mn (mg/L)	EC (μ S/cm)	pH	ORP (mV)	Fe (mg/L)	Ca (mg/L)	SO ₄ ²⁻ (mg/L)
Real mine effluent (n = 292)	Minimum	0.16	0.03	250	7.11	*n.a.	0.04	37.0	15.0
	Maximum	39.0	4.50	6,600	11.0	n.a.	230	831	655
	Average	3.50	0.90	2,600	8.50	n.a.	59	267	328
S _{As} (n = 17)	As	**3.67 \pm 0.32	-	5.55 \pm 0.20	8.75 \pm 0.14	238 \pm 15	0.01 \pm 0.01	n.a.	n.a.
S _{Mn} (n = 12)	Mn	-	4.45 \pm 0.20	20.1 \pm 2.6	5.82 \pm 0.14	431 \pm 20	0.01 \pm 0.01	n.a.	n.a.
S _{As+Mn} (n = 17)	As + Mn	3.42 \pm 0.04	4.31 \pm 0.09	26.7 \pm 3.6	7.62 \pm 0.48	233 \pm 8	0.01 \pm 0.01	n.a.	n.a.
Surrogate effluent	E _{low}	1.60	0.05	3,030	7.71	260	0.23	471	1,755
	E _{high}	4.05	4.27	3,020	7.89	270	0.23	483	1,784

* n.a.: not available, ** mean \pm standard deviation

The EC, as an indicator of the dissolved species, was close to that measured on the mine site (EC: 2.9-3.0 mS/cm for E_{low} and E_{high} vs. EC: 2.6 mS/cm for the real mine effluent). For E_{low} , As and Mn concentrations (1.6 and 0.05 mg/L, respectively) were lower than the target (i.e., average and maximum concentrations of As and Mn, respectively, found at the mine site). Therefore, the surrogate effluent was spiked with NaAsO_2 (2.3 mg As/L) and $\text{MnSO}_4 \cdot \text{H}_2\text{O}$ (4.2 mg Mn/L) salts to reach the desired As and Mn concentrations in E_{high} (4.05 mg/L for As and 4.27 mg/L for Mn).

5.5.2 Performance of Fe(VI) on As and Mn removal from synthetic effluents

5.5.2.1 Effect of ferrate type, ferrate dose, and pH on Fe(VI) performance

The performance of Fe(VI)_{w} and Fe(VI)_{s} to remove As(III) and Mn(II) from effluents S_{As} and S_{Mn} was evaluated using various Fe(VI) doses (14-56 mg/L as Fe(VI) for As vs. 2-7 mg/L for Mn) and at different pH_a (6.0 and 5.5 for As vs. 6.5 and 5.5 for Mn). For As, the results showed a similar removal efficiency for Fe(VI)_{s} and Fe(VI)_{w} , at both pH_a (Fig. 5.2a), except for the tests performed at 14 mg/L Fe(VI). Indeed, higher removal efficiencies were obtained for 14 mg/L Fe(VI)_{s} compared to the same dose of Fe(VI)_{w} . For Mn, an opposite effect to the one observed for As was detected. Indeed, Fe(VI)_{w} seemed a little more efficient than Fe(VI)_{s} except at high doses (7 mg/L of Fe(VI)) (Fig. 5.2b). The higher Mn removal efficiencies observed at 2 and 5 mg/L for Fe(VI)_{w} relative to Fe(VI)_{s} can be due to the stronger oxidizing conditions of Fe(VI)_{w} ($\text{ORP}_{\text{final}}$: 800 mV for Fe(VI)_{w} vs. 500 mV for Fe(VI)_{s}), mainly because of the residual NaOCl (used for Fe(VI)_{w} synthesis). It should be noted that strong oxidizing conditions are required to oxidize Mn(II) to Mn(IV) at pH below 8.0 (Freitas et al., 2013; Oruê et

al., 2020). Despite slightly lower Mn removal efficiencies, Fe(VI)_s was selected for the further tests because of the 13–14 times lower residual salinity (and therefore lower potential associated toxicity) of the treated effluent when using Fe(VI)_s rather than Fe(VI)_w (Fig. 5.2c,d). The use of large amounts of NaOH and NaOCl to synthesize Fe(VI)_w can explain the higher residual salinity.

Better As removal was obtained at a pH_a of 5.5 relative to 6.0 regardless of the type of Fe(VI) used (Fig. 5.2a), while Mn removal seemed to be slightly affected by the pH_a tested (between 5.5 and 6.5), except at the lowest Fe(VI)_w dose (Fig. 5.2b). Similar tendencies were observed in previous studies using different Fe(VI) doses or initial As/Mn concentrations (Lan et al., 2016; Prucek et al., 2013; Wang et al., 2020). For example, Prucek et al. (2013) found that As removal efficiency increased from 80 to up to 100% as the pH decreased from 10 to 6.6. Consistently, in a recent study, a decrease in pH from 6.5 to 4.0 resulted in a slight increase in As removal, while leading to a decrease in the required Fe(VI) dose for efficient As removal (> 99%, [As]_{initial} = 0.05 mg/L) from a synthetic effluent (Wang et al., 2020). The higher As removal efficiency observed as the pH_a decreased could be explained by the higher oxidation potential of Fe(VI) at slightly acidic pH and the lower solubility of Fe(OH)₃ under these conditions (Wang et al., 2020). Indeed, the predominant species of Fe(VI) at pH 5.5 is the protonated form HFeO₄⁻, which is known to react faster and more efficiently with As than the unprotonated form present at pH > 7 (Lee et al., 2003; Sharma, 2011). Moreover, the dominant species of As(V) is negatively charged (H₂AsO₄⁻) at pH 5.5, which is more easily adsorbed on the surface of Fe(III)-hydroxides (Wang et al., 2020). This lower Fe(VI) dose requirement as the pH decreased from 6.0 to 5.5 was also observed in the present study (Table 5.2). An almost complete removal of As (98% removal and [As]_{final}: 0.05 mg/L) was obtained using only 22 mg/L of Fe(VI)_s at pH 5.5, while requiring twice the amount of Fe(VI)_s at pH 6 to achieve the same performance. However, lowering the dose of Fe(VI)_s required to efficiently remove As resulted in an important decrease in residual salinity

(EC = 0.19 vs. 0.42 mS/cm when using 22 mg/L vs. 56 mg/L of Fe(VI)_s), and hence a decrease in the associated operating costs and amount of produced sludge. In contrast, Mn(II) is known to be more efficiently removed at high pH (9–10) after its oxidation to Mn(IV) using conventional oxidants such as ozone or potassium permanganate (Gordon et al., 1989; Goodwill et al., 2016). However, the oxidation of Mn(II) to Mn(IV) can occur under slightly acidic pH and strong oxidizing conditions. In the present study, the strong oxidizing power of Fe(VI) obtained at Fe(VI) doses higher than 5 mg/L at pH_a of 5.5 overcomes the requirement for high pH to oxidize Mn(II) to Mn(IV), which can explain the efficient removals observed (> 80%) for most of the Fe(VI) doses tested at both pH_a. Of note, a slightly lower Mn removal efficiency (decrease of 10 to 20% depending on the type of Fe(VI) used) was obtained at a pH_a of 5.5 vs. 6.5 at the lowest Fe(VI) dose tested (2 mg/L). The Mn removal efficiency was similar to that obtained by Lim and Kim (2010) under similar pH conditions for the treatment of synthetic effluents. Indeed, in this last study, it was observed that the Mn removal efficiency from an effluent initially containing 5.5 mg Mn/L increased from 40 to 80% as the pH increased from 3 to 6.

Additional experiments were conducted to evaluate the effect of Fe(VI)_s dose on the performance of As and Mn removal at a pH_a of 5.5 from S_{As} and S_{Mn} (Table 5.2). Removal efficiency increased as the applied Fe(VI)_s dose increased from 14 to 56 mg/L, which is consistent with the literature (Prucek et al., 2013; Sharma et al., 2007; Wang et al., 2020). For example, Prucek et al. (2013) reported increased As removal ([As]_i: 100 mg/L) from a synthetic effluent with an increasing Fe(VI) dose, from 200 to 2,000 mg/L. This positive correlation was attributed to better contact between Fe and As because of a higher amount of coagulant produced (i.e., Fe(III)-hydroxides), providing more sorption sites for As(V) (Prucek et al., 2013; Sharma et al., 2007; Wang et al., 2020).

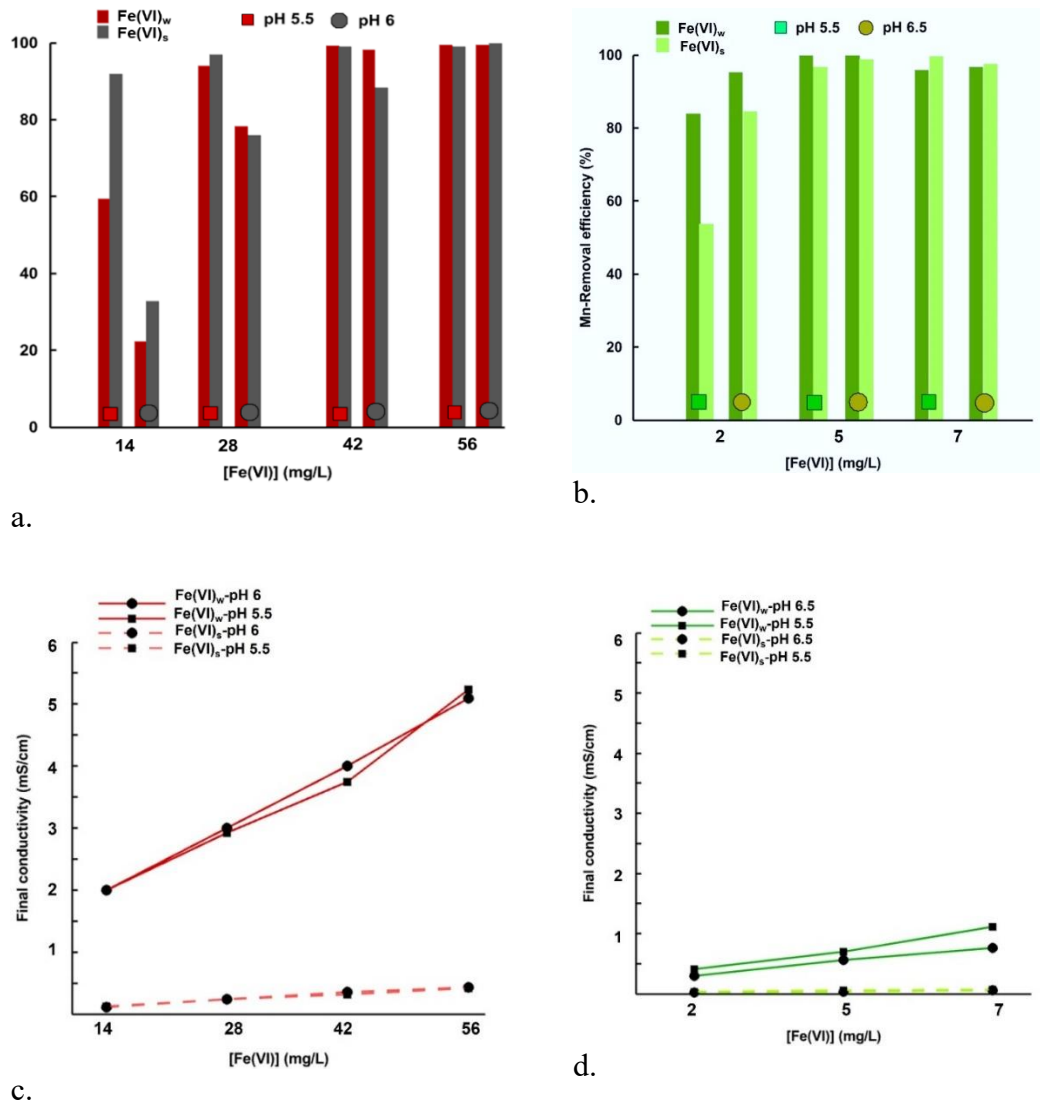


Figure 5.2 Effect of Fe(VI) type at different doses and pH_a on As (a) and Mn (b) removal efficiency and residual salinity (c,d) from S_{As} and S_{Mn} (reaction time: 20 min; settling time: 30 min)

Table 5.2 Effect of Fe(VI)_s dose on As (average [As]_{initial}: 3.5 ± 0.3 mg/L) or Mn (average [Mn]_i: 4.5 ± 0.2 mg/L) removal from S_{As} and S_{Mn} at pH_a = 5.5 (reaction time: 20 min; settling time: 30 min)

Contaminant	[Fe(VI)] (mg/L)	Fe(VI)/cont. Molar ratio	pH _a	[cont.] _f (mg/L)	[Fe] _f (mg/L)	pH _f	EC _f (mS/cm)	ORP _f (mV)
As	14	2.5/1	5.58	0.28	0.16	6.84	0.12	288
	17	3.0/1	5.49	0.27	0.20	7.13	0.15	328
	22	4.0/1	5.60	0.05	0.02	7.04	0.19	381
	28	5.0/1	5.42	0.12	0.01	6.74	0.24	294
	42	7.5/1	5.49	0.05	0.04	6.21	0.31	368
	56	10.0/1	5.48	0.03	0.05	6.78	0.42	342
Mn	2	0.25/1	5.45	2.14	0.01	6.55	0.04	373
	5	0.5/1	5.60	0.15	0.01	6.63	0.06	426
	7	0.75/1	5.53	0.01	0.03	6.76	0.07	497

*cont.: contaminant

This explanation is consistent with the decrease of residual Fe (from 0.16 to 0.05 mg/L) observed in the present study when Fe(VI)_s doses increased from 14 to 56 mg/L. For Mn, an important increase in removal efficiency was also observed when Fe(VI)_s increased from 2 to 7 mg/L for all tested pH (6.5 and 5.5) (Fig. 5.2b and Table 5.2). A small loss of efficiency (nearly 4%) was observed for 7 mg Fe(VI)_w/L at pH_a 6.5 and 5.5, probably due to the stronger oxidizing conditions (ORP_{final} was around 870 mV for 7 mg Fe(VI)_w/L vs. 490 mV for all other Fe(VI)_s doses), leading to further oxidation of insoluble Mn(IV) to soluble Mn(VII), as evidenced by the light pink color of the final solution. This phenomena was previously reported by Goodwill et al. (2016) when using a Fe(VI)/Mn molar ratio greater than 2/3, which is close to the actual Fe(VI)/Mn molar ratio of 0.5/1 in the present study (Table 5.2), indicating that Fe(VI) doses higher than 5 mg/L can be problematic.

Based on these results, Mn was efficiently (99%) removed using a low dose of Fe(VI)_s, while As required higher dose to achieve the same removal efficiency (Fe(VI)/Mn molar ratio of 0.5/1 vs. Fe(VI)/As molar ratio of 10/1). The most performant treatment conditions for As and Mn removal from S_{As} and S_{Mn} (meeting the regulatory criteria of [As]_{final} < 0.2 mg/L corresponding to 98% removal and [Mn]_{final} < 2 mg/L corresponding to 97% removal) and residual salinity were identified as the following: (i) pH_a of 5.5 and Fe(VI)_s dose of 22 mg/L (Fe(VI)/As molar ratio of 4/1) for As, and (ii) pH_a of 5.5 and Fe(VI)_s dose of 5 mg/L (Fe(VI)/Mn molar ratio of 0.5/1) for Mn. The difference in dose requirements could be due to the mechanisms involved in contaminant removal (oxidation for Mn vs. oxidation and coagulation/sorption for As).

5.5.2.2 Effect of reaction time on As and Mn removal using Fe(VI)

The evolution of As(III) and Mn(II) removal efficiencies with time was assessed after addition of 22 mg/L of Fe(VI)_s for As and 5 mg/L of Fe(VI)_s for Mn and adjustment of the pH to 5.5 (Fig. 5.3). Results indicated similar As(III) and Mn(II) treatment efficiencies, with almost complete removal within the first minute of reaction. This could be due to the low pH_a at which Fe(VI) is highly reactive (Sharma et al., 2007), favoring As(III) and Mn(II) oxidation and removal. Most previous studies evaluated the kinetics of Fe(VI) oxidation reactions at high pH (8 to 12), due to greater Fe(VI) stability under alkaline conditions (Goodwill et al., 2016; Lee et al., 2003; Sharma, 2011). For example, pH of 8.8 and 9.2 were selected for the evaluation of the reaction kinetics of Fe(VI) and Mn(II), even if pH of 6.2 and 7.5 were used for the removal of Mn, because at pH lower than 7.5 the reaction was too fast to measure the kinetics (Goodwill et al., 2016). Similarly, the reaction rate between As and Fe(VI) was too fast to be measured at pH below 8.4 (Lee et al., 2003). The second-order rate constant decreased from 3.54×10^5 to 1.23×10^3 M/s when the pH of the reaction increased from 8.4 to 11. In the present study, both As(III) and Mn(II) were removed within the

first minute, indicating very fast kinetics and potential competition between the contaminants for the oxidant once they are both present. Despite high removal efficiencies within the first minutes (99% for As and 98% for Mn), additional reaction and settling times were required for the precipitation of Fe(III)-hydroxide nanoparticles as well as sorption, incorporation, or co-precipitation of As(V) (Lee et al., 2003; Prucek et al., 2013) and the precipitation of Mn-oxides (Goodwill et al., 2016). The reaction time was decreased from 20 to 5 min in the following tests. Two settling times (15 and 30 min) were tested to evaluate their impact on the removal of As and Mn to optimize the treatment performance and associated capital costs related to the size of the settling tank. Similar removal efficiencies (99% for As and 98% for Mn) as well as size and settling of generated flocs were found for both settling times. Thus, the settling time was reduced to 15 min.

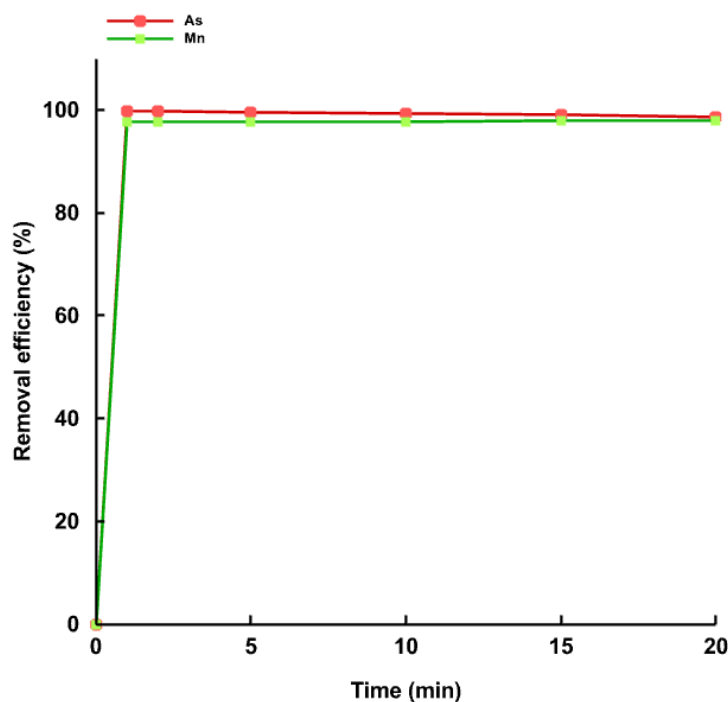


Figure 5.3 Evolution of As and Mn removal efficiency with time (Fe(VI)_s dose: 22 mg/L for As; 5 mg/L for Mn; $\text{pH}_a = 5.5$)

Treatability tests were conducted in triplicate (Table 5.3) under the most performant conditions (Fe(VI)_s dose of 22 mg/L for As and 5 mg/L for Mn, pH_a of 5.5, reaction time of 5 min, settling time of 15 min) to evaluate the reproducibility of Fe(VI) treatment to remove As and Mn from effluents S_{As} and S_{Mn}. Similar treatment performances were obtained in terms of final As and Mn concentrations as well as pH, ORP, and EC, indicating the reproducibility of the treatment. Based on these findings, Fe(VI)_s can be considered a promising, reproducible, and highly efficient process for the removal of As and Mn from mine effluent.

Table 5.3 Performance of Fe(VI)_s treatment on As and Mn removal from S_{As} and S_{Mn} (Fe(VI) dose: 22 mg/L for As and 5 mg/L for Mn; [As]_{initial}: 3.4 mg/L or [Mn]_{initial}: 4.7 mg/L; pH_a: 5.5; reaction time: 5 min and settling time: 15 min)

Contaminant	Triplicate	[cont.] _{final}	pH _{final}	EC _{final} (mS/cm)	ORP _{final} (mV)
As	1	0.03	6.45	0.18	411
	2	0.02	6.41	0.19	420
	3	0.02	6.65	0.19	395
Mn	1	0.04	6.42	0.042	357
	2	0.05	6.41	0.045	358
	3	0.04	6.45	0.045	354

cont.: contaminant

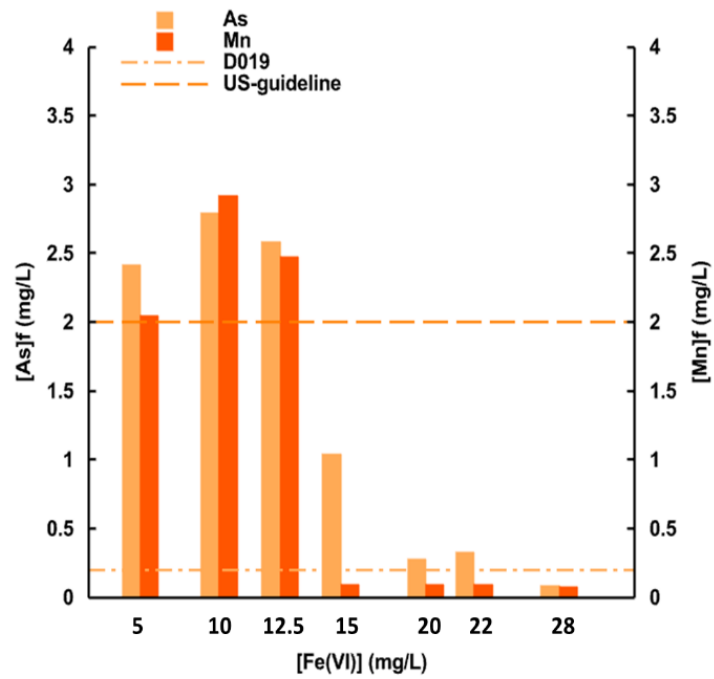
5.5.3 Performance of Fe(VI) on As and Mn removal from synthetic effluent S_{As+Mn}

5.5.3.1 Effect of Fe(VI) on the simultaneous removal of As and Mn

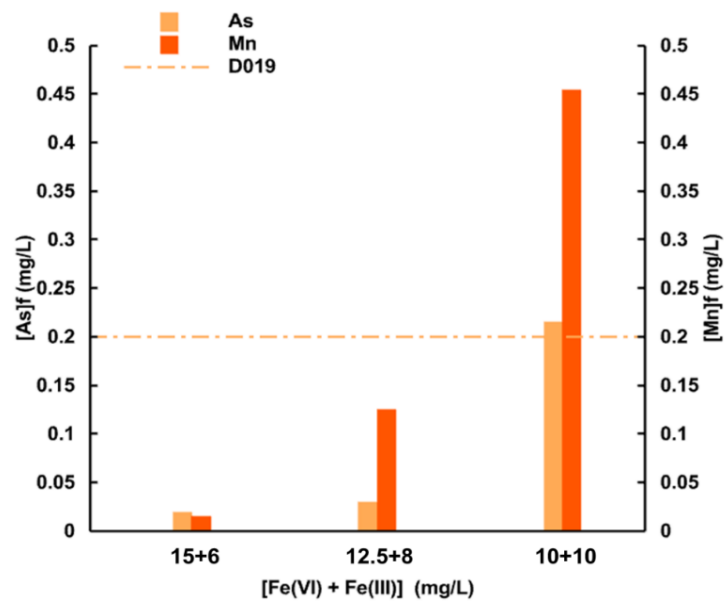
Different Fe(VI)_s doses (from 5 to 28 mg/L) were applied to the effluent S_{As+Mn} at $pH_a = 5.5$ to evaluate their effect on the simultaneous removal of As and Mn (Fig. 5.4a). As observed for the effluents S_{As} and S_{Mn} (Table 5.2), an increase in Fe(VI)_s doses led to a progressive improvement of both As and Mn treatment from the effluent S_{As+Mn} . The results indicated that Fe(VI)_s simultaneously and efficiently removed 99% of As and 98% of Mn from the effluent S_{As+Mn} in a one-step treatment. However, simultaneous removal of As and Mn required a slight increase in the Fe(VI)_s dose, from 22 mg/L for S_{As} or 5 mg/L for S_{Mn} (Table 5.2) to 28 mg/L for S_{As+Mn} to achieve the same performance, i.e., to meet regulatory criteria. It should be noted that to reach the 0.2 mg/L criteria for As (D019) and 2 mg/L for Mn (US CFR), the required dose of Fe(VI)_s was increased 1.3- and 3.0-fold, respectively (28 mg/L for S_{As+Mn} vs. 22 mg/L for S_{As} and 15 mg/L for S_{As+Mn} vs. 5 mg/L for S_{Mn}) (Fig. 5.4a, Table S5.1). However, the total amount of Fe(VI)_s required for S_{As+Mn} was close to the combined amount required to treat S_{As} and S_{Mn} . The loss of Mn removal efficiency (45% vs. 98% for S_{As+Mn} and S_{Mn} , respectively) observed when using 5 mg/L of Fe(VI)_s can be explained by the competition between As(III) and Mn(II) during the oxidation step. This is consistent with the similar evolution of As and Mn concentrations with time observed in the effluents S_{As} and S_{Mn} (Fig. 5.3). Similar competition between Mn(II) and organic matter or As(III) and Sb(III) for intermediate Fe(VI) oxidizing species was observed by Goodwill et al. (2016) and Wang et al. (2020), respectively. Competition between As(III) and Mn(II) for intermediate oxidizing species (i.e., Fe(IV)) produced at $pH = 5.5$ was also noted during the treatment of an As-contaminated groundwater using an electrocoagulation process (Catrouillet et al., 2020). The higher loss of Mn removal

efficiency vs. As (3.0-fold vs. 1.3-fold increase in the required amount of Fe(VI)_s) could be attributed to the fact that Mn(II) needs to be oxidized to Mn(IV) before its subsequent precipitation as MnO₂, while the removal of As(III) requires oxidation to As(V) prior to co-precipitation and sorption on Fe(III)-hydroxides. As a result, the removal of As(III) seems to be more impacted by the presence of Fe(III) than the use of a strong oxidant, as compared to the removal of Mn(II).

However, using a higher dose of Fe(VI)_s for satisfactory As(III) and Mn(II) removal efficiencies led to higher residual salinity (EC = 0.23 mS/cm for the effluent S_{As+Mn} vs. 0.19 and 0.04 mS/cm for the effluents S_{As} and S_{Mn}) (Table S5.1 and Table 5.3) and potentially associated operating costs. Therefore, additional experiments were conducted using a new source of Fe in the place of Fe(VI)_s to produce Fe(III)-hydroxide sorption sites for As removal.



a.



b.

Figure 5.4 Influence of Fe(VI)_s (a) and $\text{Fe(VI)}_s + \text{Fe(III)}$ (b) on the simultaneous removal of As and Mn from the effluent $S_{\text{As+Mn}}$ (pH_a : 5.5; reaction time: 5 min; settling time: 15 min)

5.5.3.2 Addition of ferric salt effect

The use of Fe(III) as a supporting coagulant for the treatment of As by Fe(VI) was previously attempted to reduce the necessary Fe(VI)_s dose, residual salinity, and operating costs (Jain et al., 2009; Lee et al., 2003). The amount of Fe(VI)_s required to remove As from a solution decreased from 2 to 0.5 mg/L when using Fe(III) (Lee et al., 2003). Several doses of Fe₂(SO₄)₃ (6, 8, 10 mg/L as Fe(III)) were tested in the present study as a coagulant to enhance the performance of Fe(VI)_s for As(III) and Mn(II) removal, while reducing the dose of Fe(VI)_s required. The amount of Fe(III) was calculated depending on the results obtained for the treatment of the effluent S_{As+Mn} by Fe(VI)_s only, targeting the same total amount of Fe. Residual As and Mn concentrations measured in the effluent after treatment with different doses of Fe(VI)_s and Fe(III) are presented in Fig. 5.4b.

Based on the results presented in Fig. 5.4b, the gradual replacement of Fe(VI) by Fe(III) slightly deteriorated the removal of Mn (from 99.6 to 90%) and to an even lesser extent of As (from 99.4 to 94%), when increasing the Fe(III) added from 0 to 10 mg/L. These findings confirm that As removal is more impacted by the number of available sorption sites on Fe(III)-hydroxides than by the use of an oxidizing agent (i.e., Fe(VI)), while the removal of Mn(II) requires stronger oxidizing conditions for its oxidation to Mn(IV) and precipitation as Mn-oxides. Nevertheless, the addition of Fe(III) decreased the amount of Fe(VI)_s needed by nearly 50% (12.5 mg/L with Fe(III) vs. 28 mg/L without Fe(III)) to achieve satisfactory As and Mn removal efficiencies (> 99% for As and > 97% for Mn) from the effluent S_{As+Mn} and meet the criteria for effluent discharge in the environment. The amount of Fe(VI)_s could be decreased from 15 to 12.5 mg/L when adding Fe(III) to the system to efficiently remove Mn ([Mn]_{final} < 2 mg/L). This small decrease in Fe(VI)_s dose could be attributed to the pH decrease (around 3.5) after Fe(III) addition. Indeed, Fe(VI) is a stronger oxidizing agent under acidic conditions,

improving Mn(II) oxidation to Mn(IV). However, the pH needs to be increased at the end of the treatment to reach the regulatory criteria ($6 < \text{pH} < 9$). It should be noted that the amount of neutralizing agent required to adjust the pH is quite negligible, leading to a slight increase in residual salinity. Because Fe(VI) is more expensive than Fe(III) and produces more residual salinity (because of its low purity, around 25% FeO_4^{2-}), the combined use of a smaller amount of Fe(VI)_s as an oxidant and of Fe(III) as an additional coagulant is promising to efficiently remove As (99%) and Mn (97%), while meeting the regulatory criteria ($[\text{As}]_{\text{final}} = 0.03 \text{ mg/L} < 0.2 \text{ mg/L}$, $[\text{Mn}]_{\text{final}} = 0.13 \text{ mg/L} < 2 \text{ mg/L}$), lowering residual salinity (Table S5.1), and cutting operating costs.

5.5.4 Performance of Fe(VI)_s and Fe(III) on As and Mn removal from surrogate mine effluent

5.5.4.1 Treatment by Fe(VI) and Fe(III)

E_{low} and E_{high} were treated using Fe(VI)_s and Fe(III) under the optimal conditions ($[\text{Fe(VI)}]: 12.5 \text{ mg/L}$, $[\text{Fe(III)}]: 8 \text{ mg/L}$; $\text{pH}_a: 5.5$, reaction time: 5 min, settling time: 15 min) identified in previous treatability testing performed on the effluent $S_{\text{As+Mn}}$ (Table 5.4). For the treatment of E_{low} , the amounts of Fe(VI)_s and Fe(III) were adjusted to 4.3 and 2.0 mg/L, respectively, to maintain the same contaminant/Fe(VI)+Fe(III) ratio, as the initial concentrations of As and Mn were lower than for the effluent $S_{\text{As+Mn}}$ (Table 5.1).

High As and Mn removal efficiencies were achieved for both E_{low} (97% for As and 80% for Mn) and E_{high} (> 99% for As and 99% for Mn) using the most performant conditions previously identified. A slight increase in Mn removal (from 97 to 99%) was observed between the effluents $S_{\text{As+Mn}}$ and E_{high} (with similar initial As and Mn concentrations), while comparable As removal was achieved (99%). This improvement in Mn removal could be explained by the presence of Ca (470–480 mg/L), which promotes the formation of larger $\text{Fe}(\text{OH})_3$ flocs, allowing for better removal of residual Mn(II) through sorption on the surface of the flocs (Ruiping et al., 2007). The attraction between Mn(II) and the negatively charged Mn-oxides (pH_{PZC} of $\text{MnO}_2 = 1.8$) could also contribute to a better Mn(II) removal (Xie et al., 2018). The amount of sludge produced was relatively low ($8 \cdot 10^{-2}$ – $3 \cdot 10^{-1}$ g of wet sludge/ m^3 , which is equivalent to $4 \cdot 10^{-2}$ – $1 \cdot 10^{-2}$ g of dry sludge/ m^3), facilitating its handling and storage. These results are in agreement with the literature, with minimal sludge production as one of the advantages of Fe(VI) treatment (Heřmánková et al., 2020).

Table 5.4 Effect of Fe(VI)_s+Fe(III) addition on As and Mn removal (pH_a: 5.5; reaction time: 5 min; settling time: 15 min) from E_{low} and E_{high}.

Effluent		E _{low}	E _{high}
[Fe(VI)] (mg/L)		4.3	12.5
[Fe(III)] (mg/L)		2.0	8.0
[contaminant] _{initial} (mg/L)	As	1.56	4.05
	Mn	0.05	4.27
[contaminant] _{final} (mg/L)	As	0.04	0.01
	Mn	0.01	0.04
Efficiency (%)	As	97	100
	Mn	80	99
[Fe] _{final} (mg/L)		0.25	0.22
pH _{final}		5.55	5.69
pH _a after filtration		6.15	6.14
EC _{final} (mS/cm)		2.97	3.08
ORP _{final} (mV)		415	448
Mass of dry sludge (g)		0.12	0.24

5.5.4.2 Toxicity

Based on the results, the untreated and treated effluents S_{As+Mn} were deemed acutely toxic to *D. magna* (results not presented), which may be mainly attributed to the low hardness of the deionized water used (< 0.05 mg/L CaCO₃). A hardness greater than 80 mg/L CaCO₃ is recommended to eliminate hardness as a factor of toxicity towards *D. magna* (Environment Canada, 1996). Results also showed that the mortality of

D. magna decreased from 70% to less than 10% in undiluted E_{high} after treatment by $\text{Fe(VI)}_s + \text{Fe(III)}$, while a total absence of mortality for both untreated and treated E_{high} was found for other dilutions (Fig. 5.5b). A mortality of 30% was observed in the treated E_{low} at 100% dilution (% - v/v), while E_{low} before treatment showed no mortality with all dilutions (Fig. 5.5a). This mortality, which is equivalent to three dead *D. magna* species, could be due to unhealthy organisms used in this test and should be considered with caution. Another potential cause of this mortality might be the presence of Ba (420 mg/L) and Na (540 mg/L) in high concentrations, which can be problematic for this sensitive organism (Okamoto et al., 2014). With a 48 h $\text{LC}_{50} > 100\%$ (v/v) (equivalent to < 1 acute toxic units—TUa; defined as $100/\text{LC}_{50}$), untreated and treated E_{low} and treated E_{high} were non-toxic (Fig. 5.5), while before treatment E_{high} was considered acutely toxic with a 48 h LC_{50} of 85.4% (v/v) (equivalent to 1.17 TUa) (Ministry of Justice, 2022). The observed toxicity in E_{high} before treatment could be a result of relatively high As (4.05 mg/L) and Mn (4.27 mg/L) contents compared to the acceptable concentrations defined for aquatic life protection (0.005 mg As/L (CCME, 1999); 0.6–1.9 mg Mn/L (Reimer, 1999)). Based on these results, it can be concluded that toxic by-products were not generated during treatment by Fe(VI), which is consistent with previous studies performed on different organisms (e.g., *Spirostomum ambiguum*, *Spinacia oleracea*) (Drzewicz et al., 2018; Malik et al., 2017).

The non-toxicity observed for untreated and treated E_{low} and treated E_{high} confirm that the toxicity observed for the effluent $S_{\text{As+Mn}}$ was not due to the presence of potentially toxic Fe(VI) by-products or the final concentration of As or Mn (which were similar). This confirms that the hardness of the water can be a potential factor of toxicity to *D. magna* (< 0.05 vs. 1,200 mg/L CaCO_3 for the effluent $S_{\text{As+Mn}}$ vs. E_{low} and E_{high}). Indeed, Ca^{2+} plays an important role in the protection of *D. magna* by binding on its surface, thus decreasing the toxicity effect of other contaminants (Heijerick et al., 2002; Paulauskis et al., 1988; Yim et al., 2006).

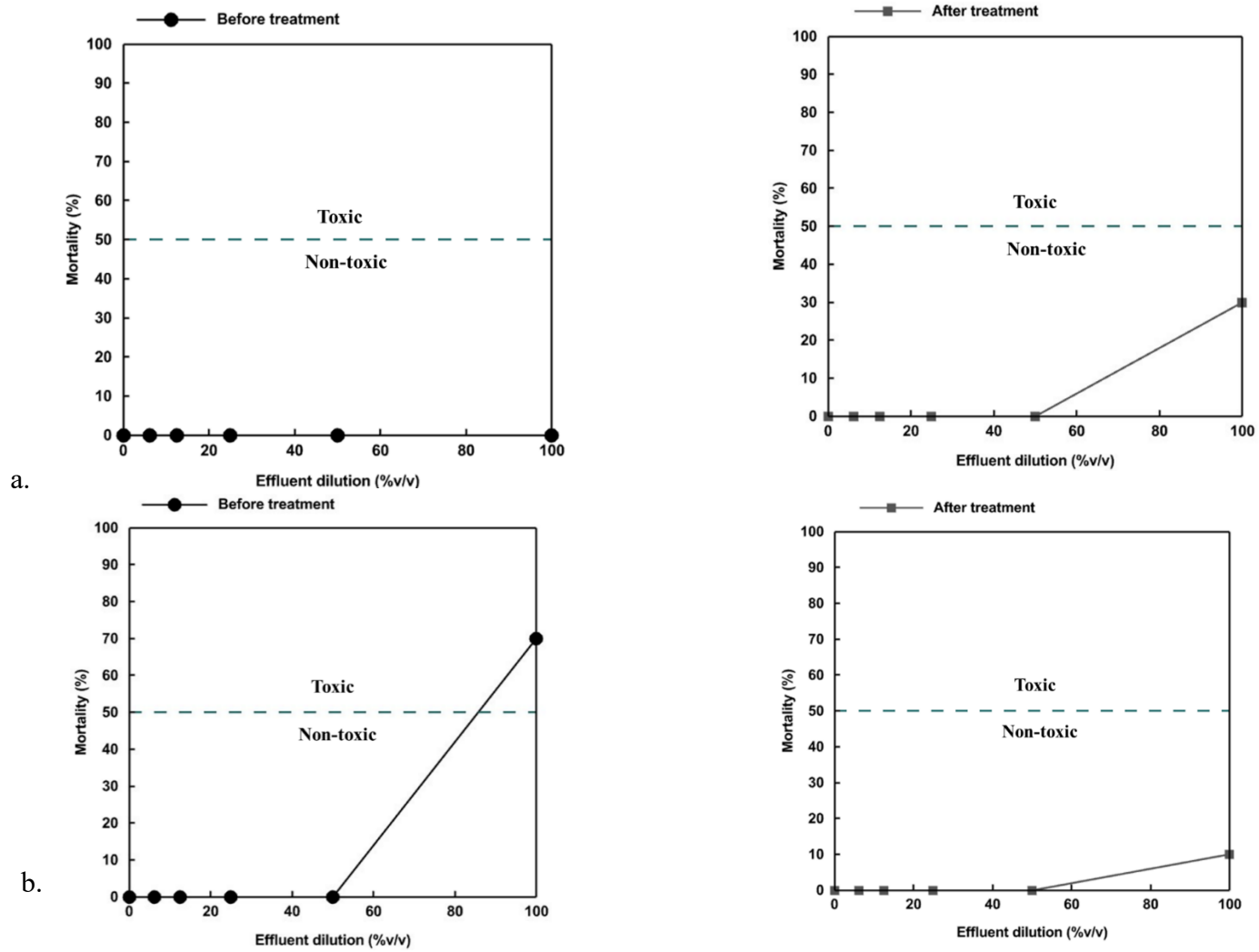


Figure 5.5 Mortality evolution of *D. magna* for untreated and treated E_{low} (a) and E_{high} (b).

5.6 Conclusion

This study evaluated the performance of Fe(VI), alone or in combination with Fe(III), for the simultaneous removal of As and/or Mn from synthetic and surrogate neutral mine effluents. Both Fe(VI)_s and Fe(VI)_w showed similar As removal efficiency from the effluent S_{As}, while Fe(VI)_w showed higher Mn removal efficiency from the effluent S_{Mn}. However, Fe(VI)_w greatly increased the residual salinity and justified the use of Fe(VI)_s for further tests. Fe(VI)_s efficiently removed As (98%) and Mn (97%) at pH_a = 5.5 in the first minute of the reaction time from the effluents S_{As} and S_{Mn}, respectively. An increase in Fe(VI)_s doses led to an efficiency improvement. Fe(VI)_s doses of 22 mg/L and 5 mg/L, respectively, were required to remove As from the effluent S_{As} and Mn from the effluent S_{Mn} to meet the regulatory criteria (< 0.2 and < 2 mg/L for As and Mn, respectively). The application of 28 mg Fe(VI)/L efficiently removed As (99%) and Mn (98%) from the effluent S_{As+Mn} in a one-step treatment. A higher Fe(VI)_s dose was required to efficiently treat S_{As+Mn} than for S_{As} or S_{Mn}, probably because of the competition between As(III) and Mn(II). The amount of Fe(VI) had a greater impact on Mn than As removal efficiency, as stronger oxidizing conditions are required for Mn(II) oxidation, while As removal is affected by the amount of Fe(III)-hydroxides produced. The combination of Fe(VI)_s+Fe(III) showed efficient removal of As (99%) and Mn (97%), with a lower Fe(VI)_s dose vs. Fe(VI)_s alone, lower residual salinity, and lower associated operating costs. Finally, the Fe(VI)_s+Fe(III) treatment was tested with the most performant conditions for the removal of As and Mn from two neutral surrogate mine effluents, E_{low} and E_{high}. Efficient As and Mn removal was found, while resulting in a low amount of dry sludge. Lastly, the Fe(VI)_s+Fe(III) treatment eliminated E_{high} toxicity to *D. magna*, while no toxicity was measured for untreated and treated E_{low}. The findings suggest that Fe(VI) alone or in combination with Fe(III) could be a promising option for the simultaneous

removal of metal(loid)s from synthetic or real mine effluents. Forthcoming studies will have to focus on the stability of the produced sludge.

Credit authorship contribution statement

Reem Safira: Conceptualization, Methodology, Visualization, Formal analysis, Investigation, Writing - original draft. Lucie Coudert: Conceptualization, Methodology, Formal analysis, Visualization, Supervision, Project administration, Funding acquisition, Writing - review & editing. Carmen M. Neculita: Conceptualization, Methodology, Visualization, Formal analysis, Supervision, Writing - review & editing, Funding acquisition. Étienne Bélanger: Methodology, Formal analysis, Writing – review & editing. Eric Rosa: Conceptualization, Methodology, Visualization, Formal analysis, Supervision, Writing - review & editing.

Declaration of competing interest

The authors declare that there is no conflict of interest.

Acknowledgments

This study was funded by the Natural Sciences and Engineering Research Council of Canada (NSERC), Canada Research Chairs Program (CRC) and the industrial partners of the Research Institute on Mines and Environment (RIME) - University of Québec in Abitibi-Témiscamingue (UQAT) - Polytechnique Montréal, including Agnico Eagle, Newmont Éléonore, Iamgold, Canadian Malartic Mine, Raglan Mine – a Glencore Company and Rio Tinto.

Table S5.1 Effect of Fe(VI) and Fe(VI)+Fe(III) doses on the performance of As and Mn removal from a binary contaminant effluent

Binary contaminant-Fe(VI) _s													
[Fe(VI)]	Fe(VI)/As(III) molar ratio	Fe(VI)/Mn(II) molar ratio	pH _a	[contaminant] _i (mg/L)		[contaminant] _f (mg/L)		Efficiency (%)		[Fe] _f (mg/L)	pH _f	EC _f (mS/cm)	ORP _f (mV)
				As	Mn	As	Mn	As	Mn				
5	0.88/1.0	0.5/1.0	5.46	3.45	4.30	2.42	2.05	30	52	0.84	6.10	0.06	277
10	1.76/1.0	1.0/1.0	5.60	3.45	4.30	2.84	3.08	18	28	0.75	6.20	0.09	253
10	1.76/1.0	1.0/1.0	5.43	3.47	4.45	2.75	2.76	21	38	3.13	6.04	0.08	373
12.5	2.2/1.0	1.25/1.0	5.40	3.41	4.15	2.51	2.34	26	44	3.50	6.20	0.11	450
12.5	2.2/1.0	1.25/1.0	5.45	3.42	4.34	2.66	2.62	22	40	4.67	6.30	0.12	447
15	2.64/1.0	1.5/1.0	5.54	3.42	4.29	1.10	0.12	68	97	0.10	6.17	0.13	437
15	2.64/1.0	1.5/1.0	5.42	3.36	4.38	0.99	0.08	71	98	0.15	6.10	0.13	419
20	3.52/1.0	2.0/1.0	5.46	3.45	4.30	0.21	0.09	94	98	0.16	6.10	0.17	477
20	3.52/1.0	2.0/1.0	5.52	3.38	4.20	0.35	0.10	90	98	0.19	6.25	0.17	516
22	4.0/1.0	2.3/1.0	5.60	3.38	4.20	0.33	0.10	90	98	0.22	6.34	0.18	522
28	5.0/1.0	2.9/1.0	5.48	3.34	4.27	0.05	0.08	99	98	0.03	6.23	0.23	466

Table S5.1 (continued) Effect of Fe(VI) and Fe(VI)+Fe(III) doses on the performance of As and Mn removal from a binary contaminant effluent

Binary contaminant-Fe(VI) _s + Fe(III)												
[Fe(VI)] (mg/L)	[Fe(III)] (mg/L)	pH _a	[contaminant] _i (mg/L)		[contaminant] _r (mg/L)		Efficiency (%)		[Fe] _r (mg/L)	pH _r	EC _r (mS/cm)	ORP _r (mV)
			As	Mn	As	Mn	As	Mn				
10	10	5.30	3.42	4.29	0.02	0.05	99	99	< 0.01	5.52	0.14	397
10	10	5.41	3.42	4.29	0.41	0.86	88	80	0.12	5.58	0.14	353
12.5	8	5.42	3.42	4.34	0.03	0.13	99	97	< 0.01	6.04	0.13	343
12.5	8	5.40	3.42	4.34	0.03	0.12	99	97	< 0.01	5.98	0.13	293
15	6	5.42	3.47	4.45	0.02	0.01	99	100	< 0.01	6.08	0.12	412
15	6	5.40	3.47	4.45	0.02	0.02	99	100	0.03	6.06	0.13	408

CHAPTER 6

COMPARATIVE ASSESSMENT OF AS- AND MN-RICH SLUDGE STABILITY FROM NEUTRAL MINE WATER TREATMENT BY FE(VI) VS ELECTROCOAGULATION

ÉVALUATION COMPARATIVE DE LA STABILITÉ DES BOUES DE TRAITEMENT D'EAUX MINIÈRES NEUTES TRAITÉS PAR LES FE(VI) ET ÉLECTROCOAGULATION

Reem Safira¹, Abdellatif Elghali², Mostafa Benzaazoua², Lucie Coudert^{1,*}, Eric
Rosa^{1, 3}, Carmen M. Neculita¹

¹Research Institute on Mines and Environment (RIME), University of Québec in
Abitibi-Témiscamingue (UQAT), Rouyn-Noranda, QC, Canada

²Geology and Sustainable Mining Institute (GSMI), Mohammed VI Polytechnic
University (UM6P), Benguerir 43150, Morocco

³Groupe de Recherche sur l'Eau Souterraine (GRES - Groundwater Research Group),
RIME, UQAT, Amos, QC, Canada

This chapter will be submitted to Journal of Cleaner Production (in preparation)

6.1 Abstract

The electrocoagulation (ECG) and ferrate (Fe(VI))-based processes are increasingly acknowledged as efficient for the simultaneous removal of As and Mn from synthetic and real mine effluents. Prior to design of full-scale applications, more information on the physicochemical, mineralogical, and environmental characterization of the produced sludge is required. The main objective of this study was to characterize and evaluate the leaching potential of problematic elements in As- and Mn-rich sludge produced during ECG and Fe(VI) treatment of circumneutral surrogate mine water. To do so, PHREEQC modelling was carried out on the effluents, both before and after ECG and Fe(VI) treatment, to calculate the saturation index of dissolved As, Fe, and Mn species. A physicochemical and mineralogical characterization of the sludge was also performed using powder X-ray diffraction (PXRD) and a scanning electron microscope equipped with an energy dispersive spectrometer (SEM-EDS). Then, a non-sequential selective extraction procedure (N-SEP) combined with a USGS field leaching test (FLT) was conducted to evaluate the environmental behaviour of the As- and Mn-rich sludge. Geochemical modelling indicated that the Fe(VI) and ECG processes favour the precipitation of Fe-(oxy)hydroxides (lepidocrocite, schwertmannite, ferrihydrite). Chemical characterization showed that the Fe(VI)-sludge contained higher As and Mn concentrations and lower Fe concentrations than the ECG-sludge (3.8% As, 5.3% Mn, and 34% Fe for the Fe(VI) sludge vs. 1.2% As, 0.77% Mn, and 52% Fe for the ECG-sludge). These findings can be explained by the smaller amount of sludge produced during the Fe(VI) treatment and the higher removal efficiency of this method, especially for Mn. The PXRD patterns suggested the formation of poorly crystalline Fe-(oxy)hydroxides (lepidocrocite or β -FeO(OH) in the ECG-sludge vs. ferrihydrite in the Fe(VI) sludge); however, no As- or Mn-bearing minerals were identified. Findings from N-SEP tests showed different speciation of As and Mn in the sludge, with a higher proportion of As bound to poorly crystalline Fe-(oxy)hydroxides in the Fe(VI) sludge than the ECG-sludge (97% and 71%,

respectively), and higher proportion of Mn associated with the residuals in the Fe(VI)-sludge than the ECG-sludge (57% and 5.7%, respectively). Finally, FLT results indicated that very low concentrations of As (<0.05 mg/L) and Mn (<0.5 mg/L) were leached from the ECG- and Fe(VI) sludge, with the Fe(VI) treatment resulting in slightly better As and Mn immobilization in the sludge relative to the ECG process. Nevertheless, both treatment processes were satisfactory in terms of efficient removal of As and Mn and their immobilization in the produced sludge.

Keywords: advanced oxidation processes, mine water, As and Mn contamination, metal(loid)s removal, mineralogy, sludge stability

6.2 Résumé

Les procédés de traitement par électrocoagulation (ECG) et utilisation des ferrates (Fe(VI)) sont de plus en plus reconnus comme efficaces pour enlever simultanément l'As et le Mn des eaux minières synthétiques et réelles. Avant la conception d'unités de traitement à pleine échelle, des informations additionnelles sur la caractérisation physico-chimique, minéralogique et environnementale des boues produites sont nécessaires. L'objectif principal de cette étude était de caractériser et d'évaluer le potentiel de lixiviation des éléments problématiques présents dans les boues riches en As et en Mn produites lors du traitement par ECG ou par Fe(VI) des eaux minières contaminées. Pour ce faire, une modélisation PHREEQC a été réalisée sur les effluents, avant et après traitement par ECG ou par Fe(VI), afin de calculer l'indice de saturation des espèces dissoutes (e.g., As, Fe et Mn). Une caractérisation physicochimique et minéralogique des boues a également été réalisée à l'aide de diffraction des rayons X sur poudre (PDRX) et d'un microscope électronique à balayage équipé d'un spectromètre à dispersion d'énergie (MEB-EDS). Ensuite, une extraction non séquentielle (N-SEP) combinée à un test de lixiviation sur le terrain (Field leaching test - FLT) de l'USGS ont été réalisées pour évaluer le comportement environnemental des boues riches en As et en Mn. La modélisation géochimique a indiqué que les procédés de traitement par Fe(VI) ou par ECG favorisent la précipitation des oxydes/hydroxydes de Fe (lépidocrite, schwertmannite, ferrihydrite). La caractérisation chimique a montré que des teneurs plus élevées en As et Mn et des teneurs plus faibles en Fe sont présentes dans les boues de Fe (VI) (3,8% As, 5,3% Mn, et 34% Fe) par rapport aux boues d'ECG (1,2% As, 0,77% Mn, et 52% Fe). Ces résultats peuvent s'expliquer par la plus faible quantité de boues produites lors du traitement par les Fe(VI) et par une efficacité d'enlèvement plus élevée, en particulier pour le Mn. Les diffractogrammes PDRX suggèrent la formation d'(oxy-)hydroxydes

de Fe faiblement cristallins (lépidocrocite ou β -FeO(OH) pour les boues ECG vs. ferrihydrite pour les boues de Fe (VI)), alors qu'aucun minéral porteur d'As ou de Mn n'a été identifié. Les résultats des tests N-SEP ont montré une spéciation différente de l'As et du Mn dans les boues ECG et Fe(VI), avec une proportion plus élevée d'As lié aux (oxy-)hydroxydes de Fe faiblement cristallins (97% pour les boues Fe(VI) vs. 71% pour les boues ECG) et une proportion plus élevée de Mn associé à la fraction résiduelle dans les boues de Fe(VI) (57% pour les boues Fe(VI) vs. 5,7% pour les boues ECG). Enfin, les résultats FLT ont indiqué que de très faibles concentrations d'As (<0,05 mg/L) et de Mn (<0,5 mg/L) étaient lixiviées à partir des boues d'ECG et de Fe(VI), le traitement au Fe(VI) entraînant une légère meilleure immobilisation de l'As et du Mn dans les boues par rapport au procédé ECG. Néanmoins, les deux procédés de traitement se sont révélés satisfaisants en termes d'enlèvement efficace de l'As et du Mn et de leur immobilisation dans les boues produites.

Mots clés: procédés d'oxydation avancés, eaux de mine, contamination par l'As et le Mn, enlèvement des métaux/métalloïdes, minéralogie, stabilité des boues

6.3 Introduction

Growing exploitation of low-grade gold deposits is partially responsible for the co-occurrence of As and Mn in contaminated mine and natural waters (Bondu et al., 2020; Luo et al., 2020; Tiwari et al., 2017). Efficient treatment of As and Mn is required prior to the release of mine water to the environment to reduce potential health and environmental impacts related to the toxicity of these elements (Neculita and Rosa, 2019; Ryskie et al., 2021; USEPA, 2002). Several conventional and emerging technologies, including advanced oxidation processes using ferrate (Fe(VI)) and electrocoagulation (ECG), have been successfully applied for the efficient removal of As and Mn from synthetic or real mine water (Del Àngel et al., 2014; Reátegui-Romero et al., 2018; Safira et al., 2023). Previous studies have documented the removal of As(III) and Mn(II) from contaminated water using Fe(VI), beginning with oxidation to As(V) and Mn(IV), followed by (co-)precipitation and adsorption on newly formed Fe(III)-hydroxides (Goodwill et al., 2016; Wang et al., 2020). The partial incorporation of As into the structure of Fe(III)-hydroxide nanoparticles has also been reported (Prucek et al., 2013; Wang et al., 2020). During ECG treatment using Fe-electrodes as sacrificial anodes, As(III) is oxidized to As(V) and removed by (co-)precipitation and adsorption onto newly formed Fe(III) hydroxides. Mn(II) is removed by adsorption or trapping (sweep coagulation) by the Fe(III)-hydroxides or by precipitation as Mn(OH)_2 at $\text{pH} > 7$ (Kobyá et al., 2022; Li et al., 2012; Oncel et al., 2013; Shafaei et al., 2010). In both processes, As and Mn are removed from contaminated mine water as (co-)precipitated or sorbed species; as such, the produced sludge could be prone to leaching under changing environmental conditions (pH or Eh). Although several studies have evaluated the efficiency of Fe(VI) or ECG for the removal of As and Mn from synthetic and real wastewater (and, to a lesser extent, contaminated mine water), there is still limited knowledge on the chemical and mineralogical composition of the

produced sludge as well as its stability over time. If improperly managed, this As- and Mn-rich sludge may represent a secondary source of contamination (Coudert et al., 2020; Jouini et al., 2019a; 2020a).

To better anticipate the environmental stability of the sludge and provide solutions for improving its management, it is crucial to characterize in detail its chemistry and mineralogy, and to assess metal(loid) mobility. Physical and chemical characteristics of the produced sludge are highly dependent on the quality of the wastewater and the treatment used (Amanda and Moersidik, 2019; Coudert et al., 2020; Jouini et al., 2019a,b). Previous studies have documented that the stability of metal(loid)-rich sludge is affected by its physical (particle size), chemical, and mineralogical (mineralogy, crystallinity) composition, as well as the site related disposal characteristics (pH, Eh, salinity, hydrological conditions, freeze-thaw cycles, temperature) (Coudert et al., 2020; Jouini et al., 2019a, 2020c; Kousi et al., 2018; Neculita and Rosa, 2019; Neil et al., 2014; Northrup et al., 2018).

The identification and quantification of mineral phases encountered in post-treatment sludge, in terms of the surface morphology, elemental content, and distribution of the flocs within the phase, can provide information on the possible attenuation processes that occurred during the selected treatment. This improved understanding of the immobilization methods (co-precipitation, adsorption, precipitation) can contribute to further insights on the potential mobility of metal(loid)s and the short- or long-term stability of reactive metal(loid)-bearing minerals under different environmental disposal conditions (redox conditions) (Jamieson, 2011; Jamieson et al., 2015). The mineralogical characterization of As-bearing sludge from the treatment of synthetic and sometimes real effluents and the short-term stability of this material has been extensively studied (Clancy et al., 2013; Harris, 2000; Welham et al., 2000), whereas the characterization of Mn-bearing sludge from mine water treatment is sparsely documented (Butler, 2011; Ginder-Vogel and Remucal, 2016; LeBourre et al., 2020).

However, the mineralogical characterization of As- and Mn-bearing sludge produced from the treatment of real mine effluents can be challenging (Nazari et al., 2017; Pantuzzo and Ciminelli, 2010), depending on the initial composition of the effluent to be treated and aging of the sludge. Precipitation of As in the form of scorodite ($\text{FeAsO}_4 \cdot 2\text{H}_2\text{O}$) is considered an attractive option for its immobilization, as scorodite is known to be stable under mildly acidic ($\text{pH} > 2$) to neutral conditions. However, high concentrations of As can be released from scorodite under strongly acidic ($\text{pH} < 2$; 20-206 mg/L of As) and alkaline conditions ($\text{pH} > 8$; 45-787 mg/L of As) (Coudert et al., 2020). The reductive dissolution of scorodite may also result in the release of As to the environment (Demopoulos, 2005; Lagno et al., 2010; Revesz et al., 2015). Ferric arsenate ($\text{FeAsO}_4 \cdot 4-7\text{H}_2\text{O}$), another well-known As bearing precipitate formed during mine water treatment, is stable under slightly acidic medium ($\text{pH} 3-4$) and is considered a suitable form for the safe disposal of As-bearing sludge under typical environmental disposal conditions (Harris, 2000). Previous studies have shown that oxidative precipitation of Mn(II) produces more stable sludge, even at low pH (3.5), than that produced from the precipitation of Mn(II) at high pH (Watzlaf, 1987; Watzlaf, and Casson, 1990). Another study reported an increase in Mn mobility with decreasing pH from Mn-bearing residues produced from sorption on Fe(III) hydroxides or precipitation at high pH (> 9) (Ginder-Vogel and Remucal, 2016). Anaerobic conditions, such as those found in tailings impoundment facilities, can affect the stability of hydrous Mn-oxides, resulting in reductive dissolution and the release of Mn and any other metal(loid)s adsorbed on the mineral surface (Butler, 2011; Ginder-Vogel and Remucal, 2016; Tobiasson et al., 2016). For As- and Mn-rich residues generated from the sorption of As on Mn-oxides, a lower release of As has been observed under neutral ($\text{pH} 6.5-7$) than under acidic ($\text{pH} 3$) and alkaline conditions ($\text{pH} 8$) (Ettler et al., 2015). However, the presence of competing ions such as PO_4^{3-} and Ca^{2+} can be responsible for As release from the surface of Mn-oxides (Lafferty et al., 2011).

To evaluate the potential release of problematic metal(loid)s from mine residues, including post treatment sludge, several leaching tests such as the toxicity characteristics leaching procedure (TCLP; Pinto et al., 2014), the synthetic precipitation leaching procedure (SPLP; Kim et al., 2005; Pinto et al., 2014), the Ph-dependent leaching test (pH-stat; Cappuyns and Swennen, 2008; Van Herreweghe et al., 2002), (non-)sequential extraction (Fernández-Ondoño et al., 2017; Rakotonimaro et al., 2021), and the field leaching test (FLT; Hageman, 2007) have been developed. Most of these tests are standardized and used to assess the short-term stability of the sludge or to classify them as hazardous, non-hazardous, valuable, or non-valuable materials (Jouini et al., 2019b). Each of these leaching tests has advantages and drawbacks. For example, the sequential extraction procedure (SEP) was designed to assess the mobility of metals from low to moderately contaminated soils and sediments; however, the speciation of metal(loid)s and their mobility can be impacted by the previous leaching step in the test (re-adsorption of As on other mineral phases and desorption in the subsequent extraction step) (Caraballo et al., 2018; Rakotonimaro et al., 2021; Wenzel et al., 2001). The non-sequential selective extraction procedure (N-SEP, or parallel extraction procedure) was developed to better evaluate the mobile and solid-phase fractionation of As by separately mixing solid samples with reagents of increasing dissolution strength (Ma et al., 2019; Turunen et al., 2016). The main limitations of the TCLP test for the evaluation of metal(loid) release from mine residues are related to the use of acetic acid and acidic pH conditions, potentially leading to an underestimation of As release (Ghosh et al., 2004). The FLT test was developed by the U.S. Geological Survey (USGS) to assess the mobility of metal(loid)s from mine waste (Hageman, 2007; Hageman et al., 2015). The main challenge associated with the FLT is the lack of specific criteria for the allowable metal(loid) concentration. In previous studies using FLT, alone or along with other leaching tests, the authors compared the concentration of metal(loid)s found in the FLT leachate with the TCLP criteria for regulated metal(loid)s (e.g., As) or drinking water and aesthetic objective criteria for non-regulated metals (e.g., Mn) (Akhavan and

Golchin, 2021; Al-Abed et al., 2006; Hageman et al., 2015; McCann and Nairn, 2022). Up to the best of our knowledge, a chemical and mineralogical characterization of As- and Mn-rich sludge produced during ECG and Fe(VI) treatment, as well as an assessment of the potential release of metal(loid)s using static tests, has not yet been conducted.

In this context, the main objective of the present study was to characterize As- and Mn-rich sludge produced during ECG and Fe(VI) treatment of circumneutral surrogate mine water and to evaluate the possible leaching of problematic elements from these post treatment-sludges. The methodological approach included chemical and mineralogical characterization combined with static leaching tests and thermodynamic equilibrium calculations to better understand the composition of the As- and Mn rich sludge produced during ECG and Fe(VI) treatment and the stability of these materials (Fig. 6.1).

6.4 Materials and methods

6.4.1 Preparation of surrogate mine water and sludge production

The surrogate mine water (E_{high}) was prepared by washing desulfurized mine tailings collected from an active mine site located in Northern Quebec with deionized water (solid/liquid: 1:1); the resulting liquid was spiked with NaAsO_2 and $\text{MnSO}_4 \cdot \text{H}_2\text{O}$ salts to reach the target concentrations encountered on the mine site (3.5 mg/L of As and 4.5 mg/L of Mn; Safira et al., 2023). E_{high} was characterized for its physicochemical parameters (pH and oxidation-reduction potential (ORP)) using a VWR Symphony®

multimeter equipped with electrodes that were calibrated daily (Orion 915 BNWP double junction Ag/AgCl electrode for pH; Orbisint CPS 12D Pt electrode for ORP). Electrical conductivity (EC) was determined using a VWR Traceable® Expanded Range Conductivity Meter equipped with an epoxy probe that was calibrated daily. Metal(loid) concentrations were measured, after sample filtration using syringe filter (pore size of 0.45 μm , diameter of 30 mm), using inductively coupled plasma optical emission spectroscopy (ICP OES; Agilent 5800-Vertical Dual View (VDV), Canada); the instrument was calibrated before each series of analyses using certified multi-elements standard solutions (Agilent Technologies; TruQ).

Several experiments for the treatment of E_{high} using ECG and Fe(VI) were conducted to produce the required amount of sludge for further analyses. The tests were executed under the most performant operating parameters, which were identified in previous studies (Safira et al., 2023; Safira et al., 2024). For ECG, a 2 L Pyrex reactor was used to perform the experiments, with a 1.80 L working volume. Two iron electrodes (dimensions: 110 mm \times 110 mm \times 2 mm; total submerged area: 121 cm^2 ; purity: $\geq 99.5\%$) were directly connected to a DC power supply (ARKSEN 605D, USA; voltage: 0–30 V; electrical current: 0–10 A), with an inter-electrode distance of 10 mm (Safira et al., 2024). For the Fe(VI) treatment, a 20 L plastic pail was used as the reactor vessel, with a 10 L working volume. A digital agitator was utilized to continuously mix the water. The steps involved in the ECG and Fe(VI) treatment processes are presented in Fig. S6.1. For both processes, the effluent was left to settle after treatment and filtered using Whatman filter papers (nylon, diameter of 90 mm, pore size of 0.45 μm) to collect the solid sludge. The collected wet residue was air-dried for 24 h, ground using a mortar and pestle, and homogenized. Sub-samples of dried sludge were collected for chemical (0.50 g) and mineralogical (synchrotron powder X-ray diffraction (PXRD): 1 g; scanning electron microscope equipped with an energy dispersive spectrometer (SEM-EDS): 0.50 g for ECG and 0.80 g for Fe(VI))

characterization, as well as for the evaluation of the leaching potential of metal(loid)s using the N-SEP and FLT (2.20-2.50 g) (Fig. 6.1).

6.4.2 Geochemical modeling and thermodynamic equilibrium calculations

Geochemical calculations were conducted using PHREEQC-Version 3 (Parkhurst and Appelo, 2013) with the minteq.v4.dat thermodynamic database; these calculations helped in the evaluation of the mineral precipitation processes likely to occur under the conditions prevailing during the treatment of E_{high} by ECG and Fe(VI). The speciation-solubility models were constructed based on defined pe–pH–temperature conditions and concentrations of dissolved solids to represent as accurately as possible the physicochemical conditions prevailing at different stages of contaminated mine water treatment. The focus was on determining saturation indices for Fe- and Mn-(oxy)hydroxides and the speciation of Fe, Mn, and As in solution during treatment. The simulation steps for ECG treatment involved: i) calculation of mineral saturation indices for the initial solution; ii) simulation of the solution after pH adjustment with HCl; iii) simulation of the solution after current application, and iv) simulation of the final solution, after treatment. The simulation steps for the Fe(VI) treatment model included: (i) calculation of mineral saturation indices for the initial solution; (ii) simulation of the solution after Fe(VI) addition; (iii) simulation of the solution after ferric sulfate addition; (iv) simulation of the solution after pH adjustment with H_2SO_4 , and (v) simulation of the final solution, after treatment (Fig. S6.1).

6.4.3 Physicochemical and mineralogical composition of the sludge

The physicochemical characterization of the ECG and Fe(VI) sludge consisted of determining the water content and the chemical elemental composition, while the mineralogical characterization consisted of identifying the As- and Mn-bearing phases using PXRD and SEM-EDS analyses.

Water content was determined by drying the sludge sample, collected after 30 min of settling, at 60°C for 48 h. Then, the dried sample was left to cool in a desiccator for 2 h before weighting twice successively to obtain a fixed measurement (ASTM, 2010). The mass water content was then calculated by dividing the mass of water in the sample by the total mass (mass of water in the sample + mass of dry sample). Dried sludge produced from the ECG and Fe(VI) treatments were subjected to strong acid digestion (HNO₃, Br₂, HCl, and HF) to determine their chemical composition (USEPA, 1996). The concentrations of metal(loid)s in the digestate were determined using inductively coupled plasma mass spectrometry (ICP-MS; relative precision of 5%). The analyses were performed at the SGS Canada Inc. laboratories.

PXRD for phase identification of minerals was performed at the Canadian Light Source, University of Saskatchewan, Canada. Samples were mounted in polyimide capillaries with an inside diameter of 0.5 mm. The Canadian Macromolecular Crystallography Facility Bend Magnet beamline (CMCF-BM or 08B1-1) was used for the collection of PXRD patterns. The 08B1-1 utilizes a Si (111) double crystal monochromator. Data collection was performed using a photon energy of ~18 keV (wavelength $\lambda = 0.68880 \text{ \AA}$) and a sample–detector distance of ~350 mm. Two-dimensional (2D) diffraction patterns were collected using a Pilatus3 S 6M detector with an active area of 423.6 mm x 434.6 mm.

SEM analyses were conducted on the produced sludges at the Geology and Sustainable Mining Institute labs (GSMI) at the Mohammed VI Polytechnic University (Morocco). The SEM (TESCAN TIMA) was equipped with two 30 mm² energy dispersive spectrometers (Element EDAX 30) for the micro-analysis of phases. The analysis was conducted at 25 KeV energy and a beam current of 8 nA. Prior to SEM analysis, the samples were mounted into 25 mm carbon coated polished sections.

6.4.4 Leaching tests

Two static leaching tests (N-SEP and FLT) were performed to assess the potential mobility of As and Mn from the ECG and Fe(VI) post-treatment sludge. The N-SEP procedure subjected separate sludge samples to different reagents of increasing dissolution strength to evaluate As and Mn speciation (Rakotonimaro et al., 2021). The different reagents and operating conditions (solid-to-liquid ratio (S/L) and retention time) used for the three extraction steps (Step 1, 2 and 3) are presented in Fig. 6.1. Since the stronger extractants were expected to dissolve the phases leached in weaker conditions, the amount of As and Mn associated with each fraction (F1+F2: soluble and readily exchangeable (Step 1), F3: bound to poorly crystalline/amorphous Fe-(oxy)hydroxides (Step 2 - Step 1), F4: adsorbed onto crystalline Fe-(oxy)hydroxides (Step 3 - (Step 2 + Step 1)), and F5: residual (Total digestion - (Step 3 + Step 2 + Step 1)) was calculated by subtracting the amount obtained in the weaker fractions from the amount extracted in the next strongest extraction (Fig. 6.1). The amount of As and Mn associated with the residual fraction (F5) was calculated by subtracting the amount leached from the sum of Steps 1, 2, and 3 from the total digestion performed using HNO₃, Br₂, HCl, and HF. For quality control, blank samples were analyzed. The N-SEP was selected to limit the desorption or re adsorption of As on mineral phases, which may occur during oxidative and reducing steps of conventional sequential extraction (Rakotonimaro et al., 2021; Wenzel et al., 2001).

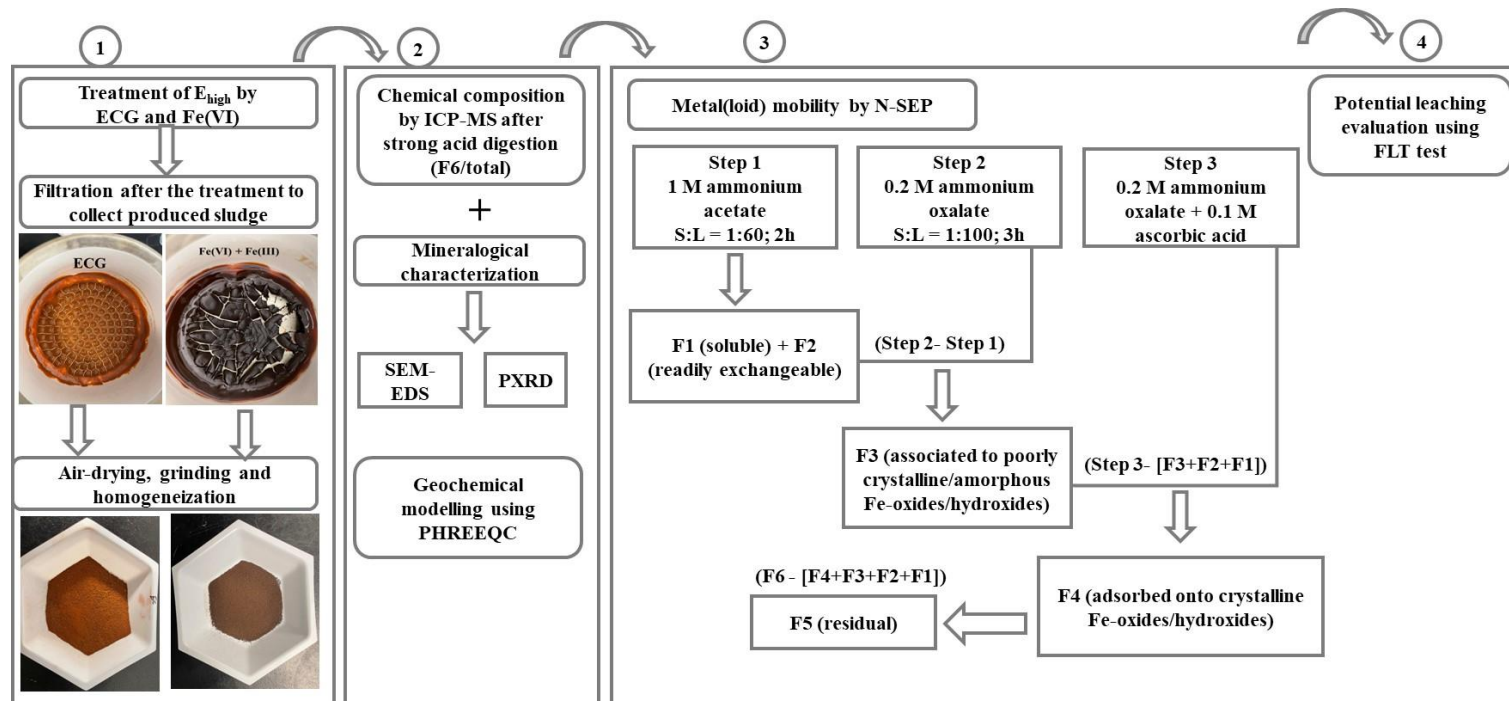


Figure 6.1 Experimental approach used for chemical and mineralogical characterization as well as stability assessment of As- and Mn-rich sludge from Fe(VI) and ECG treatment

The USGS-FLT was performed by mixing the dried sludge samples with deionized water at a solid/liquid ratio of 20/1 (similar to TCLP and SPLP tests). The mixtures were shaken by hand for 5 min and then settled for 10 min (Hageman, 2007). After settling, the leachate samples were collected and characterized for pH, EC, and ORP. The leachates were then filtered at 0.45- μm and acidified (2% HNO_3) prior to the determination of metal(loid) concentrations by ICP-OES.

6.5 Results and discussion

6.5.1 Treatment performance, geochemical modelling, and thermodynamic equilibrium calculations

Both the ECG and Fe(VI) treatments efficiently removed As (99.4% and 99.7%, respectively) and Mn (58.5% and 98.6%, respectively) from circumneutral surrogate mine water (Table S6.1). The removal efficiencies obtained in this study were consistent with previous results obtained during identification of the most performant operating conditions (Safira et al., 2023; 2024). The amount of sludge produced during the ECG treatment was estimated at 1,277 mg of sludge per L of treated effluent (wet basis after 30 min of settling, equivalent to 278 mg/L in dry basis), whereas 440 mg/L sludge (wet basis, equivalent to 80 mg/L in dry basis) was produced during the Fe(VI) treatment.

The geochemical models tested in PHREEQC were designed to improve the understanding of the processes likely to affect Fe, Mn, and As concentrations during Fe(VI) and ECG treatments. The relevant mineral phases for both treatment processes

are reported in Table 6.1, and the corresponding saturation index are presented in Table S6.2. Ferrihydrite and lepidocrocite were selected first, as they are mineral phases that were likely to precipitate according to rapid reaction kinetics (Bigham et al., 2002); this was confirmed by the mineralogical analysis using PXRD (see section 6.5.3.2). However, other phases were also considered here (Table 6.1) as mineralogical analyses were only performed on a fraction of the precipitated sludge; other mineral phases may have been present if the sludge was heterogeneous.

A five-step model was proposed for the Fe(VI) treatment (Fig. 6.2), representing the solution chemistry at various stages in the treatment process: (i) initial solution chemistry (E_{high}), including calculation of the saturation indices of relevant minerals; (ii) solution chemistry after the addition of Fe(VI) in the form K_2FeO_4 ; (iii) solution chemistry after the addition of iron sulfate ($\text{Fe}_2(\text{SO}_4)_3 \cdot 5\text{H}_2\text{O}$); (iv) solution chemistry after the addition of sulfuric acid (H_2SO_4) for pH adjustment; and (v) final solution chemistry, after treatment. The pH and ORP (used for pe calculations) were measured at all steps, while the concentrations of dissolved species were measured only at steps 1 and 5. All measured parameters were used as inputs for the model. For steps 2-3-4, concentrations are calculated (estimated) from known quantities of added reagents, assuming that all reagents were dissolved. For steps 2, 3, and 4, concentrations were calculated (estimated) from known quantities of added reagents, assuming that all reagents were dissolved. The results showed that pH slightly increased between steps 1 and 2 and significantly decreased thereafter, while pe increased between step 1 and step 2 and remained stable thereafter (Fig. 6.2).

Table 6.1 Mineral phases selected during the geochemical modeling and corresponding reactions

Minerals	Formula	Reaction	log k	ΔH (kJ)
Ferrihydrite	$\text{Fe}(\text{OH})_3$	$\text{Fe}(\text{OH})_3 + 3 \text{H}^+ = \text{Fe}^{3+} + 2 \text{H}_2\text{O}$	3.19	0.00
Goethite	FeOOH	$\text{FeOOH} + 3 \text{H}^+ = \text{Fe}^{3+} + 2 \text{H}_2\text{O}$	-1.00	-14.48
Hematite	Fe_2O_3	$\text{Fe}_2\text{O}_3 + 6 \text{H}^+ = 2 \text{Fe}^{3+} + 3 \text{H}_2\text{O}$	-4.01	-30.85
Jarosite (K)	$\text{KFe}_3(\text{SO}_4)_2(\text{OH})_6$	$\text{KFe}_3(\text{SO}_4)_2(\text{OH})_6 + 6 \text{H}^+ = \text{K}^+ + 3 \text{Fe}^{3+} + 2 \text{SO}_4^{2-} + 6 \text{H}_2\text{O}$	-9.21	-31.28
Lepidocrocite	FeOOH	$\gamma\text{-FeOOH} + 3\text{H}^+ = \text{Fe}^{3+} + 2 \text{H}_2\text{O}$	1.37	0.00
Schwertmannite	$\text{Fe}_8\text{O}_8(\text{SO}_4)_{1.26}(\text{OH})_{5.48}$	$\text{Fe}_8\text{O}_8(\text{SO}_4)_{1.26}(\text{OH})_{5.48} + 21.48 \text{H}^+ = 8 \text{Fe}^{3+} + 1.26 \text{SO}_4^{2-} + 13.48 \text{H}_2\text{O}$	18.5	NA

Measured and estimated dissolved species concentrations suggested that Fe increased significantly between steps 1 and 2 and decreased between steps 4 and 5 (Fig. 6.2). Based on previous studies, the other dissolved solids were expected to exhibit stable concentrations between steps 1 and 4, while a decrease might occur during the precipitation phase, which is accompanied by the formation of coagulants upon pH adjustment (between steps 4 and 5) (Fig. 6.2). The saturation index calculations suggested that all Fe-bearing phases identified in Table 6.1 were supersaturated during the five steps of the model, except for jarosite-K, which was undersaturated in the initial effluent (E_{high}) and became supersaturated between steps 2 and 5.

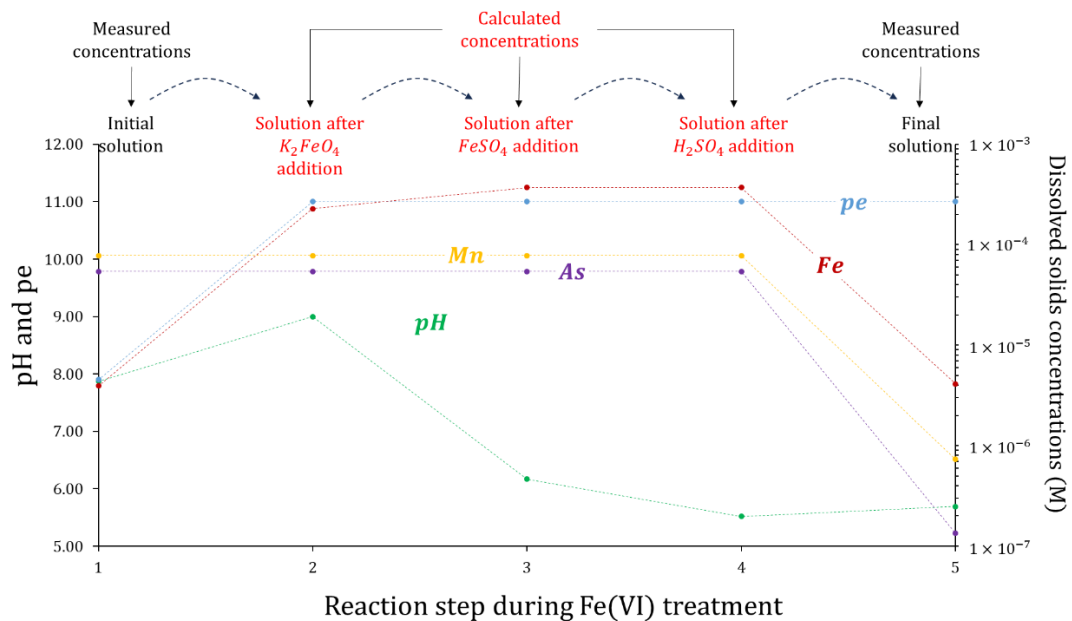


Figure 6.2 Evolution of pH, pe and dissolved concentrations considered in the 5-steps Fe(VI) model

For the ECG treatment, a four-step model was suggested (Fig. 6.3) to characterize the solution chemistry at various stages in the treatment process: (i) initial solution chemistry, including calculations of the saturation indices for all minerals; (ii) solution chemistry after the addition of HCl to adjust the pH; (iii) solution chemistry after application of the current; and (iv) final solution chemistry, after treatment. The pH and ORP were measured during the experiments at all steps except step 3 (current application), while concentrations of dissolved species were measured only for steps 1 and 4. All measured parameters were used as inputs for the model. For steps 2 and 3, concentrations were calculated (estimated) from known amounts of added reagents, assuming that all reagents were dissolved. The amount of Fe at step 3 was calculated according to the applied current, using Faraday's law. The results indicated that pH increased between steps 3 and 4 (6.54 to 7.15), while the ORP remained stable at the beginning and decreased significantly between steps 3 and 4 (Fig. 6.3). Measured and calculated dissolved solids concentrations showed that Fe increased considerably between steps 2 and 3 and decreased between steps 3 and 4 (Fig. 6.3). Based on previous studies, the other dissolved species were anticipated to remain stable during steps 1 to 3 and to decrease during the precipitation phase, which followed the formation of coagulant species (steps 3 and 4). The results also showed that the Mn concentration decreased slightly during the precipitation step, unlike the As concentration, which significantly decreased in this step (Fig. 6.3). The saturation index calculations suggested that all Fe-bearing phases presented in Table 6.1 were supersaturated during the four stages of the model, except for jarosite-K, which was undersaturated in the initial effluent (between steps 1 and 2) and became supersaturated between steps 3 and 4.

Saturation indices (Table S6.2) do not provide direct information on the precipitation or dissolution of solids, as these processes depend on the reaction kinetics for the physicochemical conditions prevailing during the experiments. Nevertheless, the models suggested that the Fe(VI) and ECG treatments generated conditions conducive

to the precipitation of several Fe(III)-(oxy)hydroxides (lepidocrocite, schwertmannite, ferrihydrite), which is consistent with the literature. However, the mineral phases identified in the mineralogical analyses for the Fe(VI) treatment, ferrihydrite, did not show significant variation in saturation indices in the model, whereas the mineral phase identified for the ECG treatment, lepidocrocite, showed variation between steps 2 and 3 (Section 6.5.3.2). Thus, the model results were consistent with mineralogical observations, but they did not allow more precise identification of the precipitated mineral phases. The formation of solid phases such as goethite, hematite, and manganite and the incorporation of metals into the Fe-(oxy)hydroxide phases were predicted to be thermodynamically favorable, but may not be kinetically favored during the short timeframe of Fe(VI) and ECG treatment; however, these phases might be formed during long-term storage of the sludge (Coudert et al., 2020; Freitas et al., 2013).

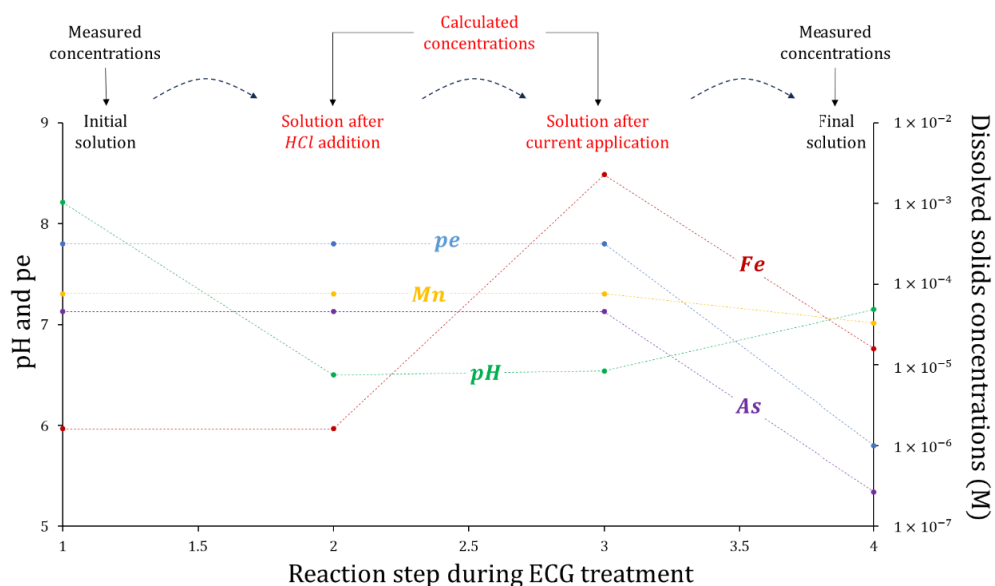


Figure 6.3 Evolution of pH, pe and dissolved concentrations considered in the 4-steps ECG model

6.5.2 Chemical composition of post-treatment sludges

The physicochemical characterization of the sludge produced during Fe(VI) and ECG treatment is presented in Table 6.2. The ECG-treated sludge exhibited concentrations ranging from 290 mg/kg for Mg to 520,000 mg/kg for Fe, in the sequence Fe > As > Ca > Mn > S > Na > K > Al > Ba > Mg. The Fe(VI)-treated sludge exhibited concentrations ranging from 150 mg/kg for Ba to 340,000 mg/kg for Fe, in the sequence Fe > Mn > As > Ca > S > K > Al > Na > > Mg > Ba.

Table 6.2 Humidity and chemical composition of sludge produced from Fe(VI) and ECG treatment

Parameter	Fe(VI)	ECG
Water content (%)	80	78
Al (mg/kg)	2,000	670
As (mg/kg)	38,000	12,000
Ba (mg/kg)	150	380
Ca (mg/kg)	9,900	11000
Fe (mg/kg)	340,000	520,000
K (mg/kg)	2,600	940
Mg (mg/kg)	920	290
Mn (mg/kg)	53,000	7,700
Na (mg/kg)	1,700	1,800
S (mg/kg)	7,000	3,500

Concentrations of Al, K, Mg, S, Mn, and As were higher in the Fe(VI) sludge, whereas Ba, Fe, and, to a lesser extent, Ca and Na were more concentrated in the ECG sludge (Fig. 6.4). The higher Fe concentration in the ECG sludge is attributed to the higher amount of Fe added to the system (133 mg/L) through the dissolution of the Fe-electrode at a current density of 2 mA/cm², compared to the addition of only 20.50 mg/L in the Fe(VI) treatment (12.5 mg Fe(III)/L added as Fe(VI) and 8 mg/L added as Fe(III)). The 3.2- and 6.9-times higher concentrations of As and Mn measured in the Fe(VI) sludge in comparison to the ECG sludge could be attributed to the superior removal of Mn (99.1% for Fe(VI) vs. 57.0% for ECG) and As (99.8% for Fe(VI) vs. 99.4% for ECG), when using Fe(VI); in addition to the 3.5-times smaller amounts of dried sludge produced (0.08 g/L for Fe(VI) vs. 0.28 g/L for ECG). The high amounts of K and S in the Fe(VI) sludge are attributed to the addition of the solid potassium ferrate (K₂FeO₄) reagent and to the pH adjustment (H₂SO₄). The higher Mg and Al contents in the Fe(VI) sludge may have resulted from a small variation between the initial composition of the surrogate mine water used for the ECG treatment (Mg: 2.48 mg/L; Al: 0.03 mg/L) and that used for the Fe(VI) treatment (Mg: 5.2 mg/L; Al: 0.07 mg/L); in addition, the smaller volume of sludge produced during the Fe(VI) treatment resulted in a higher factor of concentration of these elements. The Ba and Ca contents were slightly higher in the ECG sludge than the Fe(VI) sludge, which could be partially explained by greater adsorption of these elements during the ECG treatment (Esmailirad et al., 2015; Nigri et al., 2020).

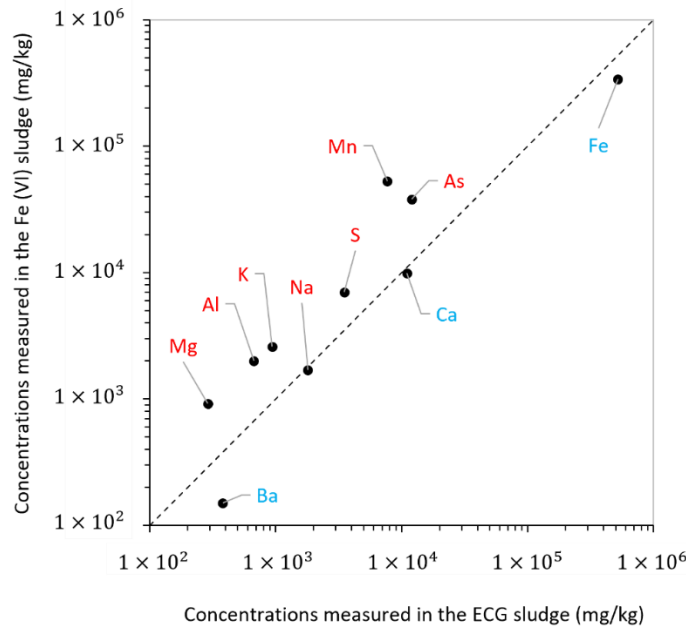


Figure 6.4 Comparison of element concentrations measured in the Fe(VI) and ECG sludge

Mass balance calculations ensured the quality of the results and allowed the recovery of As and Mn initially present in E_{high} . For the ECG treatment, the mass balance calculations showed almost complete As recovery in the sludge, with nearly no As mass loss during the treatment process (input/output = 0.99). However, for Mn, the results showed that 52.0% was trapped in the sludge, while 41.5% remained in the final solution, leading to mass loss of 6.4%. For the Fe(VI) treatment, 82% of the As initially present in E_{high} was recovered in the sludge, while 0.27% remained in the final solution. Based on the mass balance calculation, an 18% mass loss of As occurred in the Fe(VI) treatment, perhaps due to some errors in the estimation of the amount of dry sludge produced. For Mn, 96% was recovered in the produced sludge, with only 1.36%

of the Mn remaining in the final solution, indicating a negligible loss of 2.49% during the treatment.

6.5.3 Mineralogical characterization of ECG- and Fe(VI)-sludge

6.5.3.1 Scanning electron microscope (SEM-EDS)

The X-maps from the SEM analysis on polished sections suggested the presence of a relatively homogeneous precipitate for the ECG-sludge (Fig. 6.5a) and a heterogeneous precipitate in the case of the Fe(VI)-sludge (Fig. 6.5b). Indeed, during ECG treatment As and Mn distributions were relatively distributed within the analyzed particle. However, during Fe(VI) treatment, As and Mn showed different distributions within the analyzed particle. Within the analyzed particle (Fig. 6.5.b), all the zone depleted in Fe is enriched in As, but only a small area of this zone is enriched in Mn. The elemental punctual microanalysis conducted by EDS ($n = 48$) for the ECG sample (Fig. 6.6a) indicated that Fe (5.19–49.4 wt.%) and O (43.2–53.3 wt.%) (Table 6.3) were the main chemical elements in the precipitate; this was consistent with the geochemical modelling and the PXRD patterns, suggesting the presence of poorly crystalline Fe-(oxy)hydroxides, most likely consisting of lepidocrocite (γ -FeOOH) or β -FeO(OH).

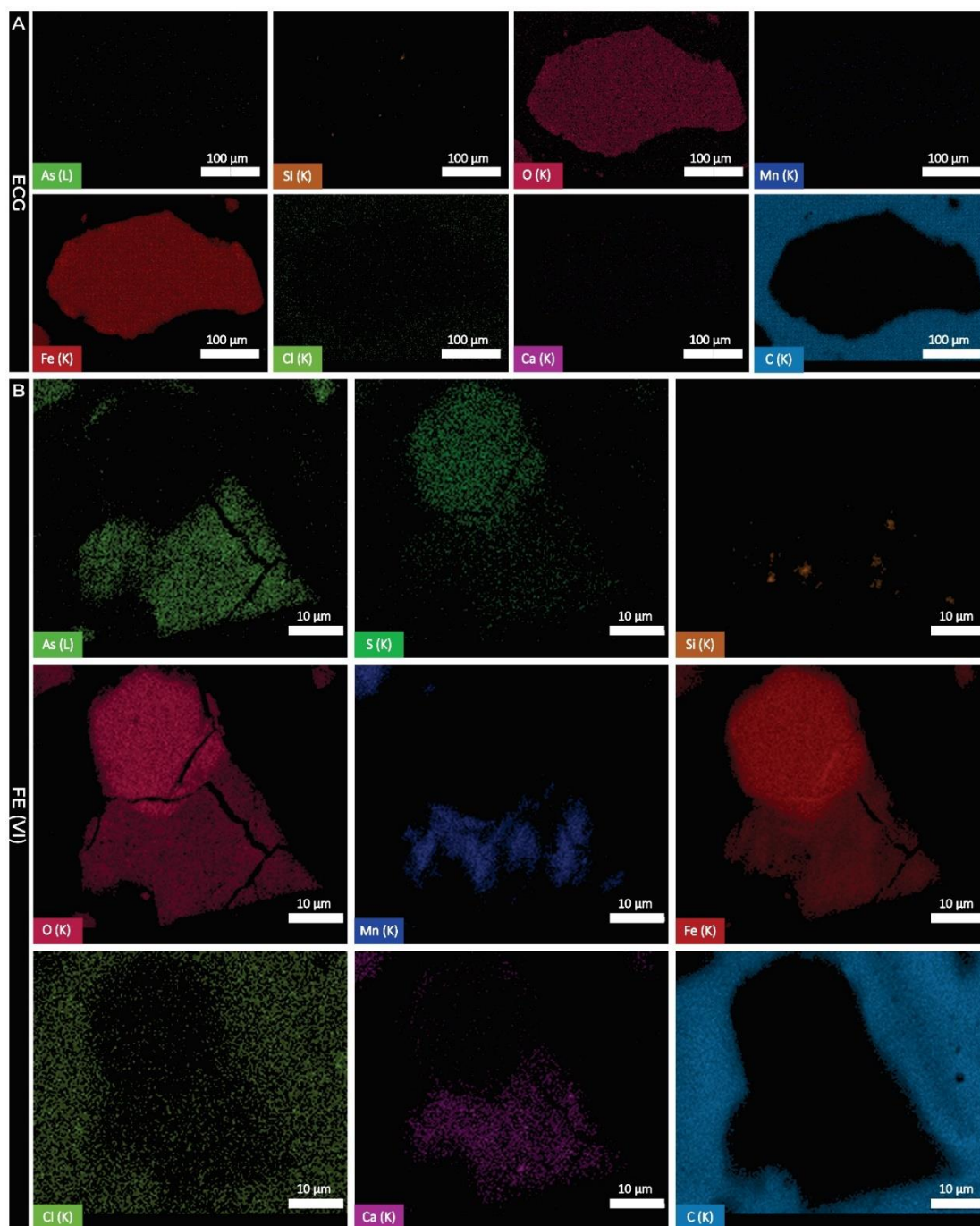


Figure 6.5 X-mapping of selected areas from (A) precipitate formed during ECG and (B) precipitate formed during Fe(VI) treatment of E_{high}

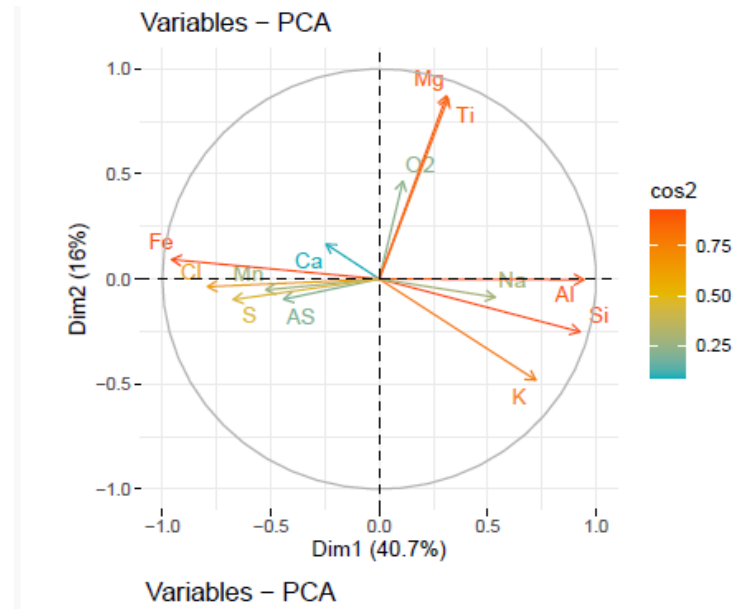
The high Fe content found in the ECG-sludge was attributed to the Fe-electrode dissolution to produce coagulant for As and Mn removal, while the other species were initially present in the water.

The presence of other elements filling the matrix of the Fe-(oxy)hydroxides was confirmed by EDS microanalysis. Other chemical species that were detected in the formed precipitate include As, Mn, Ca, Cl, Si, S, Al, K, Na, and Mg (Table 6.3). In general, the ECG sludge was richer in As (avg. 1.87 wt.%) than Mn (avg. 0.19 wt.%). Considering the results of circular hierarchical cluster analysis, the data can be divided, considering all variables, into three groups (Fig. 6.6). The average chemical composition of the identified groups is illustrated in Table 6.3. For As-bearing precipitates, three groups of precipitates, based on As content, were identified as follows: (i) the first category is characterized by an As content of 1.87 ± 0.42 wt.%, (ii) the second and the third categories are characterized by relatively low As content of about 0.03 ± 0.07 wt.% and 0.01 ± 0.01 , respectively. The Mn-bearing minerals can be grouped into three different categories: (i) the first one is identified with Mn content of 0.19 ± 0.14 wt.%, (ii) the second category is distinguished by a Mn content of 0.15 ± 0.16 wt.%, and (iii) the third group is characterized by comparatively low Mn content of 0.01 ± 0.01 wt.%. Fig. S6.2 reflects a low positive correlation between As and Fe of about 0.301, which means that high As-content bearing minerals are accompanied by high Fe-content bearing minerals. The correlation between Fe and Mn appears to be significant and positive ($r = 0.476$), meaning that medium Mn-content bearing minerals (0.15–0.19 wt.%) are associated with high Fe-content bearing minerals. A low positive correlation between As and Mn is observed ($r = 0.221$). Therefore, it appears that both contaminants are mostly associated to different Fe-bearing particles, which might be attributed to the different mechanisms involved in their removal (i.e., (co-)precipitation and sorption for As vs. sweep coagulation and sorption for Mn) (Gomes et al., 2007; Oncel et al., 2013).

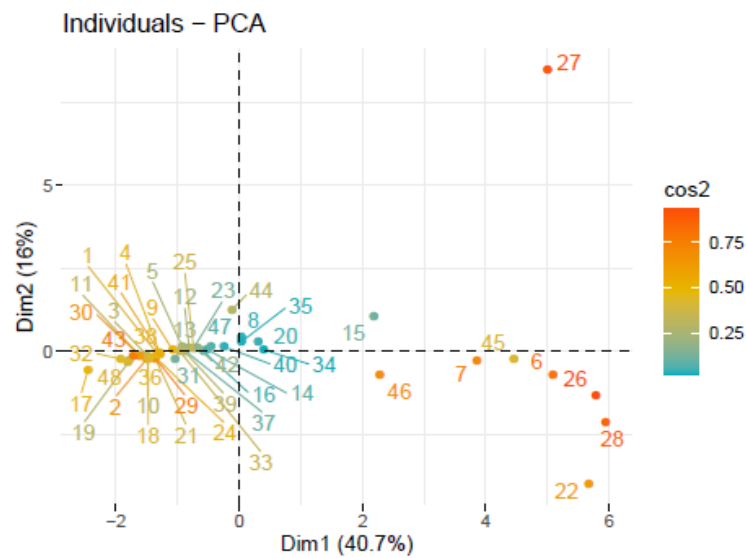
For the Fe(VI) treatment, the elemental analysis by EDS ($n = 29$) also showed that O (39.8–45.6 wt.%) and Fe (34.1–50.7 wt.%) were the major chemical components in the newly formed precipitate (Fig. 6.7, Table 6.3), which was consistent with the geochemical modelling. These results were also consistent with PXRD patterns showing the presence of a poorly crystalline phase most likely corresponding to ferrihydrite ($\text{Fe}_{10}\text{O}_{14}(\text{OH})_2$). The following chemical species were identified in the precipitate as well: As, Mn, Ca, Si, S, Al, K, and Na (Table 6.3). The high Fe content measured in Fe(VI) sludge was mainly introduced to the system from the potassium ferrate reagent (K_2FeO_4) used as strong oxidant and coagulant for the simultaneous removal of As and Mn. Multivariate and circular hierarchical analysis (Fig. 6.7) shows the precipitated phases can be divided into 5 groups; the chemistry of these groups is presented in Table 6.3. The As content was about 7.20 ± 0.41 wt.% for group 1, 5.30 ± 0.68 wt.% for group 2, 4.96 ± 2.61 wt.% for group 3, 2.80 ± 2.19 wt.% for group 4, and 0.29 ± 0.47 wt.% for group 5. Further, five categories of Mn-bearing minerals (Table 6.3) were identified: (i) the first category is of 3.61 ± 1.49 wt.% Mn content, (ii) the second one, Mn content is 12.9 ± 3.42 wt.%, (iii) the third group is with Mn content of 4.14 ± 3.19 wt.%, (iv) the fourth group is identified by Mn content of 1.33 ± 0.51 wt.% and (v) the last group is with 0.48 ± 0.76 wt.% Mn content.

Fig S6.3 shows a negative correlation between Fe and both As and Mn ($r = -0.384$ for As and -0.721 for Mn) and a positive correlation between As and Mn ($r = 0.488$) in the Fe(VI) precipitate. This means that As- and Mn-bearing minerals with high content of these elements are associated to low Fe-content bearing mineral. On the other hand, As and Mn are positively correlated, indicating that high As-content bearing minerals are also Mn-bearing minerals, or associated with high Mn-content bearing minerals, which is the opposite of what was previously observed for ECG-sludge. Based on these results, both contaminants were present within the same Fe-bearing precipitates, indicating that sorption or incorporation onto newly formed Fe-(oxy)hydroxides might be the main mechanisms involved in their removal. Additional mineralogical

characterization (X-ray absorption fine structure (EXAFS)) will be needed to validate this hypothesis.

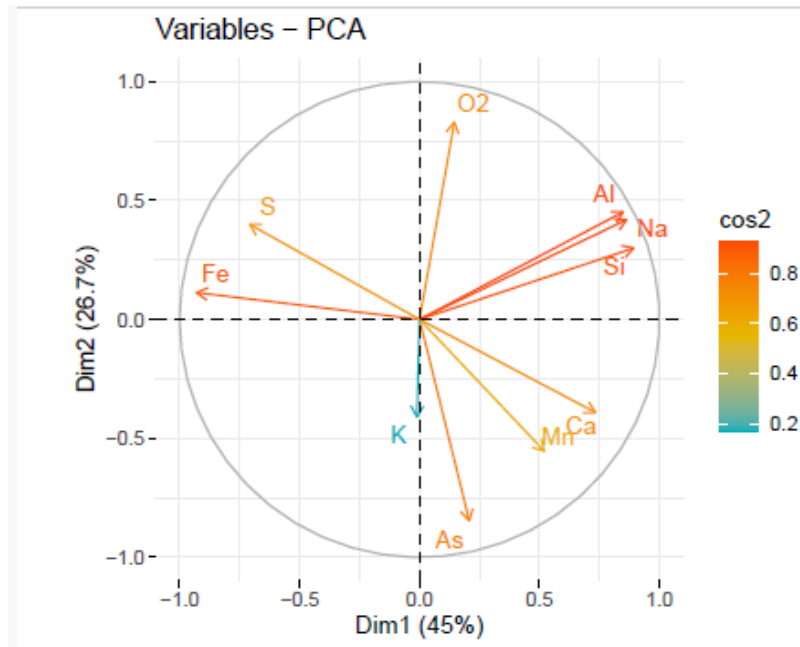


a.

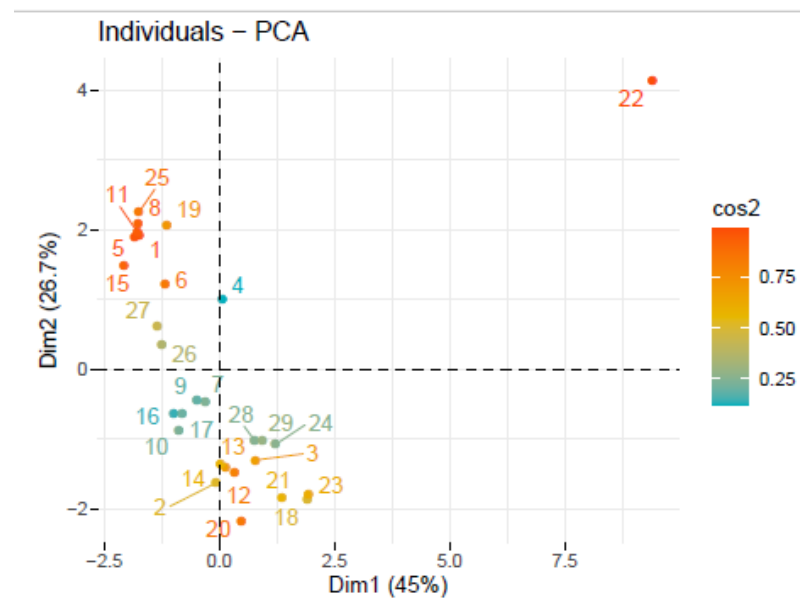


b.

Figure 6.6 Multivariate analysis of EDS data in ECG sample



a.



b.

Figure 6.7 Multivariate analysis of EDS data in Fe(VI) sample

Table 6.3 Summary of the chemical composition (wt. %) of the identified groups as analyzed using SEM-EDS.

		As	Ca	Cl	Fe	Mn	O ₂	Si	S	Al	K	Na
ECG												
Group 1	Average	1.87	1.37	0.80	49.4	0.19	43.2	2.39	0.72	-	0.01	-
	SD*	0.42	0.20	0.26	2.3	0.14	2.7	0.19	0.21	-	0.06	-
Group 2	Average	0.03	1.27	0.71	48.9	0.15	45.2	2.35	0.50	0.65	0.21	-
	SD*	0.07	0.52	0.28	5.9	0.16	3.1	2.66	0.38	0.97	1.02	-
Group 3	Average	0.01	0.31	0.06	5.19	0.01	53.4	25.5	-	7.93	5.46	2.13
	SD*	0.01	0.43	0.08	6.78	0.01	4.4	5.5	-	2.49	5.72	1.82
Fe(VI)												
Group 1	Average	7.20	1.90	-	43.5	3.61	39.8	1.73	0.97	0.08	0.72	-
	SD*	0.41	0.19	-	1.4	1.49	1.3	0.26	0.03	0.18	0.18	-
Group 2	Average	5.30	2.04	-	34.1	12.9	42.4	1.40	0.69	0.16	0.77	0.27
	SD*	0.68	0.09	-	4.4	3.4	1.3	0.96	0.46	0.33	0.03	0.54
Group 3	Average	4.96	2.45	-	42.9	4.14	43.1	1.71	0.45	-	-	-
	SD*	2.61	0.82	-	4.3	3.19	1.3	0.45	0.52	-	-	-
Group 4	Average	2.80	1.00	-	50.5	1.33	40.8	1.39	1.06	0.10	0.94	-
	SD*	2.19	0.94	-	3.1	0.51	2.0	0.19	0.15	0.18	0.17	-
Group 5	Average	0.29	0.65	-	50.7	0.48	45.6	0.16	1.79	-	0.31	-
	SD*	0.47	0.36	-	1.7	0.76	1.1	0.33	0.13	-	0.19	-

* SD : standard deviation

6.5.3.2 Synchrotron powder X-ray diffraction (PXRD)

The PXRD patterns suggested that the ECG (Fig. 6.8) and Fe(VI) (Fig. 6.9) sludge were mainly composed of poorly crystalline Fe-(oxy)hydroxide hydrates, which is consistent with the literature. The PXRD patterns for the ECG sample showed a broad, poorly crystalline feature most likely consisting of lepidocrocite (FeOOH) and/or β -FeO(OH) (Fig. 6.8). Lepidocrocite is known to adsorb arsenate (Gomes et al., 2007; Wang and Giammar, 2015). The formation of poorly crystalline Fe-(oxy)hydroxide

phases such as lepidocrocite, magnetite, and Fe hydroxide during ECG treatment using Fe-electrodes has been noted in previous studies (Gomes et al., 2007; Kobya et al., 2022). The red-brown color of the ECG sludge (Fig. 6.1) was consistent with the presence of lepidocrocite (Scheinost and Schwertmann, 1999). No other crystalline mineral phases could be identified.

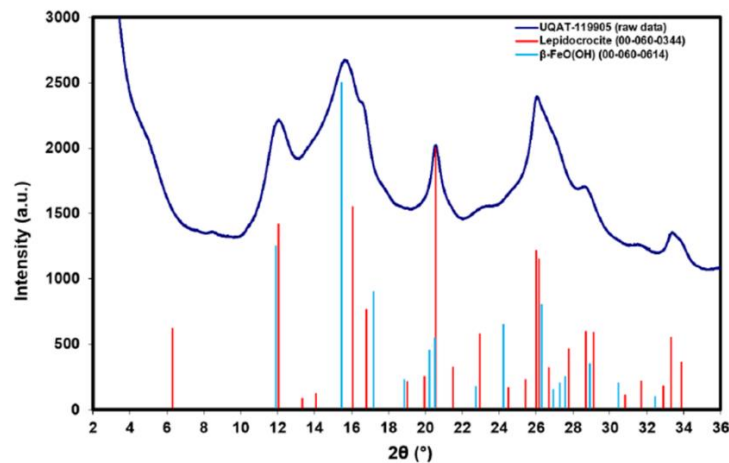


Figure 6.8 PXR D pattern used for phase identification of ECG sludge sample

The PXR D patterns for the Fe(VI)-sludge showed a poorly crystalline phase most likely corresponding to ferrihydrite ($\text{Fe}_{10}\text{O}_{14}(\text{OH})_2$), a mineral known to adsorb arsenate species (Alarcón et al., 2014) (Fig. 6.9a). The low angle shoulders of the features could also suggest the presence of amorphous ferric arsenate ($\text{FeAsO}_4 \cdot x\text{H}_2\text{O}$) (Fig. 6.9a). The formation of poorly crystalline Fe-(oxy)hydroxides during As removal by Fe(VI) and the adsorption of As(V) have been previously reported (Kong et al., 2023; Wang et al., 2020). The dark brown color of the produced sludge appeared to be consistent with the presence of significant amounts of ferrihydrite and/or Mn-

oxides (Fig. 6.1) (Michel et al., 2007; Post, 1999). However, Mn-oxide minerals were not detected in the Fe(VI) sludge PXRd spectrum.

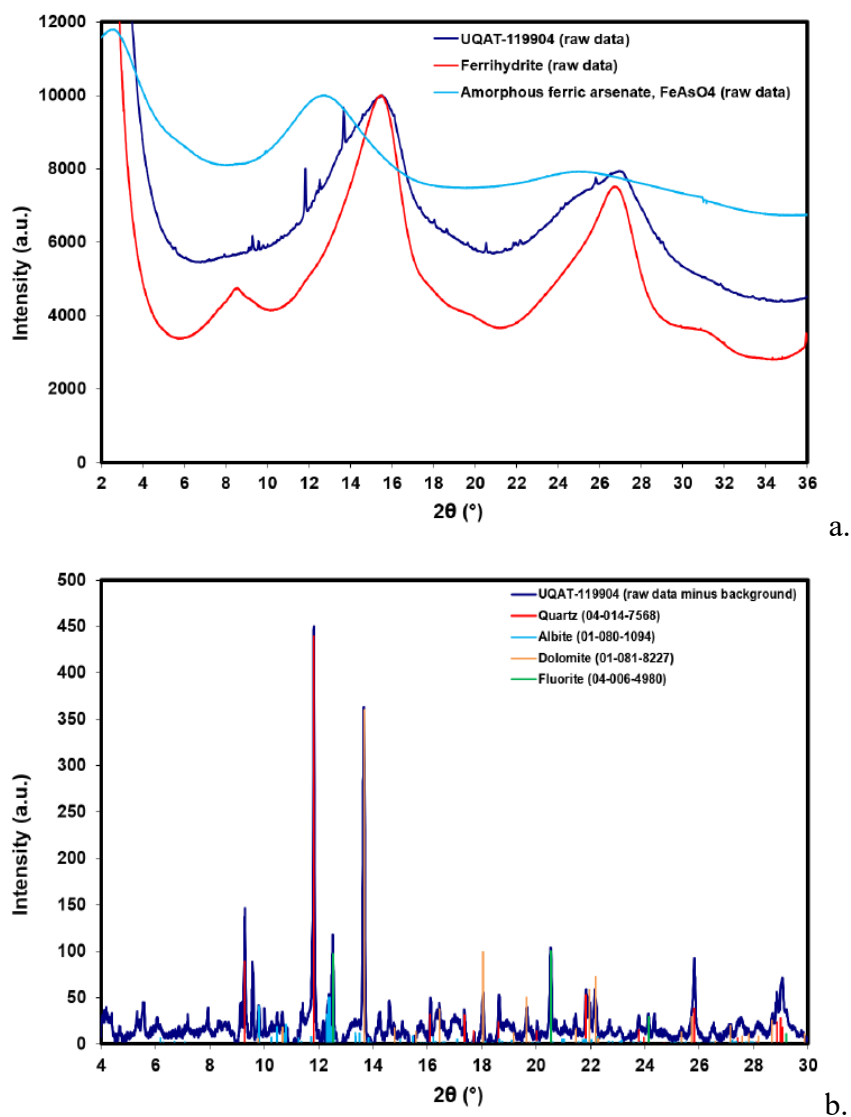


Figure 6.9 The PXRd pattern for Fe(VI) sludge sample, compared to ferrihydrite and amorphous ferric arsenate (a), and crystalline mineral phase identification (background subtracted PXRd pattern) (b)

These findings could partially be explained by the preferential sorption of Mn(II) on Fe-(oxy)hydroxides (especially ferrihydrite) at a low Fe/Mn molar ratio ($< 16/1$), rather than catalytic oxidation and precipitation as hausmannite ($\text{Mn(II,III)}_2\text{O}_4$), resulting in the formation of manganite with time (Lan et al., 2021). The crystalline mineral phases identified in the Fe(VI) sludge sample were quartz, albite, dolomite, and fluorite (Fig. 6.9b); these were most likely fine particles originating from the mine tailings from which the surrogate mine water was produced.

6.5.4 Environmental characterization of the sludge

6.5.4.1 As and Mn fractionation in the sludge using N-SEP

Four extraction steps (including total digestion and 3 N-SEP extraction steps) were performed on the sludge to determine the fractions and total concentrations of As and Mn (Fig. 6.10). Ammonium acetate-extractable for As was low in both treatments (0.15–0.45%), while Mn ranged from 1.6% in the Fe(VI)-sludge to 24% in the ECG-sludge; this indicated a mostly negligible presence of easily exchangeable or low solubility As and Mn from these materials (F1 + F2; Fig. 6.10). The results of the second extraction step suggested that 97% of the As in the Fe(VI)-sludge was bound to poorly crystalline Fe-(oxy)hydroxides (F3; Fig. 6.10), which was consistent with previous PXRD patterns (Fig. 6.9), while only 71% of the As was bound to the Fe-(oxy)hydroxide surfaces in the ECG-sludge. These findings indicated that adsorption of As on poorly crystalline Fe (oxy)hydroxides was one of the mechanisms of As retention occurring during both the ECG and Fe(VI) treatment, which is consistent with the literature (Kobya et al., 2022; Li et al., 2012; Sharma et al., 2007). Furthermore, the Fe/As molar ratio was six times lower in Fe(VI)-sludge

(Fe/As : 10.6/1) than the ECG-sludge (61.2/1), suggesting that As in the Fe(VI)-sludge was probably hosted in the Fe (oxy)hydroxides through co-precipitation or incorporation (Rakotonimaro et al., 2021); this is consistent with a previous study highlighting a partial incorporation of As into the structure of Fe-(oxy)hydroxide nanoparticles (Prucek et al., 2013). A slightly higher proportion of Mn (F3: 54%) was bound to poorly crystalline or amorphous Fe-(oxy)hydroxides in the ECG-sludge relative to the Fe(VI) sample (F3: 42%). This difference can be explained by the different removal mechanisms involved in ECG and Fe(VI) treatment. During ECG treatment, Mn is removed as Mn(II) trapped in the formed flocs; in contrast with Fe(VI) treatment for which Mn(II) is oxidized and removed as an oxide, and only the residual soluble Mn(II) is adsorbed onto Fe-(oxy)hydroxide surfaces. This could explain the higher Mn fraction associated to poorly crystalline or amorphous Fe-(oxy)hydroxides in the ECG sludge. This observation is consistent with the larger proportion of Mn associated with the residual fraction in the Fe(VI)-sludge vs. that in the ECG-sludge (56.7% and 5.56%, respectively), suggesting the formation of Mn-oxides during Fe(VI) treatment that are not dissolved in the first extraction steps of the N-SEP. The findings showed that none of the As or Mn was adsorbed onto crystalline Fe-(oxy)hydroxides (F4) in either treatment, which may further support the identification of only poorly crystalline Fe-bearing phases in the PXRD patterns. The co-precipitation of As with Fe (oxy)hydroxides or the incorporation of As into these phases, as well as the formation of Mn-oxides during Fe(VI) treatment, will likely favour the immobilization of these contaminants and lower their mobility in the field.

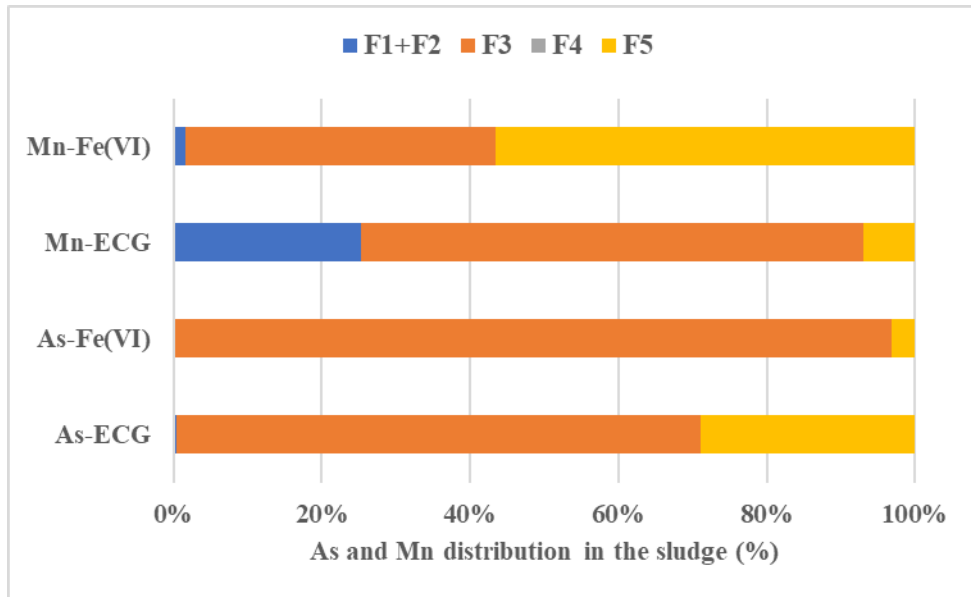


Figure 6.10 As, and Mn fractions of the As- and Mn-rich sludge produced from ECG and Fe(VI) treatment: F1+F2: soluble or readily exchangeable; F3: fraction bound to poorly crystalline or amorphous Fe-oxides/hydroxides; F4: fraction adsorbed onto crystalline Fe-oxides/hydroxides and F5: residual fraction

6.5.4.2 Evaluation of As and Mn mobility from the sludge using FLT approach

A FLT was performed on fresh sludge to assess the potential mobility of As and Mn from these post treatment residues. Metal(loid) concentrations in the FLT leachate were compared to: (1) Quebec's provincial criteria of Directive 019 (MELCC, 2012), (2) the surface water quality criteria (SWQC) for a hardness between 10 and 400 mg/L CaCO₃ (SWQC1 and SWQC2 correspond to SWQC at water hardness of 10 and 400 mg/L CaCO₃, respectively; MELCCFP, 2023), and (3) the TCLP criteria (USEPA, 1992) (Table 6.4). Despite the high concentrations in the sludge, very low amounts of Fe, As, and Mn were leached from the ECG- and Fe(VI)-sludge. Indeed, less than 0.1% of the

total amount of Fe, As, and Mn initially present in the sludge were mobilized through the FLT, indicating that the target elements were efficiently immobilized in the sludge at near-neutral pH.

Table 6.4 Concentrations of the main metal(loid)s in the eluates collected after FLT relative to standard regulations

Elements	ECG (mg/L)	Fe(VI) (mg/L)	SWQC1 (mg/L)	SWQC2 (mg/L)	D019 (mg/L)	TCLP (mg/L)
Arsenic	0.03	0.05	0.15	0.15	0.2	5
Calcium	74.8	63.6	-	-	-	-
Iron	0.13	0.09	1.30	1.30	3	-
Potassium	38.1	45.5	-	-	-	-
Manganese	0.49	0.10	0.26	6.52	-	-

The concentrations of As measured in the FLT leachate were 3–5 times lower than the SWQC and 4-7 times lower than the Directive 019 criteria, highlighting that this element is poorly mobilized from ECG- and Fe(VI)-sludge at near neutral pH and under oxidizing conditions. This low mobility of As could be explained by the mechanisms involved in ECG and Fe(VI) treatment, favoring oxidation to As(V) followed by (co-)precipitation and sorption onto the Fe-(oxy)hydroxide structure. The concentration of As leached from the Fe(VI) sludge was slightly higher than that from the ECG sludge; this can be explained by the three-times higher initial amount of As in the Fe(VI)-sludge rather than its higher mobility from the sludge. When considering the proportion of As mobilized (amount of As leached divided by the initial amount of As), it can be noted that the Fe(VI) sludge was more stable than the ECG sludge

(fraction leached of 0.0026% and 0.0055%, respectively). These findings could be explained by the (co-)precipitation and internal sphere complex adsorption of As that occurred during the Fe(VI) treatment, as well as its incorporation into the structure of Fe (oxy)hydroxides (Kong et al., 2023; Nkele et al., 2022; Pucek et al., 2013). In addition, the As concentrations released from the FLT did not exceed the criteria set for TCLP (< 5 mg/L, Directive 019, 2012) for either the ECG or the Fe(VI) sludge. A previous study showed similar results for As release from different mine wastes using FLT and TCLP tests (Hageman et al., 2015), despite different pH conditions (near neutral vs. pH 4.9) and retention times (5-min and 18-h for FLT vs. 18-h for TCLP). By comparing FLT results to the TCLP criteria, both the ECG and Fe(VI) sludges can be classified as a non-hazardous waste. These results are consistent with previous studies evaluating the mobility of As from Fe-bearing sludge, with scorodite, schwertmannite, ferrihydrite, and ferrous arsenate identified as the main Fe-bearing minerals (Raghav et al., 2013; Rait et al., 2010).

Despite its 7-times lower initial content in the sludge, the concentration of Mn was higher in the FLT leachate from the ECG-sludge than that from the Fe(VI)-sludge. This increased amount of Mn leached from the ECG-sludge, which exceeded the SWQC1 criteria, may be attributed to its removal as Mn(II) by trapping or sweep coagulation by the Fe-(oxy)hydroxides (Oncel et al., 2013). In contrast, during Fe(VI) treatment, Mn is oxidized to Mn(IV) and precipitated as Mn oxides or immobilized by adsorption or (co-)precipitation with newly-formed Fe (oxy)hydroxides (Goodwill et al., 2016; Sharma, 2010), resulting in the production of more stable sludge under the FLT conditions. This finding is in agreement with the high stability of Mn-bearing sludge produced from oxidative precipitation treatments relative to high pH Mn(II) precipitation methods (Watzlaf, 1987; Watzlaf and Casson, 1990). The leaching of Fe from the ECG- and Fe(VI)-sludge was very low, with concentrations 10-times and 14-times lower than the SWQC and D019 criteria, respectively. The low Fe concentrations were related to the stability of Fe-(oxy)hydroxides under oxidizing

conditions at near-neutral pH (Acero et al., 2006; Coudert et al., 2020; Raghav et al., 2013). The leaching of Fe could be explained by the partial dissolution of poorly crystallized Fe-(oxy)hydroxides (Coudert et al., 2020; Theng and Yuan, 2008). Overall, the concentrations of As, Fe, and Mn generally met the SWQC and D019 criteria, except for Mn leaching from the ECG-sludge, which exceed SWQC1 criteria; this highlighted that the ECG and Fe(VI) processes efficiently immobilized As and Mn during the treatment of circumneutral contaminated mine water.

6.6 Conclusion

A physicochemical, mineralogical, and environmental characterization of ECG- and Fe(VI)-sludge was conducted to assess the potential mobility of As and Mn. The efficient removal of As (99%) and Mn (58–98%) by ECG and Fe(VI) resulted in the production of As- and Mn-rich sludges (1.2–3.8 wt.% As and 0.77–5.3 wt.% Mn). SEM-EDS characterization showed relatively homogeneous As- and Mn particles in the ECG sample. Different categories of As- and Mn-bearing particles were identified, with a low positive correlation between the As and both Mn and Fe contents, as well as significant positive correlation between Fe and Mn contents, in the different classes of precipitates, indicating that As and Mn were mostly immobilized into different Fe-bearing particles. A relatively heterogeneous phase was identified in the Fe(VI)-sludge, with a positive correlation observed between the As and Mn contents, as well as a negative correlation between Fe and both As and Mn contents, indicating that As and Mn were immobilized within the same type of particles. PXRD patterns indicated the formation of poorly crystalline Fe-(oxy)hydroxide (lepidocrocite or β -FeO(OH)) for the ECG-sludge and ferrihydrite for the Fe(VI)-sludge), which are known for their ability to adsorb As(V); however, no As- or Mn-bearing minerals were

identified. Results from N-SEP showed that As was mainly associated with poorly crystalline Fe-(oxy)hydroxides (70–97%), which is consistent with the mineralogical characterization, while Mn was distributed within the soluble and easily exchangeable (20%) and poorly crystalline Fe-(oxy)hydroxide (54%) fractions in the ECG-sludge and within the poorly crystalline Fe-(oxy)hydroxide (42%) and residual (57%) fractions in the Fe(VI)-sludge. All contaminants in the FLT leachate were below the D019 or surface water quality criteria, except for Mn in the ECG sludge, which exceeded SWQC1 for a water hardness at 10 mg/L CaCO₃. This non compliance of SWQC1 for Mn leaching from the ECG-sludge is not deemed as a major limitation for full-scale ECG and Fe(VI) applications. New studies are necessary to better evaluate the long-term stability of the sludge using similar conditions to the mine site, such as performing kinetic tests.

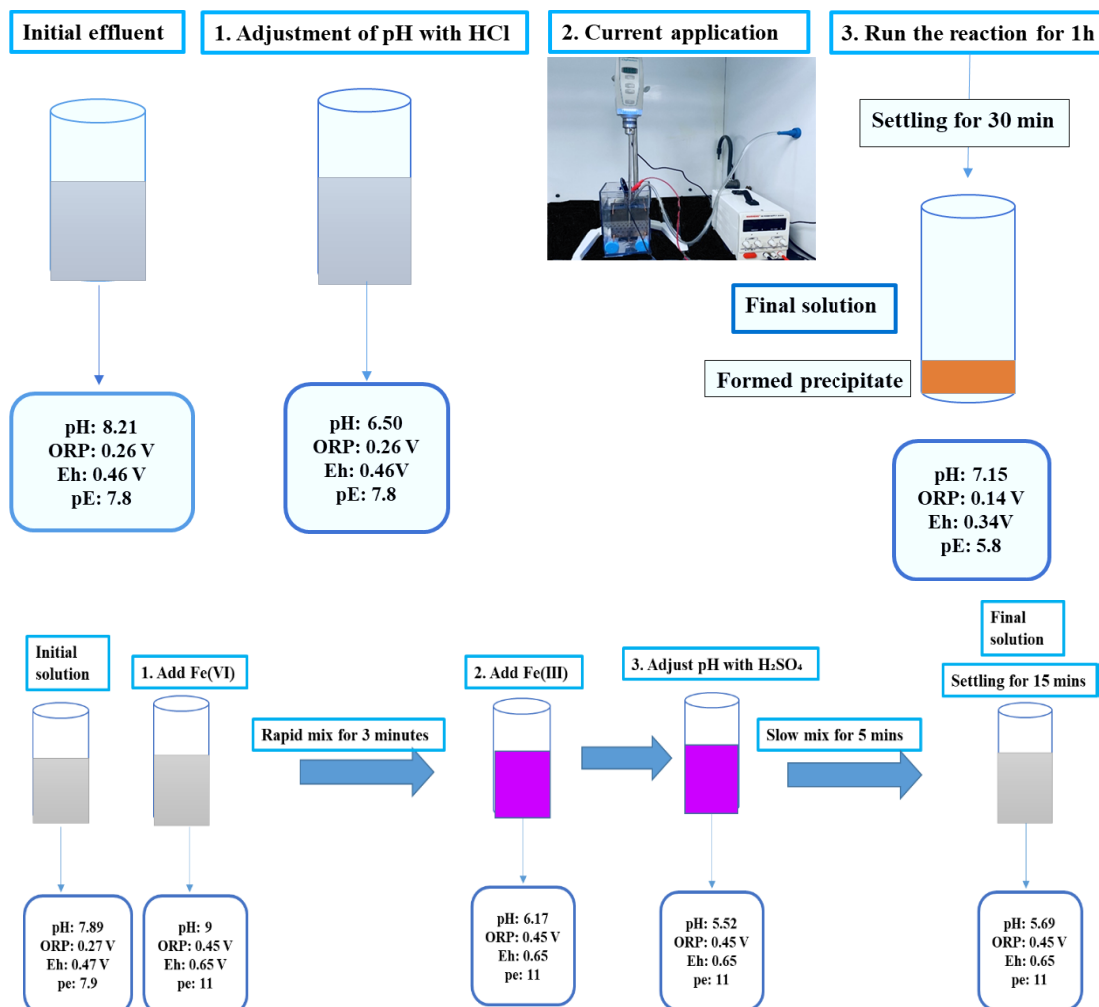


Fig. S6.1 Process steps followed for the treatment of circumneutral contaminated mine water using ECG (a) and Fe(VI) (b).

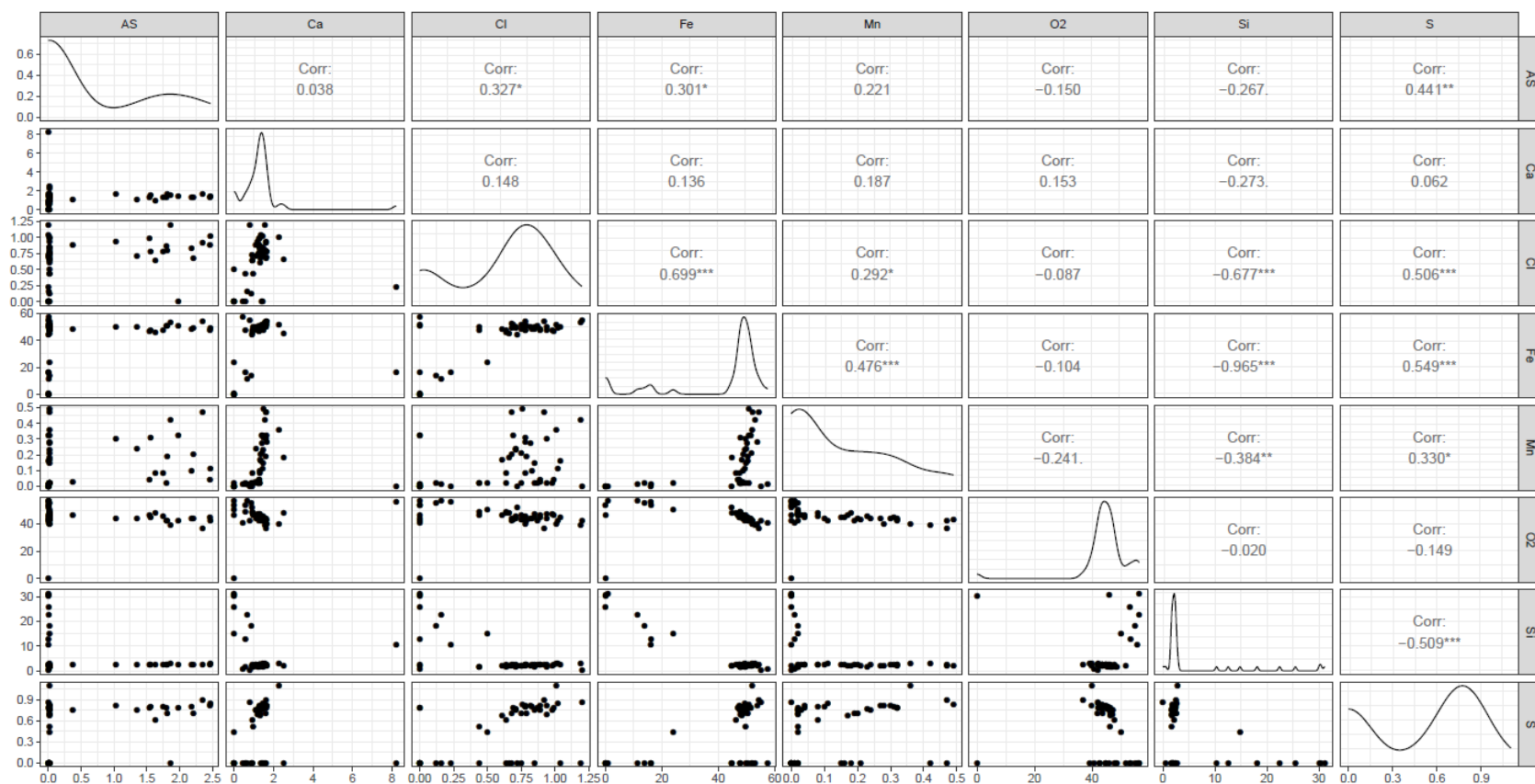


Figure S6.2 Elemental distribution and correlation between the analyzed elements in the precipitated minerals in ECG sample

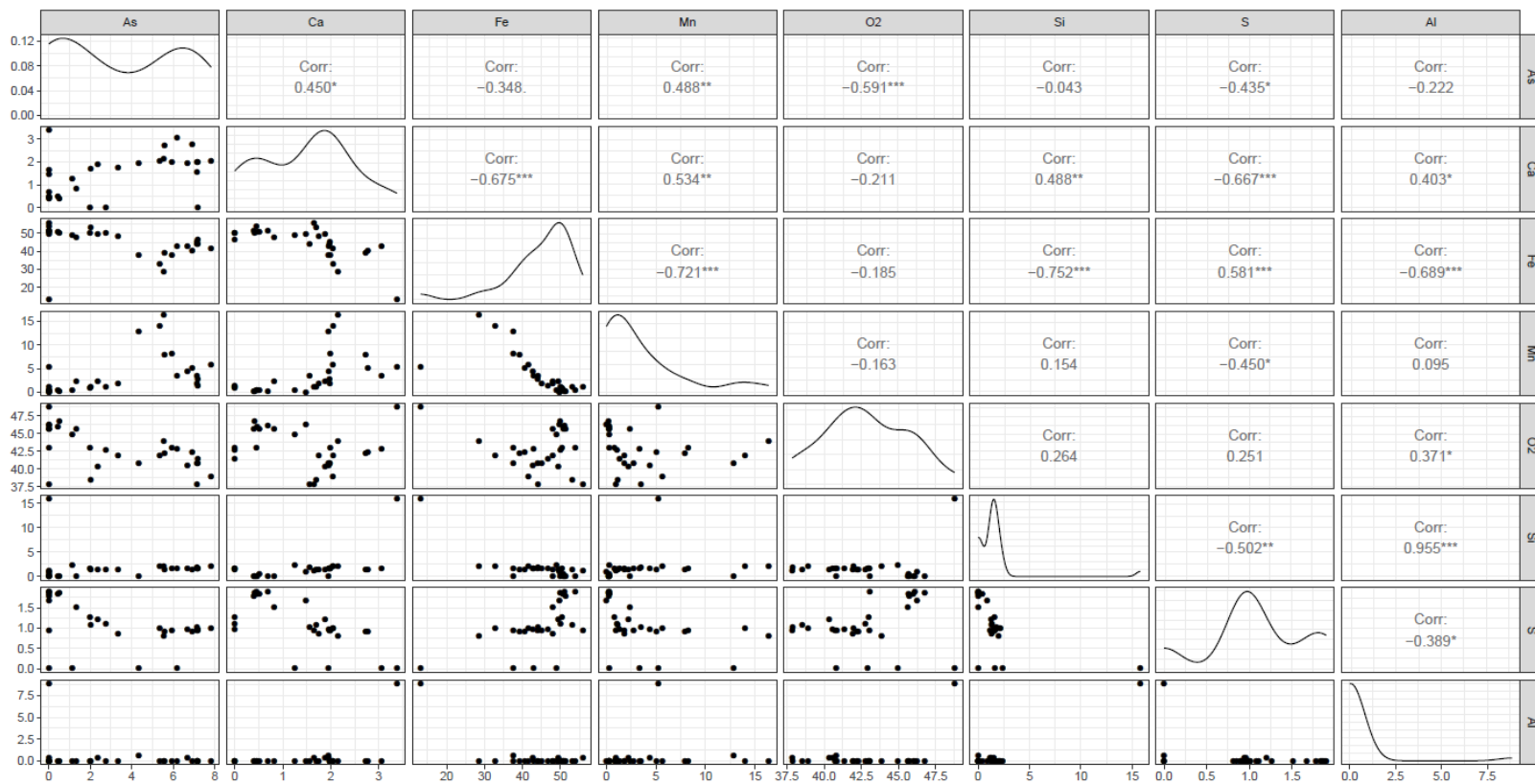


Figure S6.3 Elemental distribution and correlation between the analyzed elements in the precipitated minerals in Fe(VI) sample

Table S6.1 Physicochemical composition of Ehigh before and after ECG and Fe(VI) treatment and associated removal performance.

Treatment	ECG			Fe(VI)		
	Initial	Final	Removal (%)	Initial	Final	Removal (%)
pH	8.21	7.15		7.87	5.69	
pe	7.8	5.8		7.9	11	
Al (mg/L)	0.05	0.03	40.0	0.06	0.04	33.3
As (mg/L)	3.41	0.02	99.4	4.05	0.01	99.8
Mn (mg/L)	4.17	1.81	56.6	4.27	0.04	99.1
Fe (mg/L)	0.09	0.89	-	0.22	0.23	-
B (mg/L)	0.49	0.49	-	0.4	0.39	2.5
Ba (mg/L)	115	112	3.8	435	420	3.4
Ca (mg/L)	219	216	1.5	483	472	2.4
Cu (mg/L)	0.08	0.08	-	0.08	0.08	-
Cd (mg/L)	0.003	0.003	-	0.003	0.003	-
Li (mg/L)	0.08	0.08	-	0.08	0.08	-
K (mg/L)	115	112	2.6	125	145	-
Mg (mg/L)	5.78	5.05	12.6	9.84	9.63	2.1
Na (mg/L)	265	261	1.3	535	522	2.4
Ni (mg/L)	0.003	0.003	-	0.003	0.003	-
Pb (mg/L)	0.1	0.1	-	0.1	0.008	92.0
S (mg/L)	320	312	2.6	534	526	1.4
Si (mg/L)	3.35	0.32	90.4	3.64	3.26	10.4
Se (mg/L)	0.02	0.02	-	0.02	0.02	-
Cl (mg/L)	143	138	3.5	68.0	72.3	-6.4
Br (mg/L)	0.1	0.1	-	0.1	0.1	-
P (mg/L)	0.1	0.1	-	0.1	0.1	-
F (mg/L)	0.1	0.1	-	0.1	0.1	-
N (mg/L)	32	28	12.5	91.0	93.7	-3.0

Table S6.2 Saturation index for the selected mineral phases during geochemical modeling.

Minerals		Ferrihydrite	Goethite	Hematite	Jarosite (K)	Lepidocrocite	Schwertmannite
Fe(VI) treatment steps	1	3.94	8.15	18.3	-1.08	5.89	16.2
	2	5.49	9.70	21.4	0.31	7.44	25.8
	3	5.07	9.28	20.6	7.49	7.02	29.5
	4	4.45	8.67	19.3	7.59	6.40	26.2
	5	2.67	6.88	15.7	1.69	4.62	11.5
ECG treatment steps	1	3.55	7.76	17.5	-3.44	5.50	12.1
	2	2.99	7.20	16.4	-0.01	4.94	11.9
	3	6.17	10.38	22.8	9.41	8.12	37.3
	4	4.35	8.56	19.1	2.11	6.30	21.2

CHAPTER 7

GENERAL DISCUSSION

Mine water, including processing effluents and mine drainage, can entail the release of several contaminants into the surrounding environment, if not properly managed or treated. The co-occurrence of As and Mn in mine-impacted waters (i.e, mine water, groundwater and surface water in the vicinity of mining activities) is attracting increasing attention because of their detrimental effects on aquatic ecosystems and human health. As a proof of the current awareness related to As and Mn contamination, regulation controlling their concentration in mine and drinking water are becoming more and more stringent, leading to new challenges for their efficient removal to meet lower concentrations. Conventionally, As is removed from mine water by chemical co-precipitation in the presence of Fe(III) at pH 4-7, while Mn(II) is oxidized to insoluble Mn(IV) using strong oxidants before its precipitation as Mn-oxides at pH 9-10. However, these treatments have shown multiple limitations for the simultaneous removal of As and Mn from mine water such as: (i) the requirement of large amounts of oxidants, (ii) the contradictory effect of Fe on As or Mn removal ($Fe/As > 4/1$ vs. $Fe/Mn < 4/1$), and (iii) the different pH conditions needed for their removal. Recently, ECG and Fe(VI) have been proven to be efficient for the removal of As or Mn from synthetic effluents and to a lesser extent from real effluents. Despite the increasing co- occurrence of As and Mn in mine water, there are only few studies targeting the simultaneous removal of these contaminants from lightly contaminated mine water using these technologies. Moreover, the identification of the most performant operating conditions (i.e, CD, ionic strength and retention time for ECG and Fe(VI) nature and dose, pH_a and retention time for Fe(VI)) on the simultaneous removal of As and Mn is still ongoing. It is worthy to mention that little is known about the acute toxicity of the effluents treated using ECG or Fe(VI) as well as on the stability

of the sludge produced, even if these parameters are crucial for the identification of the most performant treatment option. Therefore, there is a requirement for developing innovative treatment methods for the simultaneous removal of As and Mn from mine water and for better considering removal efficiency, residual salinity, acute toxicity, sludge stability and operating costs to assess the performance of the treatment.

The following sections will focus on further discussion of the results obtained to answer to the specific objectives and hypothesis formulated at the beginning of this research project on: (i) the effect of the presence of both As and Mn on the most performant operating conditions required for the treatment of S_{As+Mn} compared to S_{As} or S_{Mn} only using ECG and Fe(VI); (ii) the effect of competing ions (i.e., SO_4^{2-} , Cl^-) on the performances of ECG and Fe(VI), (iii) the potential mobility of As and Mn from the sludge produced by ECG and Fe(VI), and (iv) the identification of the most performant treatment for the simultaneous removal of As and Mn from circumneutral mine water.

7.1 Effect of operating conditions on the simultaneous removal of As and Mn using ECG and Fe(VI)

A comparison of the most performant operating conditions required for the removal of As and Mn from S_{As} and S_{Mn} vs. S_{As+Mn} was performed to confirm our hypothesis that the simultaneous removal of As and Mn from lightly contaminated mine water will result in the reinforcement of critical operating conditions (i.e., CD for ECG and Fe(VI) dose for Fe(VI)) and higher retention time to achieve satisfactory removal efficiencies compared to the effluents containing only As or Mn.

7.1.1 Current density

Controlling the degree of electrode dissolution and the amount of produced cationic species, which act as coagulant, as well as the production rate of the gas bubbles and the size of the flocs, CD is one of the most critical parameters of ECG. Depending on the quality of the effluent to be treated (i.e., synthetic vs. real effluent or the co-presence of different contaminants and their concentrations), the amount of coagulant required may vary, resulting in the application of different CD (Koby et al., 2011; Reátegui--Romero et al., 2018; Safwat et al., 2023). From previous studies, the CD is known to positively affect the contaminant removal and therefore, the removal efficiency of As and Mn from contaminated mine water is expected to be improved when increasing the CD (Gomes et al., 2007; Koby et al., 2011, Parga et al., 2005; Reátegui- Romero et al., 2018; Shafaei et al., 2010). However, little is known about the effect of the presence of both As and Mn on the required CD for their simultaneous removal using ECG, despite the fact that As and Mn removal are Fe-dependent.

In the current study, different CD (0.25-10 mA/cm²) were tested for the treatment of S_{As} , S_{Mn} , S_{As+Mn} to remove As and Mn below the targeted values (< 0.2 mg As/L and < 2 mg Mn/L). As was efficiently removed from S_{As} (97-99%) at low CD (0.5, 1 mA/cm²), with a plateau (>99%) achieved at CD higher than 2.5 mA/cm². Satisfactory Mn removal (60-70%) required CD higher than 2.0 mA/cm², with a gradual increase up to 98% at 10 mA/cm². The difference observed in the required CD between As and Mn removal could be attributed to the different mechanisms involved in their removal: (i) (co-)precipitation or adsorption on the Fe(III)-hydroxide surfaces for As, requiring the production of Fe(III) at the anode and (ii) sorption on Fe-hydroxides, trapping (sweep coagulation) by these hydroxides, or deposition on the cathode surface for Mn, resulting in the importance of producing more Fe-hydroxides (Koby et al., 2022; Oncel et al., 2013; Shafaei et al., 2010; Xu et al., 2017). These

results indicated that a 4-times higher CD was required for the efficient removal of Mn ($> 2 \text{ mA/cm}^2$) from S_{Mn} compared to As ($> 0.5 \text{ mA/cm}^2$) from S_{As} , highlighting the importance to select the appropriate CD for the simultaneous removal of these contaminants and identify if higher CD are required when both contaminants are present or not. Therefore, the efficiencies of two CDs (0.5 and 2 mA/cm^2) were evaluated for the simultaneous removal of As and Mn from $S_{\text{As+Mn}}$. Based on the results presented in Table 7.1, the presence of both As and Mn did not affect their removal efficiencies at 0.5 and 2 mA/cm^2 , evidencing that there is no antagonistic or synergistic effect between the two contaminants for their removal using ECG (Fig. 4.4). However, the results indicated that for an efficient simultaneous removal of As and Mn, the higher CD required for Mn removal is needed for the simultaneous removal of both contaminants below the targeted values. At low CD (0.5 mA/cm^2), only 30% of Mn was removed after 1 h, while at 2 mA/cm^2 , more than 58% of Mn was removed within the same time, decreasing final concentrations below the targeted value (Fig. 4.4).

Table 7.1 Effect of the co-occurrence of As and Mn on the CD required to achieve similar removals for S_{As} , S_{Mn} and $S_{\text{As+Mn}}$

	Removal from S_{As} (%)	Removal from S_{Mn} (%)	Removal from $S_{\text{As+Mn}}$ (%)
CD : 0.5 mA/cm^2			
As	97	-	94-96
Mn	-	27	26-30
CD : 2 mA/cm^2			
As	-	-	99
Mn	-	58-67	59-64

However, no increase of CD at values higher than the ones required for Mn removal from S_{Mn} is required because of the presence of both As and Mn in S_{As+Mn} , which may be attributed to the different mechanisms involved in their removal (i.e., Fe(III) required for As co-precipitation or sorption vs. Fe(III)-hydroxides for Mn sorption or trapping). In summary, the presence of As and Mn did not impact the required CD for the efficient removal of As and Mn from synthetic single and binary effluents. However, the presence of Mn in the effluent to be treated is the driving factor for the selection of the optimal CD, because of the higher CD required for its efficient removal compared to As. The requirement for the higher CD (2 vs. 0.5 mA/cm²) as optimal value confirms the first formulated hypothesis (H1) regarding the effect of the co-occurrence of As and Mn on the needs for more stringent operating parameters for their simultaneous removal.

7.1.2 Fe(VI) dose

The dose of Fe(VI) required for the efficient removal of As and Mn below the targeted criteria is a critical parameter that directly affect the performance of Fe(VI) treatment. Acting as a strong oxidant for both As(III) and Mn(II) oxidation and as coagulant for As(V) co-precipitation and sorption, the dose of Fe(VI) to be added is strongly dependent of the quality of the effluent to be treated and the concentration of contaminants to be removed. The ratio of Fe(VI)/As or Fe(VI)/Mn required for the efficient removal of these contaminants from synthetic effluent (with simplified composition – no competing ions) is not clearly established in the scientific literature. In the present study, several Fe(VI)_s doses were tested for the removal of As from S_{As} (14-56 mg Fe(VI)/L) and Mn from S_{Mn} (2-7 mg Fe(VI)/L) at pH_a 5.5. The results indicated a slight increase in As removal efficiencies from S_{As} with final concentrations ranging from 0.28 to 0.03 mg/L with the increase of Fe(VI)_s dose from 14 to 56 mg/L.

At doses higher than 22 mg Fe(VI)/L, the final concentration of As met the regulations (0.2 mg/L), with no important improvement in terms of As removal while increasing the Fe(VI) dose. An important increase (from 54 to 97%) in Mn removal was observed when increasing Fe(VI) from 2 to 5 mg/L, while a small decrease of Mn removal (nearly 4%) was observed at Fe(VI)_w dose of 7 mg/L, which can be explained by the oxidation of insoluble Mn(IV) to soluble Mn(VII) (Goodwill et al., 2016). These results showed that the dose of Fe(VI) to be added for Mn removal should be carefully selected, because doses higher than the optimal Fe(VI)/Mn ratio of 0.5/1 (2/3 identified by Goodwill et al., 2016) could entail the oxidation of Mn(IV) to Mn(VII), resulting in Mn release from the sludge. The different requirements of Fe(VI) doses for As and Mn removal (22 vs. 5 mg Fe(VI)/L, respectively) could be explained by the different mechanisms involved in their removal. For the efficient removal of As, sufficient amounts of Fe(III)-hydroxides must be produced to favour (co-)precipitation, adsorption or incorporation after the oxidation step. For Mn(II), oxidation to Mn(IV) prior to precipitation as MnO₂ seems to be the driving step in its efficient removal. To evaluate the effect of the co-occurrence of As and Mn in synthetic effluents, several doses of Fe(VI)_s (5-28 mg/L) were assessed for their simultaneous removal from S_{As+Mn} at pH_a 5.5. The Fe(VI)_s dose required to achieve similar removal efficiencies was approximately 28 mg/L, which is 1.3-5.6 times higher than the dose required for S_{As} (22 mg/L) and S_{Mn} (5 mg/L) (Table 7.2). This increase in the Fe(VI) dose, which is close to the sum of the doses required for S_{As} and S_{Mn} (28 mg/L vs. 22+5 mg/L), reflects a competition between As and Mn, particularly for the oxidation step, and emphasizes that Mn removal depends on the oxidation step, while As removal could be more impacted by the produced Fe(III)-hydroxides. Despite the addition of larger amounts of Fe(VI) added compared to the Fe(VI)/Mn ratio of 0.5/1 to avoid the oxidation of Mn(IV) to Mn(VIII), no production of insoluble and purple Mn(VIII) was observed, confirming the competition between As and Mn for Fe(VI) during the oxidation step. It is also worthy to mention that the increase of Fe(VI) dose would result in an increase in the residual salinity, which may affect the associated acute toxicity as well as

operating costs. In addition, the increase of Fe(VI) dose required for the simultaneous removal of As and Mn supports the first hypothesis (H1) postulated in this study in terms of higher demands of operating parameters when As and Mn are both present in mine water.

Table 7.2 Effect of the co-occurrence of As and Mn on the dose of Fe(VI) required to achieve similar removals for S_{As} , S_{Mn} and S_{As+Mn}

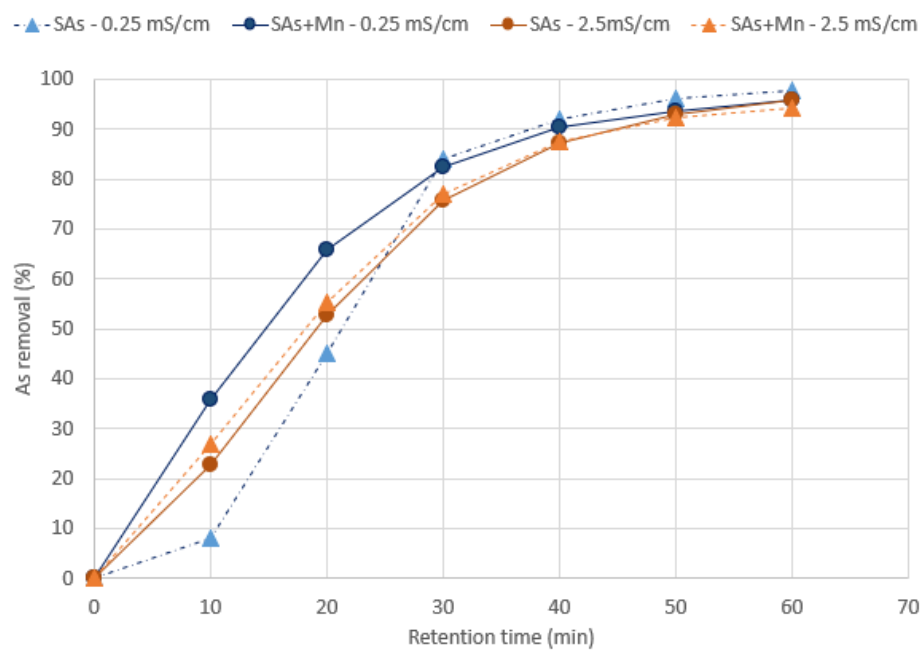
	Removal from S_{As} (%)	Removal from S_{Mn} (%)	Removal from S_{As+Mn} (%)
Fe(VI) – 5 mg/L			
As	-	-	30
Mn	-	97	52
Fe(VI) – 22 mg/L			
As	98	-	90
Mn	-	-	98
Fe(VI) – 28 mg/L			
As	97	-	99
Mn	-	-	98

Additional experiments were performed using a Fe(III) salt as a supporting coagulant, in the endeavour to decrease the Fe(VI) dose and confirm the hypothesis that the removal of As was mainly impacted by the amount of Fe(III)-hydroxide produced and, to a lesser extent, by the dose of oxidant used. Several doses of Fe(III) salt (6, 8, 10 mg Fe(III)/L) were tested and selected to obtain a total amount of Fe equivalent to the dose of 28 mg Fe(VI)/L. Upon the addition of 8 mg Fe(III)/L, the dose of Fe(VI) was decreased to 12.5 mg/L without affecting the removal of As and Mn, while reducing the residual salinity by 44% (0.231 mS/cm for Fe(VI) only; 0.130 mS/cm for

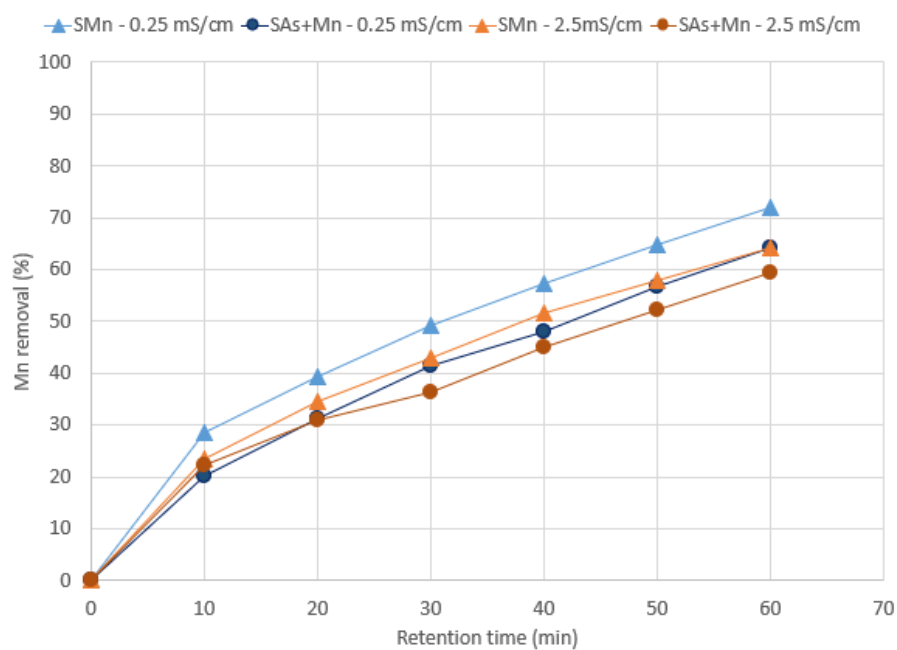
Fe(VI)+Fe(III)). However, the addition of the Fe(III) salt led to a slight decrease in the final pH (6.23 vs. 5.98), which must be adjusted prior the final effluent discharge.

7.1.3 Retention time

The retention time is an important factor to consider for the optimization of an ECG process to reduce the consumption of energy and associated costs as well as the size of the equipment required to accommodate a certain flowrate. In previous studies performed on the removal of As and Mn using ECG, the retention treatment time varied from few minutes (5 min) to several hours (60-180 min), depending on the operating conditions applied (e.g, CD, number of electrodes), and the targeted removal efficiencies (Banerji and Chaudhari, 2016; Reátegui- Romero et al., 2018; Shafaei et al., 2010). Here, the kinetics of As and Mn removal from S_{As+Mn} was investigated at 0.5 and 2 mA/cm², which were the optimal CDs identified for the treatment of S_{As} and S_{Mn} , respectively (Fig. 7.1). From Fig 7.1a, it can be observed that the removal of As appears to be slightly faster in the presence of Mn in the solution, within the first 20 minutes of treatment at 0.5 mA/cm², while after 30 minutes, no difference was observed in terms of As removal for the different conditions tested. This slightly faster As removal observed in the first minutes of treatment at low CD in the presence of Mn can be explained by the co-precipitation of Fe-As-Mn-hydroxides or its sorption on Fe-/Mn- hydroxides. It can be noticed that the Mn removal efficiencies were slightly better and faster for the effluents containing only Mn compared to S_{As+Mn} at both low and high ionic strength (Fig 7.1b). There is no evidence that the small differences observed in Mn removal efficiencies between S_{Mn} and S_{As+Mn} can only be attributed to the presence of As, as it could also be due to the slightly higher initial Mn concentrations in S_{As+Mn} (4.5-4.7 mg/L) compared to S_{Mn} (4.01 mg/L) or to the lower final pH (5.9-6.1 for S_{As+Mn} vs. 6.3-6.5 for S_{Mn}) (Parga et al., 2005).



a.



b.

Figure 7.1 Evolution of As and Mn removal from S_{As} and S_{As+Mn} at 0.5 mA/cm^2 (a.) and from S_{Mn} and S_{As+Mn} at 2.0 mA/cm^2 (b)

With the Fe(VI) treatment, experiments carried out on S_{As} and S_{Mn} showed that the removal of As and Mn was very fast, occurring within the first minute of the reaction. This can be due to the strong oxidizing power of Fe(VI) under the slightly acidic conditions (pH_a : 5.5) used for the treatment of S_{As} and S_{Mn} . At a pH_a of 5.5, the Fe(VI) species are highly reactive, thus promoting the oxidation of As(III) to As(V) and Mn(II) to Mn(IV). However, considering the similar behaviour of As and Mn removal from S_{As} and S_{Mn} within the first minute of reaction, a possible competition between both contaminants can be expected if they are present in the same effluent. When both contaminants were present in the effluents to be treated, a loss of efficiency of Mn removal (from 98% for S_{Mn} to 52% for S_{As+Mn}) was observed when using 5 mg Fe(VI)/L (optimal dose identified for Mn removal from S_{Mn}), while a lower loss of efficiency was observed for As (from 99% for S_{As} to 90% for S_{As+Mn}) when using 22 mg Fe(VI)/L (optimal dose identified for As removal from S_{As}). The greater loss of removal efficiency observed for Mn compared to As can be explained by the competition between As(III) and Mn(II) during the oxidation step and by the fact that Mn(II) needs to be oxidized to Mn(IV) before its subsequent precipitation as MnO_2 , while the removal of As(III) requires oxidation to As(V) prior to co-precipitation and sorption on Fe(III)-hydroxides.

In summary, the removal of As(III) seems to be more impacted by the presence of Fe(III) than by the use of a strong oxidant, as compared to the removal of Mn(II). Similar competition between As(III) and Sb(III) or Mn(II) and organic matter for intermediate Fe(VI) oxidizing species was observed by Wang et al. (2020) and Goodwill et al. (2016), respectively. Consequently, the co-occurrence of As and Mn seems to be more detrimental to the effective removal of Mn than As, if the dose of Fe(VI) is not adequately adapted to the initial composition of the mine water to be treated. Indeed, the treatment using Fe(VI) can be considered competitive in terms of required retention time (only 23 min: 3 min mixing, 5 min reaction time and 15 min settling) compared to ECG and conventional precipitation processes. ECG retention

time (1.5 h: 1 h reaction time and 30 min settling) is quite comparable to the typical retention time of conventional precipitation ranging from 1.5 to 2.5 h (10-30 min of reaction time followed by 1-2 h of settling time) depending on the water quality and contaminants concentrations (Stuetz and Stephenson, 2009).

7.1.4 Effect of competing ions on treatment performance

A comparison of the removal efficiencies of As and Mn from S_{As+Mn} and E_{high} was performed to confirm/infirm the hypothesis that the presence of competing ions commonly found in real mine water (i.e., Ca, Na, Ba, Cl^- , SO_4^{2-} , NO_3^-) will negatively impact the performance of treatment processes, especially when using ECG (Table 7.3). From the literature review, it is expected that the presence of different cations or anions (e.g., Ca, Na, Ba, Cl^- , SO_4^{2-} , NO_3^-) found in real mine water in variable concentrations may improve or worsen the treatment performance, in terms of contaminant removal efficiency and acute toxicity of final effluent (Banerji and Chaudhari, 2016; Foudhaili et al., 2020b; Lakshmipathiraj et al., 2010; Maitlo et al., 2018; Radić et al., 2014; Xu et al., 2017). For example, studies reported an enhancement of Mn removal using the ECG treatment in the presence of Cl^- ions (1.40 mg/L), which was explained by an increase of the oxidizing conditions due to the formation of strong oxidizing species (i.e., ClO^-), leading to the oxidation of Mn(II) to Mn(IV) and its subsequent removal as MnO_2 (Xu et al., 2017). The positive effect of Cl^- (3.5 mg/L) on As removal was also reported and attributed to the prevention of passivation layer formation on the anode surface, leading to a better dissolution of sacrificial electrodes (Lakshmipathiraj et al., 2010). On the contrary, the presence of SO_4^{2-} and NO_3^- hinder the anode dissolution, because of promoting the passivation of the anode. The presence of carbonate may, as well, affect the As removal due to its

competition with arsenate for sorption onto Fe-hydroxide surfaces (Banerji and Chaudhari, 2016; Lakshmipathiraj et al., 2010; Maitlo et al., 2018).

Table 7.3 Effect of the presence of competing ions on the performances of ECG and Fe(VI) treatment for the simultaneous removal of As and Mn

	S_{As+Mn}	E_{high}
As removal (%)	96	99
Mn removal (%)	61	57
ECG		
Acute toxicity (before → after)	n.a.	non toxic → non toxic
Mortality (before → after - expressed in %)	n.a.	5 → 0
As removal (%)	99	> 99.9
Mn removal (%)	97	99
Fe(VI)		
Acute toxicity	toxic → toxic	toxic → non toxic
Mortality (%)	100 → 70	70 → 10

Here, the ECG treatment results showed a slight increase in As removal efficiency for E_{high} compared to S_{As+Mn} (Table 4.4, Table 7.3), while a slight diminution of Mn removal (from 61% for S_{As+Mn} to 57% for E_{high}) was observed. For the Fe(VI) treatment, similar removal efficiencies were obtained for the removal of As and Mn from S_{As+Mn} and E_{high} , indicating that there is no detrimental effect related to the presence of competing ions in the surrogate mine water. The slight improvement in As removal (from 96 to 99%) by ECG and Mn removal (from 97 to 99%) by Fe(VI) can be attributed to the presence of Ca^{2+} ions in surrogate mine water, promoting the production of larger Fe-hydroxides flocs and therefore increasing the sorption of As and Mn (Ruiping et al., 2007). The attraction between Mn(II) and the negatively

charged Mn-oxides (pH_{PZC} of $\text{MnO}_2 = 1.8$) could also contribute to a better Mn(II) removal during the Fe(VI) treatment (Xie et al., 2018). The decrease in Mn removal efficiencies when treating E_{high} by ECG can be attributed to the passivation of Fe-electrodes by SO_4^{2-} , leading to a less efficient dissolution of the cathode and therefore a lower production of OH^- ions. The slower removal of Mn compared to As by the ECG treatment could explain why only Mn was affected by the passivation of the sacrificial electrodes over time (El-Taweel et al., 2015; Lakshmipathiraj et al., 2010). In terms of toxicity of the final effluent, it can be noticed that a toxicity was observed for $S_{\text{As+Mn}}$ before and after treatment by Fe(VI), while for E_{high} , all the effluents were non-toxic after treatment by Fe(VI) and ECG. Untreated E_{high} was found to be toxic for the experiments performed with Fe(VI), while no toxicity was observed for the experiments performed with ECG. This difference in untreated E_{high} between Fe(VI) and ECG experiments might be due to some variations in Ba (420 mg/L) and Na (540 mg/L) concentrations, in addition to the hardness of the water, as previously reported by Okamoto et al. (2014). Another potential source of this inconsistent toxicity for untreated E_{high} might be the higher salinity and sulfate content, as previously reported (Schuyttema et al., 1997; Semsari and Megateli, 2007). The presence of toxicity in $S_{\text{As+Mn}}$ in the effluent before and after treatment by Fe(VI), while untreated E_{high} for ECG, which has the same initial and final As and Mn concentrations was non-toxic, can be attributed to the lower hardness of the effluent (< 0.05 for $S_{\text{As+Mn}}$ vs. 1,200 mg CaCO_3/L for E_{high}). Based on these results, it can be concluded that toxic by-products were not generated during treatment by Fe(VI) or ECG on the surrogate mine effluent, with a composition similar to real contaminated mine water. In summary, the results indicated that the competing ions can positively or negatively affect the performance of the treatment in terms of removal efficiency or toxicity. This observation is partially consistent with the second hypothesis (H2) of the current study, which stated that the competing ions negatively affect the treatment performance.

7.2 Potential mobility of As and Mn from the sludge produced from ECG and Fe(VI)

The immobilization of As and Mn from contaminated mine water using ECG and Fe(VI) produces metal-rich sludges that may represent a secondary source of contamination if not properly managed. Therefore, chemical, mineralogical and environmental characterization are required to characterize ECG- and Fe(VI)-sludge and to evaluate their stability, and to better understand the removal mechanism. The assessment of sludge stability aimed at testing the hypothesis that the mobility of As and Mn from the sludge produced by Fe(VI), through incorporation of As into the structure of Fe-oxides/hydroxides nanoparticles and oxidation of Mn followed by precipitation as Mn-oxides, adsorption or (co-)precipitation with Fe-hydroxides, is expected to be lower than for ECG. A few studies have been performed to characterize the sludge produced by ECG and Fe(VI) treatments (Gomes et al., 2007; Kong et al., 2023). And to the best of the author's knowledge, there is no study focusing on the evaluation of As and Mn mobility from the ECG- and Fe(VI)-sludge. According to previous studies, during As removal by Fe(VI), a partial incorporation into the Fe- hydroxide nanoparticles was noted as one of the removal mechanisms, with adsorption, (co-)precipitation or precipitation as ferric arsenate (Prucek et al., 2013; Wang et al., 2020). This partial incorporation is expected to retain As better than its sequestration by adsorption or (co-)precipitation. According to previous studies, the removal of Mn by oxidative precipitation is expected to increase the Mn stability in the produced sludge than its removal by high-pH neutralization (Watzlaf, 1987; Watzlaf, and Casson, 1990). To better anticipate the processes that impact the concentrations of As, Mn and Fe during the ECG and Fe(VI) treatments, geochemical calculations were performed with PHREEQC. The calculations for both ECG and Fe(VI) treatments suggest that the mineral phases likely to precipitate during treatment are primarily Fe-oxides/hydroxides. The two mineral phases that were selected among others as the

most likely precipitating phases are ferrihydrite and lepidocrocite due to their rapid reaction kinetics (Bigham et al., 2002). Further, these two mineral phases were identified in the mineralogical characterization using PXRD. In the current study, PXRD patterns showed the formation of poorly crystalline Fe-(oxy)hydroxide hydrates. For the ECG sludge, the generated phase appeared to be lepidocrocite (FeOOH) or β -FeO(OH), while for the Fe(VI) sludge, the dominant phase appeared to be ferrihydrite. The two phases are amenable to adsorb species such as arsenate (Alarcón et al., 2014; Gomes et al., 2007; Wang and Giammar, 2015). Additionally, the findings from PXRD analyses are in agreement with previous studies, which reported the formation of poorly crystalline phases such as lepidocrocite during ECG and Fe(OH)₃ or Fe₂O₃ nanoparticles during Fe(VI) treatment for As removal (Gomes et al., 2007; Kong et al., 2023; Prucek et al., 2013; Wang et al., 2020). To evaluate the mobility and fractionation of As and Mn from the Fe(VI) and ECG sludges, the environmental behaviour of the sludges was investigated using N-SEP and FLT tests. The N-SEP results revealed that the major As fraction (97% for Fe(VI); 71% for ECG) was associated to the poorly crystalline Fe-(oxy)hydroxides. These findings are consistent with previous studies that have reported that As adsorption is a potential removal mechanism during ECG and Fe(VI) treatment (Kobyas et al., 2022; Li et al., 2012; Sharma et al., 2007). In addition, the co-precipitation or incorporation of As into Fe-(oxy)hydroxides nanoparticles during the Fe(VI) treatment are potential immobilization mechanisms for As. This could be explained by the lower Fe/As molar ratio (10.6/1) in Fe(VI) treatment than in ECG (61.2/1) treatment (Rakotonimaro et al., 2021). Similar findings were previously reported in literature and the partial incorporation of As into the Fe-(hydr-)oxide nanoparticles is recognized as a possible removal mechanism of As during Fe(VI) (Prucek et al., 2013). The Mn removal through trapping by the generated flocs during ECG and by oxidation from Mn(II) to Mn(IV) and formation of Mn-oxides in Fe(VI) treatment resulted in slightly higher fraction of Mn bound to poorly crystalline Fe-(oxy)hydroxides in the ECG-sludge (54%) than in the Fe(VI)-sludge (42%). Indeed, the co-precipitation or incorporation

of As, the oxidation of Mn and formation of Mn-oxides during Fe(VI) treatment are factors enhancing the stability of the produced sludge and decreasing the potential leaching of both elements on the environment. This result is in line with the hypothesis (H4) of the lower mobility of As and Mn from the Fe(VI)-sludge than for the ECG- sludge. This low As mobility was also found in the FLT leachate for both ECG and Fe(VI) treatments. The concentrations of As measured in the FLT leachate are 3- to 5-times lower than those of the SWQC and 4-7 times lower than the D019 criteria. The oxidation of As(III) to As(V) and its subsequent co-precipitation and sorption onto the Fe-(oxy)hydroxide surfaces can explain the increased As immobilization during the two treatments. The concentration of As mobilized from Fe(VI) sludge (0.05 mg/L) is slightly higher than that from ECG (0.03 mg/L). This could be attributed to the higher initial As content in the Fe(VI) sludge, the latter being more stable than the ECG-sludge, when the proportion of As mobilized is considered (0.0026% of leached from Fe(VI)-sludge vs. 0.0055% for ECG-sludge). Furthermore, the Fe(VI)- and ECG-sludge can be considered as non-hazardous when the FLT leachate concentrations are compared to TCLP criteria (< 5 mg/L). In terms of Mn leaching during FLT test, the Fe(VI)-sludge could be more stable than the ECG-sludge. The Mn concentration in the ECG-sludge exceeded the SWQC1 criteria (0.26 mg/L). This finding may confirm the hypothesis related to the higher Fe(VI)-sludge stability and can be related to the suspected Mn removal mechanism (trapping as Mn(II) in ECG vs. oxidation and removal as Mn-oxide in Fe(VI)). Furthermore, this higher stability of Mn after oxidative precipitation was already reported in literature (Watzlaf, 1987; Watzlaf and Casson, 1990).

7.3 Comparison between ECG and Fe(VI) performances

The findings from the current study are consistent with the results from previous studies on the removal efficiencies of As and Mn by ECG and Fe(VI) from synthetic and real effluents (Tables 2.3; 2.5) (Goodwill et al., 2016; Lakshmipathiraji et al., 2010; Lee et al., 2003; Parga et al., 2005; Shafaei et al., 2010; Wang et al., 2020). The results presented here also revealed that ECG and Fe(VI) can remove As and Mn efficiently and simultaneously from E_{high} without deteriorating the efficiency achieved with the treatment of synthetic effluents ($S_{\text{As+Mn}}$). However, the Fe(VI) treatment allowed for removing As (99.7%) and Mn (98.6%) almost completely from E_{high} , which initially contained 4.05 mg As/L and 4.27 mg Mn/L (Table 7.4). ECG was found to be less efficient in removing Mn (58.5%) from E_{high} which contained 4.17 mg Mn/L, and highly efficient for As removal (99.4%) with an initial concentration of 3.41 mg As/L (Table 7.4). These results are in accordance with the hypothesis (H3) on the higher performance using Fe(VI) than ECG for the removal of As and Mn from slightly contaminated mine water. The removal mechanism of Mn and the more demanding operating conditions for its treatment compared to As are probably the reasons for the different efficiencies between the ECG and Fe(VI) treatments. Indeed, the As removal relies on the production of Fe(III)-hydroxides to promote its (co-)precipitation or adsorption after the oxidation step. This observation was confirmed with the experiments performed using Fe(VI) in combination with Fe(III) as supporting coagulant. During the experiments, the amount of Fe(VI) decreased from 28 mg/L to 12.5 mg/L after the addition of 8 mg/L as Fe(III), the As removal did not deteriorate, suggesting the dependency of As removal on the production of coagulant species, with lower amount of the oxidant. On the other hand, the removal of Mn required more oxidizing conditions, and thus it was more affected by the amount of Fe(VI) added.

In the case of Mn removal by ECG, which depends on the production of OH^- (higher final pH), and the Fe-hydroxides, the identification of the most performant CD value to achieve satisfactory Mn removal (60% - equivalent to final $[\text{Mn}] < 2 \text{ mg/L}$) lead to the application of higher CD (2 mA/cm^2) compared to As removal (CD: 0.5 mA/cm^2). This difference in CD requirements could be attributed to the dependency of As on the produced Fe-hydroxides which was achieved at this low CD, even at low pH value. Eventually, the more critical operating conditions required for Mn removal (higher amounts of Fe(VI) and higher value of CD) may have an important effect on the overall treatment performances and costs.

The amount of sludge produced at the end of a treatment is a critical factor in the evaluation of its performance. The importance of considering the produced sludge lies in its further handling, discharging, and storage. The sludge may further be exploited for the recovery of valuable materials. In fact, the treatment by Fe(VI), according to the current study results (Table 7.4), produced considerably lower amounts of sludge in wet basis (440 g/m^3), and lower masses of dry sludge (80 g/m^3) compared to the ECG ($1,227 \text{ g/m}^3$ in wet basis; 300 g/m^3 in dry basis). From a practical standpoint, the differences in the amounts of generated sludge can lead to increased difficulties and costs associated with the handling of ECG-sludge. These challenges would probably affect the evaluation of the process performance. The salinity is a known cause of toxicity to aquatic organisms. Therefore, the residual salinity of an effluent after the treatment is a crucial factor to consider before the final discharge. Due to the addition of chemicals (K_2FeO_4 , $\text{Fe}_2(\text{SO}_4)_3 \cdot x\text{H}_2\text{O}$, H_2SO_4) when using the Fe(VI)_s for the As and Mn removal, the residual salinity (expressed in EC (mS/cm)) was slightly increased with respect to the initial effluent salinity (Table 7.4). However, when the ECG treatment was performed, no change of salinity was observed, because no chemicals were added, except few drops of HCl for the pH adjustment before the treatment. Finally, it is worthy to mention that due to the addition of $\text{Fe}_2(\text{SO}_4)_3 \cdot x\text{H}_2\text{O}$ salt in combination with Fe(VI), the final pH required a slight adjustment to respect the

regulations (MELCC, 2012, $6 < \text{pH} < 9$). However, the amount of neutralizing agent (NaOH) added for this purpose was low and did not considerably contribute to the observed increase of the residual salinity.

Table 7.4 Comparison between Fe(VI) and ECG performances for simultaneous removal of As and Mn from lowly-contaminated mine water

Treatment	Parameter						
	Removal efficiency (%)		pH		EC (mS/cm)		Mass of dry sludge (g/m ³)
	As	Mn	Adjusted	Final	Initial	Final	
ECG	99.4	58.5	6.50	7.15	2.50	2.50	278
Fe(VI)	99.7	98.6	5.50	5.69	3.02	3.08	80

The evaluation of the total operating costs (OCs) per 1 m³ of treated effluent by ECG and Fe(VI) was performed according to the variables and costs defined in Tables 3.1 and 3.2. The estimated costs for each variable considered in the preliminary techno-economic evaluation for ECG and Fe(VI) are shown in Table 7.5. The ECG treatment cost evaluation indicated that the major component of the treatment contributing to the total cost was the electrodes' cost. As shown in Table 7.5, the total cost of the ECG treatment was \$2.04 CAD/m³. The cost of energy and neutralizing agent was very low compared to the estimated cost of the electrodes' consumption. For the Fe(VI) treatment, as indicated in Table 7.5, the cost of the required Fe(VI)_s was the main contributor to the total cost, which was 2.51 \$ CAD/m³, with lower contribution of the other components (i.e Fe(III) salt, deionized water, neutralizing agents and the cost of equipment).

Table 7.5 Preliminary OCs evaluation for the treatment of E_{high} by ECG and Fe(VI)

Parameter	Total cost (\$ CAD/m ³)
ECG	
C_{energy}	0.083
$C_{\text{neutralizing agent}}$	0.01
$C_{\text{Electrodes}}$	1.95
Fe(VI)	
C_{reagents}	
Fe(VI) _s	2.48
Fe(III) salt	0.01
Deionized water-Fe(VI) solution	0.01
Deionized water-Fe(III) solution	0.004
H ₂ SO ₄	0.0005
NaOH	0.0002

CHAPTER 8

GENERAL CONCLUSION

The main objective of this study was to evaluate the performance of ECG and Fe(VI) treatments to simultaneously remove As and Mn from slightly contaminated mine water. To do so, treatability tests were performed on synthetic mine effluent containing only As (S_{As}), only Mn (S_{Mn}) and As and Mn (S_{As+Mn}) as well as surrogate mine water (E_{low} and E_{high}) to evaluate the effect of operating conditions on the removal of As and Mn. The physicochemical, mineralogical and environmental characterization of As- and Mn-rich sludge originating from the treatment of mine water using ECG and Fe(VI) was performed to assess the potential leaching of these contaminants with time. Then, the performances of ECG and Fe(VI) were compared.

For ECG, the CD was the main operating factor influencing the removal of Mn and to a lesser extent of As, while the dose of Fe(VI) highly affected the performances of the treatment. Moreover, the results showed that ECG can efficiently treat S_{As} and S_{Mn} , even at low CD (0.5 mA/cm^2 for As and 2.0 mA/cm^2 for Mn) and ionic strength (from 0.25 to 2.5 mS/cm), resulting in low residual salinity and potential associated toxicity. Neither antagonistic nor synergistic effects were observed for the simultaneous removal of As and Mn from S_{As+Mn} using the most performant conditions identified for S_{As} and S_{Mn} . The effect of inter-electrode distance (between 10 and 50 mm) and ionic strength (from 0.25 to 2.5 mS/cm) was quite negligible on the removal of As and Mn from S_{As} , S_{Mn} or S_{As+Mn} , while significantly increasing the consumption of sacrificial Fe-electrodes as well as energy. The removal of As was faster and more efficient from S_{As+Mn} than Mn (20 vs. 60 min and 97–98% vs. 59–64%, respectively) at a CD of 2.0 mA/cm^2 . Finally, efficient removal of As and Mn was obtained for surrogate mine

water (E_{low} and E_{high}), with no addition of toxicity toward *D. magna* after treatment by ECG.

For Fe(VI), the results highlighted that the dose of Fe(VI)_s was the main operating factor influencing the removal of both Mn and As. The high dependency of Mn removal efficiency towards the dose of Fe(VI) added was attributed to the strong oxidizing conditions required during the treatment to oxidize Mn(II) to Mn(IV) prior to its precipitation, while the removal of As through (co-)precipitation and sorption on Fe-(oxy)hydroxide was most sensitive to the amount of newly formed Fe(III)-hydroxide. A 1.3- to 5.6-times higher dose of Fe(VI)_s was required to efficiently remove As and Mn from $S_{\text{As+Mn}}$ compared to S_{As} and S_{Mn} , which can be explained by some competition between As(III) and Mn(II). The combination of $\text{Fe(VI)}_s + \text{Fe(III)}$ at pH_a of 5.5 showed efficient removal of As (99%) and Mn (97%), with a lower Fe(VI)_s dose vs. Fe(VI)_s alone, lower residual salinity, and lower associated operating costs. Finally, an efficient removal (99%) of As and Mn was obtained for E_{low} and E_{high} , with no addition of toxicity toward *D. magna* after the Fe(VI) treatment.

These results suggest that ECG and Fe(VI) could be promising options for the simultaneous removal of As (>97%) and Mn (57-99%) from slightly contaminated mine water (<10 mg/L), in a one-step treatment process. However, the simultaneous removal of As and Mn required the application of more stringent operating conditions (higher CD for ECG and higher Fe(VI)_s dose for Fe(VI)) to achieve satisfactory performances (similar to the treatment of S_{As} and S_{Mn}). The results also showed that the presence of competing ions such as Ca^{2+} can positively affect the ECG treatment performance in terms of contaminant and toxicity removals through the production of larger Fe-(oxy)hydroxide flocs, while the presence of SO_4^{2-} negatively affected the removal of Mn by ECG, because of the potential formation of a passivating film at the surface of the sacrificial Fe-electrodes.

As for conventional treatment, both ECG and Fe(VI) processes produced As- and Mn-rich sludge that might represent a secondary source of contamination if not properly managed. A physicochemical and mineralogical characterization of these sludge showed that they were mainly composed of O (49-56 wt%) and Fe (56-57 wt%), with variable concentrations of As (1.2% for ECG-sludge vs. 3.8% for Fe(VI)-sludge) and Mn (0.77% for ECG-sludge vs. 5.3% for Fe(VI)-sludge). The lower content of As and Mn in ECG-sludge can be explained by the higher amounts of sludge produced and the lower removal efficiency obtained during ECG treatment, especially for Mn. The mineralogical characterization (PXRD and SEM-EDS) showed the formation of relatively homogeneous precipitate during the ECG treatment and heterogeneous precipitate with the Fe(VI) treatment, composed of poorly crystalline Fe-(oxy)hydroxides (lepidocrocite or β -FeO(OH) for ECG-sludge vs. ferrihydrite for Fe(VI)-sludge). This is in accordance with the N-SEP results, showing that a higher proportion of As was bound to poorly crystalline Fe-(oxy)hydroxide (97% for Fe(VI) vs. 71% for ECG), while a higher proportion of Mn was associated to the residuals (57% for Fe(VI) vs. 5.7% for ECG). Finally, FLT results indicated that very low amounts of As and Mn were leached out from the sludge produced by both ECG and Fe(VI) treatment. Indeed, the concentrations of As measured in the FLT leachate are 3-5 times lower than those of the SWQC and 4-7 times lower than the D019 criteria. For Mn, the concentration leached out from ECG sludge slightly exceeded the SWQC1 criteria (0.26 mg/L), while the sludge from Fe(VI) met the criteria, indicating that Fe(VI) sludge seemed to be more stable than ECG sludge. This can be related to the suspected Mn removal mechanism (trapping as Mn(II) in ECG vs. oxidation and removal as Mn-oxide in Fe(VI)).

Considering all these results, Fe(VI) treatment can be considered more performant than ECG with respect to As and, more importantly, Mn removal efficiency and sludge stability, despite higher residual salinity (that is not related to additional toxicity towards *D. magna*) and operating costs.

This study showed that Fe(VI) and ECG can be promising options for the simultaneous removal of As and Mn from mine water. Yet, few recommendations can be formulated to favor the industrial application of these technologies for the treatment of As- and Mn-contaminated mine water including:

- 1) Additional treatability tests will be recommended to better understand the effect of water quality on the performances of ECG and Fe(VI) treatment and better document how the co-occurrence of contaminants (such as identify if other inorganic contaminant can be removed) can affect their removal efficiencies as well as operating costs;
- 2) Additional mineralogical characterization of the fresh ECG- and Fe(VI)-sludge using X-ray absorption spectroscopy (XANES; XAFS) will be needed to further improve the knowledge about the mechanisms involved in As and Mn removal within the newly formed Fe-bearing precipitates by ECG and Fe(VI);
- 3) The geochemical behavior of fresh and “aged” ECG- and Fe(VI)-sludge using static (i.e., pH-dependent leaching tests, anoxic leaching tests) and kinetic tests should be studied to better evaluate the long-term stability of the sludge. The effect of chloride on the mobility of As and Mn from ECG- and Fe(VI)-sludge should also be evaluated;
- 4) The physical behavior of the ECG- and Fe(VI)-sludge in terms of its settlability, and its spontaneous tendency to separate from water can be important criteria to assess to better identify the most performant treatment process;
- 5) ECG and Fe(VI) treatability tests must be performed at pilot scale in continuous mode to better evaluate the effect of hydraulic retention time on the removal of As and Mn and the requirement for air injection during ECG treatment;
- 6) A techno-economic analysis of ECG and Fe(VI) treatment using reagent and electricity consumption values as well as considering the required space and cost of aeration in ECG from pilot scale experiments should be done.

APPENDIX

7) # Treatment of surrogate mine water (Ehigh) using ECG at current density of 2
mA/cm2
8)
9) database c:\phreeqc\database\WATEQ4F.DAT
10)
11) SELECTED_OUTPUT 1
12)
13) -file Reem_ECG_data_PHREEQC.csv
14) -pH true
15) -pe true
16) -totals Al As As(+3) As(+5) Mn Mn(2) Mn(3) Mn(6) Mn(7) Fe Fe(+2) Fe(+3)
B Ba Ca Cu Dc Li K Mg Na Ni Pb S Si Se Cl Br P F N C
17)
18) -saturation_indices Jarosite(ss) Jarosite-Na Jarosite-K JarositeH Goethite
Hematite Ferrihydrite Lepidocrocite Schwertmannite Fe(OH)3 Fe(OH)3(a)
Fe(OH)2.7Cl.3 Basaluminite Al(OH)3(a) Boehmite Pyrolusite Manganite
Birnessite Bixbyite
19)
20) END
21)
22) PHASES
23)
24) Lepidocrocite #From minteq.v4 database
25) $\text{FeOOH} + 3\text{H}^+ = \text{Fe}^{+3} + 2\text{H}_2\text{O}$
26) log_k 1.371
27) delta_h-0 kJ
28)
29) Ferrihydrite #From minteq.v4 database
30) $\text{Fe}(\text{OH})_3 + 3\text{H}^+ = \text{Fe}^{+3} + 3\text{H}_2\text{O}$
31) log_k 3.191
32) delta_h -73.374 kJ
33)
34) Schwertmannite #From Nordstrom (2020)
35) $\text{Fe}_8\text{O}_8(\text{SO}_4)_{1.26}(\text{OH})_{5.48} + 21.48\text{H}^+ = 8\text{Fe}^{+3} + 1.26\text{SO}_4^{-2} + 13.48\text{H}_2\text{O}$
36) log_k 18.5
37)
38) Basaluminite #From Nordstrom (2020)
39) $\text{Al}_4(\text{OH})_{10}\text{SO}_4 + 10\text{H}^+ = 4\text{Al}^{+3} + \text{SO}_4^{-2} + 10\text{H}_2\text{O}$
40) log_k 24.0

41)
42) Fe(OH)₃ #From Nordstrom (2020)
43) $\text{Fe(OH)}_3 + 3\text{H}^+ = \text{Fe}^{+3} + 3\text{H}_2\text{O}$
44) log_k 3.0
45)
46) Manganite
47) $\text{MnOOH} + 3\text{H}^+ + \text{e}^- = \text{Mn}^{+2} + 2\text{H}_2\text{O}$
48) log_k 25.34
49) delta_h-0 kJ
50)
51) END
52) SOLUTION 1 # initial Ehigh composition before the application of the current,
and the adjustment of pH (i.e before the Fe electrode dissolution)
53)
54) units mg/L
55) temperature 22
56) pH 8.21
57) pe 7.8
58) Al 0.05
59) As 3.41
60) Mn 4.17
61) Fe 0.09
62) B 0.49
63) Ba 115
64) Ca 219
65) Cu 0.08
66) Cd 0.003
67) Li 0.08
68) K 115
69) Mg 5.78
70) Na 265
71) Ni 0.003
72) Pb 0.1
73) S 320
74) Si 3.35
75) Se 0.02
76) Cl 143
77) Br 0.1
78) P 0.1
79) F 0.1
80) N 32
81) C 1 charge
82)

- 83) END
- 84)
- 85) SOLUTION 2 # Ehigh (with the same composition of solution 1) after pH adjustment with 0.034 mL of 1 M HCl (change of Cl concentration is negligible)
- 86)
- 87) units mg/L
- 88) temperature 22
- 89) pH 6.50
- 90) pe 7.8
- 91) Al 0.05
- 92) As 3.41
- 93) Mn 4.17
- 94) Fe 0.09
- 95) B 0.49
- 96) Ba 115
- 97) Ca 219
- 98) Cu 0.08
- 99) Cd 0.003
- 100) Li 0.08
- 101) K 115
- 102) Mg 5.78
- 103) Na 265
- 104) Ni 0.003
- 105) Pb 0.1
- 106) S 320
- 107) Si 3.35
- 108) Se 0.02
- 109) Cl 143.002
- 110) Br 0.1
- 111) P 0.1
- 112) F 0.1
- 113) N 32
- 114) C 1 charge
- 115) END
- 116)
- 117) SOLUTION 3 # This is the composition of Ehigh after the application of the current. Fe concentration after the Fe electrode dissolution. Fe according concentration calculated according to the current density applied using Faradays law, and assuming that the composition of the Ehigh is the same.
- 118)
- 119) units mg/L
- 120) temperature 22

121) pH 6.54
122) pe 7.8
123) Al 0.05
124) As 3.41
125) Mn 4.17
126) Fe 127
127) B 0.49
128) Ba 115
129) Ca 219
130) Cu 0.08
131) Cd 0.003
132) Li 0.08
133) K 115
134) Mg 5.78
135) Na 265
136) Ni 0.003
137) Pb 0.1
138) S 320
139) Si 3.35
140) Se 0.02
141) Cl 143
142) Br 0.1
143) P 0.1
144) F 0.1
145) N 32
146) C 1 charge
147) END
148)
149) Solution 4 # Final solution composition (sample collected after 1 h of
reaction and 30 min of settling)
150)
151) units mg/L
152) temperature 22
153) pH 7.15
154) pe 5.8
155) Al 0.03
156) As 0.02
157) Mn 1.81
158) Fe 0.89
159) B 0.49
160) Ba 110.59
161) Ca 215.71
162) Cu 0.08

163) Cd 0.003
164) Li 0.08
165) K 112.03
166) Mg 5.05
167) Na 261.43
168) Ni 0.003
169) Pb 0.1
170) S 311.76
171) Si 0.32
172) Se 0.02
173) Cl 138
174) Br 0.1
175) P 0.1
176) F 0.1
177) N 28
178) C 1 charge
179)
180) END

```

181) # Title Ferrate treatment for As and Mn removal (step by step)
182) database c:\phreeqc\database\WATEQ4F.DAT
183)
184) SELECTED_OUTPUT 1
185)
186) -file Reem_data_PHREEQC.csv
187) -pH true
188) -pe true
189) -totals Al As As(+3) As(+5) Mn Mn(2) Mn(3) Mn(6) Mn(7) Fe Fe(+2)
      Fe(+3) B Ba Ca Cu Dc Li K Mg Na Ni Pb S Si Se Cl Br P F N C
190) -saturation_indices Jarosite(ss) Jarosite-Na Jarosite-K JarositeH
      Goethite Hematite Ferrihydrite Lepidocrocite Schwertmannite Fe(OH)3
      Fe(OH)3(a) Fe(OH)2.7Cl.3 Basaluminite Al(OH)3(a) Boehmite Pyrolusite
      Manganite Birnessite Bixbyite
191)
192) END
193)
194) PHASES
195)
196) Lepidocrocite #From minteq.v4 database
197) FeOOH + 3H+ = Fe+3 + 2H2O
198) log_k 1.371
199) delta_h-0 kJ
200)
201) Ferrihydrite #From minteq.v4 database
202) Fe(OH)3 + 3H+ = Fe+3 + 3H2O
203) log_k 3.191
204) delta_h -73.374 kJ
205)
206) Schwertmannite #From Nordstrom (2020)
207) Fe8O8(SO4)1.26(OH)5.48 + 21.48H+ = 8Fe+3 + 1.26SO4-2 +
      13.48H2O
208) log_k 18.5
209)
210) Basaluminite #From Nordstrom (2020)
211) Al4(OH)10SO4 + 10H+ = 4Al+3 + SO4-2 + 10H2O
212) log_k 24.0
213)
214) Fe(OH)3 #From Nordstrom (2020)
215) Fe(OH)3 + 3H+ = Fe+3 + 3H2O
216) log_k 3.0
217)
218) Manganite

```

219) $\text{MnOOH} + 3\text{H}^+ + \text{e}^- = \text{Mn}^{2+} + 2\text{H}_2\text{O}$
220) \log_k 25.34
221) ΔH^0 kJ
222)
223) END
224)
225)
226) SOLUTION 1 #Initial composition of the water, metals concentrations
analyzed by ICP, anions by IC
227)
228) units mg/L
229) temperature 22
230) pH 7.87
231) pe 7.9
232) Al 0.06
233) As 4.05
234) Mn 4.27
235) Fe 0.22
236) B 0.4
237) Ba 435
238) Ca 483.23
239) Cu 0.08
240) Cd 0.003
241) Li 0.08
242) K 125
243) Mg 9.84
244) Na 535
245) Ni 0.003
246) Pb 0.1
247) S 533.56
248) Si 3.64
249) Se 0.02
250) Cl 68
251) Br 0.1
252) P 0.1
253) F 0.1
254) N 91
255) C 1 charge
256)
257) END
258)
259) SOLUTION 2 #Water composition after addition of 12.50 mg/L as
FeO₄²⁻ (solution prepared from K₂FeO₄ solid), (pH, pe higher than initial

conditions), to assume that the concentrations are still the same as in solution 1 except Fe and K (because they can be calculated and there is no analysis for the metals during this step). Followed by 3 min rapid mixing.

260)
 261) units mg/L
 262) temperature 22
 263) pH 9
 264) pe 11
 265) Al 0.06
 266) As 4.05
 267) Mn 4.27
 268) Fe 12.72
 269) B 0.4
 270) Ba 435
 271) Ca 483.23
 272) Cu 0.08
 273) Cd 0.003
 274) Li 0.08
 275) K 150
 276) Mg 9.84
 277) Na 535
 278) Ni 0.003
 279) Pb 0.1
 280) S 533.56
 281) Si 3.64
 282) Se 0.02
 283) Cl 68
 284) Br 0.1
 285) P 0.1
 286) F 0.1
 287) N 91
 288) C 1 charge
 289)
 290) END
 291)
 292) SOLUTION 3 #Water composition after the addition of ferric sulfate solution as supporting coagulant, the addition was 8 mg Fe(III)/L (here also we will assume the same composition as in solution 2, except Fe, S and the pH value. pe no change)
 293)
 294) units mg/L
 295) temperature 22
 296) pH 6.17

297) pe 11
298) Al 0.06
299) As 4.05
300) Mn 4.27
301) Fe 20.72
302) B 0.4
303) Ba 435
304) Ca 483.23
305) Cu 0.08
306) Cd 0.003
307) Li 0.08
308) K 150
309) Mg 9.84
310) Na 535
311) Ni 0.003
312) Pb 0.1
313) S 541.56
314) Si 3.64
315) Se 0.02
316) Cl 68
317) Br 0.1
318) P 0.1
319) F 0.1
320) N 91
321) C 1 charge
322)
323) END
324)
325) SOLUTION 4 #Water composition after pH adjustment with 0.15 mL,
0.1 M H₂SO₄, directly after the addition of Fe(III) solution (to assume the same
composition as in solution 3, except the S concentration and the pH value).
326)
327) units mg/L
328) temperature 22
329) pH 5.52 #During the experiment, the color of ferrate vanishes after
adjustment of pH. During the pH adjustment, the precipitate starts to form.
330) pe 11
331) Al 0.06
332) As 4.05
333) Mn 4.27
334) Fe 20.72
335) B 0.4
336) Ba 435

337) Ca 483.23
338) Cu 0.08
339) Cd 0.003
340) Li 0.08
341) K 150
342) Mg 9.84
343) Na 535
344) Ni 0.003
345) Pb 0.1
346) S 542.04
347) Si 3.64
348) Se 0.02
349) Cl 68
350) Br 0.1
351) P 0.1
352) F 0.1
353) N 91
354) C 1 charge
355)
356) END

RÉFÉRENCES

- Acero, P., Ayora, C., Torrentó, C., Nieto, J.M. (2006). The behavior of trace elements during schwertmannite precipitation and subsequent transformation into goethite and jarosite. *Geochimica et Cosmochimica Acta*, 70, 4130-4139. <https://doi.org/10.1016/j.gca.2006.06.1367>.
- Adhoum, N., Monser, L., Bellakhal, N., Belgaied, J.E. (2004). Treatment of electroplating wastewater containing Cu^{2+} , Zn^{2+} and Cr(VI) by electrocoagulation. *Journal of Hazardous Materials*, 112(3)-207-213. <https://doi.org/10.1016/j.jhazmat.2004.04.018>.
- Ahmad, A., van der Wal, A., Bhattacharya, P., van Genuchten, C.M. (2019). Characteristics of Fe and Mn bearing precipitates generated by Fe(II) and Mn(II) co-oxidation with O_2 , MnO_4 and HOCl in the presence of groundwater ions. *Water Resources*, 15, 505-516. <https://doi.org/10.1016/j.watres.2019.06.036>.
- Akhavan, A., Golchin, A. (2021). Estimation of arsenic leaching from Zn–Pb mine tailings under environmental conditions. *Journal of Cleaner Production*, 295, 126477. <https://doi.org/10.1016/j.jclepro.2021.126477>.
- Akyol, A. (2012). Treatment of paint manufacturing wastewater by electrocoagulation. *Desalination*, 285, 91-99. <https://doi.org/10.1016/j.desal.2011.09.039>.
- Al-Abed, S.R., Hageman, P.L., Jegadeesan, G., Madhavan, N., Allen, D. (2006). Comparative evaluation of short-term leach tests for heavy metal release from mineral processing waste. *Science of the Total Environment*, 364, 14-23. <https://doi.org/10.1016/j.scitotenv.2005.10.021>.
- Alarcón, R., Gaviria, J., Dold, B. (2014). Liberation of adsorbed and co-precipitated arsenic from jarosite, schwertmannite, ferrihydrite, and goethite in seawater. *Minerals*, 4, 603-620. <https://doi.org/10.3390/min4030603>.

- Ali, I., Gupta, V.K., Khan, T. A., Asim, M. (2012). Removal of arsenate from aqueous solution by electro-coagulation method using Al-Fe electrodes. *International Journal of Electrochemical Science*, 7, 1898-1907. [https://doi.org/10.1016/S1452-3981\(23\)13848-X](https://doi.org/10.1016/S1452-3981(23)13848-X).
- Amanda, N., Moersidik, S. S. (2019). Characterization of sludge generated from acid mine drainage treatment plants. *Journal of Physics: Conference Series*, 1351, 012113. <https://doi.org/10.1088/1742-6596/1351/1/012113>.
- An, B., Steinwinder, T.R., Zhao, D. (2005). Selective removal of arsenate from drinking water using a polymeric ligand exchanger. *Water Research*, 39, 4993-5004. <https://doi.org/10.1016/j.watres.2005.10.014>.
- Ansone, L., Klavins, M., Viksna, A. (2013). Arsenic removal using natural biomaterial-based sorbents. *Environmental Geochemistry and Health*, 35, 633-642. <https://doi.org/10.1016/j.gsd.2022.100740>.
- Asselin, M., Drogui, P., Benmoussa, H., Blais, J-F. (2008). Effectiveness of electrocoagulation process in removing organic compounds from slaughterhouse wastewater using monopolar and bipolar electrolytic cells. *Chemosphere*, 72, 1727-1733. <https://doi.org/10.1016/j.chemosphere.2008.04.067>.
- ASTM, 2010. D2216-10S. Standard Test Methods for Laboratory Determination of Water (Moisture) Content of Soil and Rock by Mass. ASTM Int., West Conshohocken, PA.
- Babechuk, M.G., Weisener, Ch.G., Fryer, B.J., Paktunc, D., Maunders, Ch. (2009). Microbial reduction of ferrous arsenate: Biogeochemical implications for arsenic mobilization. *Applied Geochemistry*, 24, 2332-2341. <https://doi.org/10.1016/j.apgeochem.2009.09.006>.

- Babu, D.S., Singh, T.S. A., Nidheesh, P.V., Kumar, M.S. (2019). Industrial wastewater treatment by electrocoagulation process. *Separation Science and Technology*, 55, 1-33. <https://doi.org/10.1080/01496395.2019.1671866>.
- Baig, J.A., Kazi, T.G., Mustafa, M.A., Solangi, I.B., Mughal, M.J., Afridi, H.I. (2016). Arsenic exposure in children through drinking water in different districts of Sindh, Pakistan. *Biological Trace Element Research*, 173(1), 35-46. <https://doi.org/10.1007/s12011-016-0636-0>.
- Balasubramanian, N., Kojima, T., Basha, C.A., Srinivasakannan, C. (2009). Removal of arsenic from aqueous solution using electrocoagulation. *Journal of Hazardous Material*, 167, 966-969. <https://doi.org/10.1016/j.jhazmat.2009.01.081>.
- Bandaru, S.R.S., van Genuchten, C.M., Kumar, A., Glade, S., Hernandez, D., Nahata, M., Gadgil, A. (2020). Rapid and efficient arsenic removal by iron electrocoagulation enabled with in situ generation of hydrogen peroxide. *Environmental Science and Technology*, 54, 6094-6103. <https://doi.org/10.1021/acs.est.0c00012>.
- Banerji, T., Chaudhari, S. (2016). Arsenic removal from drinking water by electrocoagulation using iron electrodes- an understanding of the process parameters. *Journal of Environmental Chemical Engineering*, 4, 3990-4000. <http://dx.doi.org/10.1016/j.jece.2016.09.007>.
- Barisci, S., Dimoglo, A. (2016). Review on the stability of ferrate (VI) species in aqueous medium and oxidation of pharmaceuticals and personal care products (PPCPs) by ferrate(VI): Identification of transformation by-products. *American Chemical Society Symposium*. Ferrites and Ferrates: Chemistry and Applications in Sustainable Energy and Environmental Remediation, Chapter 12, 287-335. <http://dx.doi.org/10.1021/bk-2016-1238.ch012>.

- Bejan, D., Bunce, N.J. (2015). Acid mine drainage: electrochemical approaches to prevention and remediation of acidity and toxic metals. *Journal of Applied Electrochemistry*, 45, 1239-1254. <https://doi.org/10.1007/s10800-015-0884-2>.
- Biesinger, K.E., Christensen, G.M. (1972). Effects of various metals on survival, growth, reproduction and metabolism of *Daphnia magna*. *Journal Fisheries Research Board of Canada*, 29, 1691-1700. <https://doi.org/10.1139/f72-269>.
- Bigham, J.M., Fitzpatrick, R.W., Schulze, D., Schulze, D.G., Dixon, J.B (2002). Iron Oxides. In: Soil Mineralogy with Environmental Applications (Chapter 10, SSSA Book Series, no. 7, pp. 324-333). <https://doi.org/10.2136/sssabookser7.c10>.
- Boinpally, S., Kolla, A., Kainthola, J., Kodali, R., Vemuri, J. (2023). A state-of-the-art review of electrocoagulation technology for wastewater treatment. *Water Cycle*, 4, 26-36. <https://doi.org/10.1016/j.watcyc.2023.01.001>.
- Bondu, R., Cloutier, V., Rosa, E., Benzaazoua, M. (2017). Mobility and speciation of geogenic arsenic in bedrock groundwater from the Canadian Shield in western Quebec, Canada. *Science of the Total Environment*, 574, 509-519. <https://doi.org/10.1016/j.scitotenv.2016.08.210>.
- Bondu, R., Cloutier, V., Rosa, E., Roy, M. (2020). An exploratory data analysis approach for assessing the sources and distribution of naturally occurring contaminants (F, Ba, Mn, As) in groundwater from southern Quebec (Canada). *Applied Geochemistry*, 114, 104500. <https://doi.org/10.1016/j.apgeochem.2019.104500>.
- Bora, A.J., Mohan, R., Dutta, R.K. (2018). Simultaneous removal of arsenic, iron and manganese from groundwater by oxidation-coagulation-adsorption at optimized pH. *Water Science and Technology*, 18, 60-70. <https://doi.org/10.2166/ws.2017.092>.

- Bouchard, M., Laforest, F., Vandelac, L., Bellinger, D., Mergler, D. (2006). Hair manganese and hyperactive behaviors: pilot study of school-age children exposed through tap water. *Environmental Health Perspectives*, 115(1), 122-127. <https://doi.org/10.1289/ehp.9504>.
- Bouchard, M.F., Sauve, S., Barbeau, B., Legrand, M., Brodeur, M.E., Bouffard, T., Limoges, E., Bellinger, D.C., Mergler, D. (2011). Intellectual impairment in school-age children exposed to manganese from drinking water. *Environmental Health Perspectives*, 119, 138-143. <https://doi.org/10.1289/ehp.1002321>.
- Bourg, A.C.M., Loch, J.P.G. (1995). Mobilization of heavy metals as affected by pH and redox Conditions. In: Salomons W., Stigliani W.M. (eds) Biogeochemistry of Pollutants in Soils and Sediments. Environmental Science. Springer, Berlin, Heidelberg. https://doi.org/10.1007/978-3-642-79418-6_4.
- Bozau, E., Licha, T., Ließmann, W. (2017). Hydrogeochemical characteristics of mine water in the Harz Mountains, Germany. *Geochemistry*, 77, 614-624. <https://doi.org/10.1016/j.chemer.2017.10.001>.
- Bujanovic, L.N., Čekerevac, M., Tomic, M., Zdravkovic, M., Đokovic, M.S. (2016). Pilot plant for treatment of raw drinking water with high content of arsenic using ferrate (VI). *Acta Technica Corviniensis – Bulletin of Engineering*, ISSN: 2067-3809.
- Buschmann, J., Berg, M., Stengel, C., Sampson, M.L. (2007). Arsenic and manganese contamination of drinking water resources in Cambodia: Coincidence of risk areas with low relief topography. *Environmental Science and Technology*, 41, 2146-2152. <https://doi.org/10.1021/es062056k>.
- Butler, B.A. (2009). Effect of pH, ionic strength, dissolved organic carbon, time, and particle size on metals release from mine drainage impacted streambed sediments. *Water Research*, 43, 1392-1402. <https://doi.org/10.1016/j.watres.2008.12.009>.

- Butler, B.A. (2011). Effect of imposed anaerobic conditions on metals release from acid-mine drainage contaminated streambed sediments. *Water Research*, 45, 328-336. <https://doi.org/10.1016/j.watres.2010.07.077>.
- Byrne, P., Reid, I., Wood, P.J. (2013). Changes in macroinvertebrate community structure provide evidence of neutral mine drainage impacts. *Environmental Science: Processes and Impacts*, 15, 393-404. <https://doi.org/10.1039/c2em30447c>.
- Cai, G., Zhu, X., Li, K., Qi, X., Wei, Y., Wang, H., Hao, F. (2019). Self-enhanced and efficient removal of arsenic from waste acid using magnetite as an *in situ* iron donator. *Water Research*, 157, 269-280. <https://doi.org/10.1016/j.watres.2019.03.067>.
- Calugaru, I.L., Genty, T., Neculita, C.M. (2018a). Treatment of manganese in acid and neutral mine drainage using modified dolomite. *International Journal of Environmental Impacts*, 3, 323-333. <https://doi.org/10.2495/EI-V1-N3-323-333>.
- Calugaru, I.L., Neculita, C.M., Genty, T., Zagury, G.J. (2019). Removal efficiency of As(V) and Sb(III) in contaminated neutral drainage by Fe-loaded biochar. *Environmental Science and Pollution Research*, 26, 9322-9332. <https://doi.org/10.1007/s11356-019-04381-1>.
- Can, B.Z., Boncukcuoglu, R., Yilmaz, A.E., Fil B.A. (2014). Effect of some operational parameters on the arsenic removal by electrocoagulation using iron electrodes. *Journal of Environmental Health Science and Engineering*, 12, 95. <https://doi.org/10.1186/2052-336X-12-95>.
- Cappuyns, V., Swennen, R. (2008). The application of pHstat leaching tests to assess the pH-dependent release of trace metals from soils, sediments and waste materials. *Journal of Hazardous Materials*, 158, 185-195. <https://doi.org/10.1016/j.jhazmat.2008.01.058>.

- Caraballo, M.A., Rötting, T.S., Macías, F., Nieto, J.M., Ayora, C. (2009). Field multi-step limestone and MgO passive system to treat acid mine drainage with high metal concentrations. *Applied Geochemistry*, 24, 2301-2311. <https://doi.org/10.1016/j.apgeochem.2009.09.007>.
- Caraballo, M.A., Serna, A., Macías, F., Pérez-López, R., Ruiz-Cánovas, C., Richter, P., Becerra-Herrera, M. (2018). Uncertainty in the measurement of toxic metals mobility in mining/mineral wastes by standardized BCR-SEP. *Journal of Hazardous Materials*, 360, 587-593. <https://doi.org/10.1016/j.jhazmat.2018.08.046>.
- Catrouillet, C., Hirose, S., Manetti, N., Boureau, V., Peña, J. (2020). Coupled As and Mn redox transformations in an Fe(0) electrocoagulation system: Competition for reactive oxidants and sorption sites. *Environmental Science and Technology*, 54, 7165-7174. <https://dx.doi.org/10.1021/acs.est.9b07099>.
- CCME, (1999). Canadian water quality guidelines for the protection of aquatic life: Arsenic. Canadian Council of Ministers of the Environment, Winnipeg, Canada, 4 p.
- CCME (2001). Canadian water quality guidelines for the protection of aquatic life: Arsenic. Updated. In: Canadian environmental quality guidelines, 1999, Canadian Council of Ministers of the Environment, Winnipeg, Canada, 4 p.
- CEAEQ, (2014). Détermination des anions: méthode par chromatographie ionique, MA. 300-Ions 1.3, Rév. 3, Centre d'Expertise en Analyse Environnementale du Québec, MDDELCC, Québec, Canada, 14 p.
- CEAEQ, (2021). Détermination de la toxicité : létalité (CL50 48h) chez la daphnie *Daphnia magna*. MA. 500 – D.mag. 1.1, Rév. 3. Centre d'Expertise en Analyse Environnementale du Québec, Ministère de l'Environnement et de la Lutte contre les changements climatiques du Québec, Québec, Canada, 18 p.

- Chang, Y.J., Black, B.D., Chang, D., Gehling, D. (2006). Advanced processes for simultaneous arsenic and manganese removal. AWWA Research Foundation. American Water Works Association. IWA Publishing. ISBN 9781583214602.
- Chen, X., Guohua, C., Yue, P.L. (2000). Separation of pollutants from restaurant wastewater by electrocoagulation. *Separation and Purification Technology*, 19, 65-76. <https://doi.org/10.1080/01496390601120557>.
- Chen, G., (2004). Electrochemical technologies in wastewater treatment. *Separation and Purification Technology*, 38, 11-41. <https://doi.org/10.1016/j.seppur.2003.10.006>.
- Choong, T. S., Chuah, T. G., Robiah, Y., Koay, F. G., Azni, I. (2007). Arsenic toxicity, health hazards and removal techniques from water: an overview. *Desalination*, 217, 139-166. <https://doi.org/10.1016/j.desal.2007.01.015>.
- Christian, S.G.D. (1994). Analytical Chemistry. In 5th ed., John Wiley and Sons, Inc., New York, USA. pp. 723-724.
- Chukwura, U.O., Hursthouse, A.S. (2020). Evaluating controls on potentially toxic element release in circum-neutral mine water: a case study from the abandoned Pb–Zn mines of Leadhills and Wanlockhead, South of Scotland, United Kingdom. *Environmental Earth Sciences*, 79, 363. <https://doi.org/10.1007/s12665-020-09108-x>.
- Ciampi, L.E., Daly, L.J. (2009). Methods of synthesizing a ferrate oxidant and its use in ballast Water. *Patent US7476342B2*.
- Clancy, T.M., Hayes, K.F., Raskin, L. (2013). Arsenic waste management: a critical review of testing and disposal of arsenic-bearing solid wastes generated during arsenic removal from drinking water. *Environmental Science and Technology*, 47, 10799-10812. <https://doi.org/10.1021/es401749b>.

- Çöl, M., Çöl, C., Soran, A., Sayli, B.S., Oztürk, S. (1999). Arsenic-related Bowen's disease, palmar keratosis, and skin cancer. *Environmental Health Perspectives*, 107, 687-689. <https://doi.org/10.1289/ehp.107-1566498> .
- Coudert, L., Bondu, R., Rakotonimaro, T.V., Rosa, E.; Guittonny, M., Neculita, C.M. (2020). Treatment of As-rich mine effluents and produced residues stability: Current knowledge and research priorities for gold mining. *Journal of Hazardous Materials*, 386, 121920. <https://doi.org/10.1016/j.jhazmat.2019.121920>.
- Crichton, R.R., Wilmet, S., Leggsyer, R., Ward, R.J. (2002). Molecular and cellular mechanisms of iron homeostasis and toxicity in mammalian cells. *Journal of Inorganic Biochemistry*, 91, 9-18. [https://doi.org/10.1016/S0162-0134\(02\)00461-0](https://doi.org/10.1016/S0162-0134(02)00461-0).
- Cruz-Hernández, P., Pérez-López, R., Nieto, J.M. (2017). Role of arsenic during the aging of acid mine drainage precipitates. *Procedia Earth and Planetary Science*, 17, 233-236. <https://doi.org/10.1016/j.proeps.2016.12.079>.
- D019. Directive 019 Sur l'Industrie Minière; Government of Quebec, Quebec, Canada, (1989). Available online: https://www.environnement.gouv.qc.ca/milieu_ind/directive019/directive019-1989.pdf.
- D019. Directive 019 Sur l'Industrie Minière; Government of Quebec: Quebec, Canada, (2005). Available online: https://www.environnement.gouv.qc.ca/milieu_ind/directive019/directive019-2005.pdf.
- Dave, G. (1984). Effects of waterborne iron on growth, reproduction, survival and hemoglobin in *Daphnia Magna*. *Comparative Biochemistry and Physiology Part C: Comparative Pharmacology*, 78, 2, 433-438. [https://doi.org/10.1016/0742-8413\(84\)90111-7](https://doi.org/10.1016/0742-8413(84)90111-7).
- Davison, W. (1993). Iron and manganese in lakes. *Earth Science Review*, 34, 119-163. [https://doi.org/10.1016/0012-8252\(93\)90029-7](https://doi.org/10.1016/0012-8252(93)90029-7).

- de Meyer, C. M. C., Rodríguez, J. M., Carpio, E. A., García, P. A., Stengel, C., Berg, M. (2017). Arsenic, manganese and aluminum contamination in groundwater resources of Western Amazonia (Peru). *Science of the Total Environment*, 607-608, 1437-1450. <https://doi.org/10.1016/j.scitotenv.2017.07.059>.
- Del Ángel, P., Carreño, G., Nava, J.L., Martínez, M.T., Ortiz, J. (2014). Removal of arsenic and sulfates from an abandoned mine drainage by electrocoagulation: Influence of hydrodynamic and current density. *International Journal of Electrochemical Science*, 9, 710-719. [https://doi.org/10.1016/S1452-3981\(23\)07751-9](https://doi.org/10.1016/S1452-3981(23)07751-9).
- Demirel, T., Özmen, F.K., Yavuz, Y., Koparal A.S. (2022). The effect of electrocoagulation (EC) on total arsenic, arsenite (As^{3+}) and arsenate (As^{5+}) species removal from model groundwater investigating toxicity and sludge characteristic. *Applied Water Science*, 12, 138. <https://doi.org/10.1007/s13201-022-01660-0>.
- Demopoulos, G.P. (2005). On the preparation and stability of scorodite. *Arsenic Metallurgy*, 25-50. McGill University Mining, Metals and Materials Engineering.
- Doerfelt, C., Feldmann, T., Roy, R., Demopoulos, G.P. (2016). Stability of arsenate-bearing Fe(III)/Al(III) co-precipitates in the presence of sulfide as reducing agent under anoxic conditions. *Chemosphere*, 151, 318-323. <https://doi.org/10.1016/j.chemosphere.2016.02.087>.
- Dong, S., Mu, Y., Sun, X. (2019). Removal of toxic metals using ferrate (VI): a review. *Water Science and Technology*, 80, 1213-1225. <https://doi.org/10.2166/wst.2019.376>.
- Doudoroff, P., Katz, M. (1953). Critical review of literature on the toxicity of industrial wastes and their components to fish: II. The metals, as salts. *Sewage and Industrial Wastes*, 25, 802-839. <https://www.jstor.org/stable/25032224>.

- Drzewicz, P., Drobniewska, A., Sikorska, K., Nałęcz-Jawecki, G. (2018). Analytical and ecotoxicological studies on degradation of fluoxetine and fluvoxamine by potassium ferrate. *Environmental Technology*, 40, 3265-3275. <https://doi.org/10.1080/09593330.2018.1468488>.
- Dubuc, J., Coudert, L., Lefebvre, O., Neculita, C.M. (2022). Electro-Fenton treatment of contaminated mine water to decrease thiosalts toxicity to *Daphnia magna*. *Science of the Total Environment* 835, 155323. <https://doi.org/10.1016/j.scitotenv.2022.155323>.
- Ebba, M., Asaithambi, P. Alemayehu, E. (2021). Investigation on operating parameters and cost using an electrocoagulation process for wastewater treatment. *Applied Water Science*, 11, 175. <https://doi.org/10.1007/s13201-021-01517-y>.
- El-Taweel, Y.A., Nassef, E.M., Elkheriany, I., Sayed, D. (2015). Removal of Cr(VI) ions from waste water by electrocoagulation using iron electrode. *Egyptian Journal of Petroleum*, 24, 183-192. <https://doi.org/10.1016/j.ejpe.2015.05.011>.
- Emamjomeh, M.M., Sivakumar, M. (2009). Review of pollutants removed by electrocoagulation and electrocoagulation/flotation processes. *Journal of Environmental Management*, 90, 1663-1679. <https://doi.org/10.1016/j.jenvman.2008.12.011>.
- Environment Canada (1996). Méthode d'essai biologique – essai de létalité aigüe sur *Daphnia* spp. Report SPE 1/RM/11, Ontario, Canada, 78 p. https://publications.gc.ca/collections/collection_2013/ec/En49-24-1-11-fra.pdf.
- Environment Canada (2000). Environmental protection series (EPS). Method development and application sections. Biological test method: acute lethality of effluents to *Daphnia magna*. Reference Method EPS 1/RM/14, Second Edition. Environmental Technology Centre, Ottawa, Canada, 34 p.

- Er, X.Y., Seow, T.W., Lim, C.K., Ibrahim, Z. (2018). Natural attenuation, biostimulation and bioaugmentation of landfill leachate management. *Earth and Environmental Science*, 140, 012034. DOI: [10.1088/1755-1315/140/1/012034](https://doi.org/10.1088/1755-1315/140/1/012034).
- Ericsson, B., Hallmans, B. (1996). Treatment of saline wastewater for zero discharge at the Debiensko coal mines in Poland. *Desalination*, 105, 115-123. [https://doi.org/10.1016/0011-9164\(96\)00065-3](https://doi.org/10.1016/0011-9164(96)00065-3).
- Esmacilrad, N., Terry, C., Kennedy, H.J., Li, G., Carlson, K.H. (2015). Optimizing metal-removal processes for produced water with electrocoagulation. *Oil and Gas Facilities*, 4, 87-96. <https://doi.org/10.2118/173899-PA>.
- Ettler, V., Tomášová, Z., Komárek, M., Mihaljevic, M., Sebek, O., Michálková, Z. (2015). The pH-dependent long-term stability of an amorphous manganese oxide in smelter-polluted soils: Implication for chemical stabilization of metals and metalloids. *Journal of Hazardous Materials*, 286, 386-394. <http://dx.doi.org/10.1016/j.jhazmat.2015.01.018>.
- Fan, M., Li, N., Chuang, C., Shi, Y., Brown, R.C., Leeuwen, J.V., Banerjee, K., Qu, J., Chen, H. (2007). Arsenite oxidation by ferrate in aqueous solution. *Trace Metals and other Contaminants in the Environment*, 9, 623-639. [https://doi.org/10.1016/S1875-1121\(06\)09024-9](https://doi.org/10.1016/S1875-1121(06)09024-9).
- Fayad, N. (2017). The application of electrocoagulation process for wastewater treatment and for the separation and purification of biological media. Chemical and Process Engineering. PhD thesis, Université Clermont Auvergne, France.
- Fernández-Ondoño, E., Bacchetta, G., Lallena, A.M., Francisco, B.N., Ortiz, I., Jiménez, M.N. (2017). Use of BCR sequential extraction procedures for soils and plant metal transfer predictions in contaminated mine tailings in Sardinia. *Journal of Geochemical Exploration*, 172, 133-141. <https://doi.org/10.1016/j.gexplo.2016.09.013>.

- Ferrari, C.R., Nascimento, H.A.F., Bruschi, A.L., Roque, C.V., Nascimento, M.R.L., Bonifácio, R.L., Rodgher, S. (2018). Acute toxicity of manganese to *Ceriodaphnia Silvestrii* and *Daphnia Magna* in bioassays and the potential toxicity of this metal in uranium mine effluent. *International Atomic Energy Agency (IAEA)*: IAEA. Poster presentation. Brazil, 424 p. https://www-pub.iaea.org/MTCD/Publications/PDF/PUB1832_web.pdf.
- Flem, B., Reimann, C., Fabian, K., Birke, M., Filzmoser, P. Banks, D. (2018). Graphical statistics to explore the natural and anthropogenic processes influencing the inorganic quality of drinking water, groundwater and surface water. *Applied Geochemistry*, 88, 133-148. <https://doi.org/10.1016/j.apgeochem.2017.09.006>.
- Foudhaili, T. (2019). Traitement de la salinité sulfatée et de la toxicité associée des effluents miniers au moyen de l'électrocoagulation. [Annexe B : Montage d'un essai batch d'électrocoagulation. Protocole expérimental] Thèse de doctorat, IRME, UQAT, Rouyn-Noranda, Canada, pp. 195-213.
- Foudhaili, T., Jaidi, R., Neculita, C.M., Rosa, E., Triffault-Boucher, G., Veilleux, E., Coudert, L., Lefebvre, O. (2020a). Effect of the electrocoagulation process on the toxicity of gold mine effluents – a comparative assessment of *Daphnia magna* and *Daphnia pulex*. *Science of the Total Environment*, 708, 134709. <https://doi.org/10.1016/j.scitotenv.2019.134739>.
- Foudhaili, T., Lefebvre, O., Coudert, L., Neculita, C.M. (2020b). Sulfate removal from mine drainage by electrocoagulation as a stand-alone treatment or polishing step. *Minerals Engineering*, 152, 106337. <https://doi.org/10.1016/j.mineng.2020.106337>.
- Freitas, R., Perilli, T.A.G., Ladeira, A.C.Q. (2013). Oxidative precipitation of manganese from acid mine drainage by potassium permanganate. *Journal of Chemistry*, 297257, 1-8. <http://dx.doi.org/10.1155/2013/287257>.

- Garcia-Segura, S., Eiband, M.M.S.G., de Melo, J.V., Martínez-Huitle, C.A. (2017). Electrocoagulation and advanced electrocoagulation processes: A general review about the fundamentals, emerging applications and its association with other technologies. *Journal of Electroanalytical Chemistry*, 801, 267-299. <http://dx.doi.org/10.1016/j.jelechem.2017.07.047>.
- Gatsios, E., Hahladakis, J.N., Evangelos Gidarakos, E. (2015). Optimization of electrocoagulation (EC) process for the purification of a real industrial wastewater from toxic metals. *Journal of Environmental Management*, 154, 117-127. <http://dx.doi.org/10.1016/j.jenvman.2015.02.018>.
- Gauthier, C., Couture, P., Pyle, G.G. (2006). Metal effects on fathead minnows (*Pimephales promelas*) under field and laboratory conditions. *Ecotoxicology and Environmental Safety*, 63, 353-364. <https://doi.org/10.1016/j.ecoenv.2005.03.019>.
- Ghosh, A., Mukiibi, M., Ela, W. (2004). TCLP underestimates leaching of arsenic from solid residuals under landfill conditions. *Environmental Science and Technology*, 38, 4677-4682. <https://doi.org/10.1021/es030707w>.
- Ghosh, D., Solanki, H., Purkait, M.K. (2008). Removal of Fe(II) from tap water by electrocoagulation technique. *Journal of Hazardous Materials*, 155, 135-143. <https://doi.org/10.1016/j.jhazmat.2007.11.042>.
- Ghosh, P., Thakur, I.S., Kaushik, A. (2017). Bioassays for toxicological risk assessment of landfill leachate: A review. *Ecotoxicology and Environmental Safety*, 141, 259-270. <http://dx.doi.org/10.1016/j.ecoenv.2017.03.023>.
- Ghosh, S., Debsarkar, A., Dutta, A. (2019). Technology alternatives for decontamination of arsenic-rich groundwater—A critical review. *Environmental Technology and Innovation*, 13, 277-303. <https://doi.org/10.1016/j.eti.2018.12.003>.

- Gilhotra, V., Das, L., Sharma, A., Kang, T.S., Singh, P., Dhuria, R.S., Bhatti, M.S. (2018). Electrocoagulation technology for high strength arsenic wastewater: Process optimization and mechanistic study. *Journal of Cleaner Production*, 198, 693-703. <https://doi.org/10.1016/j.jclepro.2018.07.023>.
- Ginder-Vogel, M., Remucal, C. (2016). Effect of source chemistry on Mn-bearing solid dissolution and reactivity in municipal water systems. University of Wisconsin Water Resources Institute. Madison, Wisconsin, United States. Groundwater Research Report, 16 p.
- Golder, A.K., Samanta, A.N., Ray, S. (2007). Removal of Cr³⁺ by electrocoagulation with multiple electrodes: Bipolar and monopolar configurations. *Journal of Hazardous Materials*, 141, 653-661. <https://doi.org/10.1016/j.jhazmat.2006.07.025>.
- Gomes, J.A.G., Daida. P., Kesmez. M., Weir. M., Moreno. H., Parga. J.R., Irwin. G., McWhinney. H., Grady. T., Peterson. E., Cocke. D.L. (2007). Arsenic removal by electrocoagulation using combined Al-Fe electrode system and characterization of products. *Journal of Hazardous Materials B*, 139, 220-231. <https://doi.org/10.1016/j.jhazmat.2005.11.108>.
- Gonçalves, A.M.M., Castro, B.T., Pardal, M.A., Gonçalves, F. (2007). Salinity effects on survival and life history of two freshwater cladocerans (*Daphnia magna* and *Daphnia longispina*). *International Journal of Limnology*, 43, 13-20. <https://doi.org/10.1051/limn/2007022>.
- Gonzalez-Merchan, C., Genty, T., Bussi ere, B., Potvin, R., Paquin, M., Benhammadi, M., Neculita, C.M. (2016). Ferrates performance in thiocyanates and ammonia degradation in gold mine effluents. *Minerals Engineering*, 95, 124-130. <https://doi.org/10.1016/j.mineng.2016.06.022>.

- Gonzalez-Merchan, C., Genty, T., Paquin, M., Gervais, M., Bussière, B., Potvin, R., Neculita, C.M. (2018). Influence of ferric iron source on ferrate's performance and residual contamination during the treatment of gold mine effluents. *Minerals Engineering*, 127, 61-66. <https://doi.org/10.1016/j.mineng.2018.07.014>.
- Goodwill, J.E., Mai, X., Jiang, J., Reckhow, D.A., Tobiason, J.E. (2016). Oxidation of manganese (II) with ferrate: Stoichiometry, kinetics, products and impact of organic carbon. *Chemosphere*, 159, 457-464. <https://doi.org/10.1016/j.chemosphere.2016.06.014>.
- Gordon, J.A., Fellow, A., Burr, J.L. (1989). Treatment of manganese from mining seep using packed columns. *Journal of Environmental Engineering*, 115. [https://doi.org/10.1061/\(ASCE\)0733-9372\(1989\)115:2\(38\)](https://doi.org/10.1061/(ASCE)0733-9372(1989)115:2(38)).
- Graham, N., Jiang, Ch-ch., Li, X-Z., Jiang, J-Q., Ma, J. (2004). The influence of pH on the degradation of phenol and chlorophenols by potassium ferrate. *Chemosphere*, 56, 949-956. <https://doi.org/10.1016/j.chemosphere.2004.04.060>.
- Habib, M.E., Ali, M.A., Fattah, K.P. (2020). Modified sand for the removal of manganese and arsenic from groundwater. *Journal of Environmental Engineering and Science*, 15, 189-196. <https://doi.org/10.1680/jenes.19.00059>.
- Hageman, P.L. (2007). U.S. Geological Survey field leach test for assessing water reactivity and leaching potential of mine wastes, soils, and other geologic and environmental materials: U.S. Geological Survey Techniques and Methods, Book 5, United States, 14 p.
- Hageman, P.L., Seal, R.R., Diehl, S.F., Piatak, N.M., Lowers, H.A. (2015). Evaluation of selected static methods used to estimate element mobility, acid-generating and acid-neutralizing potentials associated with geologically diverse mining wastes. *Applied Geochemistry*, 57, 125-139. <https://doi.org/10.1016/j.apgeochem.2014.12.007>.

- Hakizimana, J.N., Gourich, B., Chafi, M., Stiriba, Y., Vial, C., Drogui, P., Naja, J. (2017). Electrocoagulation process in water treatment: A review of electrocoagulation modeling approaches. *Desalination*, 404, 1-21. <http://dx.doi.org/10.1016/j.desal.2016.10.011>.
- Hamberg, R., Bark, G., Maurice, G., Alakangas, L. (2016). Release of arsenic from cyanidation tailings. *Minerals Engineering*, 93, 57-64. <http://dx.doi.org/10.1016/j.mineng.2016.04.013>.
- Han, Q., Wang, H., Dong, W., Liu, T., Yin, Y., Fan, H. (2015). Degradation of bisphenol A by ferrate(VI) oxidation: Kinetics, products and toxicity assessment. *Chemical Engineering Journal*, 262, 34-40. <http://dx.doi.org/10.1016/j.cej.2014.09.071>.
- Hanay, Ö., Hasar, H. (2011). Effect of anions on removing Cu^{2+} , Mn^{2+} and Zn^{2+} in electrocoagulation process using aluminum electrodes. *Journal of Hazardous Materials*, 189, 572-576. <https://doi.org/10.1016/j.jhazmat.2011.02.073>.
- Hansen, H.K., Nunez, P., Raboy, D., Schippacasse, I., Grandon, R. (2007). Electrocoagulation in wastewater containing arsenic: Comparing different process designs. *Electrochimica Acta*, 52, 3464-3470. <https://doi.org/10.1016/j.electacta.2006.01.090>.
- Harford, A.J., Mooney, T.J., Trenfield, M.A., van Dam, R.A. (2015). Manganese (Mn) toxicity to tropical freshwater species in low hardness water. *Environmental Toxicology and Chemistry*, 34, 2856-2863. <https://doi.org/10.1002/etc.3135>.
- Harris, G.B. (2000). The removal and stabilization of arsenic from aqueous process solutions: past, present and future. *Minor Elements 2000: Processing & Environmental Aspects of As, Sb, Se, Te, Bi* Courtney Young, Editor, SME-AIME, 3 p.

- Hatar, H., Abd Rahim, S., Razi, W.M., Sahrani, F.K. (2013). Heavy metals content in acid mine drainage at abandoned and active mining area. *AIP Conference Proceedings*, 1571, 641. <https://doi.org/10.1063/1.4858727>.
- Health Canada (2006). Guidelines for Canadian drinking water quality: guideline technical document. Arsenic. <https://healthycanadians.gc.ca/publications/healthy-living-vie-saine/water-arsenic-eau/alt/water-arsenic-eau-eng.pdf>. (Last access: November 11, 2023).
- Health Canada (2016). Manganese in drinking water. <https://www.canada.ca/en/health-canada/programs/consultation-manganese-drinking-water/manganese-drinking-water.html>. (Last access: November 11, 2023).
- Health Canada (2019). Guidelines for drinking water quality: Manganese. Technical report, Health Canada, Ottawa, ON, Canada, 114 p.
- Health Canada (2019). Guidelines for Canadian drinking water quality - Summary Tables. <https://www.canada.ca/en/health-canada/services/environmental-workplace-health/reports-publications/water-quality/guidelines-canadian-drinking-water-quality-summary-table.html>. (Last access: November 11, 2023).
- Heijerick, D.G., De Schampelaere, K.A.C., Janssen, C.R. (2002). Predicting acute zinc toxicity for *Daphnia magna* as a function of key water chemistry characteristics: development and validation of a biotic ligand model. *Environmental Toxicology and Chemistry*, 21, 1309-1315. <https://doi.org/10.1002/etc.5620210628>.
- Hem, J.D. (1963). Chemical equilibria and rates of manganese oxidation: Chemistry of manganese in natural water. *Geological survey water-supply paper* 1667-A.

- Heřmánková, M., Vokáč, R., Slunský, J., Filip, J. (2020). Field study IV: arsenic removal from groundwater by ferrate with the concurrent disinfecting effect: semi-pilot on-site application. *Advanced Nano-Bio Technologies for Water and Soil Treatment, Applied Environmental Science and Engineering for a Sustainable Future, eBook Chapter 13*. https://doi.org/10.1007/978-3-030-29840-1_8.
- Horvat, T., Vidaković-Cifrek, Z., Orescanin, V., Tkalec, M., Pevalek-Kozlina, B. (2007). Toxicity assessment of heavy metal mixtures by *Lemna minor L.* *Science of the Total Environment*, 384, 229-38. <https://doi.org/10.1016/j.scitotenv.2007.06.007>.
- Howe, P., Malcolm, H., Dobson, S. (2004). Manganese and its compounds: environmental aspects. World Health Organization, 70 p.
- Hsueh, Y.M., Wu, W.L., Huang, Y.L., Chiou, H.Y., Tseng, C.H., Chen, C.J. (1998). Low serum carotene level and increased risk of ischemic heart disease related to long-term arsenic exposure. *Atherosclerosis*, 141, 249-257. [https://doi.org/10.1016/S0021-9150\(98\)00178-6](https://doi.org/10.1016/S0021-9150(98)00178-6).
- Hu, G., Mian, H.R., Dyck, R., Mohseni, M., Jasim, S., Hewage, K., Sadiq, R. (2019). Drinking water treatments for arsenic and manganese removal and health risk assessment in White Rock, Canada. *Exposure and Health*, 12, 793-807. <https://doi.org/10.1007/s12403-019-00338-4>.
- Iizuka, A., Shinoda, K., Shibata, E. (2018). Scorodite synthesis in As(V)-containing Fe(II) solution in the presence of hematite as a Fe(III) source. *Materials Transactions*, 59, 843-849. <https://doi.org/10.2320/matertrans.M-M2018809>.

- Inam, M. A., Khan, R., Lee, K-H., Wie, W-M. (2021). Removal of arsenic oxyanions from water by Ferric Chloride—optimization of process conditions and implications for improving coagulation performance. *International Journal of Environmental Research and Public Health*, 18, 9812. <https://doi.org/10.3390/ijerph18189812>.
- INSPQ (2017). Valeur guide sanitaire pour le manganèse dans l'eau potable. Technical report, Institut national de santé public du Québec, Canada, 40 p.
- Jamieson, H.E. (2011). Geochemistry and mineralogy of solid mine waste: Essential knowledge for predicting environmental impact. *Elements*, 7, 381-386. <https://doi.org/10.2113/gselements.7.6.381>.
- Jamieson, H.E., Walker, S.R., Parsons, M.B. (2015). Mineralogical characterization of mine waste: Review. *Applied Geochemistry*, 57, 85-105. <https://doi.org/10.1016/j.apgeochem.2014.12.014>.
- Jain, C.K., Ali, I. (2000). Arsenic: occurrence, toxicity and speciation techniques. *Water Research*, 34, 4304-4312. [https://doi.org/10.1016/S0043-1354\(00\)00182-2](https://doi.org/10.1016/S0043-1354(00)00182-2).
- Jain, A., Sharma, V.K., Mbuya, O.S. (2009). Removal of arsenite by Fe(VI), Fe(VI)/Fe(III), and Fe(VI)/Al(III) salts: Effect of pH and anions. *Journal of Hazardous Materials*, 169, 339-344. <https://doi.org/10.1016/j.jhazmat.2009.03.101>.
- Jia, Y., Demopoulos, G.P. (2005). Adsorption of arsenate onto ferrihydrite from aqueous solution: Influence of media (sulfate vs. nitrate), added gypsum, and pH alteration. *Environmental Science and Technology*, 39, 9523-9527. <https://doi.org/10.1021/es051432i>.

- Jia, Y., Zhang, D., Pan, R., Xu, L., Demopoulos, G.P. (2012). A novel two-step coprecipitation process using Fe(III) and Al(III) for the removal and immobilization of arsenate from acidic aqueous solution. *Water Research*, 46, 500-508. <https://doi.org/10.1016/j.watres.2011.11.045>.
- Jiang, J.Q. (2014). Advances in the development and application of ferrate (VI) for water and wastewater treatment. *Journal of Chemical Technology and Biotechnology*, 89, 165-177. <https://doi.org/10.1002/jctb.4214>.
- Johnson, D.B., Hallberg, K.B. (2005). Acid mine drainage remediation options: a review. *Science of the Total Environment*, 338, 3-14. <https://doi.org/10.1016/j.scitotenv.2004.09.002>.
- Jouini, M., Rakotonimar, T.V., Neculita, C.M., Genty, T., Benzaazoua, M. (2019a). Stability of metal-rich residues from laboratory multi-step treatment system for ferriferous acid mine drainage. *Environmental Science and Pollution Research*, 26, 35588-35601. <https://doi.org/10.1007/s11356-019-04608-1>.
- Jouini, M., Rakotonimar, T.V., Neculita, C.M., Genty, T., Benzaazoua, M. (2019b). Prediction of the environmental behavior of residues from the passive treatment of acid mine drainage. *Applied Geochemistry*, 110, 104421. <https://doi.org/10.1016/j.apgeochem.2019.104421>.
- Jouini, M., Neculita, C.M., Genty, T., Benzaazoua, M. (2020a). Environmental behavior of metal-rich residues from the passive treatment of acid mine drainage. *Science of the Total Environment*, 712, 136541. <https://doi.org/10.1016/j.scitotenv.2020.136541>.
- Jouini, M., Benzaazoua, M., Neculita, C.M., Genty, T. (2020b). Performances of stabilization/solidification process of acid mine drainage passive treatment residues: Assessment of the environmental and mechanical behaviors. *Journal of Environmental Management*, 269, 110764. <https://doi.org/10.1016/j.jenvman.2020.110764>.

- Jouini, M., Neculita, C.M., Genty, T., Benzaazoua, M. (2020c). Freezing/thawing effects on geochemical behavior of residues from acid mine drainage passive treatment systems. *Journal of Water Process Engineering*, 33, 101087. <https://doi.org/10.1016/j.jwpe.2019.101087>.
- Kamachi, T., Kouno, T., Yoshizawa, K. (2005). Participation of multioxidants in the pH dependence of the reactivity of ferrate(VI). *The Journal of Organic Chemistry*, 70, 4380-4388. <https://doi.org/10.1021/jo050091o>.
- Kerr, G., Druzbecka, J., Lilly, K., Craw, D. (2015). Jarosite solid solution associated with arsenic-rich mine waters, Macraes mine, New Zealand. *Mine Water Environment*, 34, 364-374. <https://doi.org/10.1007/s10230-014-0285-5>.
- Khargarot, B.S., Ray, P.K. (1989). Investigation of correlation between physiochemical properties of metals and their toxicity to the water flea *Daphnia magna* Straus. *Ecotoxicology and Environmental Safety*, 18, 109-120. [https://doi.org/10.1016/0147-6513\(89\)90071-7](https://doi.org/10.1016/0147-6513(89)90071-7).
- Kim, J.Y., Kim, K.W., Ahn, J.S., Ko, I., Lee, CH. (2005). Investigation risk assessment modeling of As and other heavy metals contamination around five abandoned metal mines in Korea. *Environmental Geochemistry and Health*, 27, 193-203. <https://doi.org/10.1007/s10653-005-0127-2>.
- Kim, D.M., Kim, D.M., Lee, S.H. (2017). Manganese coprecipitation/adsorption behaviour and sludge volume ratios in chemical treatment systems for mine drainage: a review of the literature and a pilot-scale experiment. *Water and Environment Journal*, 1747-6585. <https://doi.org/10.1111/wej.12312>.
- Koby, M., Bayramoglu, M., Eyvaz, M. (2007). Techno-economical evaluation of electrocoagulation for the textile wastewater using different electrode connections. *Journal of Hazardous Materials*, 148, 311-318. <https://doi.org/10.1016/j.jhazmat.2007.02.036>.

- Kobyas, M., Gebologlu, U., Ulu, F., Oncel, S., Demirbas, E. (2011). Removal of arsenic from drinking water by the electrocoagulation using Fe and Al electrodes. *Electrochimica Acta*, 56, 5060-5070. <https://doi.org/10.1016/j.electacta.2011.03.086>.
- Kobyas, M., Akyol, A., Demirbas, E., Oncel, M.S. (2014). Removal of arsenic from drinking water by batch and continuous electrocoagulation processes using hybrid Al-Fe plate electrodes. *Environmental Progress and Sustainable Energy*, 33, 131-140. <https://doi.org/10.1002/ep.11765>.
- Kobyas, M., Demirbas, E., Ulu, F. (2016). Evaluation of operating parameters with respect to charge loading on the removal efficiency of arsenic from potable water by electrocoagulation. *Journal of Environmental Chemical Engineering*, 4, 1484-1494. <https://doi.org/10.1016/j.jece.2016.02.016>.
- Kobyas, M., Soltani, R.D.C., Omwene, P.I., Khataee, A. (2020). A review on decontamination of arsenic-contained water by electrocoagulation: Reactor configurations and operating cost along with removal mechanisms. *Environmental Technology and Innovation*, 17, 100519. <https://doi.org/10.1016/j.eti.2019.100519>.
- Kobyas, M., Dolaz, M., Ozaydin-Senol, B., Goren, A.Y. (2022). Removal of arsenic in groundwater from western Anatolia, Turkey using an electrocoagulation reactor with different types of iron anodes. *Heliyon*, 8, e10489. <https://doi.org/10.1016/j.heliyon.2022.e10489>.
- Kong, Y., Ma, Y., Guo, M., Huang, Z., Ma, J., Nie, Y., Ding, L., Chen, Z., Shen, J. (2023). Highly efficient removal of arsenate and arsenite with potassium ferrate: role of in situ formed ferric nanoparticle. *Environmental Science and Pollution Research*, 30, 10697-10709. <https://doi.org/10.1007/s11356-022-22858-4>.

- Kong, Y., Ma, Y., Huang, Z., Ma, J., Ding, L., Nie, Y., Chen, Z., Shen, J., Huang, Y. (2023). Characteristics and mechanisms of As(III) removal by potassium ferrate coupled with Al-based coagulants: Analysis of aluminum speciation distribution and transformation. *Chemosphere*, 313, 137251. <https://doi.org/10.1016/j.chemosphere.2023.137251>.
- Kousi, P., Remoundaki, E., Hatzikioseyan, A., Korkovelou, V., Tsezos, M. (2018). Fractionation and leachability of Fe, Zn, Cu and Ni in the sludge from a sulphate-reducing bioreactor treating metal-bearing wastewater. *Environmental Science and Pollution Research*, 25, 35883-35894. <https://doi.org/10.1007/s11356-018-1905-6>.
- Kuyucak, G., Lindvall, M., Sundqvist, T., Sturk, H. (2001). Implementation of a high density sludge (HDS) treatment process at the Kristineberg mine site. In *Proceedings Securing the Future 2001, Mining and the Environment Conference*, Seville, Spain, June.
- Lach, C.E., Pauli, C.S., Coan, A.S., Simionatto, E.L., Koslowski, L.A.D. (2022). Investigating the process of electrocoagulation in the removal of azo dye from synthetic textile effluents and the effects of acute toxicity on *Daphnia magna* test organisms. *Journal of Water Process Engineering*, 45, 102485. <https://doi.org/10.1016/j.jwpe.2021.102485>.
- Lafferty, B.J., Ginder-Vogel, M., Sparks, D.L. (2011). Arsenite oxidation by a poorly crystalline manganese oxide. Arsenic and manganese desorption. *Environmental Science and Technology*, 45, 9218-23. <https://doi.org/10.1021/es201281u>.
- Lagno, F., Rocha, S.D.R., Chryssoulis, S., Demopoulos, G.P. (2010). Scorodite encapsulation by controlled deposition of aluminum phosphate coatings. *Journal of Hazardous materials*, 181, 526-534. <https://doi.org/10.1016/j.jhazmat.2010.05.046>.

- Lakshmanan, D., Clifford, D.A., Samanta, G. (2009). Ferrous and ferric ion generation during iron electrocoagulation. *Environmental Science and Technology*, 43, 3853-3859. <https://doi.org/10.1021/es8036669>.
- Lakshmipathiraj, P., Prabhakar, S., Raju, G.B. (2010). Studies on the electrochemical decontamination of wastewater containing arsenic. *Separation and Purification Technology*, 73, 114-121. <https://doi.org/10.1016/j.seppur.2010.03.009>.
- Lan, B., Wang, Y., Wang, X., Zhou, X., Kang, Y., Li, L. (2016). Aqueous arsenic (As) and antimony (Sb) removal by potassium ferrate. *Chemical Engineering Journal*, 292, 389-397. <https://doi.org/10.1016/j.cej.2016.02.019>.
- Le Bourre, B., Neculita, C.M., Coudert, L., Rosa, E. (2020). Manganese removal processes and geochemical behavior in residues from passive treatment of mine drainage. *Chemosphere*, 259, 127424. <https://doi.org/10.1016/j.chemosphere.2020.127424>.
- Lee, Y., Um, I.K.H., Yoon, J. (2003). Arsenic (III) oxidation by iron (VI) (Ferrate) and subsequent removal of arsenic (V) by iron (III) coagulation. *Environmental Science and Technology*, 37, 5750-5756. <https://doi.org/10.1021/es034203>.
- Lee, S.H., Injeong, K., Kim, K.W., Lee, B.T. (2015). Ecological assessment of coal mine and metal mine drainage in South Korea using *Daphnia magna* bioassay. *SpringerPlus*, 4, 518. <https://doi.org/10.1186/s40064-015-1311-1>.
- Li, C., Li, X. Z., Graham, N. (2005). A study of the preparation and reactivity of potassium ferrate. *Chemosphere*, 61, 537-43. <https://doi.org/10.1016/j.chemosphere.2005.02.027>.
- Li, L., van Genuchten, C.M., Addy, S.E.A., Yao, J., Gao, N., Gadgil, A.J. (2012). Modeling As(III) oxidation and removal with iron electrocoagulation in groundwater. *Environmental Science and Technology*, 46, 12038-12045. <https://doi.org/10.1021/es302456b>.

- Li, S., Yang, X., Zheng, S., Duan, S., Zheng, X., Wang, Z. (2023). Effects of counterion type on standard anion exchange resin-based selective arsenic removal process for polluted groundwater. *Journal of Cleaner Production*, 385, 135762. <https://doi.org/10.1016/j.jclepro.2022.135762>.
- Lim, M., Kim, M.J. (2010). Effectiveness of potassium ferrate (K_2FeO_4) for simultaneous removal of heavy metals and natural organic matters from river water. *Water Air Soil Pollution*, 211, 313-322. <https://doi.org/10.1007/s11270-009-0302-7>.
- Liu, C.W., Lu, K.L., Kao, Y.H., Wang, C.J., Maji, S.K., Lee, J.F. (2014). Identifying sources and controlling factors of arsenic release in saline groundwater aquifers. *Hydrology and Earth System Sciences*, 10, 10565-10603. <https://doi.org/10.5194/hess-18-1089-2014>.
- Luo, C., Routh, J., Dario, M., Sarkar, S., Wei, L., Luo, D., Liu, Y. (2020). Distribution and mobilization of heavy metals at an acid mine drainage affected region in South China, a post-remediation study. *Science of the Total Environment*, 724, 138122. <https://doi.org/10.1016/j.scitotenv.2020.138122>.
- Lytle, D. A., Williams, D., Muhlen, Ch., Riddick, E., Pham, M. (2020). The removal of ammonia, arsenic, iron and manganese by biological treatment from a small Iowa drinking water system. *Environmental Science Water Research and Technology*, 6, 3142-3156. <https://doi.org/10.1039/D0EW00361A>.
- Ma, J., Lei, M., Weng, L., Li, Y., Chen, Y., Islam, M.S., Zhao, J., Chen, T. (2019). Fractions and colloidal distribution of arsenic associated with iron oxide minerals in lead-zinc mine-contaminated soils: comparison of tailings and smelter pollution. *Chemosphere*, 227, 614-623. <https://doi.org/10.1016/j.chemosphere.2019.04.030>.

- Machala, L., Zajíček, P., Kolařík, J., Mackuřák, T., Filip, J. (2020). Ferrates as powerful oxidants in water treatment technologies. *Advanced Nano-Bio Technologies for Water and Soil Treatment, Applied Environmental Science and Engineering for a Sustainable Future, eBook Chapter 8*. https://doi.org/10.1007/978-3-030-29840-1_8.
- Macingova, E., Ubaldini, S., Luptakova, A. (2016). Study of manganese removal in the process of mine water remediation. *Journal of the Polish Mineral Engineering Society*, 1, 121-128. <https://10.29227/IM-2016-01-19>.
- Maitlo, H.A., Kim, J.H., An, B.M., Park, J.Y. (2018). Effects of supporting electrolytes in treatment of arsenate-containing wastewater with power generation by aluminum air fuel cell electrocoagulation. *Journal of Industrial and Engineering Chemistry*, 57, 254-262. <http://dx.doi.org/10.1016/j.jiec.2017.08.031>.
- Majzlan, J., Plášil, J., Škoda, R., Gescher, J., Kögler, F., Rusznyak, A., Küsel, K., Neu, T.R., Mangold, S., Rothe, J. (2014). Arsenic-rich acid mine water with extreme arsenic concentration: Mineralogy, geochemistry, microbiology, and environmental implications. *Environmental Science and Technology*, 48, 13685-13693. <https://doi.org/10.1021/es5024916>.
- Malik, S.N., Ghosh, P.C., Vaidya, A.N., Waindeskar, V., Das, S., Mudliar, S.N. (2017). Comparison of coagulation, ozone and ferrate treatment processes for color, COD and toxicity removal from complex textile wastewater. *Water Science and Technology*, 76, 1001-1010. <https://doi.org/10.2166/wst.2017.062>.
- McBeath, S.T., Hajimalayeri, A., Jasim, S.Y., Mohseni, M. (2021). Coupled electrocoagulation and oxidative media filtration for the removal of manganese and arsenic from a raw ground water supply. *Journal of Water Process Engineering*, 40, 101983. <https://doi.org/10.1016/j.jwpe.2021.101983>.

- McCann, J.I., Nairn, R.W. (2022). Characterization of residual solids from mine water passive treatment oxidation ponds at the tar creek superfund site, Oklahoma, USA: Potential for reuse or disposal. *Cleaner Waste Systems* 3, 100031. <https://doi.org/10.1016/j.clwas.2022.100031>.
- MEND (2014). Study to identify BATEA for the management and control of effluent quality from mines. Mine Environment Neutral Drainage Program Report 3.50.1, Canada. <https://mend-nedem.org/wp-content/uploads/MEND3.50.1BATEAAppAD.pdf>. 614 p.
- Meng, X., Bang, S., Korfiatis, G. (2000). Effects of silicate, sulfate, and carbonate on arsenic removal by ferric chloride. *Water Research*, 34, 1255-1261. [https://doi.org/10.1016/S0043-1354\(99\)00272-9](https://doi.org/10.1016/S0043-1354(99)00272-9).
- Michel, F.M., Ehm, L., Antao, S.M., Lee, P.L., Chupas, J.P., Liu, G., Strongin, D.R., Schoonen, M.A.A., Phillips, B.L., John B. Parise, J.B. (2007). The structure of ferrihydrite, a nanocrystalline material. *Science*, 316, 1726. <http://10.1126/science.1142525>.
- MELCC (2012). Directive 019 sur l'industrie minière. Ministère de l'environnement et de la lutte contre les changements climatiques. Gouvernement du Québec, Québec, QC, Canada, 105 p. http://www.mddefp.gouv.qc.ca/milieu_ind/directive019/directive019.pdf.
- MELCCFP (2023). Ministère de l'Environnement, de la Lutte contre les changements climatiques, de la Faune et des Parc Critères de qualité de l'eau de surface. https://www.environnement.gouv.qc.ca/eau/criteres_eau/index.asp. (Last access 8 December 2023).
- Ministry of Justice (1975). Metal and Diamond Mining Effluent Regulations (SOR/2002-222). Government of Canada. <https://canadagazette.gc.ca/rp-pr/p2/2022/2022-07-06/html/sor-dors159-eng.html> (Last access 27 March 2024).

- Ministry of Justice (2015). Metal and Diamond Mining Effluent Regulations (SOR/2002-222). Government of Canada. <https://laws-lois.justice.gc.ca/eng/regulations/SOR-2002-222/nifnev.html> (Last access 23 December 2019).
- Ministry of Justice (2018). Metal and Diamond Mining Effluent Regulations (SOR/2002-222). Government of Canada. <https://laws-lois.justice.gc.ca/eng/regulations/sor-2002-222/20181217/P1TT3xt3.html> (Lst access 27 March 2024).
- Ministry of Justice (2019). Metal and Diamond Mining Effluent Regulations (SOR/2002-222). Government of Canada. <https://laws-lois.justice.gc.ca/eng/regulations/sor-2002-222/20190625/P1TT3xt3.html> (Lst access 27 March 2024).
- Ministry of Justice (2021). Metal and Diamond Mining Effluent Regulations (SOR/2002-222). Government of Canada. <https://laws-lois.justice.gc.ca/eng/regulations/SOR-2002-222/page-8.html#h-1293293>. (Last access 1 December 2021).
- Ministry of Justice (2022). Metal and Diamond Mining Effluent Regulations (SOR/2002-222). Government of Canada, Ottawa, ON, Canada, 82 p. <https://laws-lois.justice.gc.ca/PDF/SOR-2002-222.pdf>.
- Mohora, E., Roncevic, S., Agbaba, J., Zrnica, K., Tubic, A., Dalmacija, B. (2017). Arsenic removal from groundwater by horizontal-flow continuous electrocoagulation (EC) as a standalone process. *Journal of Environmental Chemical Engineering*, 6, 512-519. <https://doi.org/10.1016/j.jece.2017.12.042>.
- Mollah, M.Y.A., Schennach, R., Parga, J.R., Cocke, D.L. (2001). Electrocoagulation (EC)—science and applications. *Journal of Hazardous Materials*, B84, 29-41. [https://doi.org/10.1016/S0304-3894\(01\)00176-5](https://doi.org/10.1016/S0304-3894(01)00176-5).

- Mondal, P., Balomajumder, C., Mohanty, B. (2007). A laboratory study for the treatment of arsenic, iron, and manganese bearing ground water using Fe(³⁺) impregnated activated carbon: effects of shaking time, pH and temperature. *Journal of Hazardous Materials*. 144, 420-426. <https://doi.org/10.1016/j.jhazmat.2006.10.078>.
- Montefalcon, M.F.V., Chiong, M.R., Resurreccion, A.C., Garcia-Segura, S., Ocon, J.D. (2020). Arsenic removal by advanced electrocoagulation processes: The role of oxidants generated and kinetic modeling. *Catalysts*, 10, 928. <https://doi.org/10.3390/catal10080928>.
- Moussa, D.T., El-Naas, M.H., Nasser, M., Al-Marri, M.J. (2016). A comprehensive review of electrocoagulation for water treatment: Potentials and challenges. *Journal of Environmental Management*, 186, 1-18. <https://dx.doi.org/10.1016/j.jenvman.2016.10.032>.
- Müller, D., Stirn, C.N., Maier, M.V. (2021). Arsenic removal from highly contaminated groundwater by iron electrocoagulation—Investigation of process parameters and iron dosage calculation. *Water*, 13, 687. <https://doi.org/doi:10.3390/w13050687>.
- Munyengabe, A., Zvinowanda, C., Zvimba, J.N., Ramontja, J. (2020). Innovative oxidation and kinetic studies of ferrous ion by sodium ferrate (VI) and simultaneous removal of metals from a synthetic acid mine drainage. *Physics and Chemistry of the Earth*, 124, 1, 102932. <https://doi.org/10.1016/j.pce.2020.102932>.
- Munyengabe, A., Zvinowanda, C., Masindi, V. (2021). Exploring the effectiveness of in-situ sodium ferrate (VI) during the bench-scale of manganese removal from raw water collected from a South African WTP. *Research Square*. <https://doi.org/10.21203/rs.3.rs-789960/v1>.

- Nanoiron Envifer (2023). Dry potassium ferrate. <https://nanoiron.cz/en/products/potassium-ferrate>. (Last access: 04 March 2023).
- Nariyan, E., Sillanpää, M., Wolkersdorfer, C., (2017). Electrocoagulation treatment of mine water from the deepest working European metal mine – Performance, isotherm and kinetic studies. *Separation and Purification Technology*, 177, 363-373. <https://doi.org/10.1016/j.seppur.2016.12.042>.
- Nariyan, E., Wolkersdorfer, C., Sillanpää, M. (2018). Sulfate removal from acid mine water from the deepest active European mine by precipitation and various electrocoagulation configurations. *Journal of Environmental Management*, 227, 162-171. <https://doi.org/10.1016/j.jenvman.2018.08.095>.
- Nazari, A.M., Radzinski, R., Ghahreman, A. (2017). Review of arsenic metallurgy: Treatment of arsenical minerals and the immobilization of arsenic. *Hydrometallurgy*, 174, 258-281. <https://doi.org/10.1016/j.hydromet.2016.10.011>.
- Neculita, C.M., Zagury, G.J., Bussière, B. (2007). Passive treatment of acid mine drainage in bioreactors using sulfate-reducing bacteria: critical review and research needs. *Journal of Environmental Quality*, 36, 1-16. <https://10.2134/jeq2006.0066>.
- Neculita, C.M., Vigneault, B., Zagury, G.J. (2008). Toxicity and metal speciation in acid mine drainage treated by passive bioreactors. *Environmental Toxicology and Chemistry*, 27, 1659-1667. <https://10.1897/07-654>.
- Neculita, C.M., Coudert. L., Genty. T., Drapeau. M., Ryskie. S., Delay-Fortier. S. (2018). Contaminants émergents dans les effluents miniers : défis opérationnels liés à leurs traitements et besoins en recherche. *6th Mines and Environment Symposium*, Rouyn-Noranda, Canada, June 17-20.

- Neculita, C.M., Coudert, L., and Rosa, E. (2019). Challenges and opportunities in mine water treatment in cold climate. *18th Global Joint Seminar on Geo-Environmental Engineering*, Montréal, Canada, May 30- June 3.
- Neculita, C.M., Rosa E. (2019). A review of the implications and challenges of manganese removal from mine drainage. *Chemosphere*, 214, 491-510. <https://doi.org/10.1016/j.chemosphere.2018.09.106>.
- Neculita, C.M., Coudert L., Rosa E., Mulligan C. (2020). Future prospects for treating contaminants of emerging concern in water and soils/sediments – Chapter 29 – *In. Advanced nano-bio technologies for water and soil treatment*. Ed. Filip, J., Cajthaml. T., Najmanová, P., Černík, M., Zbořil, R. Springer. 657 P. DOI: [10.1007/978-3-030-29840-1](https://doi.org/10.1007/978-3-030-29840-1).
- Neil, C.W., Yang, Y.J., Schupp, D., Jun, Y.S. (2014). Water chemistry impacts on arsenic mobilization from arsenopyrite dissolution and secondary mineral precipitation: implications for managed aquifer recharge. *Environmental Science and Technology*, 48, 4395-405. <https://doi.org/10.1021/es405119q>.
- Nigri, E.M., Santos, A.L.A., Rocha, S.D.F. (2020). Removal of organic compounds, calcium and strontium from petroleum industry effluent by simultaneous electrocoagulation and adsorption. *Journal of Water Process Engineering*, 37, 101442. <https://doi.org/10.1016/j.jwpe.2020.101442>.
- Nkele, K., Mpenyana-Monyatsi, L., Masindi, V. (2022). Challenges, advances and sustainabilities on the removal and recovery of manganese from wastewater: A review. *Journal of Cleaner Production*, 377, 134152. <https://doi.org/10.1016/j.jclepro.2022.134152>.
- Nordstrom, D.K., Alpers, C.N. (1999). Negative pH, efflorescent mineralogy, and consequences for environmental restoration at the Iron Mountain Superfund Site, California. *Proceedings of the National Academy of Sciences, USA* 96, 3455–3462. <https://doi.org/10.1073/pnas.96.7.3455>.

- Nordstrom, D.K., Blowes, D.W., Ptacek, C.J. (2015). Hydrogeochemistry and microbiology of mine drainage: An update. *Applied Geochemistry*, 57, 3-16. <https://doi.org/10.1016/j.apgeochem.2015.02.008>.
- Northrup, K., Capooici, M., Seyfferth, A.L. (2018). Effects of extreme events on arsenic cycling in salt marshes. *Journal of Geophysical Research: Biogeosciences*, 123, 1086-1100. <https://DOI.org/10.1002/2017JG004259>.
- Okamoto, A., Yamamuro, M., Tatarazako, N. (2014). Acute toxicity of 50 metals to *Daphnia magna*. *Journal of Applied Toxicology*, 35, 824-30. <https://10.1002/jat.3078>.
- Olmez-Hanci, T., Arslan-Alaton, I., Dursun, D. (2014). Investigation of the toxicity of common oxidants used in advanced oxidation processes and their quenching agents. *Journal of Hazardous Material*, 278, 330-335. <http://dx.doi.org/10.1016/j.jhazmat.2014.06.021>.
- Oncel, M.S., Muhcu. A., Kobya. M. (2013). A comparative study of chemical precipitation and electrocoagulation for treatment of coal acid drainage wastewater. *Journal of Environmental Chemical Engineering*, 1, 989-995. <https://doi.org/10.1016/j.jece.2013.08.008>.
- Orescanin, V., Kollar, R., Nad, K., Halkijevic, I., Kuspilic, M., Gustek, S.F. (2014). Removal of arsenic, phosphates and ammonia from well water using electrochemical/chemical methods and advanced oxidation: A pilot plant approach. *Journal of Environmental Science and Health, Part A: Toxic/Hazardous Substances and Environmental Engineering*, 49, 1007-1014. <https://10.1080/10934529.2014.894843>.
- Oruê, B.P., Junior, A.B.B., Tenório, J.A.S.S., Espinosa, D.C.R., Baltazar, M.P.G. (2020). Kinetic study of manganese precipitation of nickel laterite leach based-solution by ozone oxidation. *Ozone: Science and Engineering*, 43, 1-15. <https://doi.org/10.1080/01919512.2020.1796580>.

- Oza, H., Anantha Singh, T.S., Jampa, S.S. (2021). Removal of arsenic from aqueous solution using combined ultrasonic and electrocoagulation process. *Materials Today Proceedings*, 47, 728-732. <https://doi.org/10.1016/j.matpr.2021.01.569>.
- Pantuzzo, F.L., Ciminelli, V.S.T. (2010). Arsenic association and stability in long-term disposed arsenic residues. *Water Research*, 44, 5631-5640. <https://doi.org/10.1016/j.watres.2010.07.011>.
- Parga, J.R., Cocke, D.L., Valenzuela, J.L., Gomes, J.A., Kesmez, M., Irwin, G., Moreno, H., Weir, M. (2005). Arsenic removal via electrocoagulation from heavy metal contaminated groundwater in La Comarca Lagunera, Mexico. *Journal of Hazardous Materials*, 124, 247-254. <https://doi.org/10.1016/j.jhazmat.2005.05.017>.
- Parkhurst, D.L., Appelo, C.A.J. (2013). Description of input and examples for PHREEQC version 3—A computer program for speciation, batch-reaction, one-dimensional transport, and inverse geochemical calculations: U.S. Geological Survey Techniques and Methods, book 6, chapter A43, 497 p. Available at <https://pubs.usgs.gov/tm/06/a43/>.
- Paulauskis, J.D., Winner, R.W. (1988). Effects of water hardness and humic acid on zinc toxicity to *Daphnia Magna* straus. *Aquatic Toxicology*, 12, 273-290. [https://doi.org/10.1016/0166-445X\(88\)90027-6](https://doi.org/10.1016/0166-445X(88)90027-6).
- Pereira, L.B., Vicentini, R., Ottoboni, L.M. (2014). Changes in the bacterial community of soil from a neutral mine drainage channel. *PLoS One*. 9, 96605. <https://doi.org/10.1371/journal.pone.0096605>.
- Pietrelli, L., Ippolito, N.M., Ferro, S., Dovì, V.G., Vocciante, M. (2019). Removal of Mn and As from drinking water by red mud and pyrolusite. *Journal of Environmental Management*, 237, 526-533. <https://doi.org/10.1016/j.jenvman.2019.02.093>.

- Pinto, P.X., Al-Abed, S.R., Holder, C., Reisman, D.J. (2014). Evaluation of metal partitioning and mobility in a sulfidic mine tailing pile under oxic and anoxic conditions. *Journal of Environmental Management*, 140, 135-144. <https://doi.org/10.1016/j.jenvman.2014.03.004>.
- Pinsino, A., Matranga, V., Carmela, M. (2012). Manganese: A new emerging contaminant in the environment. InTech. In book: Environmental Contamination. <https://10.5772/31438>.
- Pires, V.G.R., Lima, D.R.S., Aquino, S.F., Libânio, M. (2015). Evaluating arsenic and manganese removal from water by chlorine oxidation followed by clarification. *Brazilian Journal of Chemical Engineering*, 32, 409-419. <https://doi.org/10.1590/0104-6632.20150322s00003564>.
- Post, J.E. (1999). Manganese oxide minerals: Crystal structures and economic and environmental significance. Proceedings of the National Academy of Sciences, *National Acad Sciences*, 96, 3447-3454. <https://doi.org/10.1073/pnas.96.7.3447>.
- Prucek, R., Tuček, J., Kolařík, J., Filip, J., Marušák, Z., Sharma, V.K. and Zbořil, R. (2013). Ferrate(VI)-Induced Arsenite and arsenate removal by in situ structural incorporation into magnetic Iron(III) Oxide nanoparticles. *Environmental Science and Technology*, 47, 3283-3292. <https://10.1021/es3042719>.
- QMA, (2019). The mining industry, the inner strength of Quebec. <https://www.amq-inc.com/en/actualites/posts/study-of-the-economic-benefits-generated-by-quebec-s-mining-industry-who-says-that-mining-only-benefits-the-resource-regions> (Last access: 4 November 2019).
- Quino-Favero, J., Eyzaguirre, R., Mogrovejo, P., Prieto, P., Flores del Pino, L.F. (2018). Electrochemical synthesis of ferrate(VI): optimization of parameters and evaluation of their impact in production cost. *Desalination and Water Treatment*, 113, 179-186. <https://10.5004/dwt.2018.22262>.

- Quino-Favero, J., Perez, R.E., Veramendi, P.P., García, P.M., del Pino, L.F. (2021). Assessing the removal of arsenite and arsenate mixtures from the synthetic Bangladesh groundwater (SBGW) using combined Fe(VI)/Fe(III) treatments and local regression analysis. *Water*, 13, 1134. <https://doi.org/10.3390/w13091134>.
- Radić, S., Vujčić, V., Cvetković, Ž., Cvjetko, P., Oresčanin, V. (2014). The efficiency of combined CaO/electrochemical treatment in removal of acid mine drainage induced toxicity and genotoxicity. *Science of the Total Environment*, 466, 84-89. <https://doi.org/10.1016/j.scitotenv.2013.07.011>.
- Raghav, M., Shan, J., Sáez, A.E., Ela, W.P. (2013). Scoping candidate minerals for stabilization of arsenic-bearing solid residuals. *Journal of Hazardous Materials*, 263, 525-532. <https://doi.org/10.1016/j.jhazmat.2013.10.009>.
- Rai, P.K., Lee, J., Kailasa, S.K., Kwon, E.E., Tsang, Y.F., Ok, Y.S., Kim, K-H. (2018). A critical review of ferrate (VI)-based remediation of soil and groundwater. *Environmental Research*, 160, 420-448. <https://doi.org/10.1016/j.envres.2017.10.016>.
- Rait, R., Trumm, D., Pope, J., Craw, D., Newman, N., MacKenzie, H. (2010). Adsorption of arsenic by iron rich precipitate from two coal mine drainage sites on the West Coast of New Zealand. *New Zealand Journal of Geology and Geophysics*, 53, 177-193. <https://doi.org/10.1080/00288306.2010.500320>.
- Rakotonimaro, T.V., Guittony, M., Neculita, C.M. (2021). Compaction of peat cover over desulfurized gold mine tailings changes: Arsenic speciation and mobility. *Applied Geochemistry*, 128, 104923. <https://doi.org/10.1016/j.apgeochem.2021.104923>.
- Ratnaïke, R.N. (2003). Acute and chronic arsenic toxicity. *Postgrad Medical Journal*, 79, 391-396. <https://doi.org/10.1136/pmj.79.933.391>.

- Raven, K.P., Jain, A., Loeppert, R.H. (1988). Arsenite and arsenate adsorption on ferrihydrite: kinetics, equilibrium, and adsorption envelopes. *Environmental Science and Technology*, 32, 344-349. <https://doi.org/10.1021/es970421p>.
- Reátegui-Romero, W., Flores-Del Pino, L.V., Guerrero-Guevara, J.L., Castro-Torres, J., Rea-Marcos, L.M., King –Santos, M.E., Yuli-Posadas, R. (2018). Benefits of electrocoagulation in treatment of wastewater: removal of Fe and Mn metals, oil and grease and COD: three case studies. *International Journal of Applied Engineering Research*, 13, 6450-6462.
- Reimer, P.S. (1999). Environmental effects of manganese and proposed freshwater guidelines to protect aquatic life in British Columbia. Ministry of Environment, Water Protection and Sustainability Branch, Environmental Sustainability and Strategic Policy Division. British Columbia, Canada, 56 p.
- Revesz, E., Fortin, D., Paktunc, D. (2015). Reductive dissolution of scorodite in the presence of *Shewanella* sp. CN32 and *Shewanella* sp. ANA-3. *Applied Geochemistry*, 63, 347-356. <https://doi.org/10.1016/j.apgeochem.2015.09.022>.
- Rueda-Márquez, J.J., Levchuk, I., Manzano, M., Sillanpää, M. (2020). Toxicity reduction of industrial and municipal wastewater by advanced oxidation processes (photo-Fenton, UV/H₂O₂, electro-Fenton and galvanic Fenton): a review. *Catalysts*, 10, 612. <https://doi:10.3390/catal10060612>.
- Ruiping, L., Xing, L., Shengji, X., Yanling, Y., Rongcheng, W., Guibai, L. (2007). Calcium-enhanced ferric hydroxide co-precipitation of arsenic in the presence of silicate. *Water Environment Research*, 79, 2260-2264. <https://doi.org/10.2175/106143007x199324>.
- Rush, J.D., Bielski, B.H.J. (1989). Kinetics of ferrate (V) decay in aqueous solution. A pulse-radiolysis study. *Inorganic Chemistry*, 28, 3947-3951. <https://doi.org/10.1021/ic00320a004>.

- Ryskie, S., Neculita, C.M., Rosa, E., Coudert, L., Couture, P. (2021). Active treatment of contaminants of emerging concern in cold mine water using advanced oxidation and membrane-related processes: A review. *Minerals*, 11, 259. <https://doi.org/10.3390/min11030259>.
- Safi, S.R., Gotoh, T. (2021). Simultaneous removal of arsenic and manganese from synthetic aqueous solutions using polymer gel composites. *Nanomaterials*, 11, 1032. <https://doi.org/10.3390/nano11041032>.
- Safira, R., Coudert, L., Neculita, C.M., Bélanger, E., Rosa, E. (2023). Performance of ferrates for simultaneous removal of As and Mn from circumneutral contaminated mine water. *Journal of Environmental Chemical Engineering*, 11, 110421. <https://doi.org/10.1016/j.jece.2023.110421>.
- Safira, R., Coudert, L., Neculita, C.M., Rosa, E. (2024). Efficiency of electrocoagulation for simultaneous treatment of As and Mn in neutral mine effluents. *Minerals Engineering*, 207, 108546. <https://doi.org/10.1016/j.mineng.2023.108546>.
- Safwat, S.M., Mohamed, N.Y., El-Seddik, M.M. (2023). Performance evaluation and life cycle assessment of electrocoagulation process for manganese removal from wastewater using titanium electrodes. *Journal of Environmental Management*, 328, 116967. <https://doi.org/10.1016/j.jenvman.2022.116967>.
- Sahu, O., Mazumdar, B., Chaudhari, P.K. (2014). Treatment of wastewater by electrocoagulation: a review. *Environmental Science and Pollution Research*, 21, 2397-2413. <https://10.1007/s11356-013-2208-6>.
- Scheinost, A.C., Schwertmann, U. (1999). Color identification of iron oxides and hydroxysulfates: use and limitations. *Soil Science Society of America Journal*, 63, 1463-1471. <https://10.2136/sssaj1999.6351463x>.

- Schreyer, J. M., Ockerman, L. T. (1951). Stability of ferrate(VI) ion in aqueous solution. *Analytical Chemistry*, 23, 1312-1314. <https://doi.org/10.1021/ac60057a028>.
- Schuytema, G.S., Nebeker, A.V., Stutzman, T.W. (1997). Salinity tolerance of *Daphnia magna* and potential use for estuarine sediment toxicity tests. *Archives of Environmental Contamination and Toxicology*, 33, 194-198. <https://doi.org/10.1007/s002449900242>.
- Semsari, S., Megateli, S. (2007). Effect of cadmium toxicity on survival and phototactic behaviour of *Daphnia magna*. *Environmental Technology*, 28, 799-806. <https://doi.org/10.1080/09593332808618841>.
- Shafaei, A., Rezayee, M., Arami, M., Nikazar, M. (2010). Removal of Mn²⁺ ions from synthetic wastewater by electrocoagulation process. *Desalination*, 260, 23-28. <https://doi.org/10.1016/j.desal.2010.05.006>.
- Shahedi, A., Darban, A.K., Jamshidi-Zanjani, A., Homae, M. (2023). An overview of the application of electrocoagulation for mine wastewater treatment. *Environmental Monitoring and Assessment*, 195, 522. <https://doi.org/10.1007/s10661-023-11044-9>.
- Shahreza, S.O., Mokhtarian, N., Behnam, S. (2018). Optimization of Mn removal from aqueous solutions through electrocoagulation. *Environmental Technology*, 41, 890-900. <https://doi.org/10.1080/09593330.2018.1514071>.
- Sharma, V.K. (2002). Potassium ferrate (VI): an environmentally friendly oxidant. *Advances in Environmental Research*, 6, 143-156. [https://doi.org/10.1016/S1093-0191\(01\)00119-8](https://doi.org/10.1016/S1093-0191(01)00119-8).
- Sharma, V.K., Kazama, F., Jiangyong, Hu., and Ray, A.K. (2005). Ferrates (iron (VI) and iron (V)): Environmentally friendly oxidants and disinfectants. *Journal of Water and Health*, 3, 45-58. <https://10.2166/wh.2005.0005>.

- Sharma, V.K., Dutta, P.K., Ray, A.K. (2007). Review of kinetics of chemical and photocatalytic oxidation of Arsenic(III) as influenced by pH. *Journal of Environmental Science and Health, Part A: Toxic/ Hazardous Substances and Environmental Engineering*, 42, 997-1004. <http://dx.doi.org/10.1080/10934520701373034>.
- Sharma, V.K., Yngard, R.A., Cabelli, D.I., Baum, J.C. (2008). Ferrate(VI) and ferrate (V) oxidation of cyanide, thiocyanate, and copper (I) cyanide. *Radiation Physics and Chemistry*, 77, 761-767. <https://10.1016/j.radphyschem.2007.11.004>.
- Sharma, V.K. (2010). Oxidation of inorganic compounds by Ferrate (VI) and Ferrate (V): One-Electron and Two-Electron transfer steps. *Environmental Science and Technology*, 44, 5148-5152. <https://doi.org/10.1021/es1005187>.
- Sharma, V.K. (2011). Oxidation of inorganic contaminants by ferrates (VI, V, and IV)-kinetics and mechanisms: A review. *Journal of Environmental Management*, 92, 1051-1073. <https://10.1016/j.jenvman.2010.11.026>.
- Sharma, V.K., Chen, L., Zboril, R. (2016). A Review on high valent FeVI (Ferrate): A sustainable green oxidant in organic chemistry and transformation of pharmaceuticals. *Sustainable Chemistry and Engineering*, 4, 18-34. <https://10.1021/acssuschemeng.5b01202>.
- Smedley, P.L., Kinniburgh, D.G. (2002). A review of the source, behaviour and distribution of arsenic in natural waters. *Applied Geochemistry*, 17, 517-568. [https://doi.org/10.1016/S0883-2927\(02\)00018-5](https://doi.org/10.1016/S0883-2927(02)00018-5).
- Soucek, D.J., Cherry, D.S., Trent, G.C. (2000). Relative acute toxicity of acid mine drainage water column and sediments to *Daphnia magna* in the Puckett's Creek- Watershed, Virginia, USA. *Archives of Environmental Contamination and Toxicology*, 38, 305-310. <https://10.1007/s002449910040>.

- Stuetz, R. M., and Stephenson, T. (Eds.). (2009). Principles of water and wastewater treatment processes. 3rd edition, Iwa Publishing, pp. 82-84.
- Suhendrayatna, Ohki, A., Maeda, S. (1999). Arsenic accumulation, transformation and tolerance on freshwater *Daphnia magna*. *Toxicological and Environmental Chemistry*, 72, 1-11. <https://doi.org/10.1080/02772249909358820>.
- Teodorovic, I., Planojevic, I., Knezevic, P., Radak, S., Nemet, I. (2009). Sensitivity of bacterial vs. acute *Daphnia magna* toxicity tests to metals. *Central European Journal of Biology*, 4, 482-492. <https://doi.org/10.2478/s11535-009-0048-7>.
- Thakur, L.S., Mondal, P. (2016). Techno-economic evaluation of simultaneous arsenic and fluoride removal from synthetic groundwater by electrocoagulation process: optimization through response surface methodology. *Desalination Water Treatment*, 57, 1-17. <http://dx.doi.org/10.1080/19443994.2016.1186564>.
- Thakur, L.S., Varma, A.K., Goyal, H., Sircar, D., Mondal, P. (2021). Simultaneous removal of arsenic, fluoride, and manganese from synthetic wastewater by *Vetiveria zizanioides*. *Environmental Science and Pollution Research*, 28, 44216-44225. <https://doi.org/10.1007/s11356-021-13898-3>.
- Thella, K., Verma, B., Srivastava, V.C., Srivastava, K. K. (2008). Electrocoagulation study for the removal of arsenic and chromium from aqueous solution. *Journal of Environmental Science and Health*, 43, 554-562. <https://doi.org/10.1080/10934520701796630>.
- Theng, B.K.G., Yuan, G.D. (2008). Nanoparticles in the soil environment. *Elements*, 4, 395-399. <https://doi.org/10.2113/gselements.4.6.395>.
- Thimons, S., Saxena, Sh., Walter Den, W. (2022). Ferrate-pretreated directional solvent extraction for hydraulic fracturing produced water: Technical and economic feasibility studies. *Journal of Water Process Engineering*, 49, 103053. <https://doi.org/10.1016/j.jwpe.2022.103053>.

- Thompson, G.W., Ockerman, L.T., Schreyer, J.M. (1951). Preparation and purification of potassium ferrate (VI). *American Chemical Society*, 73, 1379-1381. <https://doi.org/10.1021/ja01147a536>.
- Tisler, T., Zagorc-Koncan, J. (2002). Acute and chronic toxicity of arsenic to some aquatic organisms. *Environmental Contamination and Toxicology* 69, 421–429. <https://doi.org/10.1007/s00128-002-0079-5>.
- Tiwari, D., Kim, H.Uk., Choi, B.J., Lee, S.M., Kwon, Oh.H., Choi, K.M., Yang, J.K. (2007). Ferrate(VI): A green chemical for the oxidation of cyanide in aqueous/waste solutions. *Journal of Environmental Science and Health, Part A: Toxic/Hazardous Substances and Environmental Engineering*, 42, 803-810. <https://10.1080/10934520701304674>.
- Tiwari, A.K., Singh, P.K., Mahato, M.K. (2017). Assessment of metal contamination in the mine water of the West Bokaro Coalfield, India. *Mine Water Environ*, 36, 532-541. <https://10.1007/s10230-017-0440-x>.
- Tobiason, J.E., Bazilio, A., Goodwill, J., Mai, X., Nguyen, Ch. (2016). Manganese removal from drinking water sources. *Current Pollution Reports*, 2, 168-177. <https://doi.org/10.1007/s40726-016-0036-2>.
- Torres-Sánchez, A.L., López-Cervera, S.J., de la Rosa, C., Maldonado-Vega, M., Maldonado-Santoyo, M., Peralta-Hernández, J.M. (2014). Electrocoagulation process coupled with advance oxidation techniques to treatment of dairy industry wastewater. *International Journal of Electrochemical Sciences*, 9, 6103-6112. [https://doi.org/10.1016/S1452-3981\(23\)10873-X](https://doi.org/10.1016/S1452-3981(23)10873-X).
- Touahria, S., Hazourli, S., Touahria, K., Eulmi, A., Aitbara, A. (2016). Clarification of industrial mining wastewater using electrocoagulation. *International Journal of Electrochemical Science*, 11, 5710-5723. <https://doi.org/10.20964/2016.07.51>.

- Tseng, C.H., Chong, C.K., Chen, C.J., Tai, T.Y. (1996). Dose-response relationship between peripheral vascular disease and ingested inorganic arsenic among residents in blackfoot disease endemic villages in Taiwan. *Atherosclerosis*, 120, 125-133. [https://doi.org/10.1016/0021-9150\(95\)05693-9](https://doi.org/10.1016/0021-9150(95)05693-9).
- Turan, A., Kobyas, M., Iskurt, C., Gengec, E., Alireza Khataee, A. (2023). A techno-economical assessment of treatment by coagulation-flocculation with aluminum and iron-bases coagulants of landfill leachate membrane concentrates. *Chemosphere*, 314, 137750. <https://doi.org/10.1016/j.chemosphere.2023.137750>.
- Turunen, K., Backnas, S., Neitola, R., Pasanen, A. (2016). Factors controlling the migration of tailings-derived arsenic: a case study at the Yara Siilinjärvi Site. *Mine Water and the Environment*, 35, 407-420. <https://doi.org/10.1007/s10230-016-0393-5>.
- Ucar, C., Baskan, M.B., Pala, A. (2013). Arsenic removal from drinking water by electrocoagulation using iron electrodes. *Journal of Environmental Chemical Engineering*, 30, 1889-1895. <https://doi.org/10.1007/s11814-013-0128-2>.
- US CFR (1985). Mineral resources; Chapter VII- Office of surface mining reclamation and enforcement, Department of the interior; subchapter B-initial program regulations; Part 715- General performance standards. United States Code of Federal Regulations, pp. 700-999. <https://www.ecfr.gov/current/title-30/chapter-VII>.
- US CFR (1996). Protection of the Environment. Chapter 1-EPA, Part 434-Coal Mining Point Source Categories, Subpart C-acid or Ferruginous Mine Drainage. United States Code of Federal Regulations. Washington, DC, USA, pp. 222-223.

- USEPA (1992). Method 1311: toxicity characteristic leaching procedure, SW-846: Test methods for evaluating solid waste - Physical/Chemical Methods. United States Environmental Protection Agency. Washington, USA. 35 p. <https://www.epa.gov/sites/production/files/2015-12/documents/1311.pdf>.
- USEPA (1996). Acid digestion of sediments, sludges, and soils. Method 3050B. United States Environmental Protection Agency. Washington, USA. 12 p. <https://www.epa.gov/sites/default/files/2015-12/documents/3050b.pdf>.
- USEPA (2002). Arsenic treatment technologies for soil, waste and water. EPA-542-R-02-004. United States Environmental Protection Agency. Washington, USA. 132 p. www.epa.gov/tioclui-in.org/arsenic.
- USEPA (2003). Arsenic treatment technology evaluation handbook for small systems. Office of Water (4606M). United States Environmental Protection Agency. Washington, USA. 151 p. EPA 816-R-03-014. www.epa.gov/safewater.
- USEPA (2004). Drinking Water Health Advisory for Manganese. Document was prepared under U.S. Environmental Protection Agency, lead by Health and Ecological Criteria Division, Office of Science and Technology, Office of Water, U.S. Environmental Protection Agency Health and Ecological Criteria Division. United States Environmental Protection Agency. Washington, DC, USA. 55 p.
- USEPA (2006). Drinking water requirements for states and public water systems. Chemical contaminant rules. United States Environmental Protection Agency. <https://www.epa.gov/dwreginfo/chemical-contaminant-rules>. Washington, DC, USA
- USEPA (2018). Secondary drinking water standards: guidance for nuisance chemicals. United States Environmental Protection Agency. <https://www.epa.gov/sdwa/secondary-drinking-water-standards-guidance- nuisance-chemicals-> Last updated on February 2022. (Last access on October 10, 2022).

- Valentin-Reyers, J., Coreño, O., Nava, J.L. (2022). Concurrent elimination of arsenic and hydrated silica from natural groundwater by electrocoagulation using iron electrodes. *Chemical Engineering Research and Design*, 184, 103-112. <https://doi.org/10.1016/j.cherd.2022.05.025>.
- Valenzuela, A. (2000). Arsenic management in the metallurgical industry. M.Sc. report, Université Laval, Québec, Canada. 209 p. https://www.nlc-bnc.ca/obj/s4/f2/dsk1/tape4/PQDD_0019/MQ55887.pdf?oclc_number=1006987939.
- Van Dam, R.A., Harford, A.J., Lunn, S.A., Gagnon, M.M. (2014). Identifying the cause of toxicity of a saline mine water. *PLOS One* 9, 13. <https://10.1371/journal.pone.0106857>.
- Van den Brand, T.P., Roest, K., Chen, G.H., Brdjanovic, D., van Loosdrecht, M.C. (2015). Effects of chemical oxygen demand, nutrients and salinity on sulfate-reducing bacteria. *Environmental Engineering Science*, 32, 858-864. <https://doi.org/10.1089/ees.2014.0307>.
- Van Herreweghe, S., Swennen, R., Cappuyns, V., Vandecasteele, C. (2002). Chemical associations of heavy metals and metalloids in contaminated soils near former ore treatment plants: a differentiated approach with emphasis on pHstat-leaching. *Journal of Geochemical Exploration*, 76, 113-138. [https://doi.org/10.1016/S0375-6742\(02\)00232-7](https://doi.org/10.1016/S0375-6742(02)00232-7).
- Vepsäläinen, M., Sillanpää, M. (2012). Electrocoagulation in the treatment of industrial waters and wastewaters. In Sillanpää, *Advanced Water Treatment*. Netherlands, Elsevier, 1-78. <https://doi.org/10.1016/b978-0-12-819227-6.00001-2>.
- Verep, B., Terzi, E., Besli, E.S. (2016). A research on the sensitivity of trouts (*Oncorhynchus mykiss*) to some metals (HgCl₂, ZnSO₄, PbCl₂). *Feb-Fresenius Environmental Bulletin*, 25, 4141-4147.

- Wagner, W.F., Gump, J.R., Hart, E.N. (1952). Factors affecting the stability of aqueous potassium ferrate(VI) solutions. *Analytical Chemistry*, 24, 1497-1498. <https://10.1021/ac60069a037>.
- Wang, S., Mulligan, C.N. (2006). Occurrence of arsenic contamination in Canada: Sources, behavior and distribution. *Science of the Total Environment*, 366, 701-721. <https://doi.org/10.1016/j.scitotenv.2005.09.005>.
- Wang, C.H., Hsiao, C.K., Chen, C.L., Hsu, L.I., Chiou, H.Y., Chen, S.Y., Hsueh, Y.M., Wu, M.M., Chen, C.J. (2007). A review of the epidemiologic literature on the role of environmental arsenic exposure and cardiovascular diseases. *Toxicology and Applied Pharmacology*, 222, 315-326. <https://10.1016/j.taap.2006.12.022>.
- Wang, L., Giammar, D.E. (2015). Effects of pH, dissolved oxygen, and aqueous ferrous iron on the adsorption of arsenic to lepidocrocite. *Journal of Colloid and Interface Science*, 448, 331-338. <https://doi.org/10.1016/j.jcis.2015.02.047>.
- Wang, X., Qu, R., Allam, A., A., Ajarem, J., Wei, Z., Wang, Z. (2016). Impact of carbon nanotubes on the toxicity of inorganic arsenic [As(III) and As(V)] to *Daphnia magna*: The role of certain arsenic species. *Environmental Toxicology and Chemistry*, 35, 1852-1859. <https://10.1002/etc.3340>.
- Wang, N., Wang, N., Tan, L., Zhang, R., Zhao, Q., Wang, H. (2020a). Removal of aqueous As(III) and Sb(III) by potassium ferrate (K₂FeO₄): The function of oxidation and flocculation. *Science of the Total Environment*, 726, 138541. <https://doi.org/10.1016/j.scitotenv.2020.138541>.
- Wang, X., Ding, J., Wang, L., Zhang, S., Hou, H., Zhang, J., Chen, J., Ma, M., Tsang, D., Wu, X. (2020b). Stabilization treatment of arsenic-alkali residue (AAR): Effect of the coexisting soluble carbonate on arsenic stabilization. *Environment International*, 135, 105406. <https://doi.org/10.1016/j.envint.2019.105406>.

- Wang, S., Shao, B., Qiao, B., Guan, X. (2021). Application of Fe(VI) in abating contaminants in water: State of art and knowledge gaps. *Frontiers of Environmental Science & Engineering*, 15, 80. <https://doi.org/10.1007/s11783-020-1373-3>.
- Watzlaf, G.R. (1987). Chemical stability of manganese and other metals in acid mine drainage sludge. Proceedings of American Society of Mining and Reclamation (ASMR), Pittsburgh, Pennsylvania. 83-90 p. <https://10.21000/JASMR88010083>.
- Watzlaf, G.R., Casson, L.W. (1990). Chemical stability of manganese and iron in mine drainage treatment sludge: effects of neutralization chemical, iron concentration and sludge age. Mining and Reclamation Conference and Exhibition, Charleston, West Virginia, USA. April 23-26.
- Welham, N.J., Malatt, K.A., Vukcevic, S. (2000). The stability of iron phases presently used for disposal from metallurgical systems – a review. *Minerals Engineering*, 13, 911-931. [https://doi.org/10.1016/S0892-6875\(00\)00078-9](https://doi.org/10.1016/S0892-6875(00)00078-9).
- Wenzel, W.W., Kirchbaumer, N., Prohaska, T., Stingeder, G., Lombi, E., Adriano, D.C. (2001). Arsenic fractionation in soils using an improved sequential extraction procedure. *Analytica Chimica Acta*, 436, 309-323. [https://doi.org/10.1016/S0003-2670\(01\)00924-2](https://doi.org/10.1016/S0003-2670(01)00924-2).
- White, D.A., Franklin, G.S. (1998). A Preliminary investigation into the use of sodium ferrate in water treatment. *Environmental Technology* 19, 1157-1161. <https://10.1080/09593331908616776>.
- WHO, (1993, 2011). Arsenic. World Health Organization. <https://www.who.int/news-room/fact-sheets/detail/arsenic>. (Last accessed March 28, 2024).

- Williamson, J., Pastorinho, M.R., Ranville, J.F., Meyer, J.S., Santore, R.C., Ryan, A.C., Dwyer, R.L. (2013). Toxicity of metal mixtures to *Daphnia magna*—comparison of laboratory and field data. *Reliable Mine Water Technology*, IMWA. Golden Co; USA. 6 p.
https://www.imwa.info/docs/imwa_2013/IMWA2013_Williamson_538.pdf.
- Xie, X., Zhao, W., Hu, Y., Xu, X., Cheng, H. (2018). Permanganate oxidation and ferric ion precipitation (KMnO₄-Fe(III)): process for treating Phenylarsenic compounds. *Chemical Engineering Journal*, 357, 600-610.
<https://doi.org/10.1016/j.cej.2018.09.194>.
- Xu, L., Huang, Q., Xu, X., Cao, G., He, Ch., Wang, Y., Yang, M. (2017). Simultaneous removal of Zn²⁺ and Mn²⁺ ions from synthetic and real smelting wastewater using electrocoagulation process: Influence of pulse current parameters and anions. *Separation and Purification Technology*, 188, 316-328.
<http://dx.doi.org/10.1016/j.seppur.2017.07.036>.
- Yang, A., Kookana, R.S., Williams, M., Ying, G.G., Du, J., Doan, H., Kumar, A. (2016). Oxidation of ciprofloxacin and enrofloxacin by ferrate(VI): Products identification, and toxicity evaluation. *Journal of Hazardous Materials*, 320, 296-303. <http://dx.doi.org/10.1016/j.jhazmat.2016.08.040>.
- Yang, T., Liu, Y., Wang, L., Jiang, J., Huang, Z., Pang, S., Cheng, H., Gao, D., Ma, J. (2018). Highly effective oxidation of roxarsone by ferrate and simultaneous arsenic removal with in situ formed ferric nanoparticles. *Water Research*, 147, 321-330. <https://doi.org/10.1016/j.watres.2018.10.012>.
- Yim, J.H., Kim, K.W., Kim, S.D. (2006). Effect of hardness on acute toxicity of metal mixtures using *Daphnia magna*: Prediction of acid mine drainage toxicity. *Journal of Hazardous Materials*, 138, 16-21.
<https://doi.org/10.1016/j.jhazmat.2005.11.107>.

- Ying, S.C., Schaefer, M.V., Cock-Esteb, A., Li, J., Fendorf, S. (2017). Depth stratification leads to distinct zones of manganese and arsenic contaminated groundwater. *Environmental Science and Technology*, 51, 8926-8932. <https://10.1021/acs.est.7b01121>.
- Zeng, C., Gonzalez-Alvarez, A., Orenstein, E., Field, J.A., Shadman, F., Sierra-Alvarez, R. (2017). Ecotoxicity assessment of ionic As(III), As(V), In(III) and Ga(III) species potentially released from novel III-V semiconductor materials. *Ecotoxicology and Environmental Safety*, 140, 30-36. <https://10.1016/j.ecoenv.2017.02.029>.
- Zhang, Z., Xiao, C., Adeyeye, O., Yang, W., Liang, X. (2020). Source and mobilization mechanism of iron, manganese and arsenic in groundwater of Shuangliao City, Northeast China. *Water*, 12, 534. <https://10.3390/w12020534>.
- Zhang, S., Ye, C., Zhao, W., An, L., Yu, X., Zhang, L., Sun, H., Feng, M. (2022). Product identification and toxicity change during oxidation of methotrexate by ferrate and permanganate in water. *Frontiers of Environmental Science and Engineering*, 16, 93. <https://doi.org/10.1007/s11783-021-1501-8>.
- Zuorro, A., Moreno-Sader, K.A., González-Delgado, Á.D. (2021). Evaluating the feasibility of a pilot-scale shrimp biorefinery via techno-economic analysis. *Journal of Cleaner Production*, 320, 128740. <https://doi.org/10.1016/j.jclepro.2021.128740>.